

# Analytical and Experimental Study of a PV/Thermal Transpired Solar Collector

by

Véronique Delisle

A thesis  
presented to the University of Waterloo  
in fulfilment of the  
thesis requirement for the degree of  
Master of Applied Science  
in  
Mechanical Engineering

Waterloo, Ontario, Canada, 2008

© Véronique Delisle 2008

I hereby declare that I am the sole author of this thesis. This is a true copy of the thesis, including any required final revisions, as accepted by my examiners.

I understand that my thesis may be made electronically available to the public.

# Abstract

In the last few years, unglazed transpired solar collectors (UTCs) have proven to be an effective and viable method of reducing HVAC loads and building energy consumption. With the growing interest in PV/Thermal collectors, a study of a PV/Thermal UTC with PV cells mounted directly on the absorber was carried out.

In the first part of this project, a TRNSYS model was developed to predict the performance of a PV/Thermal UTC. It was based on an actual UTC model, but modifications were made to account for the wind, the presence of PV cells and the corrugated shape of the plate. Simulations showed that mounting the cells only on the top surfaces of the corrugations prevented the cells from being shaded by the collector and consequently, presented the greatest potential. With this configuration, it was found that the addition of PV cells on the UTC decreased the thermal energy savings by 5.9%, but that 13.6% of the thermal energy savings could be recovered in the production of electricity.

In the second part of the study, a 2.5 m<sup>2</sup> prototype of a PV/Thermal UTC was constructed. The collector was mounted outdoors and tested at different air suction rates for a period of three weeks, during which the thermal output and electrical power were recorded. It was found that 10% more electricity was obtained when the fan was turned on than for zero flow conditions. It was also observed that at greater air suction rates, more cooling of the panel was achieved and potentially higher electrical power could be produced. The effect of the PV cells on the collector thermal performance could not be quantified, however, due to the small portion of PV cells on the whole collector area.

TRNSYS simulations were performed using the prototype parameters and the weather data of some experimental days. The results predicted by the component developed showed similar trends as the experimental results. The predictions were, however, not within the experimental uncertainties. The deviation in the results was attributed to the fact that the wind heat losses were not estimated accurately by the model and the non-uniform suction at the panel surface that prevented the prototype tested to work at its optimal performance.

# Acknowledgments

The work presented in this thesis could not have been completed without the help of several people that I wish, here, to acknowledge.

I would like to thank my supervisor, Professor Michael Collins. His confidence in me and his advice were fundamental to the realization of this project.

I am grateful to all the staff of the mechanical engineering department, Al Hodgson, Jim Baleshta, Andy Barber, Gordon Hitchman as well as the employees of the engineering student and machine shops. The experimental part of this project could not have been done without them sharing their experience and knowledge with me.

I would like to express my gratitude to Professor John Straube for letting me use the BEG Hut to perform my experiments. I am really thankful for his trust in me. I would also like to thank Rachel Smith from the Building Engineering Group who has been very generous of her time throughout the different stages of the experiment.

I am indebted to all my colleagues of the Solar Thermal Research Lab. I would like to thank Vivek Kansal, Chris Hadlock, Bart Lomanowski, Shohel Mahmud, Omid Nemati and Neil Norris for their daily help and support, and for making the Solar Lab an enjoyable place to work. I would also like to express my recognition to Martin Kegel for his encouragement and for proof-reading this thesis. Finally, I would like to acknowledge Nathan Kotey for his guidance as well as my officemate Victor Halder for his generosity, encouragement and support at every stage of the project.

I would like to thank Conserval Engineering Inc. for providing the panels for the experiment, especially Brett Barnes for his interest and for all the fruitful discussions.

Finally, I would like to give a special acknowledgement to the Canadian Solar Building Research Network, to the IEA Task 35 and to Yves Poissant and Lisa Dignard from Natural Resources Canada-Varenes for the financial support.

# Contents

<b>1</b>	<b>Background</b>	<b>1</b>
1.1	Introduction . . . . .	1
1.1.1	Energy Consumption and GHG Emissions . . . . .	1
1.1.2	Energy Savings Potential . . . . .	2
1.1.3	Solutions . . . . .	3
1.2	Background . . . . .	3
1.2.1	Basics of Solar Energy . . . . .	3
1.2.2	Unglazed Transpired Collectors . . . . .	5
1.2.3	Photovoltaic Cells . . . . .	6
1.2.4	Hybrid PV/Thermal Collectors . . . . .	8
1.3	Motivation and Objectives of the Research Work . . . . .	10
1.4	Thesis Outline . . . . .	10
<b>2</b>	<b>Literature Review</b>	<b>11</b>
2.1	Introduction . . . . .	11
2.2	Previous Studies of UTCs . . . . .	11
2.2.1	Heat Transfer Theory . . . . .	11
2.2.2	UTC Effectiveness . . . . .	15
2.2.3	Conductivity . . . . .	17
2.2.4	Wind Effect . . . . .	18
2.3	Numerical/Software Approach to UTCs . . . . .	19
2.4	PV/Thermal UTCs . . . . .	23
<b>3</b>	<b>PV/Thermal Transpired Collector Model</b>	<b>26</b>
3.1	Introduction . . . . .	26
3.2	Collector Configuration . . . . .	27
3.2.1	Panel Geometry . . . . .	27

3.2.2	PV/Thermal Collector Configurations . . . . .	29
3.3	Model Theory . . . . .	30
3.3.1	Assumptions . . . . .	30
3.3.2	Heat Transfer Theory . . . . .	31
3.3.3	Absorbed Radiation on the Collector . . . . .	37
3.3.3.1	Total Radiation on a Surface $i$ . . . . .	37
3.3.3.2	Diffuse Radiation on a Surface $i$ . . . . .	39
3.3.3.3	Beam Radiation on a Surface $i$ . . . . .	42
3.3.3.4	Collector Optical Properties . . . . .	45
3.3.3.5	Absorbed Solar Radiation . . . . .	47
3.3.4	Solution Method . . . . .	48
3.3.5	Control Method . . . . .	51
3.4	TRNSYS Component . . . . .	53
3.4.1	Simulation Parameters and Inputs . . . . .	53
3.4.2	Simulation Results . . . . .	56
<b>4</b>	<b>Experimental Setup</b> . . . . .	<b>60</b>
4.1	Introduction . . . . .	60
4.2	PV/Thermal Collector Prototype . . . . .	61
4.2.1	Selection of the Solar Cells . . . . .	61
4.2.2	Perforated Plate . . . . .	62
4.2.3	PV Cell Layout . . . . .	64
4.3	Experimental Setup Description . . . . .	66
4.3.1	Wall and Plenum Construction . . . . .	66
4.3.2	Suction Flow Line . . . . .	69
4.4	Instrumentation and Measurements . . . . .	70
4.4.1	Data Acquisition System . . . . .	70
4.4.2	Temperature Measurements . . . . .	71
4.4.3	Flowrate Measurements . . . . .	72
4.4.4	Irradiance Measurements . . . . .	73
4.4.5	PV Cells Maximum Power . . . . .	74
4.4.6	Data Collection . . . . .	75

<b>5</b>	<b>Experimental Results and Model Validation</b>	<b>77</b>
5.1	Introduction . . . . .	77
5.2	Experimental Results . . . . .	77
5.2.1	Experimental Conditions and Weather Data . . . . .	77
5.2.2	Experimental Data . . . . .	78
5.2.3	Effect of the Transpired Plate on the PV Cells Performance	88
5.2.4	Effect of the PV cells on the Collector Thermal Performance	92
5.3	Model Validation . . . . .	94
5.3.1	TRNSYS Simulation . . . . .	94
5.3.2	Preliminary Results . . . . .	96
5.3.2.1	PV Cells Layout Electrical Parameters . . . . .	97
5.3.3	TRNSYS Parameters and Inputs . . . . .	100
5.3.4	Simulation Results . . . . .	100
5.3.5	Discussion . . . . .	106
<b>6</b>	<b>Conclusions and Recommendations</b>	<b>113</b>
6.1	Conclusions . . . . .	113
6.2	Recommendations . . . . .	115
<b>A</b>	<b>Method for Calculating the View Factors</b>	<b>117</b>
<b>B</b>	<b>Method for Calculating the Shaded Portion</b>	<b>123</b>
<b>C</b>	<b>PV/Thermal Collector Model Fortran Code</b>	<b>127</b>
<b>D</b>	<b>Pressure Drop Calculation</b>	<b>160</b>
<b>E</b>	<b>Experimental Data</b>	<b>165</b>
E.1	Weather Data from the Roof Hut . . . . .	165
E.2	Experimental Data . . . . .	166
<b>F</b>	<b>Uncertainty Analysis</b>	<b>194</b>
F.1	Introduction . . . . .	194
F.2	Measured Quantities . . . . .	195
F.2.1	PV Cells Dimensions . . . . .	195
F.2.2	Panel Dimensions . . . . .	196
F.2.3	Barometric Pressure . . . . .	196

F.2.4	Voltage Measurements . . . . .	196
F.2.5	Shunt Resistance . . . . .	197
F.2.6	Irradiance on the East Wall . . . . .	197
F.2.7	Standard Volumetric Flowrate Measurement . . . . .	198
F.2.8	Temperature Measurements . . . . .	200
F.3	Calculated Quantities . . . . .	200
F.3.1	PV Cells Area . . . . .	200
F.3.2	Collector Projected Area . . . . .	201
F.3.3	Maximum Electrical Power . . . . .	202
F.3.4	Air Temperature Rise . . . . .	203
F.3.5	Upper Panel Temperature Rise . . . . .	204
F.3.6	PV Cells Efficiency . . . . .	204
F.3.7	Air Density . . . . .	205
F.3.8	Actual Volumetric Flowrate . . . . .	206
F.3.9	Volumetric Flowrate per Unit Area . . . . .	207
F.3.10	Mass Flowrate . . . . .	207
F.3.11	Thermal Output . . . . .	208
F.3.12	Thermal Efficiency . . . . .	209
<b>G</b>	<b>Radiation Converter Component Fortran Code</b>	<b>210</b>
	<b>Bibliography</b>	<b>216</b>

# List of Figures

1.1	Percentage of energy use and GHG emissions by end-use in Canada for the (a) residential sector (b) institutional and commercial sectors (Statistics Canada, 2006) . . . . .	2
1.2	A typical solar thermal collector . . . . .	4
1.3	Schematic diagram of a UTC mounted on a building wall . . . . .	5
1.4	Schematic diagram of the principle of PV cells . . . . .	7
1.5	Typical I-V curve for a PV module . . . . .	8
1.6	Example of a PV/Solarwall cogeneration system with PV modules mounted on the front of the absorber plate (Conserval Engineering Inc., 2007) . . . . .	9
2.1	Diagram of the unglazed transpired collector used by Kutscher et al. (1993) in the development of the UTC heat loss theory . . . . .	13
2.2	Thermal and velocity boundary layers development over the perforated plate . . . . .	14
2.3	Diagram of the sinusoidal plate used by Gawlik et al. (2002) in the development of a $h_{wind}$ correlation for corrugated UTCs . . . . .	19
2.4	UTC configuration used in Summers' model (Summers, 1995) . . . . .	21
2.5	UTC configuration used in the model of Leon and Kumar (2007) . . . . .	23
2.6	Schematic diagrams of the experimental setup used by Naveed et al. (2006) (a) Stand-alone PV module (b) Combined PV/Thermal collector . . . . .	24
3.1	Close-up of the absorber plate used in the PV/Thermal UTC model (a) trapezoidal corrugations (b) small slot perforations . . . . .	27
3.2	PV/Thermal UTC geometric variables . . . . .	28
3.3	Configurations considered in the PV/Thermal collector model (a) PV cells mounted only on the top of the corrugations (b) PV cells mounted on every surface of the absorber plate . . . . .	29

3.4	Heat transfer exchanges in the PV/Thermal collector . . . . .	31
3.5	Absorber plate divided in 8 different types of surfaces . . . . .	38
3.6	Absorber plate with the addition of 3 fictitious surfaces for the calculation of the diffuse radiation due to sky diffuse and ground reflected radiation . . . . .	39
3.7	Absorber plate with the numbering of the shaded surfaces necessary for the calculation of the diffuse radiation due to beam radiation . . . . .	41
3.8	Orientation of surface 4 of the PV/Thermal UTC with respect to surface 3 . . . . .	44
3.9	Diagram of the heating system for a building with a PV/Thermal UTC . . . . .	52
3.10	Heat transfer exchanges in the building with a PV/Thermal collector . . . . .	54
3.11	Diagram of the heating system for the base case building without a solar collector . . . . .	56
4.1	Close-up of the largest width available between two perforations on the absorber plate . . . . .	61
4.2	Solar cell cut from a Solartec photovoltaic cell of type SC2460 . . . . .	62
4.3	SW100 and SW200 SolarWall <sup>®</sup> panels dimensions (Conserval Engineering Inc., 2006) . . . . .	63
4.4	Picture of the PV/Thermal UTC prototype . . . . .	64
4.5	Diagram of the experimental setup . . . . .	66
4.6	View of the BEG Hut east wall with the plenum box installed . . . . .	67
4.7	PV/Thermal transpired solar collector prototype installed on the BEG Hut east facing wall . . . . .	68
4.8	Overall view of the duct and fan installation inside the BEG Hut . . . . .	69
4.9	Location of the thermocouples on (a) the wall (b) the absorber plate . . . . .	72
4.10	Schematic diagram of the PV cells layout connection for the maximum power point tracking . . . . .	74
5.1	Hourly data for the (a) wind direction and (b) wind speed for the clear sky days of the experiment . . . . .	79
5.2	Variation of the ambient temperature for the clear sky days . . . . .	80
5.3	Variation of the irradiance on the collector surface for the clear sky days . . . . .	80
5.4	Experimental data for August 29 (a) Temperatures and irradiance on the collector (b) Thermal output and electrical power . . . . .	81
5.5	Experimental data for August 31 (a) Temperatures and irradiance on the collector (b) Thermal output and electrical power . . . . .	82

5.6	Experimental data for September 1 (a) Temperatures and irradiance on the collector (b) Thermal output and electrical power . . . . .	83
5.7	Experimental data for September 2 (a) Temperatures and irradiance on the collector (b) Thermal output and electrical power . . . . .	84
5.8	Experimental data for September 6 (a) Temperatures and irradiance on the collector (b) Electrical power . . . . .	85
5.9	Experimental data for September 8 (a) Temperatures and irradiance on the collector (b) Thermal output and electrical power . . . . .	86
5.10	Variation of the maximum electrical power output produced for the clear sky days . . . . .	88
5.11	Variation of the upper panel back temperature and PV cells efficiency for August 29 and September 6 . . . . .	89
5.12	Variation of the upper panel back surface temperature rise with the irradiance for a wind speed measured on the roof between 2 m/s and 3 m/s . . . . .	91
5.13	Variation of the temperature rise with the irradiance for a SolarWall <sup>®</sup> (Hollick, 1994) and from the testing of the prototype . . . . .	92
5.14	Variation of the thermal efficiency with the air flowrate for a SolarWall <sup>®</sup> (Hollick, 1994) and from the testing of the prototype . . . . .	93
5.15	Electrical power measured as a function of the upper panel average temperature for different bins of irradiance . . . . .	98
5.16	Comparison between the experimental data and TRNSYS predictions for September 1 (a) Temperatures (b) Thermal and electrical output . . . . .	102
5.17	Comparison between the experimental data and TRNSYS predictions for September 2 (a) Temperatures (b) Thermal and electrical output . . . . .	103
5.18	Comparison between the experimental data and TRNSYS predictions for September 6 (a) Temperature (b) Thermal and electrical output . . . . .	104
5.19	Comparison between the experimental data and TRNSYS predictions for September 8 (a) Temperatures (b) Thermal and electrical output . . . . .	105
5.20	Variation of the wind heat transfer coefficient with the wind speed for different correlations . . . . .	110
5.21	Variation of the current and voltage recorded on September 1 . . . . .	111
A.1	2D Enclosure for Hottel's String Rule . . . . .	117

A.2	Schematic diagram of surfaces 1 and 2 in the calculation of view factor 1 . . . . .	118
A.3	Schematic diagram of surfaces 1 and 2 in the calculation of view factor 2 . . . . .	119
A.4	Schematic diagram of surfaces 1 and 2 in the calculation of view factor 3 . . . . .	119
A.5	Schematic diagram of surfaces 1 and 2 in the calculation of view factor 4 . . . . .	120
A.6	Schematic diagram of surfaces 1 and 2 in the calculation of view factor 5 . . . . .	121
A.7	Schematic diagram of surfaces 1 and 2 in the calculation of view factor 6 . . . . .	122
B.1	Sun's position relative to the solar collector . . . . .	124
B.2	Minimum and maximum angle delimiting the 5 shading cases . . . .	125

# List of Tables

3.1	Parameters and Inputs to the TRNSYS simulation . . . . .	55
3.2	Thermal energy savings and electricity produced for the 3 modes of the PV/Thermal collector model for the city of Toronto . . . . .	57
3.3	Comparison of the thermal energy savings and useful thermal energy collected obtained with Mode 1 of the PV/Thermal UTC model and with Summers' UTC component . . . . .	58
3.4	Thermal energy savings and electricity produced for different cities using Mode 2 of the PV/Thermal collector model . . . . .	59
4.1	Solartec SC2460 photovoltaic cells electrical parameters and temperature coefficients (Solartec, 2007) . . . . .	62
4.2	Results of the flash test on the PV/thermal collector prototype . . . . .	65
5.1	Average air flowrate measured for each clear sky day . . . . .	78
5.2	Parameters of the PV cells layout calculated for different bins of irradiance using the experimental measurements of September 6 . . . . .	99
5.3	Parameters and Inputs to the TRNSYS simulation of the experimental days . . . . .	101
5.4	RMSE of the collector surface and outlet temperatures predicted by TRNSYS . . . . .	106
5.5	RMSE of the collector surface and outlet temperatures predicted by TRNSYS with the local wind speed as input . . . . .	107
E.1	Weather data measured by the BEG Hut data logger . . . . .	165
E.2	Experimental Data for August 29 . . . . .	167
E.3	Experimental data for August 31 . . . . .	170
E.4	Experimental data for September 1 . . . . .	174
E.5	Experimental data for September 2 . . . . .	179
E.6	Experimental data for September 6 . . . . .	184
E.7	Experimental data for September 8 . . . . .	189

F.1	Values of the measured variables used in the uncertainty analysis	. 195
F.2	Values of the calculated variables used in the uncertainty analysis	. 200

# Nomenclature

## Symbols

a	Length of the base of the trapezoid (m)
A	Area (m <sup>2</sup> )
	Amplitude (m)
b	Length of the top of the trapezoid (m)
d	Distance between two corrugations (m)
c <sub>p</sub>	Specific heat (kJ/kg·K)
C <sub>f</sub>	Corrugation factor (dimensionless)
D	Diameter (m)
D <sub>g</sub>	Length of the diagonal in the trapezoid (m)
D <sub>h</sub>	Hydraulic diameter (m)
f	Friction (dimensionless)
F	View factor (dimensionless)
FF	Fill factor (%)
g	Gravity (9.8 m/s <sup>2</sup> )
G	Irradiation (W/m <sup>2</sup> )
h	Heat transfer coefficient (W/m <sup>2</sup> ·K)
h <sub>plen</sub>	Plenum height (m)
h <sub>T</sub>	Height of the trapezoidal corrugations (m)
HR	Relative humidity (%)
I	Current (A)
I <sub>sc</sub>	Short-circuit current (A)
I <sub>mp</sub>	Current at maximum power point (A)
J	Radiosity (W/m <sup>2</sup> )
k	Thermal conductivity (W/m·K)
K	Glazing extinction coefficient (1/m)
L	Length (m)
$\dot{m}$	Mass flowrate (kg/h)
n	Refraction index (dimensionless)
N <sub>bc</sub>	Number of corrugations (dimensionless)
Nu	Nusselt number (dimensionless)
p	Pitch (m)
P	Pressure (kPa)
P <sub>el</sub>	Electrical power (W)
P <sub>el,ref</sub>	Modified reference electrical power defined in Equation 5.3 (W)
P <sub>mp</sub>	PV cells power at maximum power point (W)
P <sub>PV</sub>	Proportion of PV cells (dimensionless)
Pr	Prandtl number (dimensionless)
P <sub>sh</sub>	Shaded portion (dimensionless)
$\dot{Q}$	Heat transfer rate (W)
$\dot{Q}''$	Heat transfer rate per unit area (W/m <sup>2</sup> )

## Symbols

$R$	Gas constant for air (0.287 kJ/kg·K)
$R_b$	Ratio of the beam radiation on a tilted surface to that on a horizontal surface (dimensionless)
$R_{sh}$	Shunt resistance (ohm)
$Re$	Reynolds number (dimensionless)
$t$	Thickness (m)
$t_T$	Length of the side of the trapezoid (m)
$T$	Temperature (K)
$T_{rise}$	Temperature rise (K)
$U$	Overall heat transfer coefficient (W/m <sup>2</sup> ·K)
$V$	Velocity (m/s)
$V_{G_{T,col}}$	Voltage recorded by the data logger associated to the measurement of the irradiance on the east wall
$V_{mp}$	Voltage at maximum power point (V)
$V_{oc}$	Open-circuit voltage (V)
$V_{PV}$	PV cells voltage (V)
$V_{PYR}$	Pyranometer voltage signal (V)
$V_{R_{sh}}$	Voltage measured across the shunt resistance (V)
$\dot{V}$	Flowmeter voltage signal (V)
$\dot{V}$	Volumetric flowrate (m <sup>3</sup> /h)
$W$	Width (m)
$W_{end}$	Width of the end surfaces of the collector (m)

## Greek Letters

$\alpha$	Absorptance (dimensionless)
	PV cells temperature coefficient (1/°C)
$\beta$	Slope (°)
	PV cells temperature coefficient (1/°C)
$\Delta$	Difference
$\delta$	Uncertainty
$\epsilon$	Surface roughness (m)
$\varepsilon$	Emissivity (dimensionless)
	Effectiveness (dimensionless)
$\gamma$	Surface azimuth angle (°)
	Mass fraction of fresh air (dimensionless)
$\gamma_s$	Solar azimuth angle (°)
$\eta$	Efficiency (dimensionless)
$\rho$	Density (kg/m <sup>3</sup> )
	Reflectance (dimensionless)
$\sigma$	Porosity (dimensionless)
$\sigma_{sb}$	Stefan-Boltzmann constant (5.67 * 10 <sup>-8</sup> W/m <sup>2</sup> ·K <sup>4</sup> )
$\tau$	Transmittance (dimensionless)
$\tau_a$	Ratio of the transmitted radiation over the total incident radiation

## Greek Letters

$\tau\alpha$	Tau-alpha product of the PV cells-cover combination (dimensionless)
$\theta$	Sun incidence angle ( $^{\circ}$ )
$\theta_{end}$	Angle between the end surface of the collector and the top surface of the corrugation ( $^{\circ}$ )
$\theta_r$	Refraction angle ( $^{\circ}$ )
$\theta_T$	Acute angle inside the trapezoid ( $^{\circ}$ )
$\theta_z$	Zenith angle ( $^{\circ}$ )
$\mu$	PV cells temperature coefficient ( $1/^{\circ}\text{C}$ )
$\nu$	Kinematic viscosity ( $\text{m}^2/\text{s}$ )
$\varsigma$	Variable in the pressure drop calculation (Kutscher, 1994) (dimensionless)
$\xi$	Angle between two vectors ( $^{\circ}$ )

## Subscripts

abs	Absorbed
acc	Acceleration
act	Actual
amb	Ambient
aux	Auxiliary heat required
avg	Average
b	Back Beam
base	Base case building
blg	Building
buoy	Buoyancy
bypass	Collector bypass
col	Collector
cond	Conductive
conv	Convective
cs	Cross-section
d	Diffuse
db	Diffuse due to beam
dcol	Diffuse radiation on the collector
dd	Diffuse due to sky diffuse
dg	Diffuse due to ground reflected
d-g	Sky diffuse or ground reflected
el	Electrical
f	Front
g	Ground reflected
glazed	Glazed solar collector
gnd	Ground
h	Hole
H	Horizontal
HX	Heat exchange
i	Surface i

## Subscripts

i-j	From surface i to surface j
int	Internal gains
i-sh	Shaded portion of surface i
max	Maximum
min	Minimum
mix	Mixing
N	Normal incidence angle
out	Outlet
pot	Potential
plen	Plenum
proj	Projected
Panel	Panel
rad	Radiative
red	Reduced
ref	Reference
s	Suction
savings	Thermal energy savings
sc	Short-circuit
sky	Sky
sol-air	Sol-air
std	Standard
sup	Supplied
sur	Surroundings
th	Thermal
T	Total
u	Useful
up	Upper panel
wall	Wall
wind	Wind
wind,loc	Local wind speed
wind,(10-11)	Wind 10 m or 11 m above the ground

## Abbreviations

BEG	Building Engineering Group
DAQ	Data acquisition system
GHG	Greenhouse gases
IAM	Incidence angle modifier
IPCC	Intergovernmental Panel on Climate Change
NSTF	National Solar Test Facility
PV	Photovoltaic
SAH	Solar air heating
STC	Standard test conditions
SWH	Solar water heating
TMY2	Typical meteorological yearly data sets
UTC	Unglazed transpired collector

# Chapter 1

## Background

### 1.1 Introduction

#### 1.1.1 Energy Consumption and GHG Emissions

In recent years, energy consumption and greenhouse gases (GHG) emissions have become a worldwide concern. According to the Intergovernmental Panel on Climate Change (IPCC, 2007), if the rate of energy consumption and GHG emissions are not reduced, global warming will accelerate and have catastrophic effects on the planet. Besides the fact that humans will have to face more frequently extreme weather such as scorching heat, flooding and draught, the IPCC report that a global warming of 1.4°C to 5.8°C could cause the sea level to rise by 0.09 m to 0.88 m by 2100 due to melting glaciers (IPCC, 2007). This last phenomenon could lead to the extinction of number of species and to significant flooding of inhabited land.

Canada has made little effort to fight climate change. From 1990 to 2004, its energy consumption and GHG emissions have increased by 22.9% and 23.9%, respectively (Statistics Canada, 2006). In order to find solutions to curb both GHG emissions and global warming, the first step consists of identifying the sectors mainly responsible for the production of GHG.

## 1.1.2 Energy Savings Potential

Figures 1.1 (a) and (b) present the distribution by end-use of the 2004 Canadian total energy consumption and GHG emissions in the residential and institutional/commercial sectors. As can be seen, for both sectors more than half of the total energy consumption and GHG emissions are due to space heating. Therefore, a small improvement in this sector could have a significant impact on the total amount of GHG emitted and ultimately, on the environment.

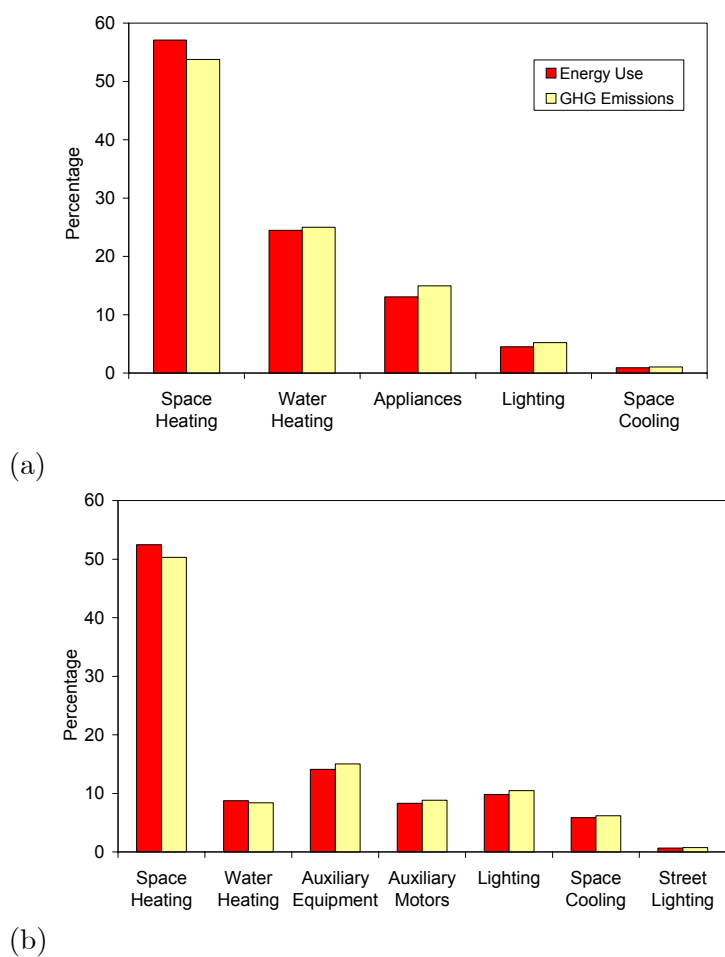


**Figure 1.1:** Percentage of energy use and GHG emissions by end-use in Canada for the (a) residential sector (b) institutional and commercial sectors (Statistics Canada, 2006)

### **1.1.3 Solutions**

There are several actions that can be taken to limit GHG emissions that are specifically related to space heating, and are applicable for all kinds of buildings. One of them consists of reducing energy consumption. For new construction, this can be done by minimizing the building heat losses by using walls and windows with better insulation. In existing buildings, installing programmable thermostats can help in reducing the heating required at night or when the building is not occupied. The use of high performance heating devices such as heat pumps can also contribute in reducing the energy consumption. Another action consists of selecting sources of energy that are clean compared to fossil fuels, such as natural gas, oil, propane and coal. Wind, water, geothermal and solar energy are all very promising sources of energy that do not produce GHG and are renewable. In certain locations, however, some cannot be used because they are simply not available in large enough quantities to be economically viable. The sun is accessible almost everywhere on the planet. Therefore, solar energy presents great potential as a source of energy.

## **1.2 Background**

### **1.2.1 Basics of Solar Energy**

Solar energy technologies transform the radiation coming from the sun to useful energy. It is typically used for:

- Passive solar heating
- Active solar heating
- Photovoltaic cells

Passive solar heating is a process that usually does not require any mechanical or electrical devices to function. It can be as simple as direct gain of energy through windows, but can also consist of any system where the working fluid is circulated

naturally, such as in thermosyphon systems. Active solar heating implies that a mechanical component like a pump or a fan, is involved. These mechanisms are used to circulate the working fluid through devices called solar collectors. Finally, solar energy can be used with photovoltaic (PV) cells that absorb the light from the sun and convert it into electricity.

Solar thermal collectors are devices that convert solar radiant energy into heat. They are available in several designs, but the basic operating principles remain the same. An absorber plate, usually of dark color, absorbs radiation from the sun and transfers this energy to a working fluid, either air or liquid. Figure 1.2 shows an example of a flat plate collector where the fluid circulates through pipes. The collector on this figure has a cover to minimize heat losses from the absorber plate.

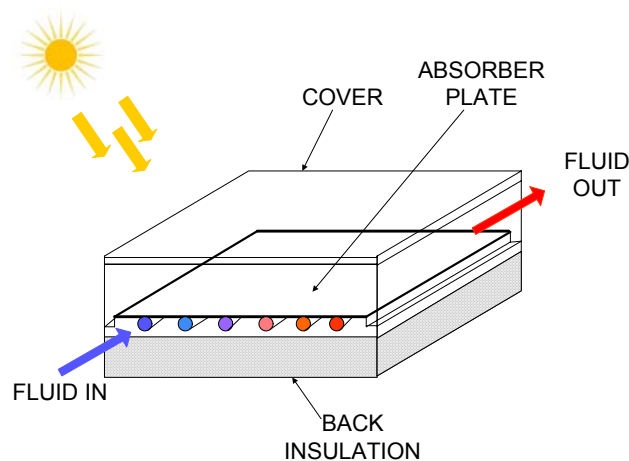


**Figure 1.2:** A typical solar thermal collector

Liquid working fluids are typically employed for solar water heating (SWH) purposes, while air is used for solar air heating (SAH). Collectors having air as their working fluid present some advantages. Contrary to liquid solar collectors, the air can be directly drawn into the building without the need for any further heat exchange. Also, in SAH systems, the problem of fluid leakage is not as critical and corrosion and freezing are not issues. With air collectors, however, high efficiencies cannot be achieved because of the low thermal capacity of air. Moreover, these

systems are generally bulky because large air channels are required to displace a small amount of energy.

### 1.2.2 Unglazed Transpired Collectors

In the last few years, a new type of air solar thermal collector, the unglazed transpired collector (UTC), has received a great deal of attention, mainly because it has proven to be an effective and viable method of reducing HVAC loads, building energy consumption and GHG emissions. SolarWall<sup>®</sup> is a well-known UTC that was developed in the early 1980s. Over 1000 SolarWall<sup>®</sup> systems have now been installed in 25 different countries on commercial, industrial, institutional and multi-residential buildings (Conserval Engineering Inc., 2007). Just like other air collectors, UTCs consist of an interesting alternative to fossil fuels for buildings requiring a large amount of hot fresh air, or for solar crop drying applications.

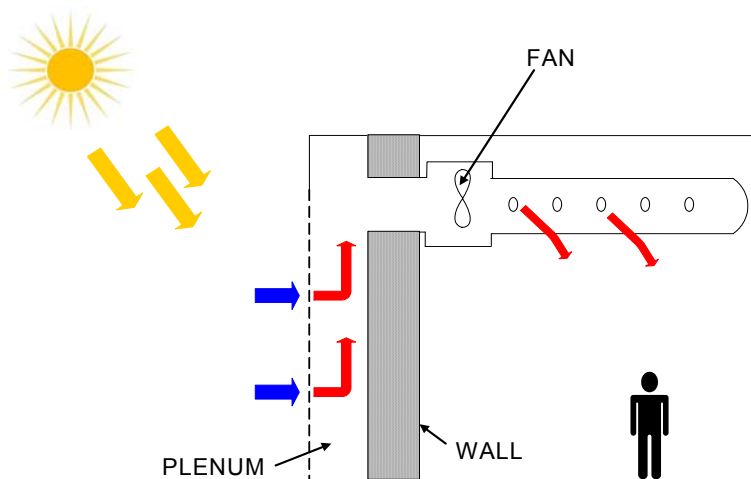


**Figure 1.3:** Schematic diagram of a UTC mounted on a building wall

Unglazed transpired collectors are dark and perforated plates, usually corrugated in a trapezoidal shape to provide structural stiffness. They are typically made out of aluminium or galvanized steel and are available in a wide range of colors to match the aesthetics of the building. They can be installed either on vertical

walls or on inclined roofs that are strongly exposed to solar radiation. In order to maximize the annual energy availability, the general rule is that a solar collector should be mounted so that its slope is equal to the latitude of the location where it is installed (Duffie and Beckman, 1991). In the case of UTCs, however, wall installations are more common, because the roofs of large commercial or industrial buildings are usually flat.

Typically, a gap of 10 to 20 cm, called the plenum, is left between the wall or roof and the absorber plate to let the air travel as it passes through the perforations of the plate (Figure 1.3). A fan, installed in the ventilation system, forces the outdoor air to pass through the perforated plate by creating a negative pressure. Therefore, when incident solar radiation hits the collector, the air going through the perforations takes back the heat gained by the absorber plate. As a result, the outdoor air is preheated when it goes into the plenum and enters the building ventilation system. A great advantage of UTCs compared to other types of solar air collectors is that since suction is occurring at the surface, the plate is kept at a relatively low temperature and the convective heat losses from the absorber plate is reduced (Kutscher et al., 1991). Therefore, there is no need for any covers, which reduces the optical losses and decreases the cost of the collector.

### **1.2.3 Photovoltaic Cells**

PV cells are typically composed of a P-type and a N-type semiconductor. The semiconductors can be made of different materials such as mono or polycrystalline silicon (Si), amorphous silicon (a-Si), cadmium sulfide (CdS) or cadmium telluride (CdTe). The P-type semiconductor has available electron-holes (+) and the N-type semiconductor has free electrons (-). Therefore, when the two semiconductors are placed back-to-back, a potential difference is created in a region called the P-N junction. When intense light or solar radiation hits a PV cell, the photons with high enough energy can displace electrons, creating hole-electron pairs. For a N-on-P silicon cell, these holes tend to collect on the back contact electrode while the free electrons move to the front contact electrode (Figure 1.4). When a load is connected to the front and back electrodes, electrons use the newly created path to

return to the P-type contact grid, creating current. Photovoltaic cells are known to convert only a small part of the solar energy they absorb into electricity. In fact, their efficiency is in the range of only 6-15%, depending on the type of cells. The main reason for this poor efficiency is that only photons with a certain amount of energy are able to create hole-electron pairs. The photons with not enough energy or the ones that are left when the maximum amount of electron-hole pairs are created cannot produce electricity. Instead, their energy is converted to heat and contributes to raising the cells temperature. This heating up is undesirable for PV cells, because it decreases their electrical conversion efficiency.

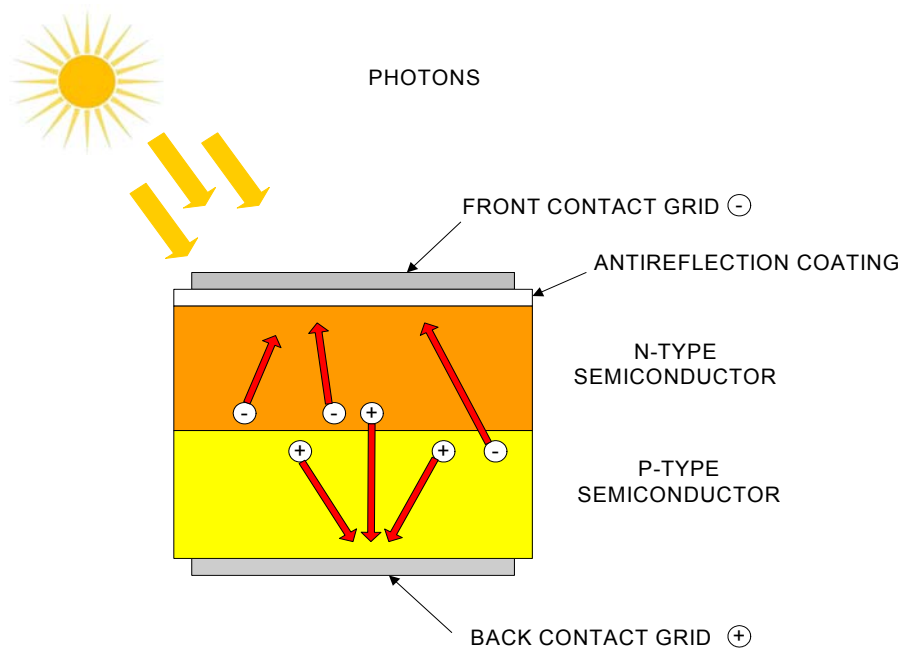


**Figure 1.4:** Schematic diagram of the principle of PV cells

A solar cell or a PV module is usually characterized by a current-voltage curve (I-V curve). An example of an I-V curve is shown in Figure 1.5. On this plot, the short-circuit current,  $I_{sc}$ , is the current at zero voltage while the open-circuit voltage,  $V_{oc}$ , corresponds to the voltage at zero current. A PV cell or PV module will always operate somewhere on its I-V curve according to the electrical load that

is applied. Ideally, it will operate at the locus on the I-V curve called the maximum power point, where the current ( $I_{mp}$ ) and voltage ( $V_{mp}$ ) generated are such that the maximum possible power is produced.

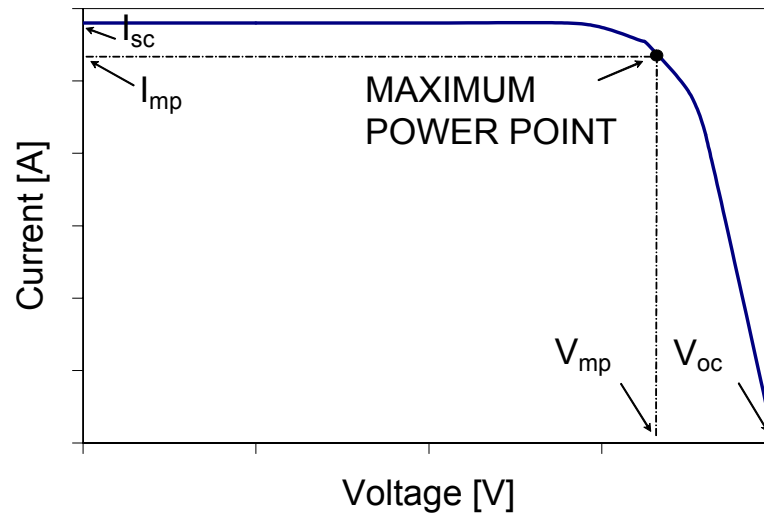


**Figure 1.5:** Typical I-V curve for a PV module

#### 1.2.4 Hybrid PV/Thermal Collectors

Hybrid photovoltaic/thermal collectors, also known as PV/Thermal collectors, consist of a PV module or PV cells mounted on the front of an absorber plate. Just like thermal collectors, they can be glazed or unglazed and can have either air or liquid as their working fluid. Contrary to stand-alone thermal collectors or PV modules, PV/Thermal collectors have the benefit of producing thermal energy and electricity simultaneously.

PV/Thermal collectors usually improve the PV modules efficiency compared to stand-alone PV modules, because the fluid circulating behind the PV removes the heat from the cells and cools them. They also contribute in decreasing the energy losses by converting the heat unused by the cells to useful energy. Combining PV with solar thermal collectors generally results in a reduction of the thermal and elec-

trical output compared to stand-alone PV modules or thermal collectors (Zondag et al., 2003). However, they are of great interest for buildings where the potential area for solar installations is limited. As shown by Zondag et al. (2003), an area covered with a PV/Thermal collector produces more energy than the same area partially covered with a PV module and a solar thermal collector. Moreover, compare to a thermal collector and a PV module side by side, PV/Thermal collectors are simpler to install and provide a greater aesthetic uniformity.

The first prototype of PV/Thermal unglazed transpired collectors was built in the late 1990's by Hollick (1998), the inventor of SolarWall<sup>®</sup>. On this collector, crystalline silicon cells encapsulated in teflon were mounted on the top of the corrugations of the SolarWall<sup>®</sup>, leaving a small gap between the cells and the absorber plate. Presently, Conservall Engineering is producing a PV/Thermal UTC where PV modules are mounted on the front of the collector (Figure 1.6). This thesis looks at a different design of a PV/Thermal UTC where the PV cells are mounted directly on some surfaces of the collector, leaving the perforations uncovered.



**Figure 1.6:** Example of a PV/Solarwall cogeneration system with PV modules mounted on the front of the absorber plate (Conservall Engineering Inc., 2007)

## 1.3 Motivation and Objectives of the Research Work

This research work was motivated by the creation of Task 35 of the International Energy Agency Solar Heating and Cooling program. The purpose of this project was to enhance the development, commercialization and general understanding of the PV/Thermal technology. One of the objectives was to provide mathematical models of different types of PV/Thermal collectors that could be used as tool to predict their performance as stand-alone devices and when they are integrated in a building.

The objectives of this thesis are as follows:

- To develop a model of a combined PV/Thermal transpired solar collector to be implemented in TRNSYS, a building energy simulation tool.
- To build a prototype of a PV/Thermal UTC and perform outdoor experiments to study its thermal and electrical performance.
- To compare the model predictions with the results from the experimental study.

## 1.4 Thesis Outline

The series of steps that were followed in order to achieve the objectives stated previously are described in this thesis. In Chapter 2, a literature review summarizes the research work performed on unglazed transpired collectors and PV/Thermal UTCs over the last years. Chapter 3 presents the development of the PV/Thermal transpired collector mathematical model. It is followed by Chapter 4 that contains the description of the construction of the prototype and the experimental setup. The experimental results as well as the comparison of the collector performance obtained experimentally and with the model developed are then discussed in Chapter 5. Finally, Chapter 6 formulates conclusions and recommendations for future work.

# Chapter 2

## Literature Review

### 2.1 Introduction

Over the past thirty years, research on UTCs has mainly focused on the understanding of the heat transfer occurring through the perforated plates. The main goals of the different studies were to improve heat transfer and to decrease the cost of the collector. There is little literature available on PV/Thermal unglazed transpired collectors.

Section 2.2 will review the different studies (analytical, numerical and experimental) that led to the development of the main aspects of the UTC heat transfer theory. Several models and pieces of software will then be discussed in Section 2.3. Finally, an overview of the work performed on PV/Thermal UTCs will be presented in Section 2.4.

### 2.2 Previous Studies of UTCs

#### 2.2.1 Heat Transfer Theory

Sparrow and Ortiz (1982) were among the first researchers to study the heat transfer through perforated plates with suction. Their objective was to determine

the heat transfer coefficients between the absorber plate and the ambient air. In order to achieve this goal, they performed experiments on plates with holes in an equilateral triangular pattern using a mass transfer method and the heat and mass transfer analogy. They obtained an expression for the Nusselt number at the front of the plate for normal flow under no-wind conditions as a function of the pitch-to-hole diameter ratio and the Reynolds number. The correlation was, however, not applicable to transpired collectors since the porosities (ratio of the total area covered by the perforations to that of the total absorber plate) were much higher (14%-22%) than the ones of the plates typically used in transpired collectors (0.1%-0.5%).

The research on perforated plates for solar collectors mainly started with Kutscher et al. (1993), with the development of the basic heat loss theory for flat plate UTCs. By performing an energy balance on the collector absorber plate, they obtained the following equation.

$$\rho c_p V_s (T_{out} - T_{amb}) = G_{T,col} \alpha_{col} - \dot{Q}''_{rad,col-sur} - \dot{Q}''_{conv,col-amb} \quad (2.1)$$

In Equation 2.1,  $\rho$  and  $c_p$  are the air density and specific heat,  $V_s$  is the air suction velocity on the panel,  $T_{out}$  is the temperature at the outlet of the collector,  $T_{amb}$  is the ambient temperature,  $G_{T,col}$  is the solar radiation incident on the collector,  $\alpha_{col}$  is the collector plate absorptance,  $\dot{Q}''_{rad,col-sur}$  is the radiative heat losses from the collector to the surroundings and  $\dot{Q}''_{conv,col-amb}$  is the convective heat losses from the plate to the ambient. By assuming the collector plate to be gray and diffuse, they expressed the radiative heat losses as

$$\dot{Q}''_{rad,col-sur} = \varepsilon_{col} \sigma_{sb} (T_{col}^4 - F_{col-sky} T_{sky}^4 - F_{col-gnd} T_{gnd}^4) \quad (2.2)$$

where  $\varepsilon_{col}$  is the collector absorber plate emissivity,  $\sigma_{sb}$  is the Stefan-Boltzmann constant,  $T_{col}$  is the absorber plate temperature,  $T_{sky}$  is the sky temperature,  $T_{gnd}$  is the ground temperature,  $F_{col-sky}$  is the view factor between the collector and the sky, and  $F_{col-gnd}$  is the view factor between the collector and the ground.

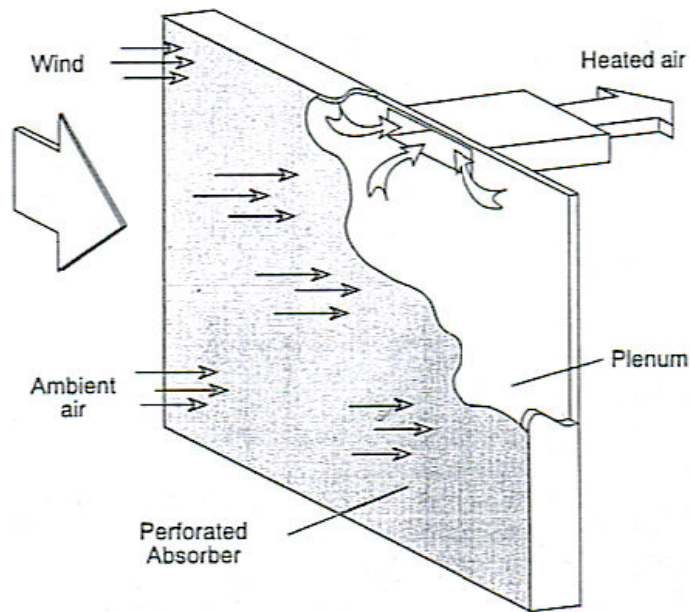


**Figure 2.1:** Diagram of the unglazed transpired collector used by Kutscher et al. (1993) in the development of the UTC heat loss theory

In order to find an expression for  $\dot{Q}''_{conv,col-amb}$ , the remaining unknown in Equation 2.1, Kutscher et al. (1993) assumed the flow on the perforated plate to be laminar with homogeneous suction (Figure 2.1). With this assumption, they showed analytically that the convective heat losses were only occurring in the region of the plate called the starting length, where the thermal and velocity boundary layers are growing. In the other part of the plate called the asymptotic region where the boundary layers reach constant thicknesses, there are no net fluxes of heat from the absorber plate into the boundary layer because the boundary layer is sucked in the plate. Therefore, there are no convective heat losses in this region and  $\dot{Q}''_{conv,col-amb}$  consist of the heat losses that occur during the starting length and that are carried all the way to the downstream edge of the plate (Figure 2.2). They considered the possibility of having turbulent flow at lower suction velocities, but not a lot of information was available regarding the velocity and temperature profiles of perforated plates with suction. The only profiles available came from experimental data that considered lower suction velocities and wind speeds than

the ones typically used in transpired collectors. Nevertheless, Kutscher et al. (1993) used this data and found that the convective heat losses were only an order of magnitude higher than in the case of a laminar asymptotic boundary layer. They concluded that for the high suction velocities used in transpired collectors, the laminar asymptotic boundary layer assumption was valid.

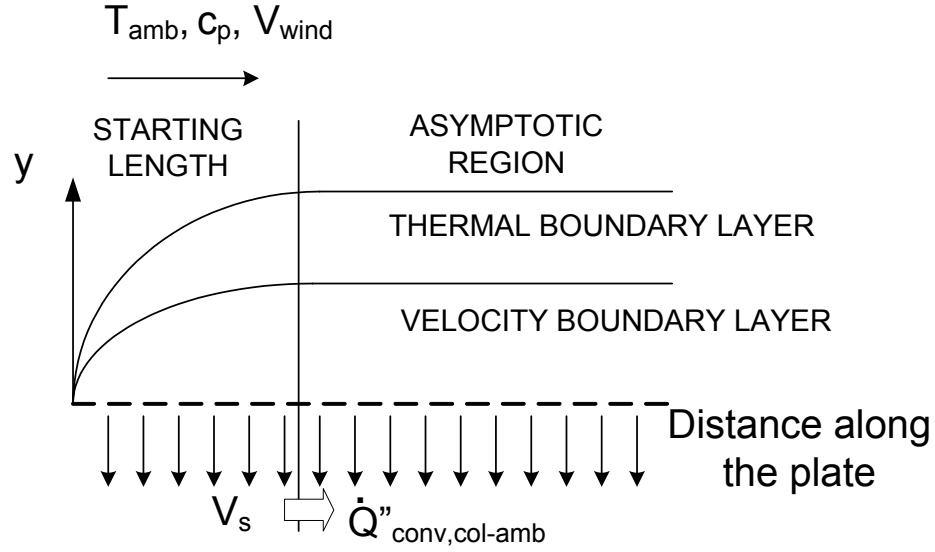


**Figure 2.2:** Thermal and velocity boundary layers development over the perforated plate

Based on this analytical study, Kutscher et al. (1991) showed that the natural convective heat losses to the ambient were negligible compared to the forced convective heat losses and expressed the convective heat loss coefficient from the collector to the ambient  $h_{conv,col-amb}$  as

$$h_{conv,col-amb} = 0.82 * \frac{V_{wind} \nu \rho c_p}{L V_s} \quad (2.3)$$

where  $V_{wind}$  is the wind velocity,  $L$  is the length of the absorber plate and  $\nu$  is the air kinematic viscosity. Considering the UTC to be isothermal, they could relate

$T_{out}$  to the collector heat exchanger effectiveness  $\varepsilon_{HX}$  with the following equation.

$$\varepsilon_{HX} = \frac{T_{out} - T_{amb}}{T_{col} - T_{amb}} \quad (2.4)$$

Using Equations 2.1 and 2.4, Kutscher et al. (1991) could express the collector thermal efficiency  $\eta_{th}$  as

$$\eta_{th} = \alpha_{col} \left[ 1 + \left( \frac{h_{rad,col-sur}}{\varepsilon_{HX}} + h_{conv,col-amb} \right) (\rho V_s c_p)^{-1} \right]^{-1} \quad (2.5)$$

where  $h_{rad,col-sur}$  is the radiative heat transfer coefficient from the collector to the surroundings. Equation 2.5 was of great interest, because once  $\varepsilon_{HX}$  was obtained, the collector efficiency could be predicted in a straightforward manner. Consequently, numerous research initiatives followed that tried to find expressions for  $\varepsilon_{HX}$ .

## 2.2.2 UTC Effectiveness

In order to find an expression for the collector heat exchange effectiveness,  $\varepsilon_{HX}$ , Kutscher (1994) performed experiments on several plates of different thicknesses, hole diameters and hole pitches having circular perforations arranged on a triangular layout. He subjected the plate to a parallel wind and studied the asymptotic region of the plate. The following Nusselt number was obtained to predict the heat exchange effectiveness

$$Nu_D = 2.75 \left[ \left( \frac{p}{D} \right)^{-1.2} Re_D^{0.43} + 0.011\sigma Re_D \left( \frac{V_{wind}}{V_s} \right)^{0.48} \right] \quad (2.6)$$

where,  $D$  is the hole diameter,  $p$  is the hole pitch (shortest distance between two adjacent holes),  $\sigma$  is the plate porosity and  $Re_D$  is the hole Reynolds number based on the hole velocity and diameter. Equation 2.6 takes into account the heat transfer occurring in all three regions of the hole: the front, the sides and the back. It is applicable for plate porosities of 0.1% to 5% and  $Re_D$  of 100 to 2000. With this experiment, Kutscher was also able to develop an empirical expression to calculate

the pressure drop for perforated plates under normal flow for the same range of porosities and Reynolds number.

Several studies conducted in the Solar Thermal Research Lab at the University of Waterloo followed the work done by Kutscher and investigated  $\varepsilon_{HX}$  for different plate designs. Cao et al. (1993) and Golneshan (1994) studied plates perforated with long narrow rectangular slots. Cao et al. (1993) conducted a two-dimensional numerical analysis by assuming the flow to be transverse to the slits but parallel to the plate, and by neglecting the heat transfer at the back of the slits. They found the velocity and temperature at the entrance of a perforation and expressed the plate effectiveness as a combination of the heat transfer occurring at the front and in the holes. Their results showed that 20% of the total heat transfer occurred in the hole. Golneshan (1994) developed a 2D momentum integral analysis and performed experiments on these plates perforated with long narrow rectangular slots (Golneshan & Hollands, 1998). The experiments were conducted on 4 different plates in the asymptotic region with the wind perpendicular to the slits. A relation between the plate effectiveness and six dimensionless parameters was obtained.

Arulanandam et al. (1999) tried to find an expression for the heat exchange effectiveness of perforated plates using a CFD model. The plate studied was perforated with circular holes laid out on a square pitch. They considered only the heat transfer occurring at the front of the plate and in the hole, modeling the back of the plate as adiabatic, and did not take the wind into account. The relation obtained was in agreement with Kutscher's work for the same conditions.

Van Decker et al. (2001) extended Kutscher's (1994) work on the plate effectiveness to a wider range of parameters by conducting experiments with the same experimental setup used by Golneshan (1994). They studied 9 plates of different materials, hole pitches, hole diameters, thicknesses and thermal conductivities in the asymptotic region. Using their experimental data and the previous work of Arulanandam et al. (1999) and Golneshan (1994), a correlation for the effectiveness of UTCs with holes laid out on a square pitch was developed by splitting the total heat transfer in three parts: the heat transfer occurring at the front face  $\varepsilon_f$ ,

in the sides of the holes  $\varepsilon_h$ , and at the back of the plate  $\varepsilon_b$ .

$$\varepsilon_{HX} = 1 - (1 - \varepsilon_f)(1 - \varepsilon_h)(1 - \varepsilon_b) \quad (2.7)$$

In Equation 2.7,  $\varepsilon_f$ ,  $\varepsilon_b$  and  $\varepsilon_h$  are expressed as

$$\varepsilon_f = 1 - \left(1 + \frac{\max(17.7, 0.708 \text{Re}_{wind}^{0.5})}{\text{Re}_s}\right)^{-1} \quad (2.8)$$

$$\varepsilon_b = 1 - \frac{1}{1 + 3.4 \text{Re}_b^{-1/3}} \quad (2.9)$$

$$\varepsilon_h = 1 - \exp\left[-0.0204 \frac{p}{D} - \frac{20.62t}{\text{Re}_h D}\right] \quad (2.10)$$

where

$$\text{Re}_{wind} = \frac{V_{wind}p}{\nu} \quad \text{Re}_s = \frac{V_s p}{\nu} \quad \text{Re}_b = \frac{V_s p}{\nu \sigma} \quad \text{Re}_h = \frac{V_s D}{\nu \sigma} \quad (2.11)$$

They found that their model could also be applied to plates with a triangular pitch by multiplying  $p$  by a scaling factor corresponding to 1/1.6. Using this factor, they were able to compare their model to the one of Kutscher (1994) and found that both models were giving similar results for the same conditions and plate geometry. Van Decker's model was, however, applicable for a wider number of plates, being valid for the following ranges of variables:  $0.028 \leq V_s \leq 0.083$  m/s,  $0 \leq V_{wind} \leq 5$  m/s,  $7 \leq p \leq 24$  mm,  $0.8 \leq D \leq 3.6$  mm,  $0.6 \leq t \leq 6.5$  mm,  $0.15 \leq k \leq 200$  W/m·K, where  $t$  and  $k$  are the plate thickness and thermal conductivity.

### 2.2.3 Conductivity

The research conducted on UTCs heat exchange effectiveness by Golneshan and Hollands (1998), Arulanandam et al. (1999) and Van Decker et al. (2001) demonstrated that plate conductivity had an important effect on the effectiveness, but only slightly influenced the collector efficiency. The effect of the plate conductivity was studied in depth by Gawlik et al. (2005) who compared numerically and experimentally the performance of a plate of high-conductivity (aluminium) and a plate of low-conductivity (styrene). Both panels were flat and perforated with holes on

a triangular layout. The two plates showed comparable efficiencies under similar conditions. This result was explained by the fact that the holes on the plate are so close to each other that a large temperature gradient between the perforations cannot be supported. They extended their result to corrugated plates, by suggesting that the plate conductivity would not affect the performance of these kinds of panels since the height of a corrugation and the distance between two corrugations were much larger than the hole pitch. This was of great interest, because using materials of low conductivity could significantly decrease the cost of UTCs.

#### 2.2.4 Wind Effect

The convective heat losses from the absorber plate to the ambient, also called the wind heat losses, are of great importance in the prediction of the performance of UTCs as it was shown in Equation 2.5. Based on the previous work done by Kutscher et al. (1993) on flat absorber plates (Equation 2.3), Gawlik and Kutscher (2002) studied numerically and experimentally the wind heat losses from UTCs with sinusoidal corrugations of amplitude  $A$  and pitch  $p$  (Figure 2.3). Assuming uniform suction and a crosswind air flow perpendicular to the corrugations, they found that after the starting length, greater than for the case of a flat plate, the thermal and velocity boundary layer thicknesses approached a constant average value over a corrugation. Moreover, the same temperature and velocity profiles were repeated cyclically on each corrugation. It was also observed that similar to the flat plate case, the convective heat losses occurred in the starting length and were carried all the way to the downstream edge of the plate. Under certain combinations of wind speed, suction velocity, and plate geometry, the flow on the plate could be either attached or separated. They obtained a criterion to determine whether the flow was attached or separated and developed a Nusselt number correlation for each case. For attached flow, the wind heat losses were similar to flat plate UTCs. In the case of a separated flow, however, the convective heat losses from plates with sinusoidal corrugations could be as much as 17 times greater than for flat plates.

Fleck et al. (2002) questioned the parallel laminar boundary layer assumption used by Kutscher et al. (1993), Kutscher (1994) and Dymond and Kutscher

(1995). Their doubt came from the fact that in real applications, the wind induces turbulence close to a building. In order to investigate the wind effects on the performance of a transpired collector in real conditions, Fleck et al. (2002) monitored the wind direction, speed and fluctuation intensity on an outdoor UTC installation. They observed that turbulence was occurring near the wall where the UTC was installed and that greater turbulence intensities were decreasing the collector efficiency. Moreover, the collector peak efficiency surprisingly did not occur at zero wind speed, but at 1-2 m/s. Finally, they stated that wind direction was likely to have an influence on the heat transfer occurring at the surface of the plate and on the collector performance.

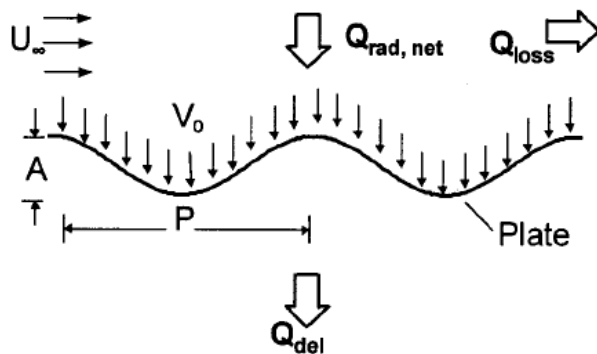


**Figure 2.3:** Diagram of the sinusoidal plate used by Gawlik et al. (2002) in the development of a  $h_{wind}$  correlation for corrugated UTCs

## 2.3 Numerical/Software Approach to UTCs

One of the first simulation tools for predicting the performance of unglazed transpired collectors was called TCFLOW and was developed by Dymond and Kutscher (1997) who modeled the flow distribution in the collector using a pipe network analogy. They assumed a parallel boundary layer flow along a smooth wall that accounted for all four pressure drops occurring in the collector: the pressure drop through the absorber plate, the friction inside the plenum, the buoyancy pressure drop and the air acceleration pressure drop. The correlations of Kutscher (1994)

were applied to model the heat exchange effectiveness. To calculate the convective heat losses from the plate to the ambient, they used Equation 2.3, but modified it slightly to account for plate corrugations, obtaining the following relation.

$$h_{conv,col-amb} = C_f \left[ 0.82 * \frac{V_{wind} \nu \rho C_p}{L V_s} \right] \quad (2.12)$$

In Equation 2.12,  $C_f$  represents the corrugation factor, an empirical coefficient corresponding to the ratio of the wind heat losses on a corrugated plate to that of a flat plate. This analysis was not as accurate as a CFD model but was meant to be used to quickly obtain predictions on the performance of UTCs.

Gunnawiek (1994) developed a 3D CFD model, later simplified to a 2D model, to predict the flow distribution in the plenum of a transpired collector under zero-wind condition (Gunnawiek et al., 1996). Their model was meant to be more accurate than the pipe network method used by Dymond and Kutscher (1997). The absorber plate was modeled under continuous suction and the convective heat losses to the ambient were neglected. They observed that in the asymptotic region, significant heat transfer could occur at the back of the plate under non-uniform flow. It was also found that at low suction velocities, reverse flow could occur in the plenum. This phenomenon was more likely to happen at the top of UTCs of large area where the buoyancy pressure could cause the air to leave through the perforations and escape from the plenum. Under no wind conditions, the CFD model showed that the suction velocity had to be at least 0.0125 m/s to avoid reverse flow. When this analysis was extended to windy conditions (Gunnawiek et al., 2002), the minimum suction velocity was estimated to be 0.017 m/s for long buildings with the collector facing the wind and 0.039 m/s for cubical buildings with the wind blowing at 45° on the UTC.

Following these two models, two programs were developed by Enermodal Engineering for Natural Resources Canada (NRCan) to facilitate the design of UTCs: SWift99 (SWift99, 2001) and RETScreen (RETScreen International, 2005). Both models predict the energy savings, the life cycle savings and the reduced amount of GHG resulting from the installation of a UTC, but use quite different approaches. RETScreen is based on empirical correlations and performs a monthly analysis

while SWift99 uses equations derived from basic thermodynamics principles and performs hourly simulation. Consequently, SWift99 is considered as being more accurate. Carpenter and Meloche (2002) performed simulations for different locations and types of buildings and concluded that both SWift99 and RETScreen predicted similar results. Gogakis (2005) also compared the two pieces of software and found that they were in acceptable agreement, obtaining a difference in annual energy savings prediction of 10%. Moreover, he identified that RETScreen had a better approach in the calculation of the irradiation when converting the solar irradiance from an horizontal plane to the plane of the collector.

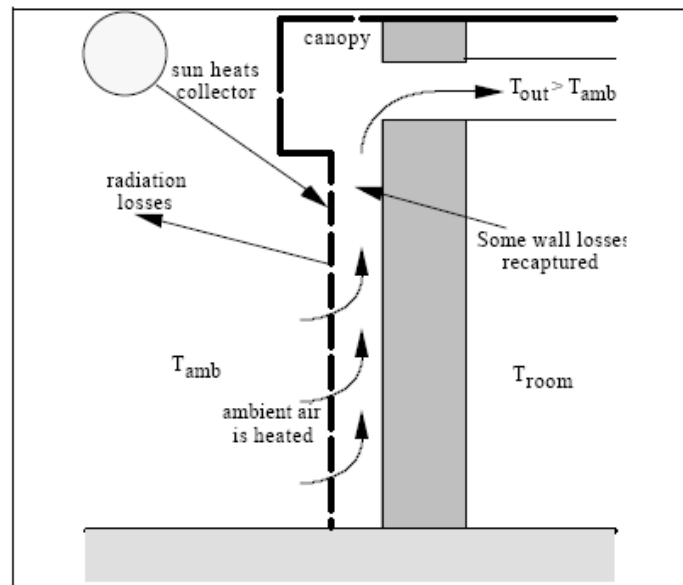


**Figure 2.4:** UTC configuration used in Summers' model (Summers, 1995)

In addition to these programs, a TRNSYS (SEL, 2005) model was developed by Summers (1995). This model solves a set of energy balances to predict the performance of the collector (Figure 2.4). It also minimizes the amount of auxiliary energy needed by optimizing the amount of air going through the collector. The model uses Kutscher's relation (Equation 2.6) to calculate the Nusselt number, but does not account for any wind effects or for the corrugated shape of the absorber plate.

Summers validated the model by comparing his simulations with results obtained from testing at the National Solar Testing Facility (NSTF) (Hollick, 1994) and with data from an operating GM battery production facility (Enermodal, 1994). The TRNSYS model was found to overpredict the air temperature rise at low suction velocity compared to the indoor results obtained at the NSTF. This deviation was attributed to the fact that the wind was not taken into account. When comparing the results to the data from the GM facility, Summers noticed that the model was under predicting the recaptured wall heat losses.

Maurer (2004) looked at the performance of UTCs in warm climates. The main goal was to verify if the collector would induce unwanted heat in the building during summer months, when the collector is bypassed. To do so, the data coming from the monitoring of an existing manufacturing facility in North Carolina where a UTC was installed were analyzed. Maurer also made some modifications to the TRNSYS model of Summers to account, for example, for the plate wind heat losses. By performing simulations for different cities, the model was found to be in reasonable agreement with Summers model, with the greatest difference in the predictions of the energy savings of 10.4%. In order to study the performance of the collector during bypass conditions, Maurer developed a Fortran code and found that the transpired collector could increase the cooling load in the summer when the collector is bypassed due to the increase of the building wall temperature. More information on the flow in the plenum was needed, however, in order to formulate a conclusion.

Leon and Kumar (2007) developed a model to predict the performance of UTCs where high temperatures are needed such as in solar crop drying applications. Like Summers, their model consisted of solving a set of energy balance equations and considered both the absorber plate and the surface at the back of the plate to be isothermal. The absorber plate was assumed to be perforated with circular holes on a triangular pitch. Contrary to Summers, the collector studied was not mounted on a wall as shown in Figure 2.5. Therefore, the model included convective and radiative heat transfer from the surface at the back of the collector to the ambient. They assumed minimum pressure drop and suction velocity of 25 Pa and 0.02 m/s and neglected the convective heat losses from the absorber plate to the ambient as

well as the effect of plate corrugation. Kutscher's relation was used to calculate the absorber plate effectiveness. A sensitivity analysis on their model, made them conclude that solar absorptivity, hole pitch and air flowrate had the strongest effect on the collector heat exchange effectiveness and efficiency.

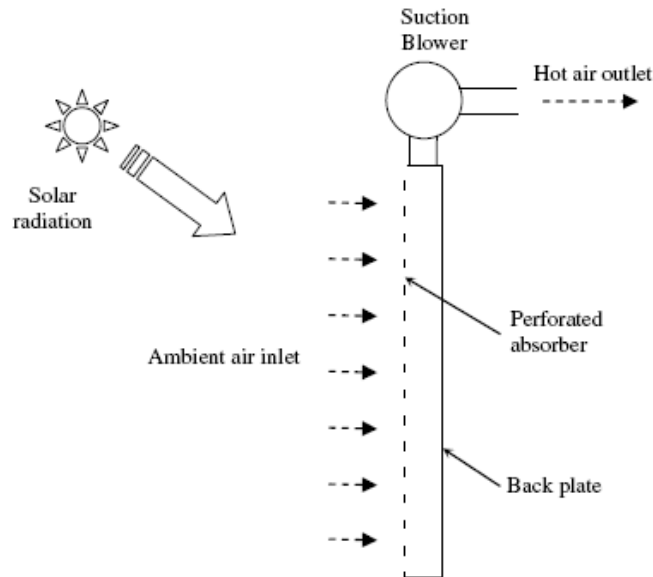


**Figure 2.5:** UTC configuration used in the model of Leon and Kumar (2007)

## 2.4 PV/Thermal UTCs

As was previously mentioned, research on PV/Thermal transpired collectors started in the late 1990's with Hollick (1998), the inventor of SolarWall<sup>®</sup>. He combined the transpired collector and photovoltaic technologies by partially covering the top of the corrugations of a SolarWall<sup>®</sup> with encapsulated crystalline silicon PV cells. The area covered by PV cells was approximately 24% of the 1.1664 m<sup>2</sup> transpired collector area. The hybrid collector was tested under a solar simulator at the NSTF. In order to assess the effect of UTCs on PV cells, the temperature of the stand-alone PV module was predicted using a model developed by CANMET Energy Technology Centre. The experiment showed that the temperature of the

cells was lower for the PV/SolarWall than the PV only, by 2-4°C for an irradiation of 600 W/m<sup>2</sup> and by 3-7°C for an irradiation of 900 W/m<sup>2</sup>. It was also found that even if the thermal efficiency of the panel was slightly decreased with the addition of PV cells, the total efficiency (electrical + thermal) was greater than for the stand-alone UTC.

Naveed et al. (2006) studied the effect of mounting a PV module on the front of a UTC absorber plate. In order to achieve their objective, they performed outdoor experiments on a stand-alone PV module and on a PV module mounted on the front of a transpired collector (Figure 2.6). The plate had an area of 6.5 m<sup>2</sup> and the PV module consisted of a 75 W polycrystalline silicon PV module. The UTC behind the module was found to decrease the temperature of the PV by 3-9°C with a 5% recovery in the electrical power output.

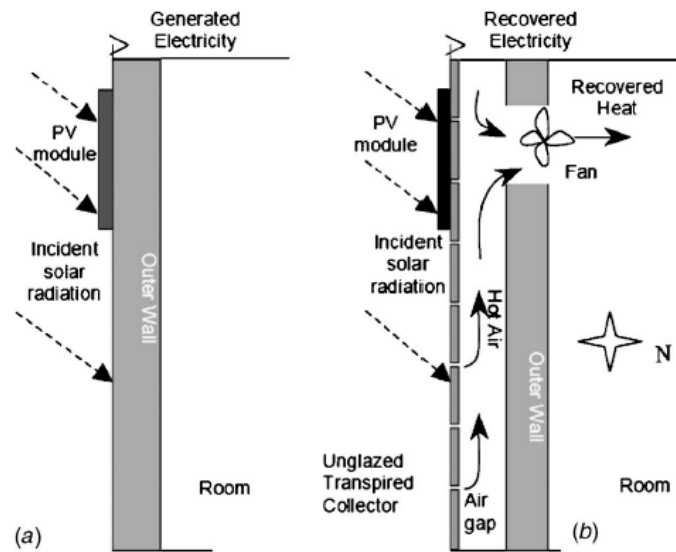


**Figure 2.6:** Schematic diagrams of the experimental setup used by Naveed et al. (2006)  
 (a) Stand-alone PV module (b) Combined PV/Thermal collector

Katic (2007) performed outdoor experiments on four different systems simultaneously: a PV/Thermal collector with a high flowrate, a PV/Thermal collector with a low flowrate, a stand-alone SolarWall<sup>®</sup>, and a PV module with a back fully

open. The PV/Thermal collector consisted of a PV module, the same than the stand-alone PV module, mounted on the front of a SolarWall<sup>®</sup> panel. The four systems were installed at 45°, facing south. He found that the PV cells temperature was lower on the stand-alone PV module than on the combined PV/Thermal collector, even at the highest air suction rate tested. Thus, Katic concluded that natural ventilation had a greater cooling effect on the PV cells than the transpired collector.

## Chapter 3

# PV/Thermal Transpired Collector Model

### 3.1 Introduction

This chapter presents the development of an analytical model for a PV/Thermal transpired solar collector, where the PV cells are mounted directly on some unperforated portions of the absorber plate. To predict the thermal and electrical performance of the PV/Thermal collector, a set of energy balances were performed. These equations were similar to the ones used in the unglazed transpired collector TRNSYS component developed by Summers (1995), but changes were made to account for the wind, the corrugated shape of the plate, and the fact that PVs are on the absorber plate. The energy equations developed were formulated as a TRNSYS component.

## 3.2 Collector Configuration

### 3.2.1 Panel Geometry

The absorber plate of the collector considered in this model consists of a perforated panel with trapezoidal corrugations and small slot perforations (Figure 3.1).

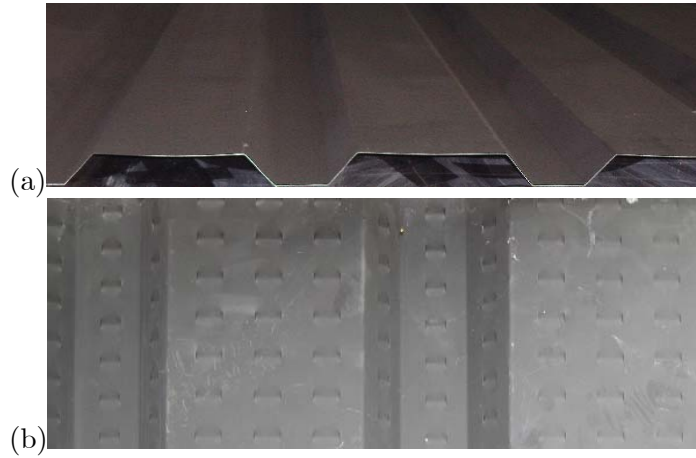


**Figure 3.1:** Close-up of the absorber plate used in the PV/Thermal UTC model (a) trapezoidal corrugations (b) small slot perforations

One of the parameters that defines the collector absorber plate is the plate porosity, which consists of the ratio of the total area covered by the perforations,  $A_h$ , to that of the total absorber plate,  $A_T$ .

$$\sigma = \frac{A_h}{A_T} \quad (3.1)$$

Van Decker et al. (2001) defined the porosity of a plate with circular holes on a square pitch as

$$\sigma = \frac{\pi D^2}{4 p^2} \quad (3.2)$$

For the geometry studied in this case, the perforations are laid out on a square pitch, but consist of slots, not holes. Considering the porosity and the pitch to be

known parameters, Equation 3.2 is used to calculate an equivalent diameter  $D$  for the slots. The rest of the absorber geometry can be fully defined with the following geometric parameters (Figure 3.2): the height of the trapezoidal corrugation ( $h_T$ ), the distance between two corrugations ( $d$ ), the plate width ( $W$ ), the plate length ( $L$ ), the plate thickness ( $t$ ), the length of the base of the trapezoid ( $a$ ) and the length of the top of the trapezoid ( $b$ ).

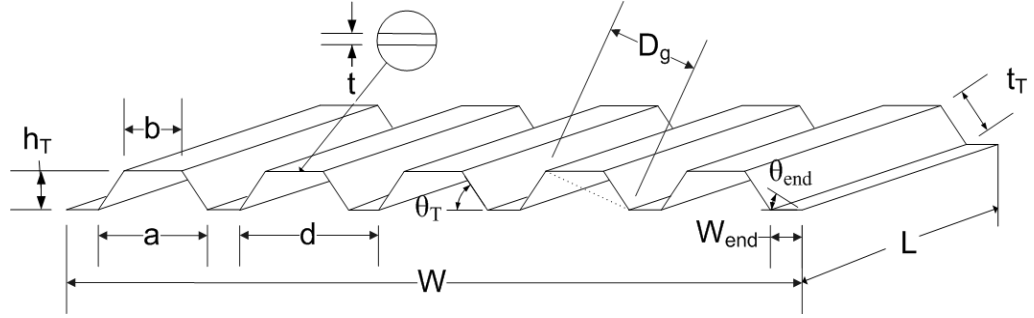


**Figure 3.2:** PV/Thermal UTC geometric variables

Once these dimensions are specified, the other variables shown in Figure 3.2 can be calculated.

$$t_T = \sqrt{h_T^2 + \left(\frac{a-b}{2}\right)^2} \quad (3.3)$$

$$\sin \theta_T = \frac{h_T}{t_T} \quad (3.4)$$

$$D_g = \sqrt{h_T^2 + \left(d + \left(\frac{a-b}{2}\right)\right)^2} \quad (3.5)$$

$$W_{end} = \frac{W - a + d(1 - N_{bc})}{2} \quad (3.6)$$

$$\tan \theta_{end} = \frac{h_T}{W_{end} + \frac{a-b}{2}} \quad (3.7)$$

In Equations 3.3 to 3.7,  $t_T$  is the length of the side of the trapezoid corrugation,  $\theta_T$  is the acute angle inside the trapezoid,  $D_g$  is the length of the diagonal in the trapezoid,  $W_{end}$  is the width of the end surfaces of the absorber plate and  $\theta_{end}$  is the angle between the end surface of the plate and the top surface of the corrugation.

### 3.2.2 PV/Thermal Collector Configurations

As mentioned in Section 2.4, the different prototypes of hybrid PV/Thermal transpired collectors that have been investigated up to now have all consisted of PV cells or PV modules mounted at a certain distance of the plate, with a small gap left between the solar cells and the absorber plate. Contrary to these previous prototypes, this analysis presents a design of a PV/Thermal UTC where the PV cells are mounted directly on the absorber plate. Figure 3.3 presents the two different configurations studied. In configuration (a), only the top of the corrugations can be covered with PV cells while in configuration (b), PV cells can be deposited on every surface of the absorber, except for the surfaces located at the panel edges.

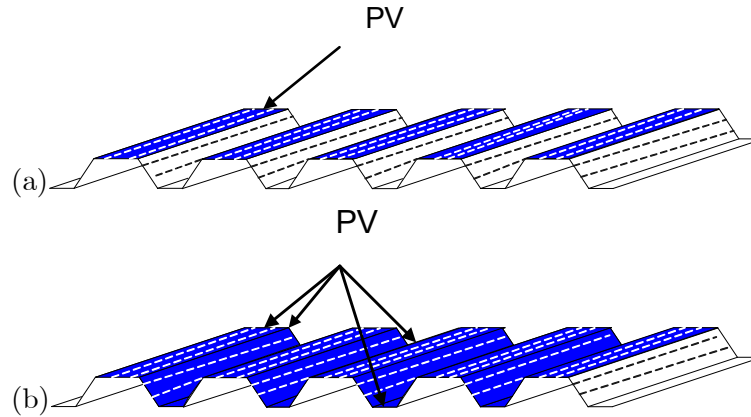


**Figure 3.3:** Configurations considered in the PV/Thermal collector model (a) PV cells mounted only on the top of the corrugations (b) PV cells mounted on every surface of the absorber plate

## 3.3 Model Theory

### 3.3.1 Assumptions

The following assumptions were made to keep the model simple and to minimize the computation time.

- The temperature of the plate is assumed to be uniform. This is a common assumption for UTCs that are used in SWift99, RETScreen and in Summers' model. In reality, there is a temperature gradient around the perforations where the convective heat transfer is greater, but Gawlik et al. (2005) showed that it does not have a great effect on the collector performance.
- The temperatures at the front and at the back of the absorber are assumed to be equal because the plate is very thin and highly conductive.
- The calculations performed at every time step are assumed to have reached steady-state. This is a valid assumption because in his experiment, Gogakis (2005) found that the response time of a UTC to a change in solar radiation was approximately 1 minute.
- The PV cells are assumed to operate at the maximum power point.
- The corrugations are parallel to the surface on which the collector is mounted, lengthwise.
- The suction and porosity are assumed to be uniform at the surface of the absorber plate, and the perforations are considered to be circular on a square pitch.
- The wall or roof on which the collector is mounted is assumed to be isothermal.
- The outside air is considered to be flowing perpendicular to the corrugations.
- The air properties used in the model are all calculated at ambient temperature.

### 3.3.2 Heat Transfer Theory

In order to predict the performance of the PV/Thermal collector, a set of ten energy balances are performed on the collector. These equations are similar to the ones used by Summers (1995), but changes were made to account for the wind, the corrugated shape of the plate and the presence of PV cells. Figure 3.4 presents the different terms associated with the heat transfer occurring in the transpired collector. In this figure, the collector is assumed to be mounted on a vertical wall, but could also be installed on an inclined roof. Therefore, the term “wall” used in this chapter refers to the surface at the back of the absorber plate that could be either a wall or a roof.

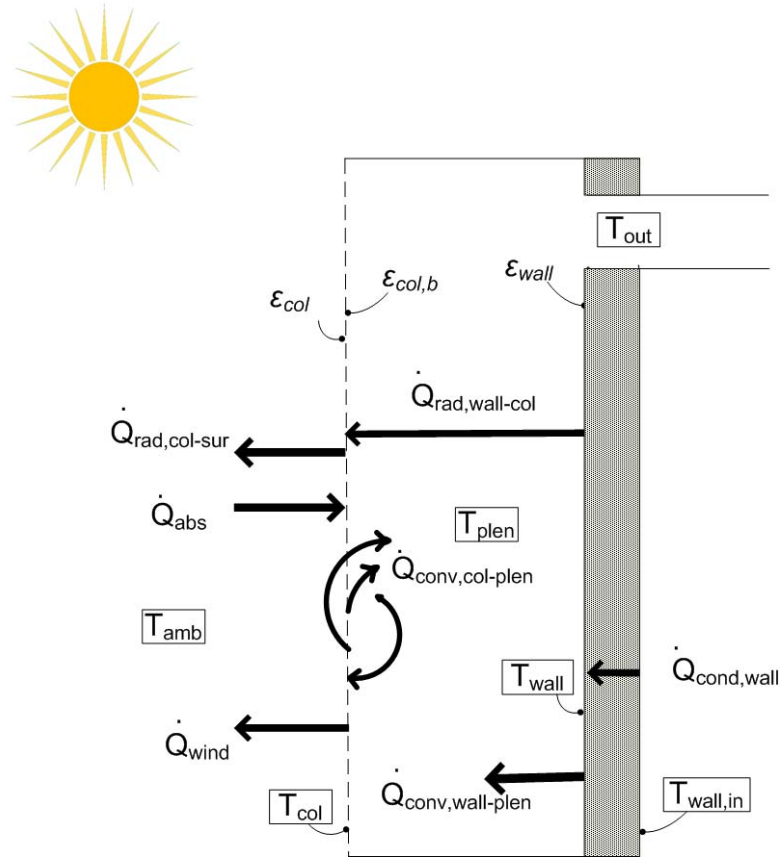


**Figure 3.4:** Heat transfer exchanges in the PV/Thermal collector

The first equation is the one developed by Kutscher et al. (1993) for an isothermal UTC that expresses the collector as a heat exchanger of effectiveness  $\varepsilon_{HX}$ .

$$\varepsilon_{HX} = \frac{T_{plen} - T_{amb}}{T_{col} - T_{amb}} \quad (3.8)$$

In Summers' model, the value of  $\varepsilon_{HX}$  in Equation 3.8 is calculated with Kutscher's (1994) correlation. In this model, it was decided to use Van Decker's correlation (Equations 2.7 to 2.11), since it applies for a greater number of panels.

The next equations are obtained by performing energy balances on the absorber plate, on the wall located at the back of the plate, and in the holes, respectively.

$$\dot{Q}_{abs} + \dot{Q}_{rad,wall-col} = \dot{Q}_{conv,col-plen} + \dot{Q}_{rad,col-sur} + \dot{Q}_{wind} \quad (3.9)$$

$$\dot{Q}_{cond,wall} = \dot{Q}_{conv,wall-plen} + \dot{Q}_{rad,wall-col} \quad (3.10)$$

$$\dot{Q}_{conv,col-plen} = \dot{m}c_p(T_{plen} - T_{amb}) \quad (3.11)$$

In Equations 3.9 to 3.11,  $\dot{Q}_{abs}$  is the total absorbed solar radiation,  $\dot{Q}_{rad,wall-col}$  is the radiation heat transfer between the wall and the back of the absorber plate,  $\dot{Q}_{conv,col-plen}$  is the convective heat transfer from the absorber plate (front, side and back) to the plenum,  $\dot{Q}_{wind}$  is the wind heat loss (or the heat transfer from the collector to the ambient),  $\dot{Q}_{rad,col-sur}$  is the radiation heat transfer from the plate to the surroundings,  $\dot{Q}_{conv,wall-plen}$  is the convective heat transfer from the wall to the plenum,  $\dot{Q}_{cond,wall}$  is the conductive heat transfer through the building wall and  $\dot{m}$  is the air mass flowrate going through the plate perforations.  $\dot{Q}_{rad,wall-col}$  can be expressed as

$$\dot{Q}_{rad,wall-col} = h_{rad,wall-col}A_{col,proj}(T_{wall} - T_{col}) \quad (3.12)$$

where  $h_{rad,wall-col}$  is the radiative heat transfer coefficient between the wall and the back surface of the absorber plate,  $T_{wall}$  is the wall temperature and  $T_{col}$  is the plate surface temperature.  $A_{col,proj}$  is the absorber plate projected area defined as

$$A_{col,proj} = WL \quad (3.13)$$

Assuming the view factor between the wall and the back of the plate to be one, i.e.

neglecting the sides of the plenum,  $h_{rad,wall-col}$  can be defined as

$$h_{rad,wall-col} = \frac{\sigma_{sb}(T_{wall}^2 - T_{col}^2)(T_{wall} + T_{col})}{\frac{1}{\varepsilon_{wall}} + \frac{1}{\varepsilon_{col,b}} - 1} \quad (3.14)$$

where  $\varepsilon_{wall}$  and  $\varepsilon_{col,b}$  are the emissivities of the outdoor wall surface and the back of the absorber plate, respectively.

The plate surface is considered to be at a uniform temperature. Therefore, the radiation losses from the collector to the surroundings,  $\dot{Q}_{rad,col-sur}$ , is given as

$$\dot{Q}_{rad,col-sur} = \sigma_{sb}\varepsilon_{col} (T_{col}^4 - T_{sur}^4) A_{col,proj}(1 - \sigma) \quad (3.15)$$

where  $T_{sur}$  is the surroundings temperature. Radiation losses from the collector surface occur both to the ground and to the sky. Thus,  $T_{sur}$  corresponds to

$$T_{sur}^4 = F_{col-sky}T_{sky}^4 + F_{col-gnd}T_{gnd}^4 \quad (3.16)$$

where  $T_{gnd}$  is assumed to be equal to the ambient temperature in this model. The view factors  $F_{col-sky}$  and  $F_{col-gnd}$  are expressed as a function of the collector slope,  $\beta_{col}$

$$F_{col-sky} = \frac{1 + \cos \beta_{col}}{2} \quad (3.17)$$

$$F_{col-gnd} = \frac{1 - \cos \beta_{col}}{2} \quad (3.18)$$

The perforated panel can be partially covered with PV cells. Therefore,  $\varepsilon_{col}$  is calculated as a weighted average of the emissivities of the panel (absorber plate),  $\varepsilon_{panel}$ , and of the PV cells,  $\varepsilon_{PV}$ .

$$\varepsilon_{col} = (1 - P_{PV})\varepsilon_{panel} + P_{PV}\varepsilon_{PV} \quad (3.19)$$

In Equation 3.19,  $P_{PV}$  is the ratio of the projected area covered with PV cells,

$A_{PV,proj}$ , to that of the total collector projected area.

$$P_{PV} = \frac{A_{PV,proj}}{A_{col,proj}} \quad (3.20)$$

The convective heat losses from the wall to the plenum,  $\dot{Q}_{conv,wall-plen}$  is expressed as

$$\dot{Q}_{conv,wall-plen} = h_{conv,wall-plen} A_{col,proj} (T_{wall} - T_{plen}) \quad (3.21)$$

where  $h_{conv,wall-plen}$  is the convective heat transfer coefficient between the outdoor wall and the plenum. It is calculated with the average Nusselt number in the plenum obtained with the following relations from Incropera and DeWitt (2002)

$$\overline{Nu}_L = 0.664 Re_L^{1/2} Pr^{1/3} \quad Re_L \leq 5 \times 10^5 \quad (3.22)$$

$$\overline{Nu}_L = \left(0.037 Re_L^{4/5} - 871\right) Pr^{1/3} \quad 5 \times 10^5 < Re_L \leq 10^8 \quad (3.23)$$

where Pr is the Prandtl number. Equation 3.22 is used for laminar flow and Equation 3.23, for mixed boundary layer conditions. The Reynolds number of the air in the plenum,  $Re_L$ , is calculated at the average velocity in the plenum,  $V_{plen,avg}$ , and corresponds to

$$Re_L = \frac{V_{plen,avg} L}{\nu} \quad (3.24)$$

Considering the mass flowrate of air to be zero at the bottom of the plenum and to reach its maximum at the top, the average velocity in the plenum corresponds to half of the maximum velocity.

$$V_{plen,avg} = \frac{1}{2} V_{plen,max} = \frac{1}{2} \frac{\dot{m}}{\rho A_{cs,plen}} \quad (3.25)$$

In Equation 3.25,  $A_{cs,plen}$  is the plenum cross-sectional area corresponding to

$$A_{cs,plen} = W h_T + N_{bC} h_T \left( \frac{a+b}{2} \right) \quad (3.26)$$

where  $N_{bC}$  is the number of corrugations on the panel. During the summer months, or at nighttime, UTCs are usually bypassed to let fresh air enter the building.

Nonetheless, it is still interesting to know the temperature of the absorber plate in the summer during bypass conditions, since the PV cells will continue producing electricity. Maurer (2004) tried to find an approximation for  $h_{conv,wall-plen}$  for two different bypass conditions. In the first scenario, the air enters the plenum at the bottom of the collector due to the plate getting heated, rises as it flows along the wall driven by natural convection, and exits at the top of the plenum. In the second scenario, Maurer assumed that there was no flow induced in the plenum and that only natural convection was taking place. For the first case, a convective heat transfer coefficient of 0.1 W/m<sup>2</sup>·K was obtained, and for the second case, the simulations predicted a value between 0.1 and 1 W/m<sup>2</sup>·K. As an approximation, the value of  $h_{conv,wall-plen}$  was set to 0.1 W/m<sup>2</sup>·K during bypass conditions.

The conduction through the wall on which the collector is mounted,  $\dot{Q}_{cond,wall}$ , is given as

$$\dot{Q}_{cond,wall} = \left( \frac{1}{U_{wall}} - \frac{1}{h_{wall}} \right)^{-1} A_{col,proj} (T_{b1g} - T_{wall}) \quad (3.27)$$

where  $T_{b1g}$  is the temperature inside the building,  $U_{wall}$  is the rate of heat transfer through the wall per unit area, also known as U-value, and  $h_{wall}$  is the heat transfer coefficient by long-wave radiation and convection at the outdoor surface of the building wall (film coefficient) assumed to be equal to 15 W/m<sup>2</sup>·°C (Enermodal, 1994). The reason why  $h_{wall}$  is subtracted from the value of  $U_{wall}$  is because the U-value usually incorporates both the radiative and convective heat transfer coefficient of the indoor and outdoor surfaces of the building wall. In this case, the energy balance is performed between the indoor space of the building and the wall outdoor surface. Thus, only the indoor heat transfer coefficient and the resistance through the wall have to be considered in the calculation of  $\dot{Q}_{cond,wall}$ .

In the model of Leon et al. (2007) and Summers (1995), the collector was assumed to be of large area with a suction velocity greater than 0.02 m/s and a pressure drop of at least 25 Pa. Therefore, according to Kutscher (1994), they could neglect the convective heat losses due to the wind. In this case, however, the model was going to be compared to experimental results performed on a collector of small surface area. Therefore, neglecting the convective heat losses was not advisable.

The convective heat losses from the absorber plate to the wind,  $\dot{Q}_{wind}$ , can be expressed as

$$\dot{Q}_{wind} = h_{wind}A_{col,proj} (T_{col} - T_{amb}) \quad (3.28)$$

where  $h_{wind}$  is the convective heat transfer coefficient from the plate to the ambient. There are several correlations available in the literature to calculate the wind heat transfer coefficient of UTCs, but none of them seem to apply directly to plates with trapezoidal corrugations. Maurer (2004) used Kutscher's (1994) relation modified for panels with a corrugated shape (Equation 2.12) and set the value of the corrugation factor  $C_f$  to 5. This was based on the IEA report (Brunger, 1999) that stated that for a plate with quasi-sinusoidal shape with a mass flowrate of  $0.03 \text{ kg/m}^2\cdot\text{s}$ , a cross wind speed of  $2 \text{ m/s}$  and a net radiation of  $750 \text{ W/m}^2$ , the heat losses were of  $83 \text{ W/m width of collector}$  compared to  $17 \text{ W/m width of collector}$  for a flat perforated plate. The ratio of these two heat losses is approximately 4.9, which can explain why Maurer chose a value of 5 for  $C_f$ . These results, however, came from experiments performed on panels with quasi-sinusoidal shape, not with trapezoidal corrugations. In this model, it was decided to use the wind heat transfer correlation of the SWift99 software (Carpenter et al., 1999) given as

$$h_{wind} = \min [h_{wind,UTC}, h_{conv,glazed}] \quad (3.29)$$

where  $h_{wind,UTC}$  is the wind heat transfer coefficient for transpired plates and  $h_{conv,glazed}$  is the convective heat transfer on a glazed solar collector.

$$h_{wind,UTC} = 0.02 \frac{V_{wind}}{V_s} \quad (3.30)$$

$$h_{wind,glazed} = 2.8 + 3.0V_{wind} \quad (3.31)$$

Equation 3.30 was developed based on experiments performed on lab-scale flat plate transpired collector by the Solar Thermal Research Laboratory at the University of Waterloo (STRL), later modified using the work of Kutscher et al. (1993) to represent better full-scale SolarWall<sup>®</sup> panels (Enermodal, 1994). The original wind

heat transfer coefficient correlation developed by the STRL was expressed as

$$h_{wind} = 6.0 + 4.0 * V_{wind} - 76 * V_s \quad (3.32)$$

Equations 3.8 to 3.12, 3.15, 3.21, 3.27 and 3.28 consist of 9 of the 10 equations that need to be solved in order to find the unknown temperatures and heat flows shown in Figure 3.4. The only equation missing is for the absorbed solar radiation,  $\dot{Q}_{abs}$ .

### 3.3.3 Absorbed Radiation on the Collector

#### 3.3.3.1 Total Radiation on a Surface $i$

In the models of UTCs described in the literature, including the one of Summers, the calculation of the total absorbed solar radiation  $\dot{Q}_{abs}$  is straight forward and is given as

$$\dot{Q}_{abs} = \alpha_{col} A_{col,proj} G_{T,col} \quad (3.33)$$

Equation 3.33 does not account for the fact that the collector can shade itself or for the multiple reflections that can occur on the surfaces located in the grooves. For thermal collectors, the shading and reflecting can be neglected since they are not expected to play significant roles in the prediction of the collector performance. In this analysis, however, they must be taken into account because PV cells can be located in the grooves. If shading occurs on the cells, the electrical performance of the collector will be significantly affected. Also, if the grooves are very deep, the multiple reflections could lead to a considerable increase in the irradiation of certain surfaces. To account for these two phenomena, the total irradiation falling on the collector was calculated considering each surface of the absorber plate separately. Assuming the corrugations to be identical along the collector width, the absorber plate can be divided in 8 different types of surfaces  $i$  (Figure 3.5) where the total

area of each type of surfaces correspond to

$$\begin{aligned}
 A_1 &= (d - a)L \cdot (N_{bC} - 1) \\
 A_2 &= A_4 = t_T L \cdot (N_{bC} - 1) \\
 A_3 &= bL \cdot N_{bC} \\
 A_5 &= A_7 = W_{end}L \\
 A_6 &= A_8 = t_T L
 \end{aligned}$$

Generally, the total radiation falling on a surface corresponds to the summation of the beam, sky diffuse and ground reflected components of the solar radiation. In this analysis, however, when one of the components of the incident radiation hits a surface in a groove, it is reflected on the other surfaces as diffuse radiation. Therefore, the diffuse radiation component for these surfaces is not only due to sky diffuse ( $G_{dd,i}$ ) and ground reflected radiation ( $G_{dg,i}$ ), but also to the beam radiation reflected diffusely ( $G_{db,i}$ ). The general expression for the total radiation falling on a surface  $i$ ,  $G_{T,i}$ , can consequently be written as

$$G_{T,i} = G_{b,i} + G_{dd,i} + G_{dg,i} + G_{db,i} \quad (3.34)$$

In Equation 3.34, the component of beam radiation,  $G_{b,i}$ , is calculated in a straight forward manner knowing the inclination of the collector and the sun's position, while the three components of diffuse radiation are obtained by performing a solar optical analysis.

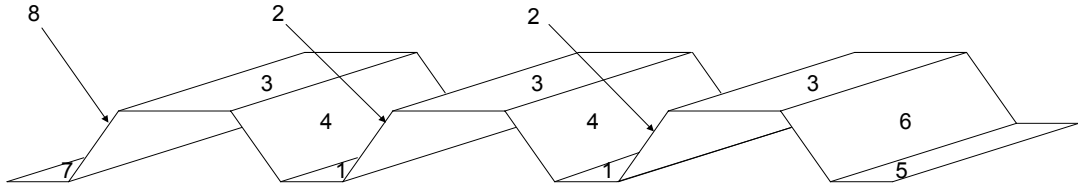


**Figure 3.5:** Absorber plate divided in 8 different types of surfaces

### 3.3.3.2 Diffuse Radiation on a Surface $i$

The general expression for the radiation falling on a surface  $i$ ,  $G_i$ , located in an enclosure of  $N$  surfaces, is given as

$$G_i = \sum_{j=1}^N F_{i-j} J_j \quad (3.35)$$

where  $F_{i-j}$  is the view factor between a surface  $i$  and a surface  $j$  and  $J_j$  is the radiosity of the  $j^{th}$  surface. In order to calculate  $G_{dd,i}$  and  $G_{dg,i}$  for the surfaces located in the grooves (surfaces 1, 2 and 4) and at the edges of the plate (surfaces 5, 6, 7 and 8), three fictitious surfaces are added at the top of the groove (surface 9) and on the sides of the plate (surfaces 11 and 10) to simulate the area from which the diffuse radiation is coming (Figure 3.6).

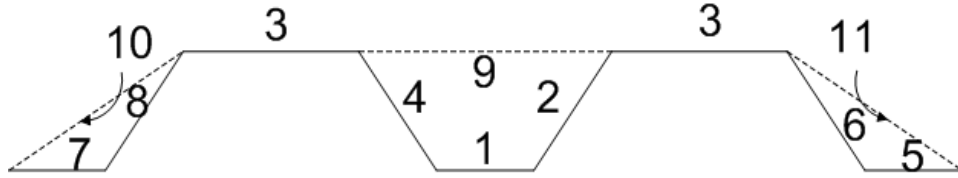


**Figure 3.6:** Absorber plate with the addition of 3 fictitious surfaces for the calculation of the diffuse radiation due to sky diffuse and ground reflected radiation

For each surface  $i$ , the radiosities  $J_{dd,i}$  and  $J_{dg,i}$  are expressed as the product of the reflectance at the incidence angle of the diffuse radiation on the collector,  $\rho_{dcol,i}$ , and the incoming diffuse radiation.

$$J_{dd,i} = G_{dd,i} \rho_{dcol,i} \quad (3.36)$$

$$J_{dg,i} = G_{dg,i} \rho_{dcol,i} \quad (3.37)$$

Surfaces 9 to 11 are fictitious surfaces considered to be the source of the sky diffuse and ground reflected radiation. Therefore, the reflectance of these surfaces is 1 and

their radiosity corresponds to the diffuse radiation (sky or ground).

$$J_{d(d-g),9} = G_{(d-g),9} \quad (3.38)$$

$$J_{d(d-g),10} = G_{(d-g),10} \quad (3.39)$$

$$J_{d(d-g),11} = G_{(d-g),11} \quad (3.40)$$

In the case of surface 3, there is no diffuse radiation coming from other surfaces.

$$J_{d(d-g),3} = G_{(d-g),3} \rho_{(d-g)col,3} \quad (3.41)$$

In Equations 3.38 to 3.41,  $G_{d,i}$  and  $G_{g,i}$  are the sky diffuse and ground reflected components of the total radiation falling on the surface  $i$ . These terms are obtained using the isotropic model of Liu and Jordan (1963) for diffuse radiation.

$$G_{d,i} = G_{d,H} \left( \frac{1 + \cos \beta_i}{2} \right) \quad (3.42)$$

$$G_{g,i} = \frac{(1 - \cos \beta_i) \rho_{gnd} G_H}{2} \quad (3.43)$$

In Equations 3.42 and 3.43,  $\rho_{gnd}$  is the ground reflectance,  $\beta_i$  is the slope of the surface  $i$  and  $G_H$  and  $G_{d,H}$  represent the total and diffuse component of the horizontal radiation.

In the case of the radiosity for the beam radiation reflected diffusely,  $J_{ab,i}$ , the surfaces in the grooves can be shaded and not receive direct beam radiation. Depending on the geometry of the plate, the shaded proportion of the surfaces in the grooves will be more or less significant on the thermal energy absorbed, but it will certainly affect the electrical output of the collector. Consequently, each surface that can be shaded is split into two surfaces; one that does not receive beam radiation due to shading (surfaces 9 to 16) and one that does (surfaces 1 to 8), as shown in Figure 3.7. Surface 1 is split into three surfaces because it can be shaded from each side.

In this case, the diffuse radiation due to beam radiation,  $J_{db,i}$ , can be expressed as the summation of both reflected beam radiation and beam radiation reflected diffusely.

$$J_{db,i} = \rho_{b,i}G_{b,i} + \rho_{dcol,i}G_{db,i} \quad (3.44)$$

In Equation 3.44,  $\rho_{b,i}$  is the reflectance of a surface  $i$  at the incidence angle of the beam radiation on that particular surface.

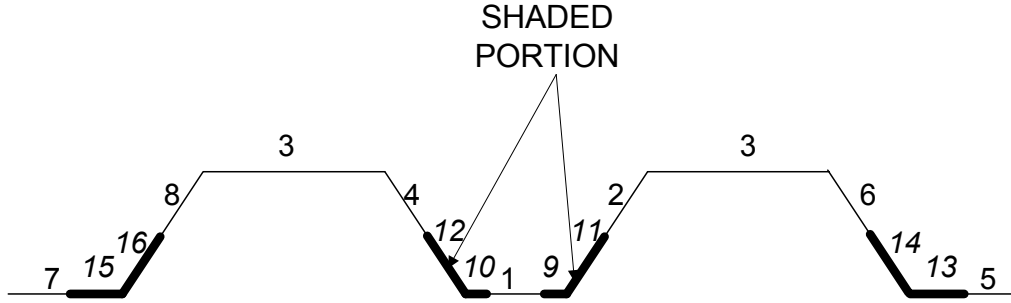


**Figure 3.7:** Absorber plate with the numbering of the shaded surfaces necessary for the calculation of the diffuse radiation due to beam radiation

Combining Equation 3.35 with Equations 3.36, 3.37 and 3.44, the following relations can be obtained for each surface  $i$

$$J_{dd,i} - \rho_{dcol,i} \sum_{j=1}^{11} F_{d,i-j} J_{dd,j} = 0 \quad (3.45)$$

$$J_{dg,i} - \rho_{dcol,i} \sum_{j=1}^{11} F_{d,i-j} J_{dg,j} = 0 \quad (3.46)$$

$$J_{db,i} - \rho_{dcol,i} \sum_{j=1}^{16} F_{b,i-j} J_{db,j} = \rho_{b,i}G_{b,i} \quad (3.47)$$

where the view factors  $F_{d,i-j}$  and  $F_{b,i-j}$  are calculated according to the method described in Appendix A. By writing Equations 3.45 to 3.47 for each surface in a matrix form, the values of the radiosities can be obtained.  $G_{dd,i}$ ,  $G_{dg,i}$  and  $G_{db,i}$  can then be calculated using Equations 3.36, 3.37 and 3.44.

### 3.3.3.3 Beam Radiation on a Surface $i$

The last unknown term in Equation 3.34 is the beam radiation component on a surface  $i$ ,  $G_{b,i}$ . It can be expressed as a function of the horizontal beam radiation  $G_{bH}$ , which is an input to the model.

$$G_{b,i} = R_{b,i}G_{b,H} \quad (3.48)$$

$R_{b,i}$  is a geometric factor defined by Duffie and Beckman (1991) as

$$R_{b,i} = \frac{\cos \theta_i}{\cos \theta_z} \quad (3.49)$$

where  $\theta_z$  is the solar zenith angle. The sun incidence angle on a surface  $i$ ,  $\theta_i$  is given by Duffie and Beckman (1991) as

$$\cos \theta_i = \cos \theta_z \cos \beta_i + \sin \theta_z \sin \beta_i \cos (\gamma_s - \gamma_i) \quad (3.50)$$

where  $\gamma_s$  is the solar azimuth angle and  $\beta_i$  and  $\gamma_i$  are the slope and azimuth angle of the surface, respectively. From Figure 3.5, it can be observed that surfaces 1, 3, 5 and 7 are in the same plane as the wall on which the collector is mounted. Therefore, the azimuth angle of these surfaces correspond to the collector azimuth angle,  $\gamma_{col}$ .

$$\gamma_1 = \gamma_3 = \gamma_5 = \gamma_7 = \gamma_9 = \gamma_{col}$$

In order to find an expression for the azimuth angle of the other surfaces, a particular approach is followed. Figure 3.8 shows the orientation of surface 4 with respect to surface 3 which is in the plane of the collector.

The orientation of surface 4 in the xyz plane can be expressed with 3 unit vectors  $\vec{U}_{1,4}$ ,  $\vec{U}_{2,4}$ , and  $\vec{U}_{3,4}$ , where  $\vec{U}_{3,4}$  is the vector normal to surface 4. From Figure

3.8, the three unit vectors can be expressed as

$$\vec{U}_{1,4} = -\cos \gamma_{col} \cos \theta_T \vec{i} + \sin \gamma_{col} \cos \theta_T \vec{j} - \sin \theta_T \vec{k} \quad (3.51)$$

$$\vec{U}_{2,4} = -\cos \beta_{col} \sin \gamma_{col} \vec{i} - \cos \beta_{col} \cos \gamma_{col} \vec{j} + \sin \beta_{col} \vec{k} \quad (3.52)$$

$$\vec{U}_{3,4} = \vec{U}_{1,4} \times \vec{U}_{2,4} \quad (3.53)$$

$$\begin{aligned} \vec{U}_{3,4} = & (\sin \beta_{col} \sin \gamma_{col} \cos \theta_T - \cos \beta_{col} \cos \gamma_{col} \sin \theta_T) \vec{i} + \\ & (\cos \gamma_{col} \cos \theta_T \sin \beta_{col} + \cos \beta_{col} \sin \gamma_{col} \sin \theta_T) \vec{j} + \\ & (\cos \theta_T \cos \beta_{col}) \vec{k} \end{aligned}$$

By projecting  $\vec{U}_{3,4}$  on the  $xy$  plane, the vector  $\vec{\gamma}_4$  is obtained.

$$\begin{aligned} \vec{\gamma}_4 = & (\sin \beta_{col} \sin \gamma_{col} \cos \theta_T - \cos \beta_{col} \cos \gamma_{col} \sin \theta_T) \vec{i} + \\ & (\cos \gamma_{col} \cos \theta_T \sin \beta_{col} + \cos \beta_{col} \sin \gamma_{col} \sin \theta_T) \vec{j} \end{aligned} \quad (3.54)$$

The angle  $\xi$  between the vectors  $\vec{\gamma}_{col}$  and  $\vec{\gamma}_4$  (Figure 3.8) corresponds to

$$\xi = \cos^{-1}(\sin \beta_{col} \cos \theta_T) \quad (3.55)$$

The azimuth angle of surface 4,  $\gamma_4$ , is the angle between the vector  $\vec{\gamma}_4$  and due south. Using  $\gamma_{col}$  as a reference,  $\gamma_4$  can be expressed as

$$\gamma_4 = \gamma_{col} - \xi = \gamma_{col} - [\cos^{-1}(\sin \beta_{col} \cos \theta_T)]$$

Repeating the same procedure for the other surfaces, the following expression for the surface azimuth angle of every surface is obtained.

$$\begin{aligned} \gamma_2 &= \gamma_8 = \gamma_{col} + \cos^{-1}(\sin \beta_{col} \cos \theta_T) \\ \gamma_4 &= \gamma_6 = \gamma_{col} - \cos^{-1}(\sin \beta_{col} \cos \theta_T) \\ \gamma_{10} &= \gamma_{col} + \cos^{-1}(\sin \beta_{col} \cos \theta_{end}) \\ \gamma_{11} &= \gamma_{col} - \cos^{-1}(\sin \beta_{col} \cos \theta_{end}) \end{aligned}$$

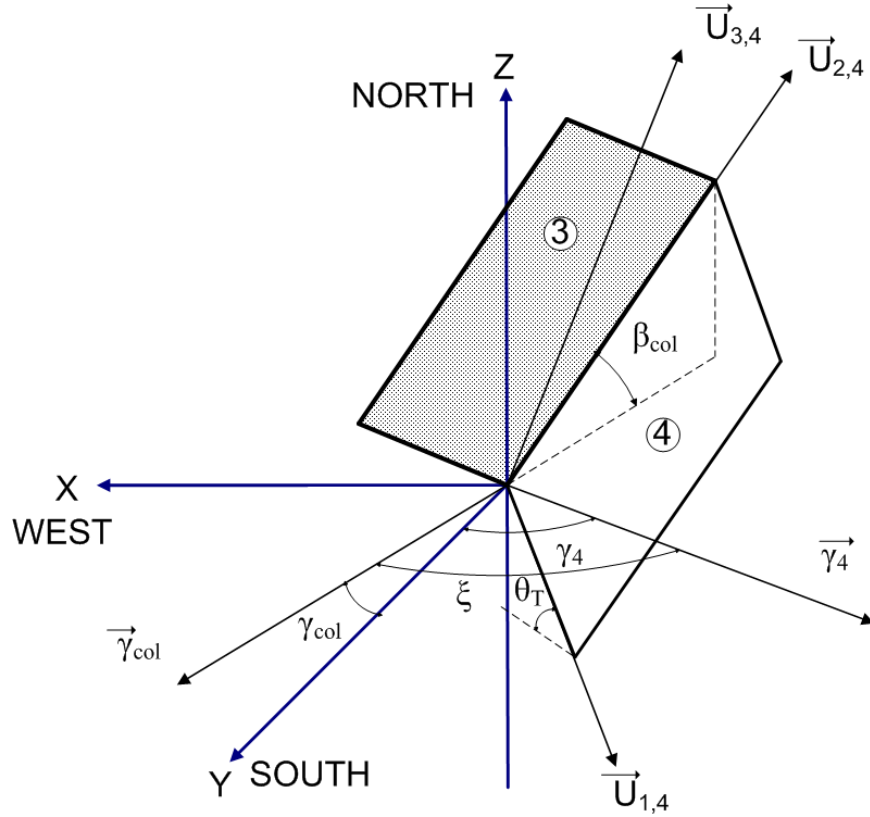


**Figure 3.8:** Orientation of surface 4 of the PV/Thermal UTC with respect to surface 3

Considering  $\gamma_s$  and  $\theta_z$  to be inputs to the model, the only unknown left in Equation 3.50 is  $\beta_i$ , the angle between the plane of the surface  $i$  and the horizontal. For the surfaces in the same plane of the wall on which the collector is mounted, this angle corresponds to the slope of that surface.

$$\beta_1 = \beta_3 = \beta_5 = \beta_7 = \beta_9 = \beta_{col}$$

For the surfaces in a different plane,  $\beta_i$  has to be calculated. Taking the slope of a surface  $i$  as the angle between the normal of a surface  $i$  and a horizontal plane, the scalar product of the normal to the surface 4,  $\vec{U}_{3,4}$ , and the normal to the

horizontal plane,  $\vec{N}$ , can be written as

$$\vec{U}_{3,4} \cdot \vec{N} = \|\vec{U}_{3,4}\| \|\vec{N}\| \cos \beta_4 \quad (3.56)$$

where

$$\vec{N} = \vec{k} \quad (3.57)$$

Substituting Equations 3.53 and 3.57 in Equation 3.56, the slope of surface 4,  $\beta_4$  can be expressed as

$$\beta_4 = \cos^{-1}(\cos \theta_T \cos \beta_{col}) = \beta_2 = \beta_6 = \beta_8$$

Repeating the same procedure for the surfaces 10 and 11, the following is obtained.

$$\beta_{10} = \beta_{11} = \cos^{-1}(\cos \theta_{end} \cos \beta_{col})$$

With all the  $\beta_i$ 's and  $\gamma_i$ 's known, Equations 3.48 to 3.50 can be solved for every surface.

### 3.3.3.4 Collector Optical Properties

The solar optical properties of a surface are dependent of the angle of incidence of the ray hitting that surface. The incidence angle of the beam radiation on a surface  $i$ ,  $\theta_i$ , is calculated with Equation 3.50 while the effective incidence angle of the sky diffuse,  $\theta_{d,i}$ , and ground reflected radiation,  $\theta_{g,i}$ , are obtained with the following relations from Brandemuehl and Beckman (1980).

$$\theta_d = 59.68 - (0.1388\beta + 0.001497\beta^2) \quad (3.58)$$

$$\theta_g = 90 - (0.5788\beta + 0.002693\beta^2) \quad (3.59)$$

From Section 3.3.2, the reflectance of the different surfaces at the beam, sky diffuse and ground reflected angles are necessary to solve for the total radiation falling on each surface. In the case of the collector studied, some surfaces of the

panel can be partially covered with PV cells. Therefore, the general expression for the reflectance of a surface  $i$  at an angle of incidence  $\theta$  is given as

$$\rho_{i(\theta)} = P_{PV,i}\rho_{PV,i(\theta)} + (1 - P_{PV,i})\rho_{Panel,i(\theta)} \quad (3.60)$$

where  $P_{PV,i}$  is the proportion of PV cells on a surface  $i$  and  $\rho_{PV,i(\theta)}$  and  $\rho_{Panel,i(\theta)}$  are the PV cells and absorber plate (panel) reflectance on that surface  $i$  at an angle  $\theta$ . The relation between the absorptance,  $\alpha$ , transmittance,  $\tau$ , and reflectance,  $\rho$ , of a surface is given by Kirchoff's law as

$$1 = \tau + \alpha + \rho \quad (3.61)$$

In this case, the absorber plate is an unglazed opaque surface. Therefore, the transmittance can be set to zero, the angular dependence of the absorptance can be neglected, and  $\rho_{Panel,i}$  can be simplified to

$$\rho_{Panel,i(\theta)} = \rho_{Panel} = 1 - \alpha_{Panel} \quad (3.62)$$

PV cells are usually covered with a thin layer of glass or plastic bonded to the cell surface. Thus,  $\rho_{PV,i(\theta)}$  in Equation 3.60 is in fact, the reflectance of the cover of the PV cells. De Soto et al. (2005) showed that a simple air-glass model could be used to represent the cover. For such a model, the refraction angle,  $\theta_r$ , is given by Snell's law (Duffie and Beckman, 1991) as a function of the refractive index of the cover  $n$ .

$$\theta_r = \sin^{-1}\left(\frac{\sin \theta}{n}\right) \quad (3.63)$$

With  $\theta_r$ , the ratio of the transmitted radiation over the total incident radiation,  $\tau_a$ , can be expressed as

$$\tau_a = \exp\left(-\frac{Kt_{PV}}{\cos \theta_r}\right) \quad (3.64)$$

where  $K$  is the glazing extinction coefficient and  $t_{PV}$  is the thickness of the PV cover. As presented by De Soto et al. (2005), the transmittance of the glazing by taking into account both the reflective losses at the interface and the absorption in

the glazing is given as

$$\tau(\theta) = \tau_a \left[ 1 - \frac{1}{2} \left( \frac{\sin^2(\theta_r - \theta)}{\sin^2(\theta_r + \theta)} + \frac{\tan^2(\theta_r - \theta)}{\tan^2(\theta_r + \theta)} \right) \right] \quad (3.65)$$

The absorptance of the cover can be calculated with the following approximation of Kirchoff's law obtained by Duffie and Beckman (1991).

$$\alpha(\theta) \simeq 1 - \tau_a \quad (3.66)$$

Using Equations 3.65 and 3.66 in Equation 3.61, the reflectance of the PV cover,  $\rho_{PV,i(\theta)}$ , can be obtained.

In a similar way than Equation 3.60, the absorptance-transmittance product of a surface can be expressed as

$$(\tau\alpha)_{i(\theta)} = P_{PV,i}(\tau\alpha)_{PV,N}IAM_{PV,i(\theta)} + (1 - P_{PV,i})\alpha_{Panel} \quad (3.67)$$

where  $(\tau\alpha)_{PV,N}$  is the tau-alpha product of the PV cells-cover combination at normal incidence and  $IAM_{PV,i(\theta)}$  is the incidence angle modifier of the PV cells located on a surface  $i$  for an incidence angle  $\theta$ . The general expression for this incidence angle modifier is given by De Soto et al. (2005) as

$$IAM = \frac{\tau(\theta)}{\tau(0)} \quad (3.68)$$

### 3.3.3.5 Absorbed Solar Radiation

With the radiation on each surface and the solar optical properties known, the total solar radiation absorbed on each surface  $i$ ,  $\dot{Q}_{abs,i}$ , can be expressed as

$$\dot{Q}_{abs,i} = \dot{Q}_{b,i} + \dot{Q}_{d,i} \quad (3.69)$$

where  $\dot{Q}_{b,i}$  and  $\dot{Q}_{d,i}$  are the beam and diffuse components of the absorbed solar

energy corresponding to

$$\dot{Q}_{b,i} = (\tau\alpha)_{b,i} A_i(1 - \sigma)(1 - P_{sh,i}) G_{b,i} \quad (3.70)$$

$$\begin{aligned} \dot{Q}_{d,i} = (\tau\alpha)_{d,i} A_i(1 - \sigma) * \\ [G_{db,i}(1 - P_{sh,i}) + G_{db,i-sh}(P_{sh,i}) + G_{dd,i} + G_{dg,i}] \end{aligned} \quad (3.71)$$

In Equations 3.70 and 3.71,  $P_{sh,i}$  is the shaded portion of a surface calculated with the method demonstrated in Appendix B and  $G_{db,i-sh}$  is the diffuse radiation due to beam radiation falling on the shaded portion of the surface. The total solar radiation absorbed by the plate can then be expressed as

$$\dot{Q}_{abs} = \sum_{i=1}^8 \dot{Q}_{abs,i} [1 - \eta_{PV} P_{PV,i}] \quad (3.72)$$

where  $\eta_{PV}$  is the PV cells efficiency. For simplicity  $\eta_{PV}$  is assumed to depend linearly on the PV cells temperature,  $T_{PV}$  (Sandnes & Rekstad, 2002).

$$\eta_{PV} = \eta_{ref} + \mu(T_{PV} - T_{ref}) \quad (3.73)$$

The PV cells are considered to be mounted directly on the absorber plate. Thus, they can be assumed to be at the same temperature as the plate and Equation 3.73 can be simplified to

$$\eta_{PV} = \eta_{ref} + \mu(T_{col} - T_{ref}) \quad (3.74)$$

In Equation 3.74,  $\eta_{ref}$  is the PV cells efficiency at the reference temperature  $T_{ref}$ , and  $\mu$  is the temperature coefficient. Thus, Equation 3.72 is a function of the collector temperature and consists of the 10<sup>th</sup> equation in the set of energy balance equations.

### 3.3.4 Solution Method

The 3 unknown temperatures and the 7 unknown heat transfer terms are obtained by solving the 10 equations (3.8 to 3.12, 3.15, 3.21, 3.27, 3.28, and 3.72) with

a matrix solver. The collector outlet temperature  $T_{out}$  can then be calculated by performing an energy balance in the plenum of the collector and the useful thermal energy  $\dot{Q}_u$  can be computed.

$$T_{out} = \frac{\dot{Q}_{conv,wall-plen} + \dot{Q}_{conv,col-plen}}{\dot{m}c_p} + T_{amb} \quad (3.75)$$

$$\dot{Q}_u = \dot{m}c_p(T_{out} - T_{amb}) \quad (3.76)$$

For configuration (a), the PV cells will never be shaded by the collector and the calculation of the electrical power output  $P_{el}$  is as follows.

$$P_{el} = \eta_{PV} P_{PV,3} \dot{Q}_{abs,3} \quad (3.77)$$

In the case of configuration (b), obtaining a value for  $P_{el}$  is more complex because of the shading of the cells. Typically, when a PV module is partially shaded, the shaded cell current drops. In order to compensate, the non-shaded cells move on their operating I-V curve closer to the open-circuit voltage. While trying to increase the current at which they are operating, the voltage of the shaded cells can then be driven in the negative voltage range. This result in the formation of a hot-spot which will reduce the PV output or in worst cases, damage the module. To avoid this, bypass diodes are generally installed. A reduction of the PV performance however, still occurs. The power output in such cases is difficult to predict because it will depend on how the cells are linked together. A 50% shading will not necessarily result in a 50% reduction of the power production. Nevertheless, to simplify the calculations, a conservative approximation similar to the one used by the TRNSYS Type 551 component (TESS, 2005) is employed to estimate the power production. When the collector is partially shaded, the PV cells layout is assumed to see the minimum of the diffuse radiation seen by any of the surfaces  $i$ .

$$P_{el} = \eta_{PV} \cdot \min \left[ \frac{\dot{Q}_{d,1}}{A_1 (\tau\alpha)_{d,1}}, \frac{\dot{Q}_{d,2}}{A_2 (\tau\alpha)_{d,2}}, \frac{\dot{Q}_{d,3}}{A_3 (\tau\alpha)_{d,3}}, \frac{\dot{Q}_{d,4}}{A_4 (\tau\alpha)_{d,4}} \right] \sum_{i=1}^4 [A_i P_{PV,i}] \quad (3.78)$$

When the collector is unshaded, the PV cells are assumed to see the minimum of the total radiation seen by any of the surfaces  $i$ .

$$P_{el} = \eta_{PV} \cdot \min \left[ \frac{1}{A_1} \left( \frac{\dot{Q}_{d,1}}{(\tau\alpha)_{d,1}} + \frac{\dot{Q}_{b,1}}{(\tau\alpha)_{b,1}} \right), \frac{1}{A_2} \left( \frac{\dot{Q}_{d,2}}{(\tau\alpha)_{d,2}} + \frac{\dot{Q}_{b,2}}{(\tau\alpha)_{b,2}} \right), \right. \\ \left. \frac{1}{A_3} \left( \frac{\dot{Q}_{d,3}}{(\tau\alpha)_{d,3}} + \frac{\dot{Q}_{b,3}}{(\tau\alpha)_{b,3}} \right), \frac{1}{A_4} \left( \frac{\dot{Q}_{d,4}}{(\tau\alpha)_{d,4}} + \frac{\dot{Q}_{b,4}}{(\tau\alpha)_{b,4}} \right) \right] \sum_{i=1}^4 [A_i P_{PV,i}] \quad (3.79)$$

This method is however, approximative and could certainly be improved if more information on the cells electrical connections are known. Once both  $P_{el}$  and  $\dot{Q}_u$  are known, the collector thermal ( $\eta_{th}$ ) and electrical efficiencies ( $\eta_{el}$ ) can be obtained.

$$\eta_{th} = \frac{\dot{Q}_u}{A_{col,proj} G_{T,col}} \quad (3.80)$$

$$\eta_{el} = \frac{P_{el}}{A_{col,proj} G_{T,col}} \quad (3.81)$$

The reduced wall heat losses,  $\dot{Q}_{red,wall}$ , corresponding to the reduction of heat losses through the wall due to the presence of the transpired collector can also be calculated.

$$\dot{Q}_{red,wall} = \dot{Q}_{pot} - \dot{Q}_{cond,act} \quad (3.82)$$

In Equation 3.82,  $\dot{Q}_{pot}$  represents the potential heat losses through the wall without the presence of a UTC and  $\dot{Q}_{cond,act}$  is the actual conduction heat losses from the inside of the building to the plenum.

$$\dot{Q}_{cond,act} = A_{wall} (T_{b1g} - T_{plen}) * \left( \frac{1}{U_{wall}} - \frac{1}{h_{wall}} + \frac{1}{h_{rad,wall-col} + h_{conv,wall-plen}} \right)^{-1} \quad (3.83)$$

$$\dot{Q}_{pot} = U_{wall} A_{wall} (T_{b1g} - T_{sol-air}) \quad (3.84)$$

In Equation 3.84,  $T_{sol-air}$  is the sol-air temperature defined in the 2005 ASHRAE Handbook-Fundamentals (ASHRAE, 2005) as the fictitious outside air temperature

for which the convective heat exchange between the surface and the outdoor is the same as the heat exchange occurring by both convection and radiation (long-wave and short-wave). For a vertical surface,  $T_{sol-air}$  is given as

$$T_{sol-air} = T_{amb} + \frac{\alpha_{wall} G_{T,col}}{h_{wall}} \quad (3.85)$$

where  $\alpha_{wall}$  is the wall absorptance.

### 3.3.5 Control Method

UTCs can be controlled in different ways depending on the type of building on which they are installed and the purpose for heating the air. In this model, the collector is controlled in a similar way as Summers' UTC model (1995) where the objective was to minimize the amount of auxiliary heat required. Thus, the electricity produced by the PV cells is considered to be additional. Figure 3.9 presents the schematic of a simple building heating system where a PV/Thermal UTC is installed. In this figure,  $T_{b1g}$ ,  $T_{sup}$  and  $\dot{m}_T$  are inputs to the model and represent the building temperature, the temperature of the air that needs to be supplied to the building and the total mass flowrate entering the building, respectively. The air supplied to the building consists of a mixing of recirculated and fresh air to which auxiliary heat can be added if the mixing temperature,  $T_{mix}$ , is below  $T_{sup}$ . The mixing temperature is calculated by performing an energy balance at the mixing point and is given as

$$T_{mix} = \gamma T_{out} + (1 - \gamma) T_{b1g} \quad (3.86)$$

In Equation 3.86,  $\gamma$  is the mass fraction of fresh air defined as

$$\gamma = \frac{\dot{m}}{\dot{m}_T} \quad (3.87)$$

where  $\dot{m}$  is the fresh air mass flowrate. The value of  $\gamma$  varies between 1 and the

minimum required mass fraction of fresh air,  $\gamma_{\min}$ , corresponding to

$$\gamma_{\min} = \frac{\dot{m}_{\min}}{\dot{m}_T} \quad (3.88)$$

where  $\dot{m}_{\min}$  is an input to the model and corresponds to the minimum amount of fresh air required in the building.

Depending on the time of year and moment of the day, the fresh air entering the building will be either preheated by going through the PV/Thermal UTC or taken directly from outside, bypassing the collector. In this model, contrary to Summers' (1995), the collector is automatically bypassed at night and both the thermal and electrical output are set to zero. In the summer, however, the user has the choice to enable or disable an option that will automatically open the collector bypass damper if the ambient temperature becomes greater than a selected bypass temperature,  $T_{bypass}$ . In such a case, the collector will be solved under bypass conditions, i.e. with a air mass flowrate of zero. If this option is disabled, the mass flowrate of air going through the collector,  $\dot{m}$ , will be set to  $\dot{m}_{\min}$ . In winter time, during the day, if at the minimum flowrate, the mixed temperature is found to be lower than  $T_{sup}$ , then the mass flowrate is set to  $\dot{m}_{\min}$ . If for the lowest and highest value of  $\gamma$ , the mixed temperature is found to be higher than  $T_{sup}$ , then the flowrate in the collector is also set to  $\dot{m}_{\min}$ , unless the summer bypass option was enabled by the user. In any other cases, the mass flowrate,  $\dot{m}$ , that minimizes the auxiliary heat required, i.e. when  $T_{mix} = T_{sup}$ , is determined using the bisection method.

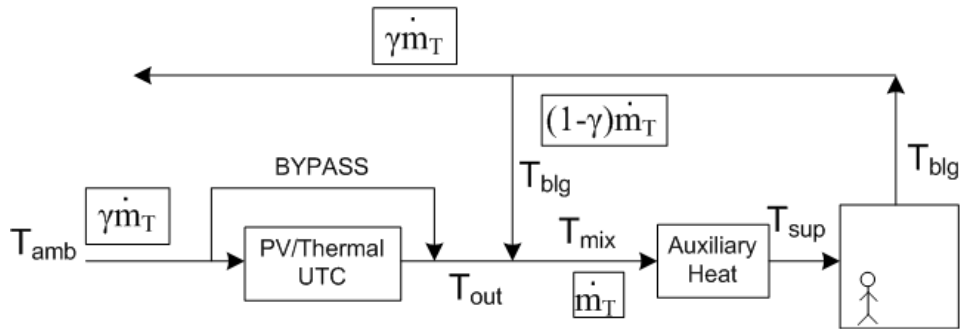


**Figure 3.9:** Diagram of the heating system for a building with a PV/Thermal UTC

## 3.4 TRNSYS Component

The model was developed in Fortran and implemented as a TRNSYS component. The component developed allows the user to choose between three different modes. Mode 1 corresponds to the case where there are no PV cells on the collector, while modes 2 and 3 are for the panel with the PV cells mounted according to configuration (a) and (b), respectively (Figure 3.3). The Fortran code of the model is available in Appendix C.

### 3.4.1 Simulation Parameters and Inputs

In order to compare the thermal and electrical performance of the different configurations, a south-facing PV/Thermal collector with an area of 100 m<sup>2</sup> was simulated in TRNSYS for each one of the three modes available. The simulations were performed hourly with the typical meteorological yearly (TMY2) data sets of solar radiation and meteorological elements for the city of Toronto (SEL, 2005). For modes 2 and 3, the fraction of the surfaces covered with PV cells was set to 75%. The PV efficiency at standard test conditions (STC) (IEC 61215, 2005) of 1000 W/m<sup>2</sup> and 25°C,  $\eta_{ref}$ , was set to 12.58% and the temperature coefficient,  $\mu$ , to -0.00058 1/°C, which are typical values for poly-crystalline cells (De Soto et al., 2005). The minimum air flowrate through the collector and the total flowrate entering the building were fixed to constant values of 8280 and 11 000 kg/h, respectively. Consequently, the amount of energy entering the building was varied by changing the temperature of the air needed to be supplied to the building,  $T_{sup}$ . This temperature was calculated at every time step with the following relation obtained from an energy balance performed on the building shown in Figure 3.10.

$$T_{sup} = \frac{\dot{Q}_{b1g} - \dot{Q}_{red,wall} - \dot{Q}_{int}}{\dot{m}_T c_p} + T_{b1g} \quad (3.89)$$

In Equation 3.89,  $\dot{Q}_{int}$  are the building internal heat gains and  $\dot{Q}_{b1g}$  represent the

heat losses from the building envelope defined as

$$\dot{Q}_{\text{blg}} = (UA)_{\text{blg}} (T_{\text{blg}} - T_{\text{amb}}) \quad (3.90)$$

where  $(UA)_{\text{blg}}$  is the overall building conductance. For the simulations,  $(UA)_{\text{blg}}$  was set to 3000 kJ/h·K and  $\dot{Q}_{\text{int}}$  was fixed to 3000 kJ/h. All the parameters and inputs of the simulations are indicated in Table 3.1.

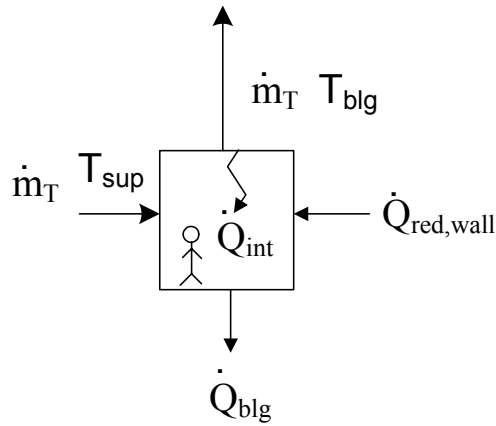


**Figure 3.10:** Heat transfer exchanges in the building with a PV/Thermal collector

With the results from the simulation, the thermal energy savings obtained from the installation of a PV/Thermal collector,  $\dot{Q}_{\text{savings}}$ , were calculated using the method of Maurer (2004). In that procedure, the thermal energy savings correspond to the difference between the auxiliary heat required for a base case building without a solar collector,  $\dot{Q}_{\text{aux,base}}$ , and for a building with a PV/Thermal UTC installed,  $\dot{Q}_{\text{aux,UTC}}$ .

$$\dot{Q}_{\text{savings}} = \dot{Q}_{\text{aux,base}} - \dot{Q}_{\text{aux,UTC}} \quad (3.91)$$

The simplified diagram of the heating system for the base case building is shown in Figure 3.11. In this context,  $\gamma_{\text{min}}$  is the fraction of fresh air that minimizes the auxiliary heat required.

**Table 3.1:** Parameters and Inputs to the TRNSYS simulation

PARAMETERS		
Length of the base of the trapezoid	a [m]	0.15
Length of the top of the trapezoid	b [m]	0.115
Height of the corrugation	$h_T$ [m]	0.033
Plate porosity	$\sigma$	0.0025
Pitch	p [m]	0.01403
Collector length	L [m]	4
Distance between two corrugations	d [m]	0.2
Collector width	W [m]	25
Absorptance of the wall	$\alpha_{wall}$	0.4
Plenum height	$h_{plen}$ [m]	0.2
Emissivity of the collector back surface	$\varepsilon_{col,b}$	0.8
Emissivity of the wall	$\varepsilon_{wall}$	0.9
Absorber plate thickness	t [m]	0.001
Panel absorptance	$\alpha_{Panel}$	0.94
Panel emissivity	$\varepsilon_{Panel}$	0.9
Wall U-Value	$U_{wall}$ [KJ/h·m <sup>2</sup> ·K]	2
1: No PV	PV Mode	Vary
2: PV cells on the top of the corrugations		
3: PV cells on every surface		
PV cells temperature coefficient at maximum power point	$\mu$ [1/°C]	-0.00058
PV cells reference efficiency	$\eta_{ref}$	0.1258
PV cells reference temperature	$T_{ref}$ [°C]	25
PV cells absorptance-transmittance product	$(\tau\alpha)_{PV,N}$	0.8
PV cells emissivity	$\varepsilon_{PV}$	0.6
Bypass collector in the summer? 1:Yes, 0: No	Bypass?	1
Bypass temperature	$T_{bypass}$ [°C]	18
PV cells refraction index	n	1.526
PV cells glazing extinction coefficient	K [1/m]	4
PV cells glazing thickness	$t_{PV}$ [m]	0.002
PV cells proportion at the top of the corrugations	$P_{PV(3)}$	0.75
PV cells proportion at the bottom of the grooves	$P_{PV(1)}$	0.75
PV cells proportion on the sides of the grooves	$P_{PV(2)}, P_{PV(4)}$	0.75
INPUTS		
Beam radiation on the collector	$G_{b,col}$ [kJ/h·m <sup>2</sup> ]	Vary
Diffuse radiation on the collector	$G_{d,col}$ [kJ/h·m <sup>2</sup> ]	Vary
Ground reflected radiation on the collector	$G_{g,col}$ [kJ/h·m <sup>2</sup> ]	Vary
Horizontal beam radiation	$G_{b,H}$ [kJ/h·m <sup>2</sup> ]	Vary
Solar zenith angle	$\theta_z$ [°]	Vary
Solar azimuth angle	$\gamma_s$ [°]	Vary
Wind velocity	$V_{wind}$ [m/s]	Vary
Ambient temperature	$T_{amb}$ [°C]	Vary
Ambient pressure	$P_{amb}$ [Pa]	Vary
Sun incidence angle on the collector	$\theta_{col}$ [°]	Vary
Building temperature	$T_{bldg}$ [°C]	21
Sky temperature	$T_{sky}$ [°C]	Vary
Minimum fresh air mass flowrate	$\dot{m}_{min}$ [kg/h]	8280
Total mass flowrate of air entering the building	$\dot{m}_T$ [kg/h]	11000
Collector slope	$\beta_{col}$ [°]	90
Collector azimuth angle	$\gamma_{col}$ [°]	0
Ground reflectance	$\rho_{gnd}$	0.2
Total horizontal radiation	$G_{T,H}$ [kJ/h·m <sup>2</sup> ]	Vary
Horizontal diffuse radiation	$G_{d,H}$ [kJ/h·m <sup>2</sup> ]	Vary
Temperature of the air supplied to the building	$T_{sup}$ [°C]	Vary

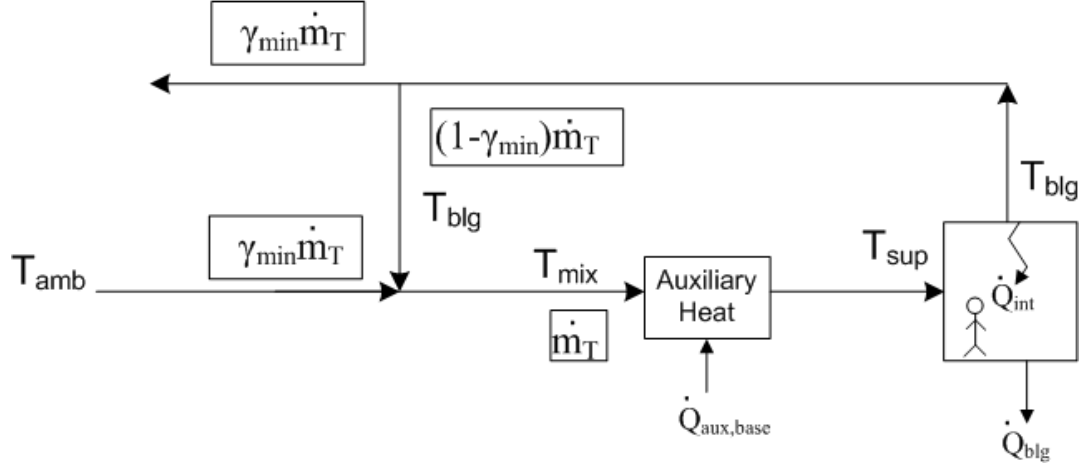


**Figure 3.11:** Diagram of the heating system for the base case building without a solar collector

By performing an energy balance on the auxiliary heat in Figures 3.9 and 3.11,  $\dot{Q}_{aux}$  can be expressed for both cases as

$$\dot{Q}_{aux} = \dot{m}_T c_p (T_{sup} - T_{mix}) \quad (3.92)$$

For the building with a PV/Thermal UTC installed,  $T_{sup}$  is calculated with Equation 3.89 and  $T_{mix}$  is an output to the model. For the base case, both temperatures can be obtained by performing energy balances on the building and at the point where the fresh and recirculated air mix (Figure 3.11).

$$T_{sup} = \frac{\dot{Q}_{blg} - \dot{Q}_{int}}{\dot{m}_T c_p} + T_{blg} \quad (3.93)$$

$$T_{mix} = \gamma_{min} T_{amb} + (1 - \gamma_{min}) T_{blg} \quad (3.94)$$

### 3.4.2 Simulation Results

The thermal energy savings were calculated using Equation 3.91 for the three modes of the PV/Thermal collector component and the yearly electricity produced

was determined. The results are presented in Table 3.2. From this table, it can be observed that the addition of PV cells on the collector surface resulted in a diminution of the thermal energy savings. This decrease was 5.9% in the case of configuration (a) and 8.2% for configuration (b). The reason for this is because the absorptance of the PV cells is not as high as the one of the absorber plate and part of the absorbed solar energy was converted into electricity instead of heat. The amount of electricity produced was estimated to be 45.3 kWh/yr·m<sup>2</sup>*panel* and 34.1 kWh/yr·m<sup>2</sup>*panel* for modes 2 and 3, respectively. Thus, even though the collector surface covered with PV cells was more than double in configuration (b), the electrical output was less compare to configuration (a). This is due to the assumption that the whole collector does not see beam radiation when one of the surfaces is partially shaded. With a better knowledge of the cells electrical connections, a more appropriate estimation of the PV output under partial shading conditions could have been obtained. Nevertheless, it can still be considered that configuration (a) would be more cost-effective since there is a possibility of always obtaining the maximum power from the PV cells.

**Table 3.2:** Thermal energy savings and electricity produced for the 3 modes of the PV/Thermal collector model for the city of Toronto

	<b>Mode 1 No PV</b>	<b>Mode 2 Conf (a)</b>	<b>Mode 3 Conf (b)</b>
Thermal energy savings [kWh/yr·m <sup>2</sup> panel]	353	332.2	324.1
Electricity produced [kWh/yr·m <sup>2</sup> panel]	-	45.3	34.1
% decrease in thermal energy savings compare to the UTC with no PV	-	5.9	8.2

From the testing of a PV/SolarWall, Hollick (1998) evaluated that the electrical energy delivered by a PV/Thermal UTC could represent approximately 10% of the collector thermal energy savings (50-100 kWh/yr·m<sup>2</sup>panel). For modes 2 and 3, the simulations results showed that the amount of electricity produced represented 13.6% and 10.5% of the thermal energy savings, respectively. The conditions under

which Hollick’s estimate was formulated are not specified, but it still shows that the model predictions are reasonable.

In order to verify the effect of the different changes made to Summers’ model on the overall collector performance, a TRNSYS simulation was performed using the original component developed by Summers with equivalent inputs and parameters than the ones indicated in Table 3.1. In his model, Summers neglected the collector wind heat losses. Therefore, the results were compared to the ones obtained with two different cases of the Mode 1 of the PV/Thermal UTC: the wind speed set to zero and  $V_{wind}$  provided by the weather data file. The thermal energy savings achieved and useful thermal energy collected are shown in Table 3.3. According to this table, the useful thermal energy predicted by the Mode 1 of the PV/Thermal UTC with zero wind was only 0.7% lower than that obtained from Summers’ component. When considering the wind, the difference increased to 11.9%. Thus, accounting for this variable is certainly the modification that had the greatest effect on the collector thermal performance. As for the thermal energy savings, the PV/Thermal UTC component predicted 12.4% less energy savings than Summers’ model under zero wind conditions and 21.8% less when accounting for the wind.

**Table 3.3:** Comparison of the thermal energy savings and useful thermal energy collected obtained with Mode 1 of the PV/Thermal UTC model and with Summers’ UTC component

	<b>Mode 1 With Wind</b>	<b>Mode 1 Zero Wind</b>	<b>Summers</b>
Thermal Energy Savings	353	395.2	451.1
[kWh/yr·m <sup>2</sup> panel]			
% Difference with Summers	-21.8	-12.4	-
Useful Thermal Energy collected [kWh/yr·m <sup>2</sup> panel]	346.5	390.6	391.5
% Difference with Summers	-11.9	-0.7	-

The simulation described in Section 3.4.1 was repeated using the hourly weather data of different climates for Mode 2 of the PV/Thermal UTC component. The results presented in Table 3.4 demonstrate that in colder climates than Toronto like

Montreal and Edmonton, more electricity and more thermal energy savings can be expected.

**Table 3.4:** Thermal energy savings and electricity produced for different cities using Mode 2 of the PV/Thermal collector model

	<b>Toronto</b>	<b>Montreal</b>	<b>Edmonton</b>
Thermal Energy Savings [kWh/yr·m <sup>2</sup> panel]	332.2	371.8	491.3
Electricity Produced [kWh/yr·m <sup>2</sup> panel]	45.3	51	60.2

# Chapter 4

## Experimental Setup

### 4.1 Introduction

In order to validate the TRNSYS model, a prototype of a PV/Thermal transpired solar collector was built and tested. The prototype consisted of 40 solar cells mounted on a SolarWall<sup>®</sup> with a corrugated shape profile. The collector was installed on a east wall of the University of Waterloo Building Engineering Group (BEG) Hut and tested outdoors for a period of three weeks, from the end of August 2007 to the beginning of September 2007. The performance of the PV/Thermal collector was studied by recording the collector outlet temperature and the solar cell power output at different air suction rates. The power output from the cells was obtained by tracing the I-V curve at every minute, by varying the load applied to the PV cells with a set of resistors. Instrumentation was put in place to monitor the solar radiation on the wall, temperatures and the air flowrate. The sensor output signals were recorded with a data acquisition system.

## 4.2 PV/Thermal Collector Prototype

### 4.2.1 Selection of the Solar Cells

The prototype was quite different from existing PV/Thermal transpired collectors. For this experiment, the PV cells needed to be directly mounted on the absorber surface, without covering the perforations. Consequently, the use of a pre-built PV module was not an option and the only possibility was to build a layout of solar cells that would fit between the perforations. This posed a challenging problem because the areas where PV cells could be mounted were very narrow rectangles. In fact, for the plates provided for the experiment, the largest width available between two perforations was 18.2 mm (Figure 4.1).

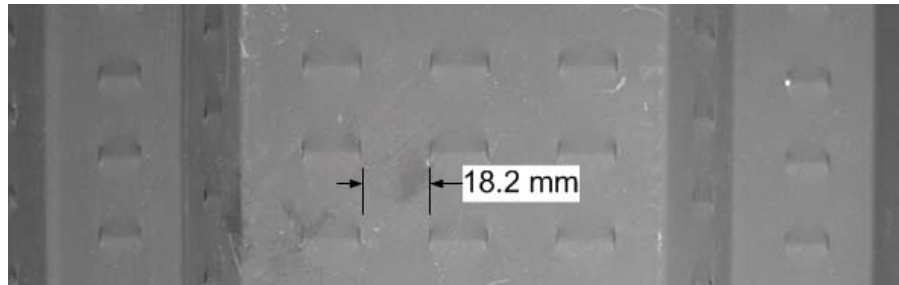


**Figure 4.1:** Close-up of the largest width available between two perforations on the absorber plate

Solar cells are sold in many different shapes, but square or rectangular cells are very rarely available with a width smaller than 100 mm. A company from Czech Republic, Solartec, was able to provide solar cells with a width of 17.1 mm and a length of 102.5 mm as shown in Figure 4.2. These cells were cut by the company from high-efficiency monocrystalline solar cells of type SC2460 that had a nominal size of 102.5 mm by 102.5 mm. The temperature coefficients of these full-size solar cells as well as their electrical parameters at an irradiance of  $1000 \text{ W/m}^2$  and a cell temperature of  $25^\circ\text{C}$  (STC conditions) are presented in Table 4.1.

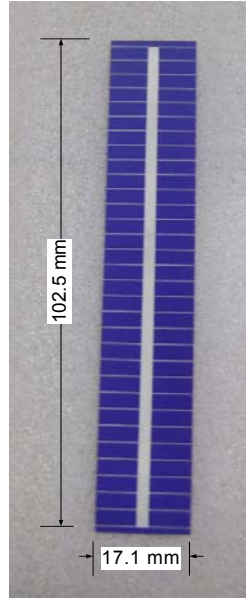


**Figure 4.2:** Solar cell cut from a Solartec photovoltaic cell of type SC2460

**Table 4.1:** Solartec SC2460 photovoltaic cells electrical parameters and temperature coefficients (Solartec, 2007)

Electrical Parameters		Temperature Coefficients	
$I_{sc}$	3.42 A	$\beta_{V_{oc}}$	-0.34 %/°C
$V_{oc}$	0.598 V	$\beta_{V_{mp}}$	-0.45 %/°C
$I_{mp}$	3.13 A	$\alpha_{I_{sc}}$	0.09 %/°C
$V_{mp}$	0.489 V	$\alpha_{I_{mp}}$	0.00 %/°C
$\eta_{sc}$	14.7 %	$\beta_{P_{mp}}$	-0.45 %/°C
$FF$	74.8 %		

## 4.2.2 Perforated Plate

The absorber plates used in the construction of the prototype were provided by Conservall Engineering Inc. and consisted of two galvanized steel SolarWall<sup>®</sup> panels

with 0.25% porosity. Both panels were of profile SW200 with a width of 1.05 m and a length of 1.25 m. The dimensions of the panel are shown in Figure 4.3.

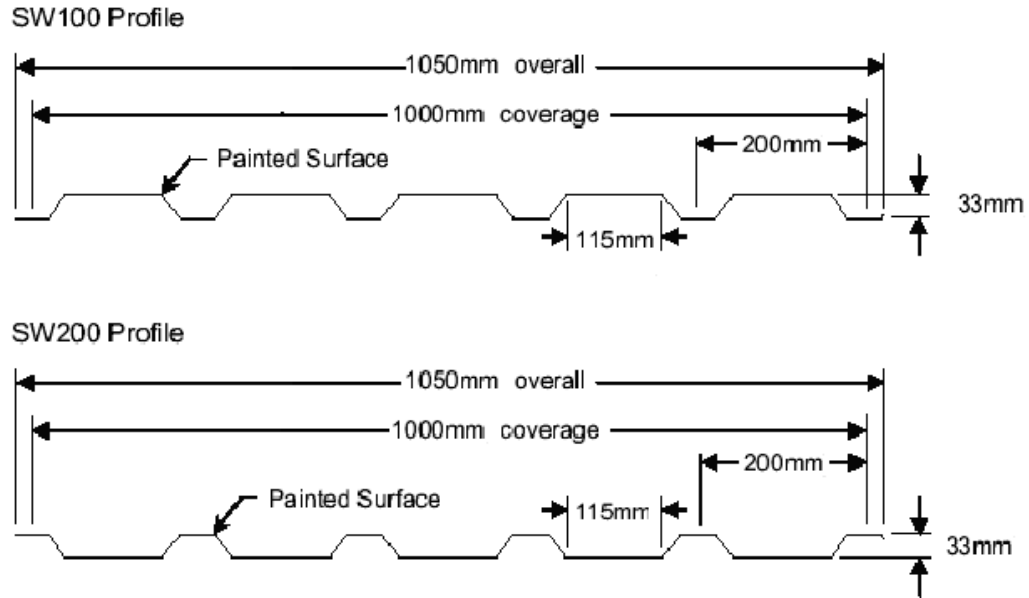


**Figure 4.3:** SW100 and SW200 SolarWall<sup>®</sup> panels dimensions (Conserval Engineering Inc., 2006)

To prevent shading on the PV cells, it was more beneficial to use a SW100 SolarWall<sup>®</sup>. Therefore, the SW200 SolarWall<sup>®</sup> was flipped and painted black. The shortwave solar reflectance of the painted surface of the panel was measured with a CARY 5000 spectrophotometer (Varian, 2005) and found to be 3.96 % (ASTM E903, ASTM E891). Knowing that for an opaque surface, the shortwave solar absorptance is given as

$$\alpha_{Panel} = 1 - \rho_{Panel}$$

The shortwave solar absorptance of the absorber,  $\alpha_{Panel}$ , was calculated to be 0.96. The emissivity of the painted surface of the absorber and the back surface of the absorber were obtained with a SOC 400T spectrometer (Surface Optics, 2001) and both found to be 0.94.

### 4.2.3 PV Cell Layout

The PV cell layout consisted of 10 rows of 4 cells mounted in parallel. Each set of 4 cells was made by soldering together the back and the front terminal of each cell with 2.38 mm wide tinned copper foil from E. Jordan Brookes Co. (E. Jordan Brookes, 2007). A crimp in the copper foil was made between each cell to avoid putting stress on the cells in case of thermal expansion. Ten sets of solar cells were connected in parallel using the same 2.38 mm wide tinned copper foil. Before putting the layout on the perforated plate, fiberglass screen was glued on the absorber at the location where it would be mounted to provide electrical insulation. The PV cells were then glued on the panel with a thin layer of silicone and the whole layout was encapsulated with optically clear silicone cut with Xylene to protect from humidity (Figure 4.4). The positive and negative busbars were wrapped in heat shrink and run along the inside of the panel.

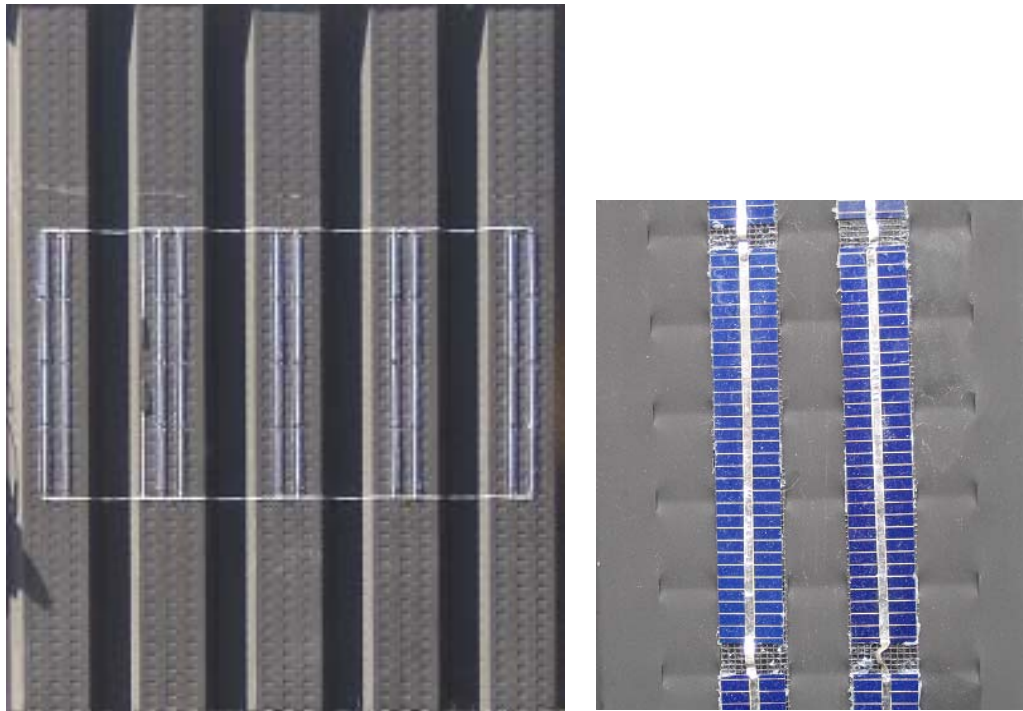


**Figure 4.4:** Picture of the PV/Thermal UTC prototype

In order to get the properties of the PV cells layout, a flash test was conducted at Photowatt in Cambridge, Ontario. A flash test consists of placing a PV module or an individual solar cell under a simulator where a lamp flashes an irradiance of  $1000 \text{ W/m}^2$  for a very short period of time (less than one second). Within this time, the I-V curve of the PV module is traced, and the temperature of the cells is recorded. Once the flash test is done, the program that controls the simulator is able to determine the electrical parameters of the module at standard test conditions (STC) of  $1000 \text{ W/m}^2$  and  $25^\circ\text{C}$ . The results obtained from the flash test of the panel are showed in Table 4.2.

**Table 4.2:** Results of the flash test on the PV/thermal collector prototype

$V_{oc}$ [V]	$I_{sc}$ [A]	$P_{mp}$ [W]	$V_{mp}$ [V]	$I_{mp}$ [A]	$FF$ [%]	$\eta_{ref}$ [%]
2.22	3.804	2.11	1.08	1.943	25.02	3.01

Unfortunately, flash tests do not provide information on the temperature coefficients of a PV module or PV cell. Therefore, a value of the temperature coefficient,  $\mu$ , for the panel was estimated by assuming the PV cells layout to have the same temperature properties as the full-size solar cells. According to Duffie and Beckman (1991),  $\mu$  can be approximated as

$$\mu = \eta_{ref} \frac{\beta_{V_{oc}}}{V_{mp}} \quad (4.1)$$

where  $\beta_{V_{oc}}$  is the temperature coefficient of the open circuit voltage,  $V_{mp}$  is the voltage at maximum power point and  $\eta_{ref}$  is the PV cells efficiency at reference conditions. Using the variables of Tables 4.1 and 4.2 in Equation 4.1, the following value for  $\mu$  was obtained.

$$\mu = 0.0301 * \frac{-0.0034[\frac{1}{^\circ\text{C}}] * 2.22 \text{ V}}{1.08 \text{ V}} = -0.00021 \frac{1}{^\circ\text{C}}$$

## 4.3 Experimental Setup Description

### 4.3.1 Wall and Plenum Construction

The PV/Thermal solar collector was set up on a east wall of the University of Waterloo BEG Hut as shown in Figure 4.5. The RSI-value of the wall was calculated to be  $3.5 \text{ m}^2 \cdot \text{K}/\text{W}$ . A hole of 0.15 m diameter was made at the top of the wall and a ventilation grid was placed in front of the hole. To act as a plenum, a wooden frame with a height of 2.49 m, a width of 1.05 m and a thickness of 0.14 m was built and mounted on the wall as shown in Figure 4.6. For aesthetic reasons and to improve the uniformity of the temperature on the collector, the frame was covered with black painted galvanized steel sheet.

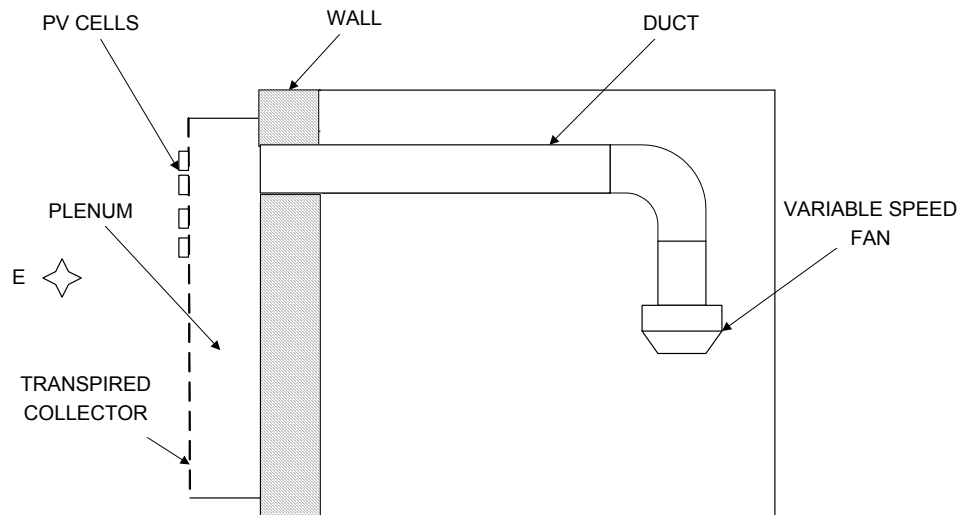


**Figure 4.5:** Diagram of the experimental setup

After the remaining spaces between the wooden box and the wall were sealed with silicone, the two panels were mounted on the plenum box by inserting the side surfaces of the panel under the galvanized steel sheet of the wooden frame (Figure 4.7). To avoid any air leakage, screws were inserted along the side surfaces of the panel and all the joints were sealed with silicone.



**Figure 4.6:** View of the BEG Hut east wall with the plenum box installed



**Figure 4.7:** PV/Thermal transpired solar collector prototype installed on the BEG Hut east facing wall

### 4.3.2 Suction Flow Line

The duct for the suction flow line consisted of an ABS (acrylonitrile butadiene styrene) plastic pipe duct with a nominal diameter of 152.4 mm (6 in). It was necessary to have a rigid material of a certain thickness for the duct, so that the flowmeter and the thermocouple measuring the collector outlet temperature could be inserted with compression fittings. Usually, it is recommended that the fan be installed as close as possible to the collector outlet to minimize the pressure drop the fan needs to overcome. In this case, however, the flowmeter required 10 diameters of straight pipe upstream of the meter and 5 diameters of straight pipe downstream of the meter to ensure fully developed flow. Thus, a total length of straight pipe of 2.3 m was necessary.



**Figure 4.8:** Overall view of the duct and fan installation inside the BEG Hut

The suction through the collector was obtained with a FG6 centrifugal DC fan from FANTECH (Fantech, 2007) used in combination with a variable speed controller. This fan was able to overcome a pressure drop of 281 Pa at 196 m<sup>3</sup>/h. As demonstrated in Appendix D, the total pressure drop through the system was calculated to be only 72 Pa at 196 m<sup>3</sup>/h. It had been noticed, however, in a previous experimental study (Maurer, 2004), that the pressure drop through the collector and in the plenum calculated with the formulae developed by Kutscher (1994) were underestimated. Therefore, it was decided to oversize the fan to ensure that the desired flowrate would be obtained. The duct and fan installation inside the hut are shown in Figure 4.8.

## 4.4 Instrumentation and Measurements

### 4.4.1 Data Acquisition System

The data acquisition system (DAQ) consisted of an OMEGA Personal Daq/56 (Omega Engineering, 2003) connected by USB port to a personal notebook. This DAQ had a high-resolution of 22 bit A/D converter and was cold-junction calibrated for the direct measurement of thermocouples. It had 10 differential ended (20 single-ended) analog inputs that could be set to record either voltages or thermocouples, 16 digital inputs/outputs and 3 frequency/pulse inputs. The configuration of the data logger channels and the record setup were done through the Personal Daq View software. Seven channels of the data acquisition system were dedicated to the measurement of the thermocouples output while two channels were used to record the DC voltage outputs of the pyranometer and the flowmeter. The measurement duration of each channel was set to 310 ms, the scan rate to 3750 ms and the averaging to 16, so that the DAQ would output average recorded values at intervals of 1 minute. With this speed of measurement, the resolution could be kept at 22 bits RMS. The accuracy of the Personal Daq/56 for voltage analog inputs was 0.01 % of the reading + 0.002 % of the selected range.

#### 4.4.2 Temperature Measurements

The temperature measurements were performed using OMEGA 30-gauge type T thermocouple wire having an accuracy of  $1^{\circ}\text{C}$ . The temperature at the collector outlet was measured by inserting a 3.17 mm diameter stainless steel tube in the duct containing a thermocouple wire. The tube was bent at  $90^{\circ}$  to minimize the effect of conduction and to avoid disturbing the flow. The tube was installed 32.5 cm from the outdoor wall surface, because it was the closest location from the duct entrance where the probe could still be reached after its installation. The tip of the tube was covered with plastic for radiation shielding. In order to investigate the temperature profile of the air in the duct, the temperature was measured at different heights in the duct when the fan was on. The largest temperature variation was found to be  $0.1^{\circ}\text{C}$ . Consequently, it was decided to measure the collector outlet temperature at the center of the duct.

The outdoor temperature was also monitored with a shielded thermocouple inserted in a stainless steel tube. This thermocouple was placed on the east wall of the building where the collector was installed.

The outdoor wall temperature was measured with four thermocouples of identical length located as shown in Figure 4.9 (a). Because of the limited number of channels of the data acquisition system, the four thermocouples were mounted in parallel through the use of a terminal block, so that the average temperature would be measured. The absorber plate was also instrumented with four thermocouples (Figure 4.9 (b)), but each temperature was recorded separately to investigate the uniformity of the plate temperature. The thermocouples were placed on the back surface of the plate, because the temperature of the front and back surfaces of the panel were expected to be similar since the plate was very thin and made of a material with high thermal conductivity. For every thermocouple mounted on a flat surface, a piece of electrical tape was used between the surface and the thermocouple, and aluminium tape was applied on the thermocouple bead to shield from any radiation. The temperature inside the hut was not measured, because it was already being recorded by a BEG Hut data logger.

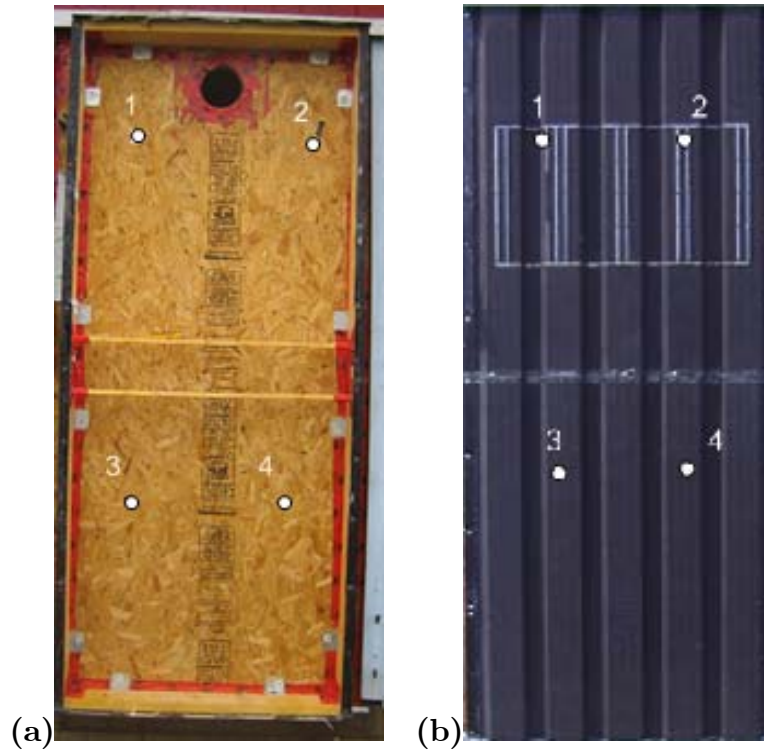


**Figure 4.9:** Location of the thermocouples on (a) the wall (b) the absorber plate

### 4.4.3 Flowrate Measurements

The air flowrate was measured with a 620S Fast-Flow insertion mass flowmeter from Sierra Instruments. This flowmeter works on the principle that the cooling effect of the flowing fluid on the sensing element is proportional to its mass flowrate. The accuracy of this instrument was stated to be  $\pm 1.0\%$  of full scale +  $0.5\%$  of reading, and the repeatability was  $\pm 0.2\%$  of full scale. In order to minimize flow disturbance and ensure accurate and repeatable results, the manufacturer suggested for this type of installation having 10 diameters of straight pipe upstream of the meter and 5 diameters downstream (Sierra Instruments, Inc., 1999). Therefore, the probe was placed at 1.52 m from the duct entrance and at 0.79 m from the elbow. The flowmeter was calibrated by Sierra Instruments for a user full scale of 155 SCFM at an output of 5 VDC. Thus, the voltage output was converted into

the volumetric flowrate at standard conditions using the following relation.

$$\frac{\dot{V}_{std}}{V_{\dot{V}}} = \frac{155 \text{ SCFM}}{5 \text{ V}} \quad (4.2)$$

In Equation 4.2,  $V_{\dot{V}}$  is the voltage signal recorded by the data logger and  $\dot{V}_{std}$  is the volumetric flowrate at standard conditions, in SCFM. The conversion of standard volumetric flowrate to actual volumetric flowrate,  $\dot{V}_{act}$ , is given as

$$\dot{V}_{act} = \dot{V}_{std} * \left[ \frac{P_{std}}{P_{act}} \right] \left[ \frac{T_{act}}{T_{std}} \right] \quad (4.3)$$

where  $P_{std}$  and  $T_{std}$  are the pressure and temperature at standard conditions. They were stated in the flowmeter calibration certificate to be 14.7 psia and 530°R, respectively. The air temperature at the actual conditions,  $T_{act}$ , was taken to be the collector outlet temperature. This is a valid assumption because by calculating the heat transfer through the duct between the thermocouple and the mass flowmeter, the maximum variation in the air temperature was estimated to be 0.2°C. The actual pressure in the duct,  $P_{act}$ , was assumed to be the same as the ambient pressure, because the pressure drop through the collector was considered to be negligible compare to the ambient pressure. Using this information and Equation 4.3, the following expression was obtained to convert the flowmeter voltage into flowrate units.

$$\dot{V}_{act} = \dot{V}_{std} * \left[ \frac{14.7}{P_{amb}} \right] \left[ \frac{T_{out}}{530} \right] * \frac{1.699 \left[ \frac{\text{m}^3}{\text{h}} \right]}{1 \text{ CFM}} \quad (4.4)$$

#### 4.4.4 Irradiance Measurements

The total radiation on the BEG Hut east wall including both beam and diffuse components was measured with a black and white Eppley Pyranometer model 8-48. The calibration certification of this instrument stated that the pyranometer was linear to within  $\pm 1$  % up to the intensity of 1400 W/m<sup>2</sup> with temperature compensation in the range of -20 to 40°C. The cosine response was  $\pm 2$  % from 0-70° incidence angle and  $\pm 5$  % from 70°-80° incidence angle. The voltage response was

linearly proportional with the incident solar radiation and the constant was  $11.80 \mu\text{V}/\text{W}\cdot\text{m}^{-2}$ . The pyranometer was mounted on the east wall of the BEG Hut, beside the solar collector, and at 13 cm from the wall to avoid being shaded by the roof. The pyranometer was used in conjunction with a Universal Single Ended Amplifier (USEA). This amplifier was set to a gain of 200 and had a constant output offset voltage of 2 to 3 mV.

#### 4.4.5 PV Cells Maximum Power

In order to track the power output from the collector, the PV cells layout was connected in series as shown in Figure 4.10, with a shunt resistance,  $R_{sh}$ , of  $0.1 \Omega \pm 5 \%$  and a variable load.

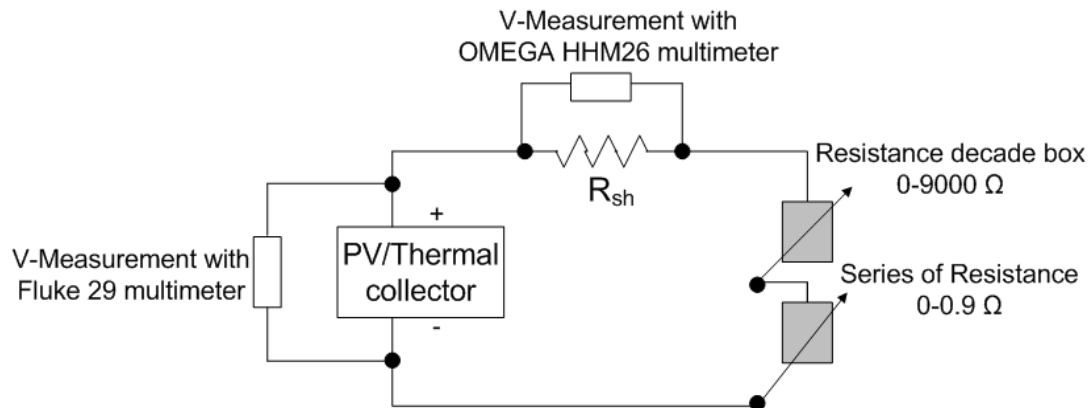


**Figure 4.10:** Schematic diagram of the PV cells layout connection for the maximum power point tracking

The load consisted of a resistance decade box varying from 0 to 9000  $\Omega$  connected in series with a set of 9 resistances of 0.1  $\Omega$ . The voltage across the PV cells,  $V_{PV}$ , was measured using a Fluke 29 multimeter with an accuracy of  $\pm 0.3 \%$ , while the voltage across the shunt resistance,  $V_{R_{sh}}$ , was obtained with a OMEGA HHM26 multimeter having an accuracy of  $\pm 0.25 \%$  of Reading + 1 digit. By measuring the voltages across the PV cells layout and across the shunt resistance, the current,  $I$ ,

and power,  $P_{el}$ , of the solar cells layout were obtained using the following equations from Ohm's law.

$$I = \frac{V_{R_{sh}}}{R_{sh}} \quad (4.5)$$

$$P_{el} = IV_{PV} \quad (4.6)$$

At the beginning of every minute, the load was varied, the voltage outputs from the multimeter were recorded and the power produced was calculated using Equations 4.5 and 4.6. By doing so, the I-V curve of the PV cells layout at the particular temperature and solar irradiance of the moment was plotted and the maximum power point was found. This process usually took less than 20 seconds. For the rest of the minute, the load of the PV cells was maintained so that the panel was operating at the maximum power point. The load at which the solar cells were producing the maximum power output would usually only change at intervals of 4 to 6 minutes and by only 0.1  $\Omega$ . Therefore, a good estimation of the resistance needed to get the maximum power point was always known and the tracking could be done very quickly.

#### 4.4.6 Data Collection

The data collection period was from August 24 to September 8, 2007 between 7:30 AM and 1:00 PM. The data were recorded in the morning since the collector was mounted on a east facing wall and after 1:00 PM, the wall would be shaded. The collector was tested under four different cases: zero flow, fan maximum speed, flowrate of 75 m<sup>3</sup>/h·m<sup>2</sup> and fan minimum speed. All the instruments were connected prior to this period to the data acquisition system and every day the following steps were taken:

1. The pyranometer was mounted on the east wall and connected to the amplifier. The power supplies for the pyranometer and flowmeter were activated.
2. The fan variable speed controller was turned on at the location where the flowmeter would indicate the desired air flowrate for the day.

3. When the measured irradiance and air flowrate reached steady-state, generally less than 5 minutes, the data recording was started.
4. The PV cell load was varied until the maximum power point was found. This step took approximately 20 seconds and was repeated at every minute.
5. When the collector outlet temperature was measured to be no more than 1°C greater than the outdoor temperature, the data collection was stopped. The data logger, the fan and the two power supplies were turned off and the pyranometer was removed.

# Chapter 5

## Experimental Results and Model Validation

### 5.1 Introduction

The first section of this chapter presents the results obtained from the monitoring of the PV/Thermal collector prototype at different air suction rates. Data were collected over a period of three weeks among which six clear sky days were chosen for the data analysis. The reason why only clear sky days were used is because it was not possible to take voltage measurements on cloudy days. The values indicated by the multimeters would fluctuate too much. The second section presents a comparison between the predictions of the TRNSYS model and the results of the experiment on the solar collector.

### 5.2 Experimental Results

#### 5.2.1 Experimental Conditions and Weather Data

The six clear sky days and suction flowrates chosen for data analysis are summarized in Table 5.1. The wind speed and wind direction were measured by a

pre-existing anemometer on the BEG Hut roof. The average values of these variables were recorded hourly by a BEG Hut data logger and are available in Appendix E. Figure 5.1 presents the variation of the wind direction and wind speed for the six days used in the data analysis.

**Table 5.1:** Average air flowrate measured for each clear sky day

Day	Average Air Flowrate [ $\text{m}^3/\text{h}\cdot\text{m}^2$ ]
Aug-29	75
Aug-31	75
Sep-01	82
Sep-02	75
Sep-06	No Flow
Sep-08	55

From Figure 5.1 (a), it can be observed that the wind was generally blowing from west to east ( $270^\circ$  north) during the time period studied, except for September 1<sup>st</sup> where it was blowing from the south-east ( $150^\circ$  north). Therefore, the wind direction was a relatively constant parameter. In Figure 5.1 (b), it can be seen that the wind speed varied for each day. Moreover, it fluctuated in the time interval where the collector was monitored. The wind speed was only roughly constant on September 1<sup>st</sup>, blowing at an average velocity around 2 m/s. The ambient temperature and irradiance profiles recorded during the six days are shown in Figures 5.2 and 5.3. From these graphs, it can be concluded that only September 6 and August 29 presented almost identical ambient temperature and irradiance profiles.

## 5.2.2 Experimental Data

The experimental data recorded by the data logger during the six clear sky days of the experiment are available in Appendix E. The variation of the seven temperatures measured, the total solar radiation on the collector surface and the electrical and thermal output are presented in Figures 5.4 to 5.9. The experimental uncertainties on the measured and calculated variables were obtained by carrying out an uncertainty analysis available in Appendix F. Only bias errors are included in the uncertainty analysis, because not enough data were collected to estimate precision errors.

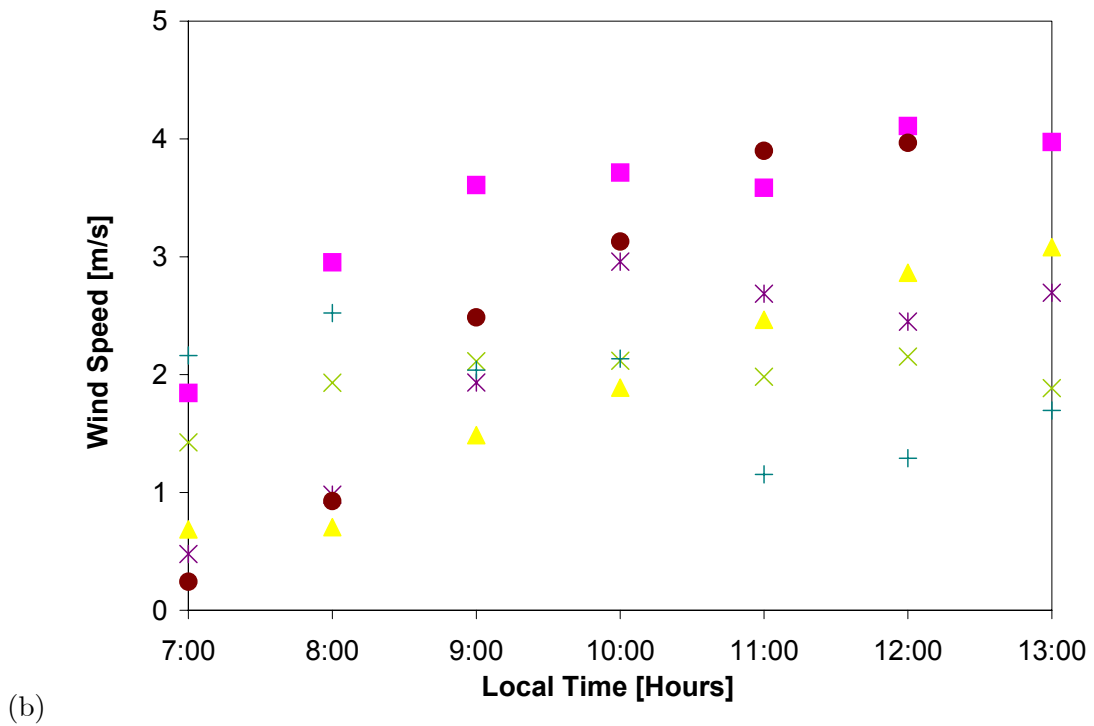
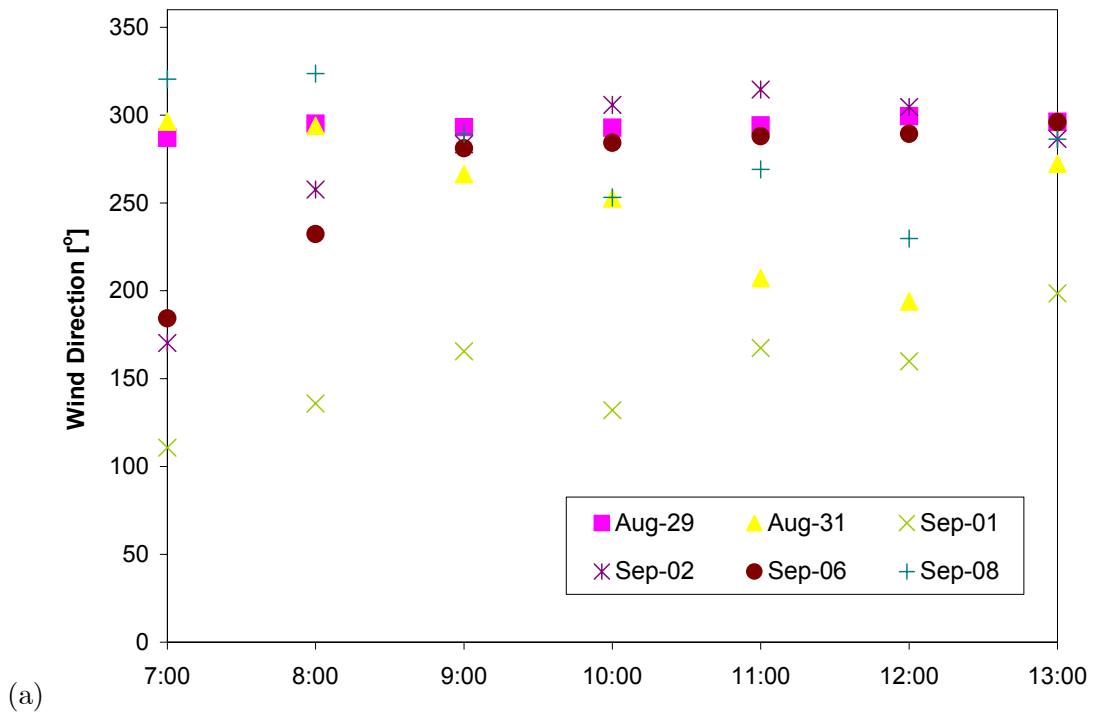


**Figure 5.1:** Hourly data for the (a) wind direction and (b) wind speed for the clear sky days of the experiment

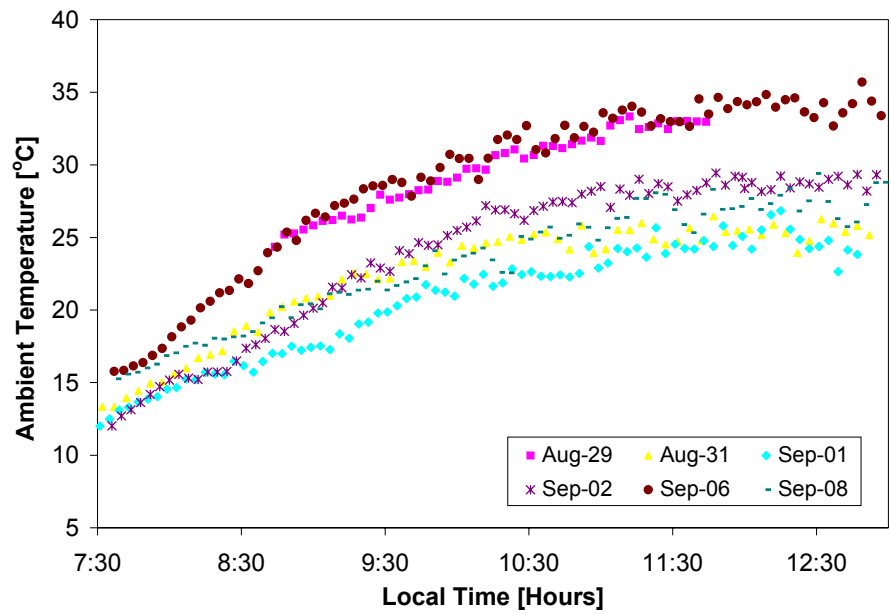


Figure 5.2: Variation of the ambient temperature for the clear sky days

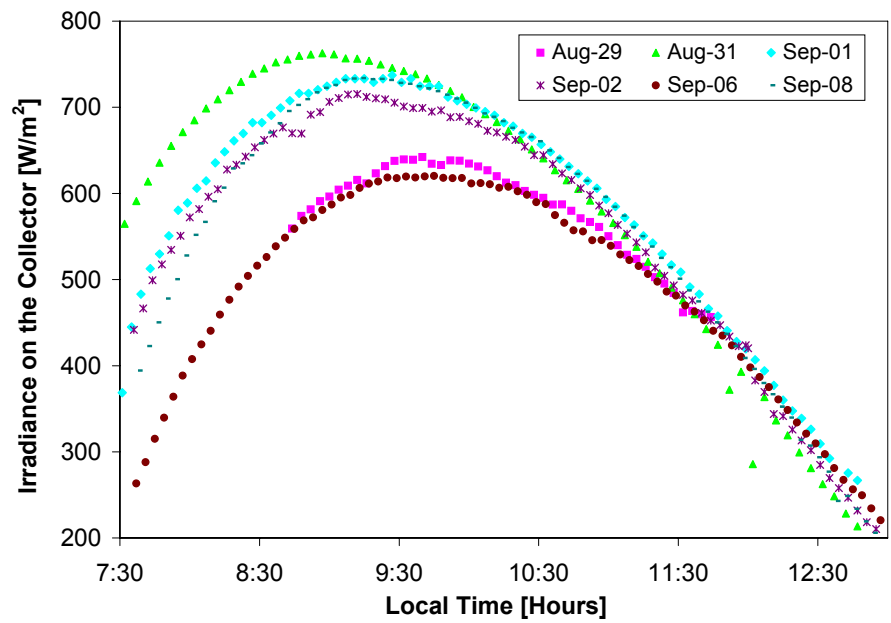
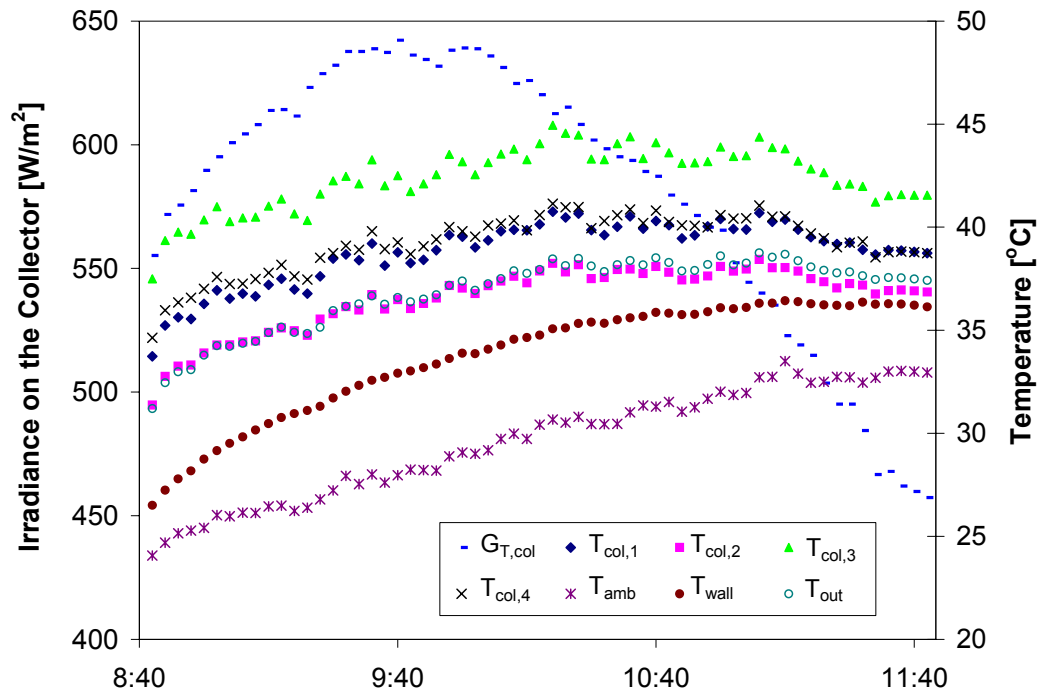
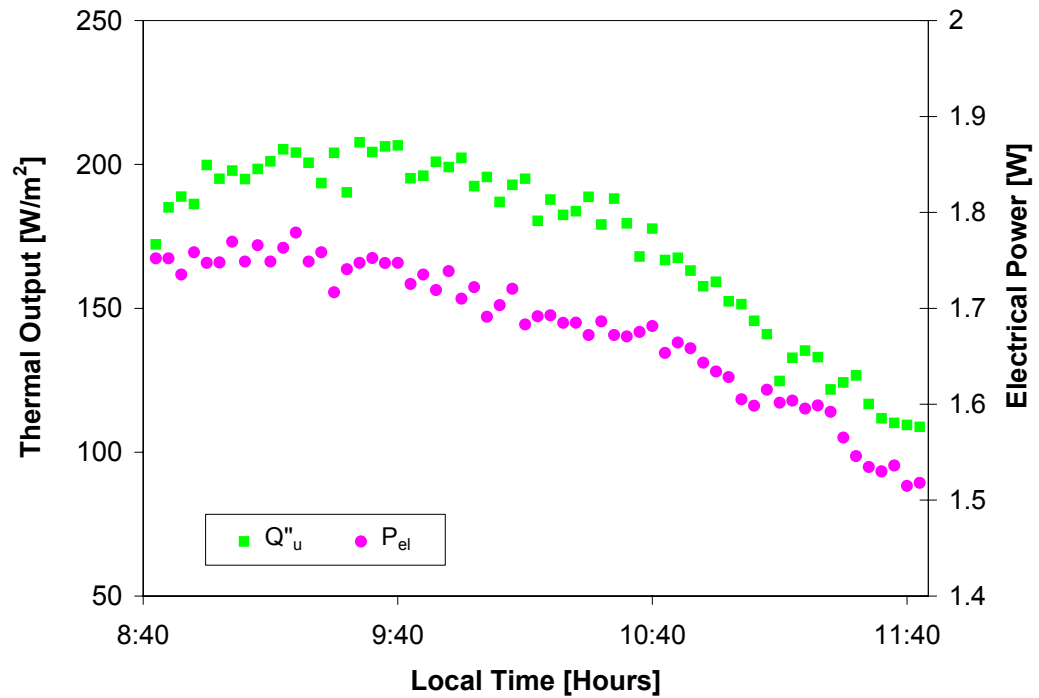


Figure 5.3: Variation of the irradiance on the collector surface for the clear sky days

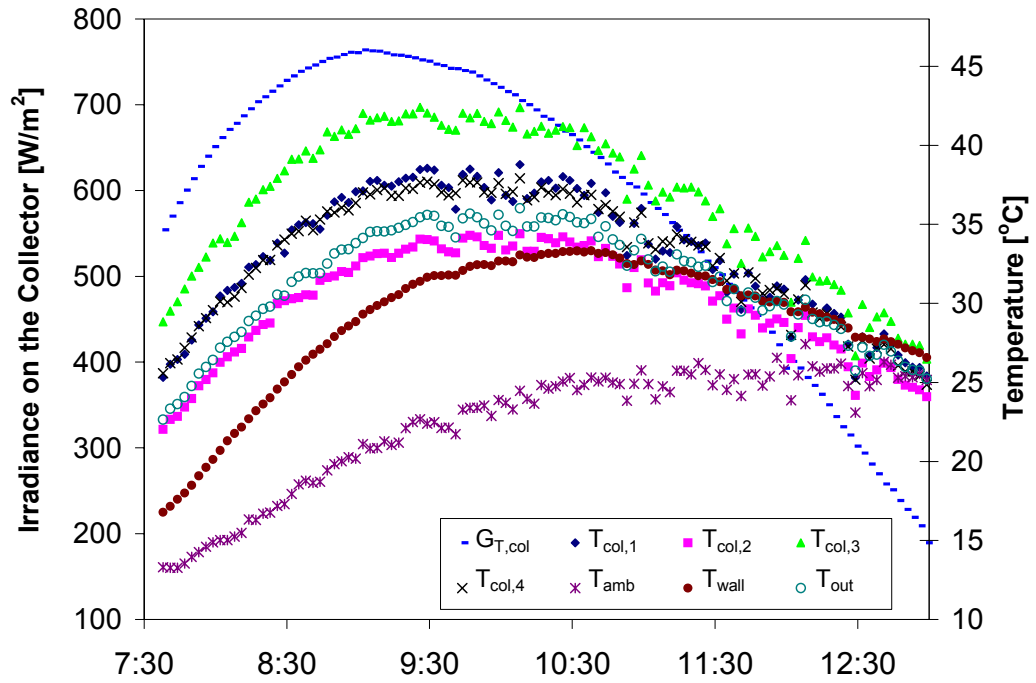


(a)

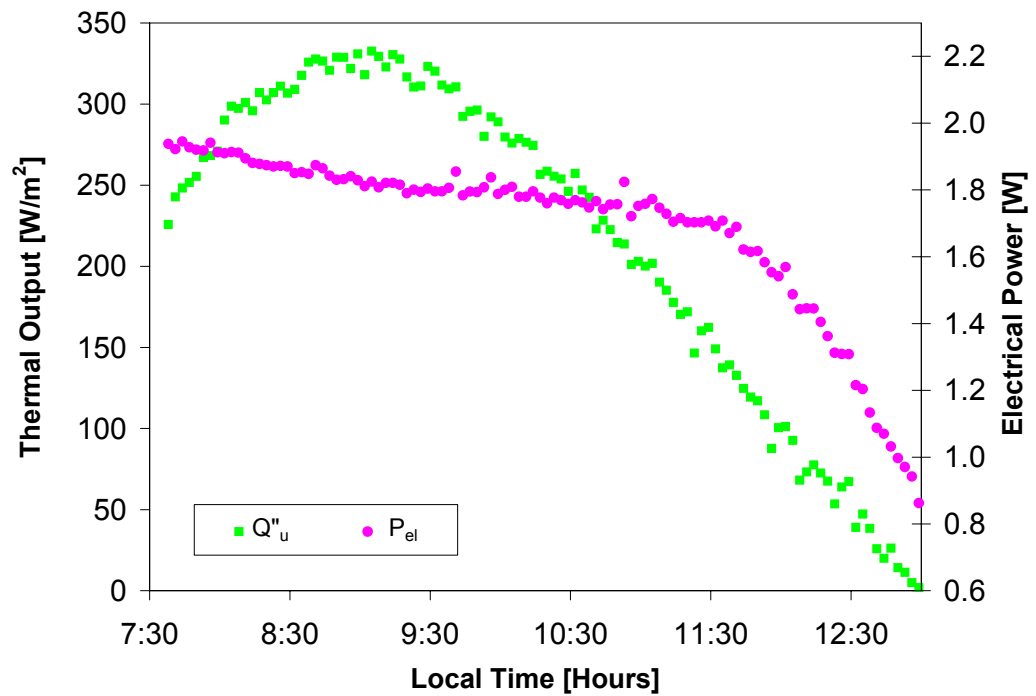


(b)

**Figure 5.4:** Experimental data for August 29 (a) Temperatures and irradiance on the collector (b) Thermal output and electrical power



(a)



(b)

**Figure 5.5:** Experimental data for August 31 (a) Temperatures and irradiance on the collector (b) Thermal output and electrical power

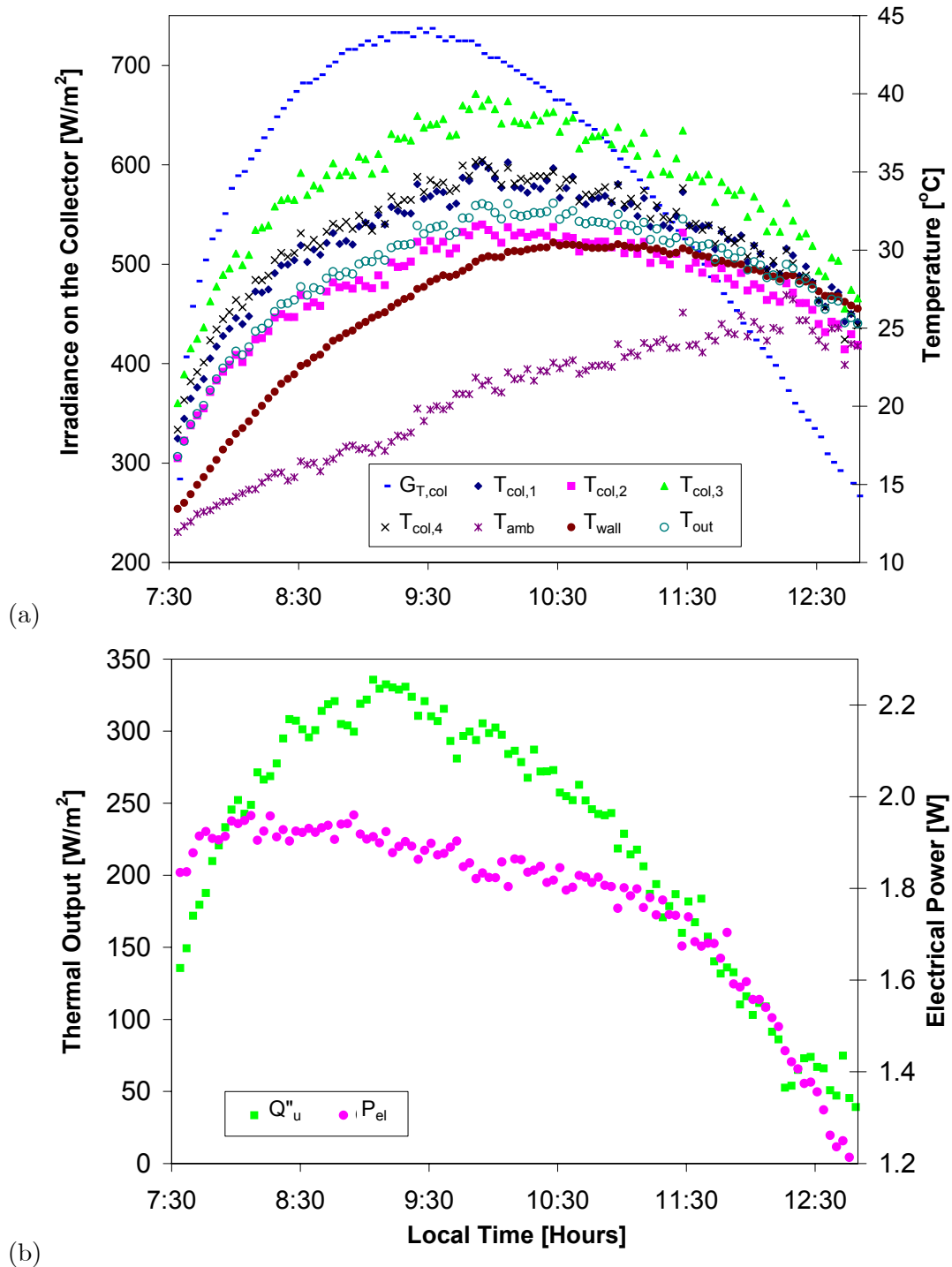
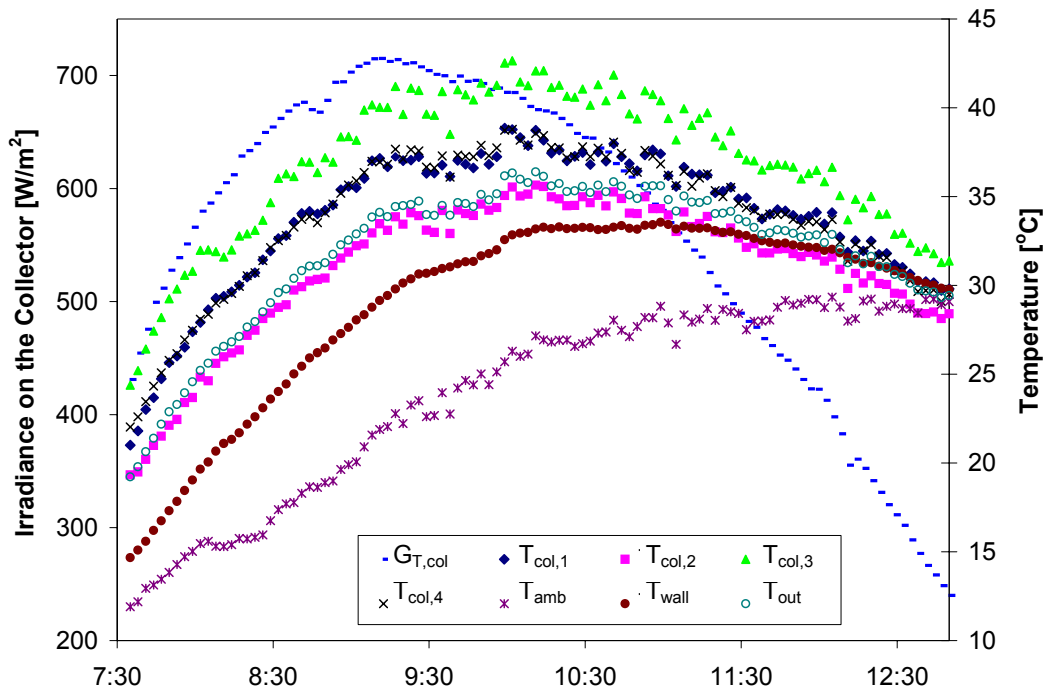
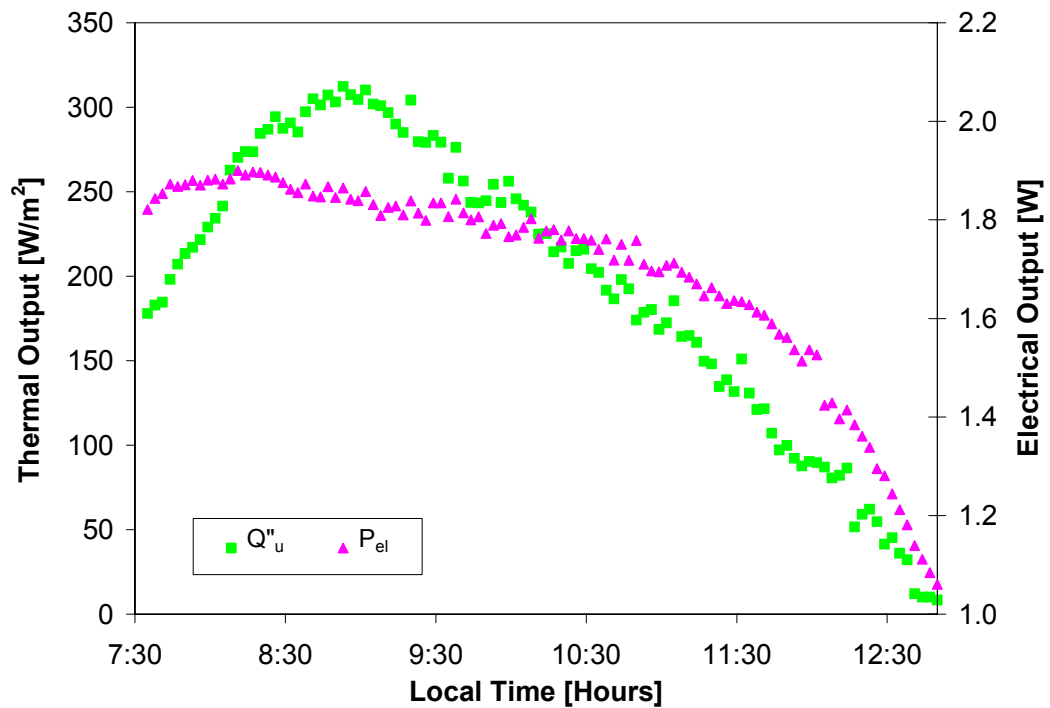


**Figure 5.6:** Experimental data for September 1 (a) Temperatures and irradiance on the collector (b) Thermal output and electrical power

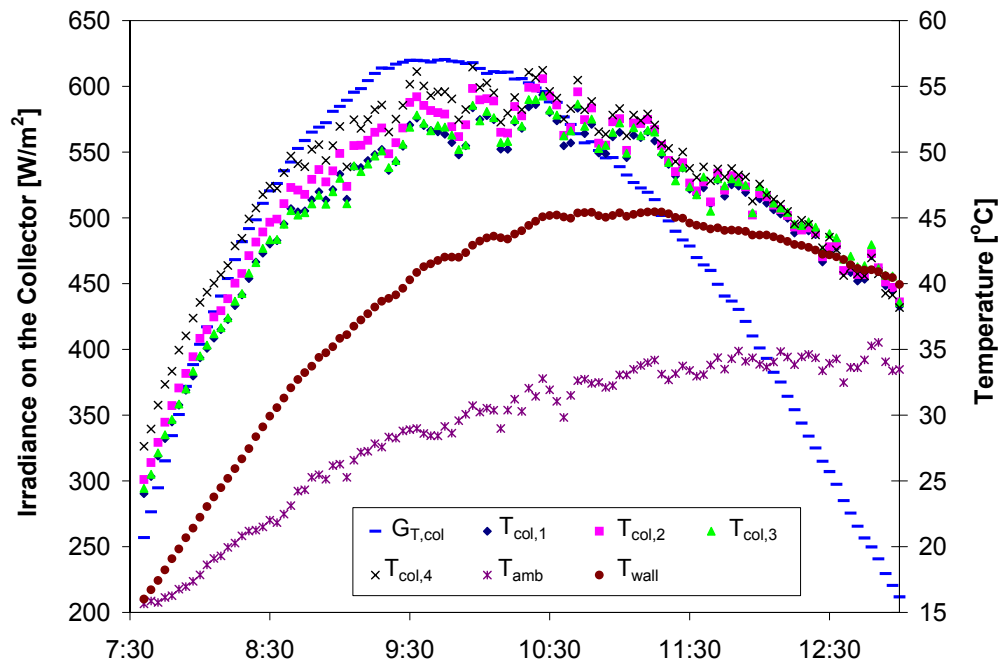


(a)

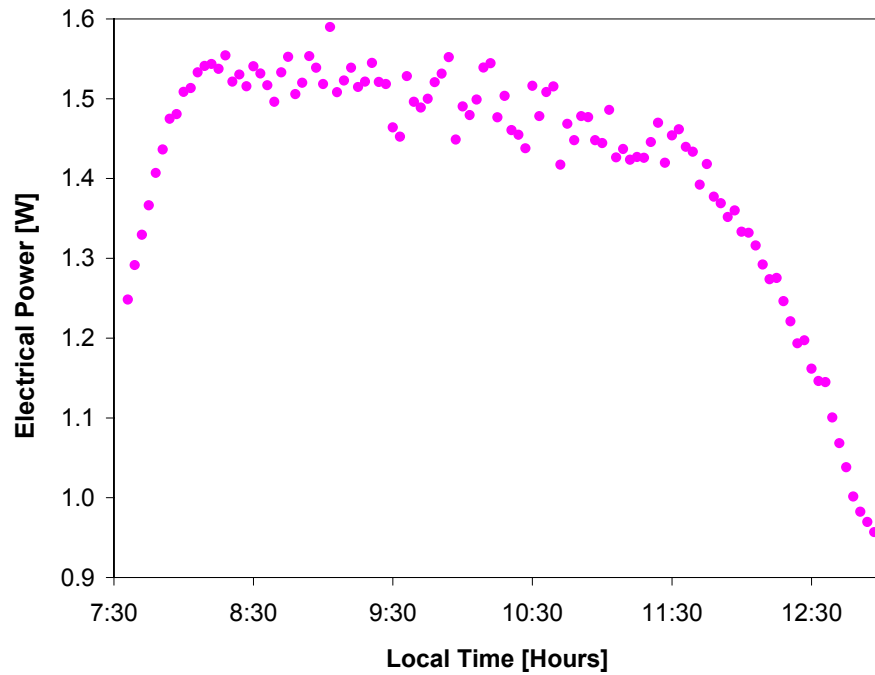


(b)

**Figure 5.7:** Experimental data for September 2 (a) Temperatures and irradiance on the collector (b) Thermal output and electrical power



(a)



(b)

**Figure 5.8:** Experimental data for September 6 (a) Temperatures and irradiance on the collector (b) Electrical power

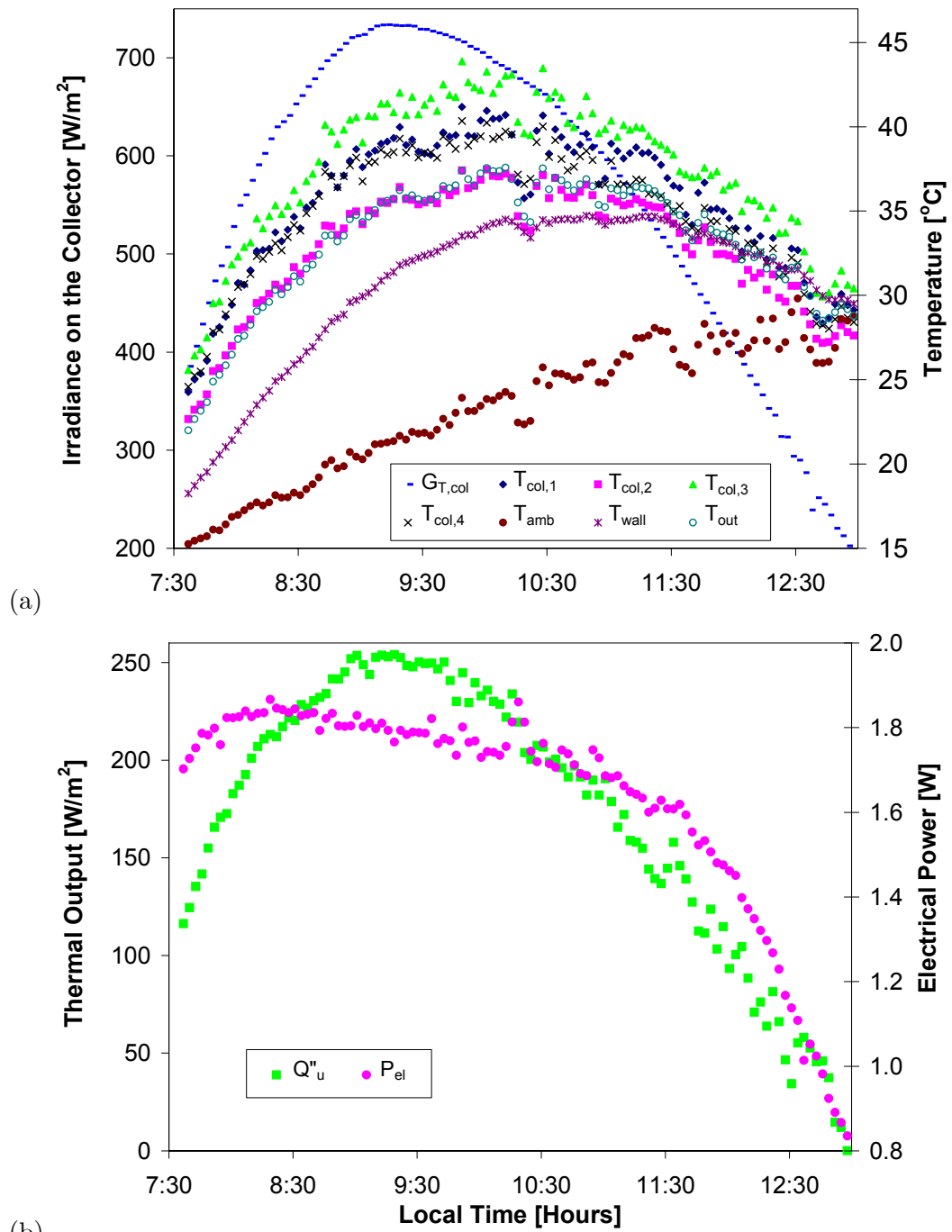


**Figure 5.9:** Experimental data for September 8 (a) Temperatures and irradiance on the collector (b) Thermal output and electrical power

The Figures 5.4 through 5.9 (a) show that the peak temperature measured by the four thermocouples located at the back of the absorber plate ( $T_{col,1@4}$ ) and on the outdoor wall ( $T_{wall}$ ) did not match the peak of irradiance. In fact, there was a delay of approximately 30 minutes for the collector and 1 hour for the outdoor wall. This was not unexpected because as the day got later, the sun continued to heat the earth and the ambient temperature increased even though there was less sun shining on the BEG Hut east wall. The time interval between the peak temperatures measured on the collector surface and on the outdoor wall is due to the fact that the wall had a greater thermal mass than the panel and thus, took longer to heat up. Another observation that can be made by looking at the trend of the different curves is that the variations of the collector outlet temperature are almost perfectly synchronized with the fluctuations of the four thermocouples located at the back surface of the panel. This shows that a change in the plate temperature had an instantaneous effect on the temperature of the air entering the building.

In Figures 5.4 to 5.9 (a), the four temperatures measured at the back of the absorber indicate that the plate temperature was not uniform. On September 1<sup>st</sup> for example, the difference between the highest and lowest recorded temperatures on the panel varied from 2.8°C to as high as 8.5°C. For each day, however, the lowest temperatures were always measured on the upper panel ( $T_{col,1}$  and  $T_{col,2}$ ) while the highest temperatures were recorded on the lower panel ( $T_{col,3}$  and  $T_{col,4}$ ). This is primarily due to the inlet duct location. Dymond and Kutscher (1997) observed that the suction velocity at the locations very close to the duct entrance were greater than anywhere else, because the air does not have to fight against the acceleration, friction and buoyancy pressure drop. Therefore, since thermocouples 3 and 4 were located further than thermocouples 1 and 2 from the duct entrance, the suction flowrate at these locations were not as high. This resulted in a poorer heat transfer between the plate and the ambient air and this is why the temperatures measured on the lower panel were higher than the ones on the upper panel. The hypothesis of a non-uniform suction is confirmed by looking at the temperatures recorded on September 6, when the fan was turned off. For that day, the highest temperature difference between two thermocouple measurements was found to be

only 4.6°C. In this case, however, the lowest temperature was always measured at the left of the upper panel ( $T_{col,1}$ ) while the hottest spot was found to be at the right of the lower panel ( $T_{col,4}$ ).

From Figures 5.4 to 5.9 (b), it can be observed that the maximum heat output coincided with the peak of irradiance. This indicates that the transpired collector responded almost instantaneously to a change in solar radiation. The highest electrical power from the PV cells, however, tended to occur approximately one hour before the peak of irradiance. This could be due to the fact that even though the irradiance was increasing, the panel electrical conversion efficiency was decreasing due to the higher panel temperature.

### 5.2.3 Effect of the Transpired Plate on the PV Cells Performance

In order to evaluate the benefits of the transpired collector on the solar cells, the variation of the electrical power output for each day was plotted.

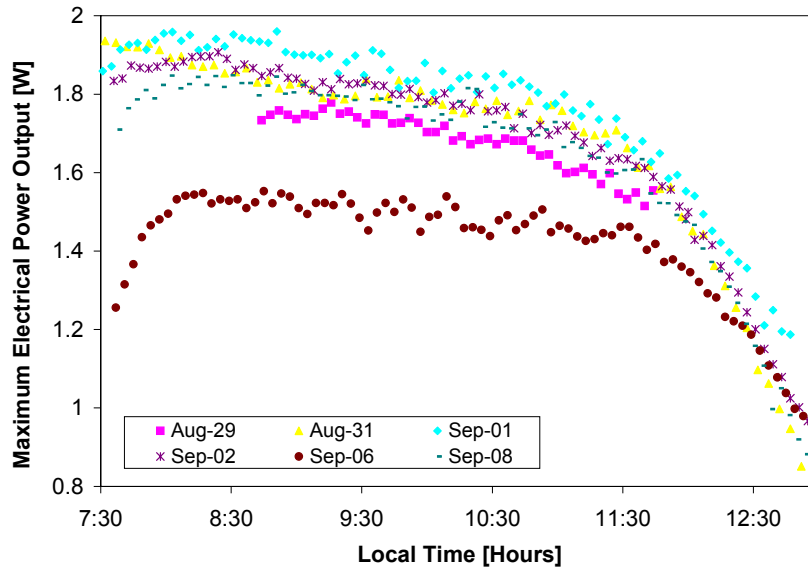


**Figure 5.10:** Variation of the maximum electrical power output produced for the clear sky days

Figure 5.10 indicates that the maximum electrical power produced was clearly less on September 6, when the fan was turned off, than on the other days when suction was occurring at the surface of the plate. The weather conditions were, however, different for each day. Therefore, only August 29 and September 6 were compared since they presented similar ambient temperature and irradiance profiles (Section 5.2.1).

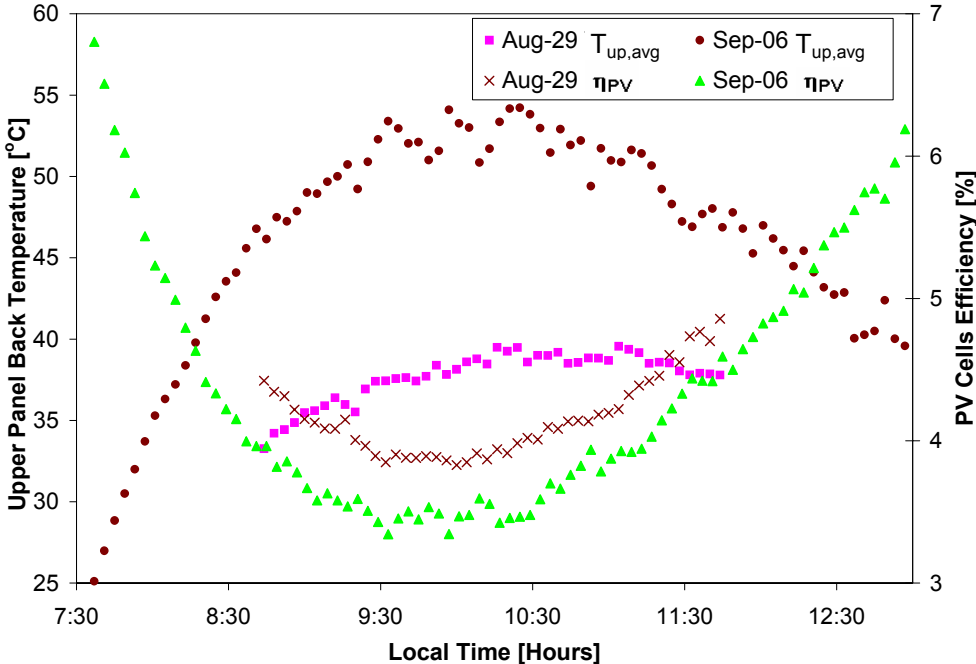


**Figure 5.11:** Variation of the upper panel back temperature and PV cells efficiency for August 29 and September 6

Figure 5.11 presents the variation of the average upper panel back surface temperature and PV cells efficiency for these two days. From this plot, it can be observed that the PV cells conversion efficiency was always greater on August 29 than on September 6. This higher efficiency can be directly attributed to the fact that the panel back surface temperature was lower when the fan was turned on (August 29). It could be argued that this lower temperature was due to the fact that the wind speed was higher on August 29 at the beginning of the day, but after

10:30, the wind was blowing at the same speed for both days. Thus, after 10:30, the higher PV cells conversion efficiency measured on August 29 had to be due to the fact that the PV cells were cooled by the air flowing through the transpired collector and in the plenum. In fact, between 10:30 and 11:30, the maximum electrical power on August 29, was about 10 % greater than on September 6, when the fan was turned off (Figure 5.10).

The other observation that can be made by looking at Figure 5.11 is, however, very surprising and consists in the fact that the electrical efficiencies calculated were always greater than 3 %. Considering that the electrical efficiency determined with the flash test was 3 % at 25°C and 1000 W/m<sup>2</sup> (Table 4.2), it is in fact unexpected that higher efficiencies were obtained at a higher cell temperature. In order to verify if the measurements from the multimeters could have been influenced by other instruments, a quick test was performed on the PV/Thermal collector. The prototype was mounted at a different location than where the experiment took place and the maximum electrical power output was tracked without the presence of the other instruments. At an irradiance of 600 W/m<sup>2</sup> and a cell temperature of approximately 40°C, a maximum electrical power output of 1.5 W was measured. This corresponded to an electrical efficiency of 3.6 % which was still higher than the maximum theoretical efficiency obtained during the flash test. Consequently, it was concluded that the settings at which the flash test had been conducted might not have been appropriate for the testing of the PV/Thermal collector.

As for the effect of the air flowrate on the electrical output, the curves of Figure 5.10 seem to indicate that the PV cells performed better at higher suction rates, since the highest power was measured on September 1<sup>st</sup> when the fan was running at its maximum speed. Unfortunately, this statement cannot be verified because there were no days that had similar ambient temperature and irradiance profiles than September 1<sup>st</sup>. Another way to predict the performance of a PV module is to look at its temperature. Comparing the panel temperature at different airflow rates would not have been appropriate, however, because the testing of the panel at the various suction flowrates were all done on different days. The back panel temperature rise, defined as the difference between the average upper panel temperature and the ambient temperature seemed to be a more relevant parameter to analyze, since it

took the ambient temperature into account. The variation of the upper panel back surface temperature rise at different suction flowrates for a wind speed measured on the roof between 2 m/s and 3 m/s is shown in Figure 5.12.

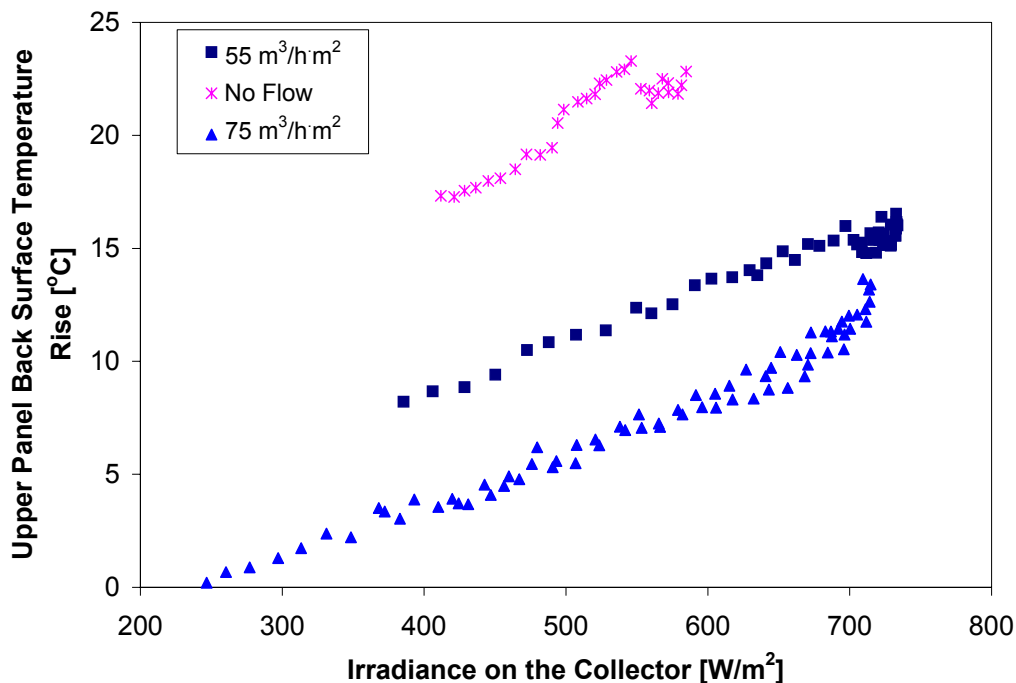


**Figure 5.12:** Variation of the upper panel back surface temperature rise with the irradiance for a wind speed measured on the roof between 2 m/s and 3 m/s

From this graph, it can be observed that the upper panel temperature rise decreased with an increase in the air flowrate. The reason for that is because with greater suction, the air spends less time in the plenum and the plate does not heat up as much. It can also be clearly seen that the temperature of the plate increased considerably when the fan was off and only natural convection was operating. In fact, at  $55 \text{ m}^3/\text{h}\cdot\text{m}^2$ , the upper panel temperature rise was generally  $9^\circ\text{C}$  lower than at zero flow, and at  $75 \text{ m}^3/\text{h}\cdot\text{m}^2$ , approximately  $14^\circ\text{C}$  lower. Therefore, it can be concluded that an increase in the suction flowrate is more likely to produce greater electrical power, because the PV cells are kept at a lower temperature.

## 5.2.4 Effect of the PV cells on the Collector Thermal Performance

In order to analyse if the PV cells affected the thermal performance of the UTC, the air temperature rise measured were compared to the ones obtained from the testing of a 5 m<sup>2</sup> SolarWall<sup>®</sup> at the NSTF (Hollick, 1994). This comparison is shown in Figure 5.13 where the experimental data and NSTF curves are plotted for different air flowrates. It was not possible to find the wind conditions associated with the NSTF measurements, but it was assumed that the data had been obtained at zero or low wind speed (< 2 m/s). Thus, only the experimental data collected when the wind speed was between 1.8 m/s and 2.3 m/s were considered.

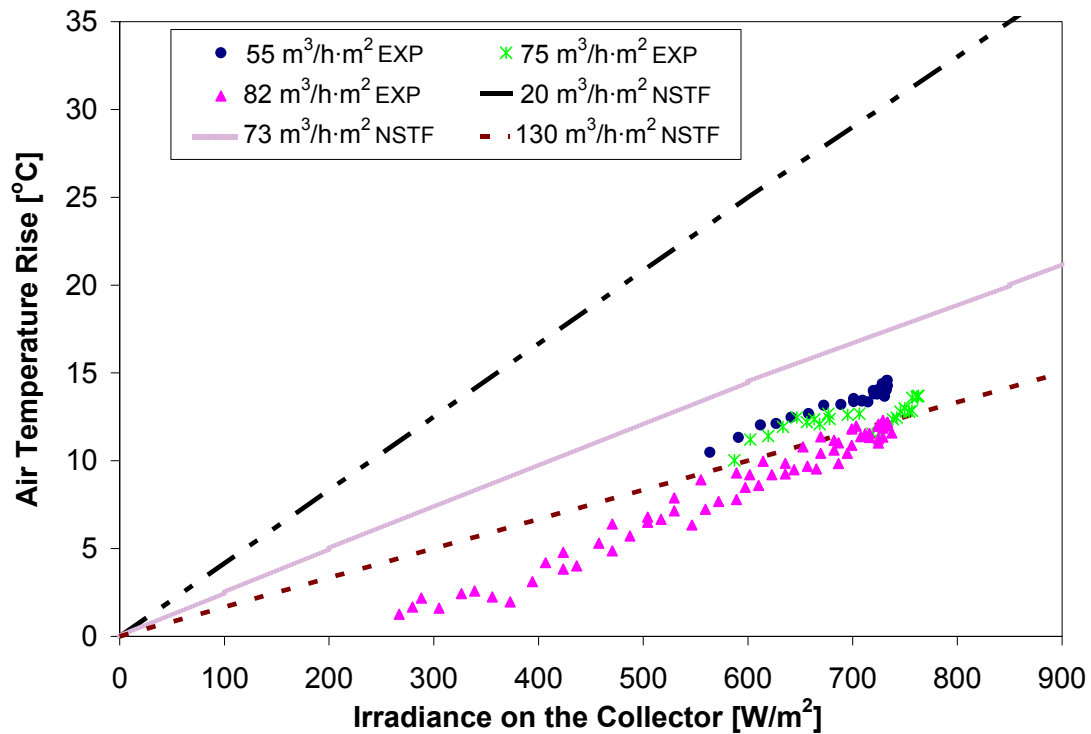


**Figure 5.13:** Variation of the temperature rise with the irradiance for a SolarWall<sup>®</sup> (Hollick, 1994) and from the testing of the prototype

From this graph, it can be observed that just like the SolarWall<sup>®</sup> tested at the NSTF, the PV/Thermal UTC showed higher air temperature rise at lower suction rates. The air temperature rise measured with the prototype were, however, always lower than the ones obtained at the NSTF. For example, at 75 m<sup>3</sup>/h·m<sup>2</sup> and 600 W/m<sup>2</sup>, the air temperature rise was of 11.2 °C for the prototype and 14.8°C for the SolarWall<sup>®</sup> tested at the NSTF. A comparison of the experimental and NSTF thermal efficiencies at different air flowrates are presented in Figure 5.14.

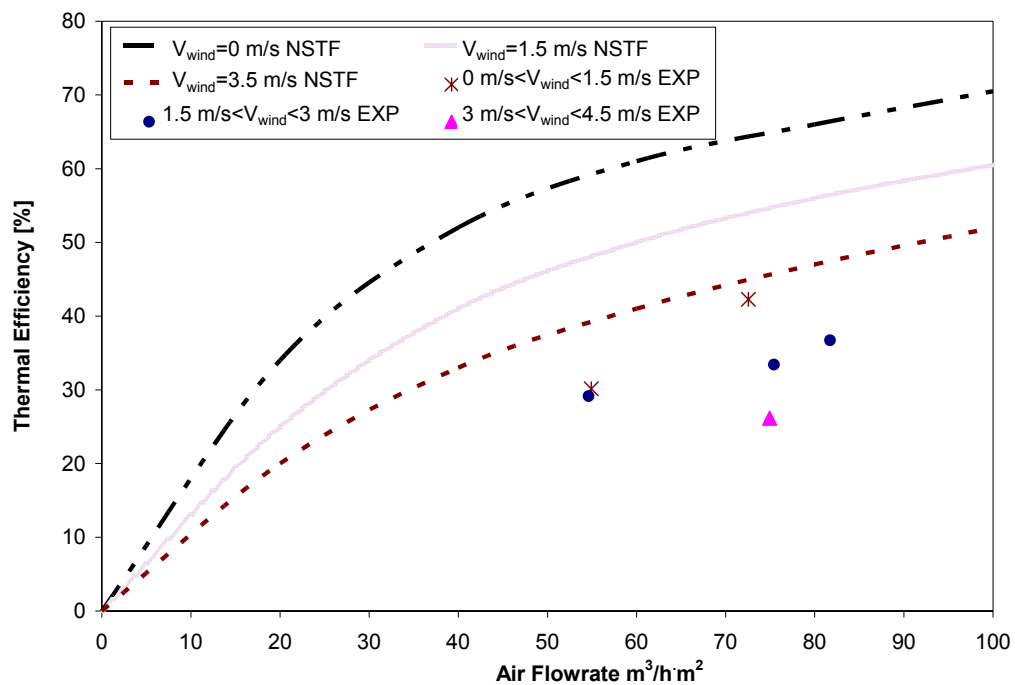


**Figure 5.14:** Variation of the thermal efficiency with the air flowrate for a SolarWall<sup>®</sup> (Hollick, 1994) and from the testing of the prototype

From this graph, it can be observed that the experiment followed a similar trend as the SolarWall<sup>®</sup> tested at the NSTF: higher thermal efficiencies were obtained at greater air flowrates and lower wind speeds. As a consequence of the lower air temperature rise achieved by the PV/Thermal UTC, the experimental thermal efficiencies were, however, lower than that obtained at the NSTF.

There are several factors that can explain why the air temperature rise and thermal efficiencies obtained during the experiment were lower than that measured at the NSTF. One reason is that the PV/Thermal UTC was about half the size of the collector tested at the NSTF. For a transpired collector, the wind heat losses occur during the plate starting length (Kutscher et al., 1993). Therefore, the smaller is the area of a collector, the more significant is the proportion of edge area to collector area, and the more important are the wind heat losses (Hollick, 1994). Thus, the convective heat losses to the ambient might have been greater on the PV/Thermal UTC tested. Another explanation for this difference can come from the definition of the ambient temperature. For the experiment, the ambient temperature was measured on the east wall. With the measurements being taken in the morning, the air on the east wall was always at a slightly higher temperature than the ambient air on the BEG Hut roof. In order to verify the effect of taking the roof temperature as the true ambient temperature, a new temperature rise was calculated by using the roof hourly averaged ambient temperature recorded by the BEG Hut data logger. For the case of an airflow of  $75 \text{ m}^3/\text{h}\cdot\text{m}^2$ , the average difference between the old and the new temperature rise was of  $1^\circ\text{C}$ . Finally, even though it is usually expected that the thermal performance of a combined PV/Thermal collector will not be as high as the one of a stand-alone thermal collector, it is less likely that the solar cells had an influence on the thermal performance in this case. The main reason being that the PV cells were covering a very small portion of the panel area. If a transpired collector of the same size without PV cells had been tested at the same time or if more solar cells had been mounted on the panel, it would have been easier to identify at which extent the solar cells were responsible for the poor thermal performance of the collector.

## **5.3 Model Validation**

### **5.3.1 TRNSYS Simulation**

In order to validate the model, TRNSYS simulations were performed using the PV/Thermal transpired collector with the prototype parameters and the weather

data of four clear sky days with different air suction rates. The following TRNSYS components were used in the simulations:

- Data Reader (Type 9c)
- Psychometrics (Type 33e)
- Sky Temperature (Type 69b)
- Radiation Converter
- Printer (Type 25a)

All these components were part of the main TRNSYS library except for the Radiation Converter that consisted of a modified version of a model originally developed by Barrett in 1987 (SEL, 2005). It was necessary to this simulation to split the radiation measured on the east wall into its beam, sky diffuse and ground reflected components and to estimate the horizontal beam and diffuse radiation. These variables were required since they are inputs to the PV/Thermal UTC model. As for the Psychometrics component, it was used to calculate the dew point temperature so that the sky temperature could be evaluated. The Fortran code of the Radiation Converter can be found in Appendix G.

The wind velocity and building temperature inputs to the model came from the records of the BEG Hut data logger (Appendix E) while the solar radiation and solar angles were all obtained from the Radiation Converter component mentioned above. The BEG Hut was not instrumented to record the ambient pressure, so the data were taken from the measurements of the Waterloo Weather Station (Waterloo Weather Station, 2007). The other inputs to the model consisted of variables measured during the experiment. In order to prevent the model from optimizing the air flowrate through the collector, the supplied temperature was fixed to 50°C and both the flowrates for the minimum amount of fresh air ( $\dot{m}_{\min}$ ) and total air required in the building ( $\dot{m}_T$ ) were set to the value of the air flowrate measured experimentally.

### 5.3.2 Preliminary Results

As a first evaluation of the model validity, a preliminary comparison of the results predicted by the TRNSYS simulations and measured experimentally was carried out. The thermal output estimated by the model was found to be much higher than that obtained with the prototype, while the electrical power predicted was significantly lower than the one measured.

The over prediction of the thermal output was directly caused by an overestimation of the panel temperature. This was expected, however, because as discussed in Section 5.2.4, the wind heat losses from the prototype tested were probably greater than on typical transpired collector installations because of the small area of the panel. Consequently, the correlation used in the model to estimate the wind heat transfer coefficient was replaced by the correlation developed by the Solar Thermal Research Laboratory from testing on a lab-scale flat plate transpired collector (Equation 3.32).

As for the electrical power produced, it was also not surprising that the TRNSYS simulation estimated much lower values. The reason being that the reference electrical efficiency entered as a parameter in the model was the one measured with the flash test. As observed in Section 5.2.3, it is more likely that the reference efficiency obtained from that test was lower than the actual PV cells reference efficiency and that a new value for this variable had to be calculated. Furthermore, considering that the flash test results had also been used to calculate the temperature coefficient  $\mu$  in Section 4.2.3, it is probable that this variable was also not accurate. Unfortunately, the manufacturer data could not be used to obtain new estimates for  $\eta_{ref}$  and  $\mu$ , because the electrical parameters were provided for individual full size solar cells, while the PV cells layout consisted of bits of cells connected together. Without resorting to the flash test results and not being able to use the manufacturer data, the only option left to obtain values for  $\eta_{ref}$  and  $\mu$  was to use the experimental results.

### 5.3.2.1 PV Cells Layout Electrical Parameters

A method suggested by Whitaker et al. (1991) was used to evaluate the PV cells layout parameters from the experimental measurements. This procedure is based on the assumption that at constant irradiance, the PV cells power is a linear function of the PV cells temperature and can be expressed as

$$P_{el} = P_{el,ref} \frac{G_{T,col}}{G_{T,col,ref}} \left[ 1 + \beta_{P_{mp}} (T_{PV} - T_{ref}) \right] \quad (5.1)$$

where  $P_{el,ref}$  is the electrical power at reference irradiance  $G_{T,col,ref}$  and PV cells temperature  $T_{ref}$ ,  $P_{el}$  is the electrical power measured at desired irradiance  $G_{T,col}$  and PV cells temperature  $T_{PV}$ , and  $\beta_{P_{mp}}$  is the temperature coefficient at maximum power point. Isolating  $\beta_{P_{mp}}$  in Equation 5.1,

$$\beta_{P_{mp}} = \frac{\frac{P_{el}}{P_{el,ref}} \frac{G_{T,col,ref}}{G_{T,col}} - 1}{T_{PV} - T_{ref}} \quad (5.2)$$

Using the following relation,

$$P'_{el,ref} = P_{el,ref} \left( \frac{G_{T,col}}{G_{T,col,ref}} \right) \quad (5.3)$$

Equation 5.2 can be simplified to

$$\beta_{P_{mp}} = \frac{1}{P'_{el,ref}} \left( \frac{P_{el} - P'_{el,ref}}{T_{PV} - T_{ref}} \right) \quad (5.4)$$

In the model developed in Chapter 3, the following equation is used to evaluate the PV cells efficiency.

$$\eta_{PV} = \eta_{ref} + \mu (T_{PV} - T_{ref}) \quad (5.5)$$

By comparing Equations 5.1 and 5.5, it can be found that these two equations are equivalent if the temperature coefficient  $\mu$  corresponds to

$$\mu = \beta_{P_{mp}} \eta_{ref} \quad (5.6)$$

In order to evaluate  $\beta_{P_{mp}}$ , Whitaker et al. (1991) suggest to plot the module power output as a function of the PV cells temperature for different bins of irradiance. The first issue with this procedure is that during the experiment, the PV cells temperature was not measured. The resistance between the back of the panel and the PV cells was considered to be negligible, however, so the average temperature measured on the upper panel was assumed to be representative of the actual PV cells temperature. The second issue that was raised by the production of this plot is that in order to obtain accurate correlations, measurements have to be taken over a period of at least two months to collect data in a wide range of cells temperatures and irradiances. In this case, only the measurements taken on September 6 could be used, because it was the only day where the PV cells were relatively isothermal. Consequently, curves could only be obtained for bins of irradiance of  $500 \text{ W/m}^2$ ,  $550 \text{ W/m}^2$  and  $600 \text{ W/m}^2 \pm 3\%$  as shown in Figure 5.15.

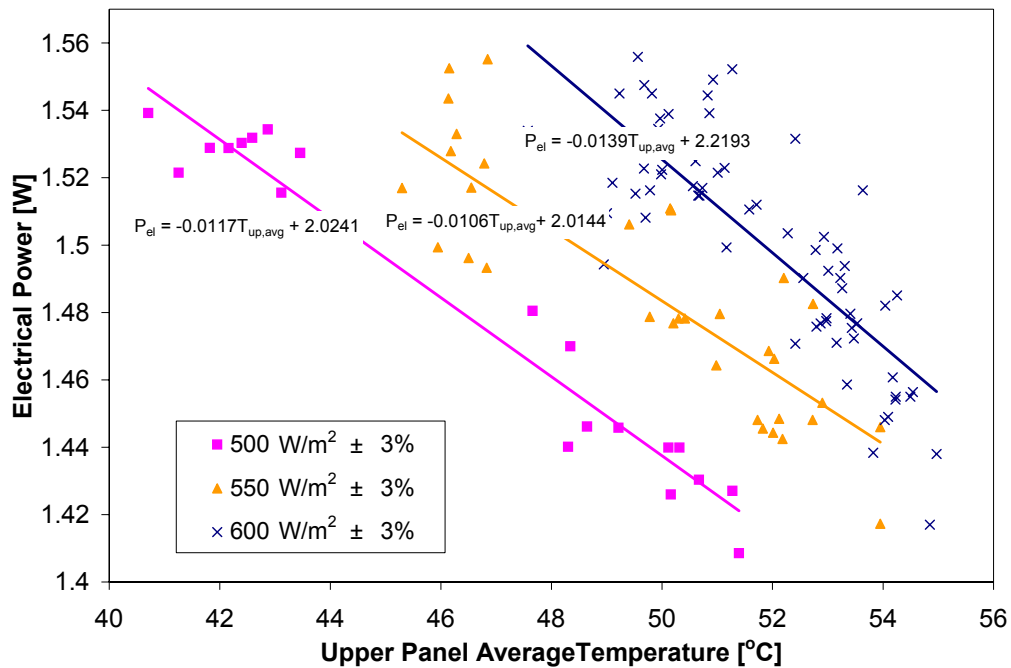


**Figure 5.15:** Electrical power measured as a function of the upper panel average temperature for different bins of irradiance

In Figure 5.15, the slope  $m$  at each reference level of irradiance is given as  $\Delta P_{el}/\Delta T_{up,avg}$ . Therefore, from Equation 5.4,  $\beta_{P_{mp}}$  corresponds to

$$\beta_{P_{mp}} = \frac{m}{P_{el,ref}} \quad (5.7)$$

Taking an arbitrary reference temperature  $T_{ref}$  of 30°C, the electrical power  $P_{el,ref}$  at each reference level of irradiance  $G_{T,col,ref}$  can be calculated using the equations of the curves shown in Figure 5.15. Taking  $G_{T,col}$  to be equal to 1000 W/m<sup>2</sup>,  $P_{el,ref}$  can be obtained for each bin of irradiance using Equation 5.3 and  $\beta_{P_{mp}}$  can be calculated with Equation 5.7. The desired temperature  $T_{PV}$  being 25°C, the electrical power  $P_{el}$  at desired temperature  $T_{PV} = 25^\circ\text{C}$  and irradiance  $G_{T,col} = 1000$  W/m<sup>2</sup> can then be estimated for each reference conditions using Equation 5.1. The PV cells efficiency,  $\eta_{PV}$ , at the desired conditions of 1000 W/m<sup>2</sup> and 25°C (STC conditions) can then be obtained using

$$\eta_{PV} = \frac{P_{el}}{A_{PV}G_{T,col}}$$

where  $A_{PV}$  is the PV cells area corresponding to 0.07 m<sup>2</sup>. The temperature coefficient  $\mu$  can also be calculated from Equation 5.6. The summary of the data obtained for each bin of irradiance is shown in Table 5.2. By averaging  $\eta_{PV}$  and  $\mu$  calculated for the three different levels of irradiance, an average temperature coefficient of -0.0002 1/°C was calculated and a PV cells efficiency at STC conditions of 25°C and 1000 W/m<sup>2</sup> was estimated to be 0.046.

**Table 5.2:** Parameters of the PV cells layout calculated for different bins of irradiance using the experimental measurements of September 6

$G_{T,col,ref}$ [W/m <sup>2</sup> ]	$P_{el,ref}$ [W]	$P'_{el,ref}$ [W]	$\beta_{P_{mp}}$ [1/°C]	$P_{el}$ [W]	$\eta_{PV}$	$\mu$ [1/°C]
500 ± 3%	1.67	3.35	-0.0035	3.40	0.049	-0.00017
550 ± 3%	1.70	3.08	-0.0034	3.14	0.045	-0.00015
600 ± 3%	1.80	3.00	-0.0046	3.07	0.044	-0.0002

### **5.3.3 TRNSYS Parameters and Inputs**

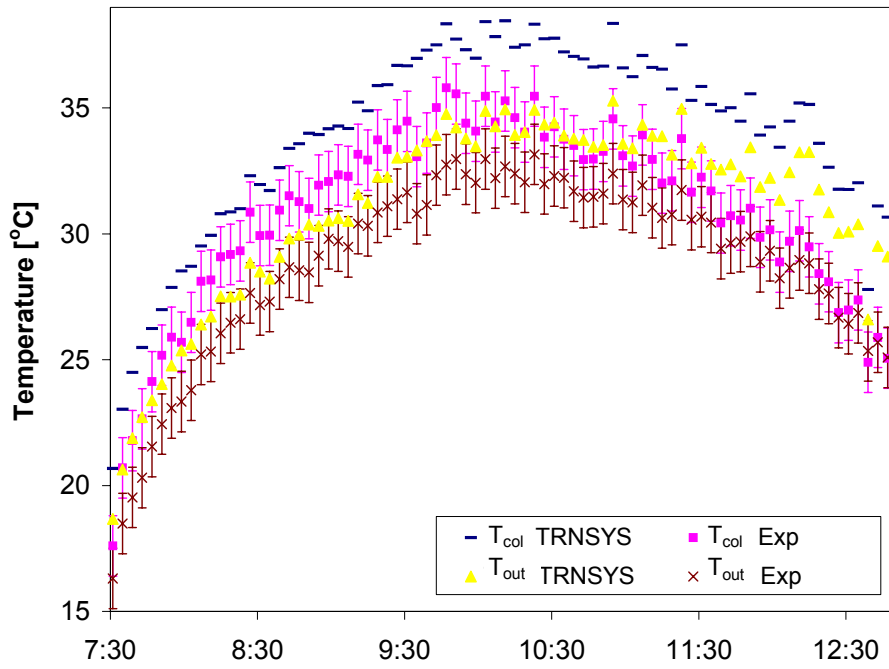
The parameters and inputs of the PV/Thermal transpired collector component used in the TRNSYS simulations with the changes described in Section 5.8.2 are shown in Table 5.3.

### **5.3.4 Simulation Results**

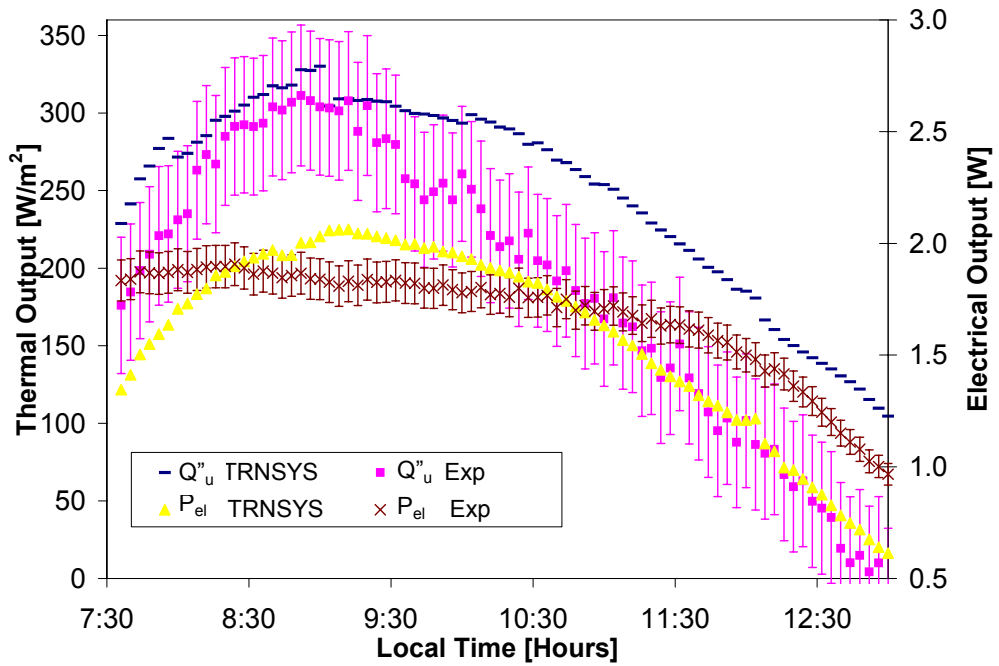
The four clear sky days selected were simulated in TRNSYS at a time step of one minute. Figures 5.16 to 5.19 present the experimental collector outlet and surface temperatures, thermal output and maximum electrical power compared with the model.

**Table 5.3:** Parameters and Inputs to the TRNSYS simulation of the experimental days

PARAMETERS		
Length of the base of the trapezoid	a [m]	0.15
Length of the top of the trapezoid	b [m]	0.115
Height of the corrugation	$h_T$ [m]	0.033
Plate porosity	$\sigma$	0.0025
Pitch	p [m]	0.01403
Collector length	L [m]	2.49
Distance between two corrugations	d [m]	0.2
Collector width	W [m]	1.05
Absorptance of the wall	$\alpha_{wall}$	0.4
Plenum height	$h_{plen}$ [m]	0.14
Emissivity of the collector back surface	$\varepsilon_{col,b}$	0.94
Emissivity of the wall	$\varepsilon_{wall}$	0.93
Collector thickness	t [m]	0.001
Panel absorptance	$\alpha_{Panel}$	0.96
Panel emissivity	$\varepsilon_{Panel}$	0.94
Wall U-Value	$U_{wall}$ [kJ/h·m <sup>2</sup> ·K]	1.02
1: No PV	PV Mode	2
2: PV cells on the top of the corrugations		
3: PV cells on every surface		
PV cells temperature coefficient at maximum power point	$\mu$ [1/°C]	-0.0002
PV cells reference efficiency	$\eta_{ref}$	0.046
PV cells reference temperature	$T_{ref}$ [°C]	25
PV cells absorptance-transmittance product	$(\tau\alpha)_{PV,N}$	0.9
PV cells emissivity	$\varepsilon_{PV}$	0.8
Bypass collector in the summer? 1:Yes, 0: No	Bypass?	0
Bypass temperature	$T_{bypass}$ [°C]	-
PV cells refraction index	n	-
PV cells glazing extinction coefficient	K [1/m]	-
PV cells glazing thickness	$t_{PV}$ [m]	0
PV cells proportion at the top of the corrugations	$P_{PV(3)}$	0.049
INPUTS		
Beam radiation on the collector	$G_{b,col}$ [kJ/h·m <sup>2</sup> ]	Vary
Diffuse radiation on the collector	$G_{d,col}$ [kJ/h·m <sup>2</sup> ]	Vary
Ground reflected radiation on the collector	$G_{g,col}$ [kJ/h·m <sup>2</sup> ]	Vary
Horizontal beam radiation	$G_{bH}$ [kJ/h·m <sup>2</sup> ]	Vary
Solar zenith angle	$\theta_z$ [°]	Vary
Solar azimuth angle	$\gamma_s$ [°]	Vary
Wind velocity	$V_{wind}$ [m/s]	Vary
Ambient temperature	$T_{amb}$ [°C]	Vary
Ambient pressure	$P_{amb}$ [Pa]	Vary
Sun incidence angle on the collector	$\theta_{col}$ [°]	Vary
Building temperature	$T_{b lg}$ [°C]	Vary
Sky temperature	$T_{sky}$ [°C]	Vary
Minimum fresh air mass flowrate	$\dot{m}_{min}$ [kg/h]	Vary
Total mass flowrate of air entering the building	$\dot{m}_T$ [kg/h]	Vary
Collector slope	$\beta_{col}$ [°]	90
Collector azimuth angle	$\gamma_{col}$ [°]	-90
Ground reflectance	$\rho_{gnd}$	0.2
Total horizontal radiation	$G_{TH}$ [kJ/h·m <sup>2</sup> ]	Vary
Horizontal diffuse radiation	$G_{dH}$ [kJ/h·m <sup>2</sup> ]	Vary
Temperature of the air supplied to the building	$T_{sup}$ [°C]	50

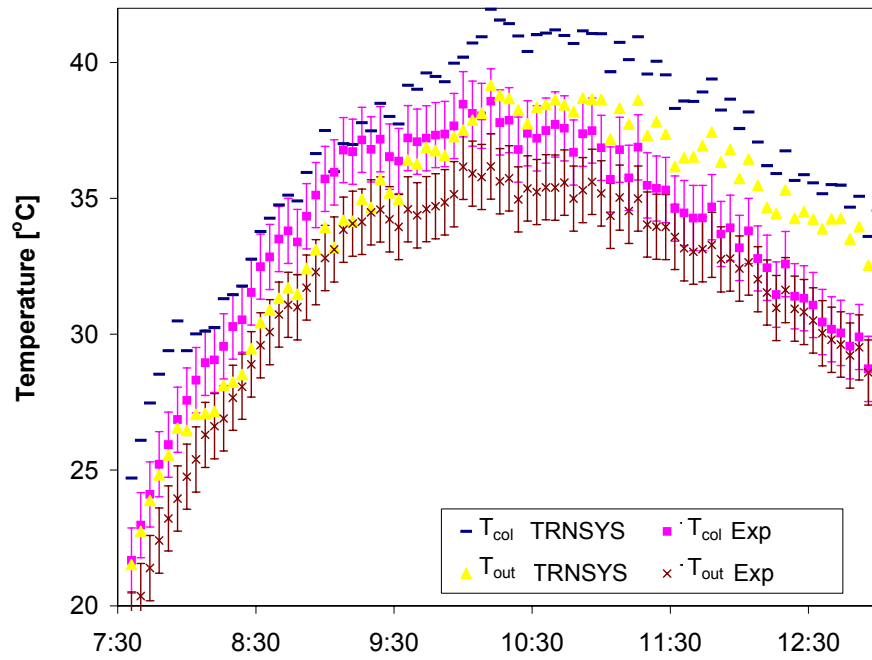


(a)

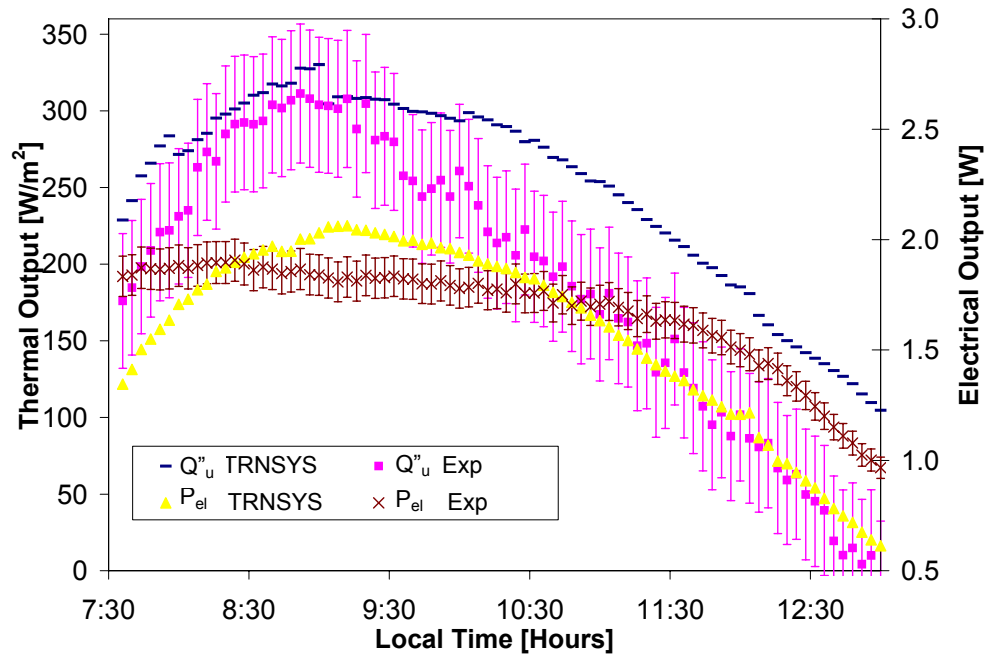


(b)

**Figure 5.16:** Comparison between the experimental data and TRNSYS predictions for September 1 (a) Temperatures (b) Thermal and electrical output

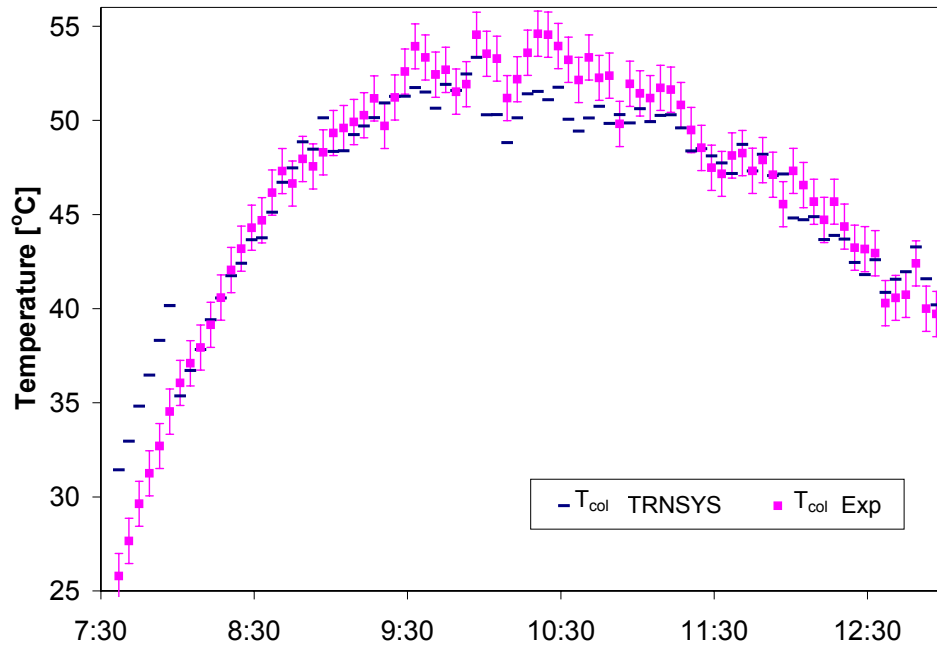


(a)

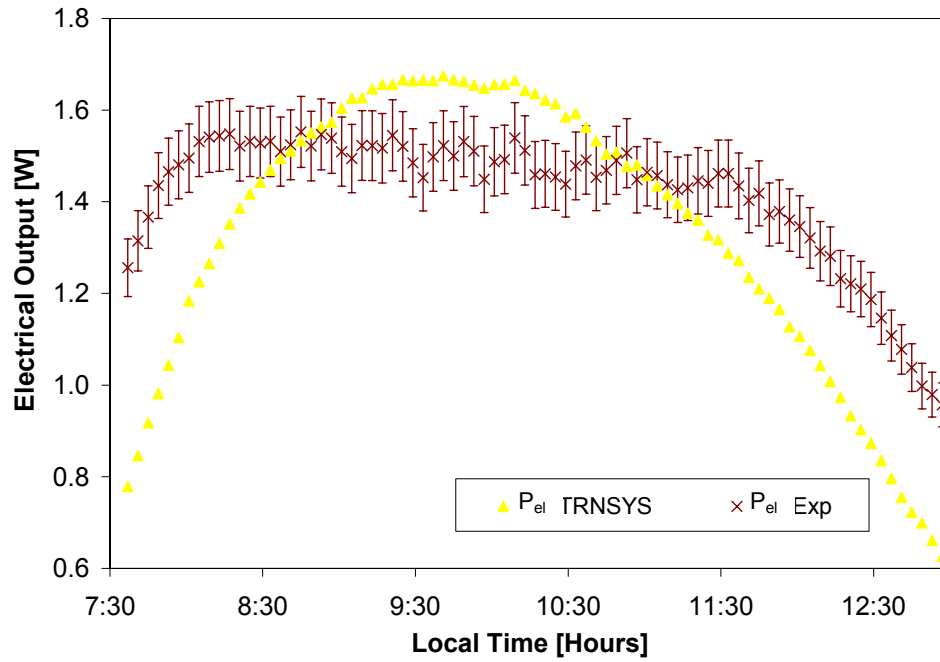


(b)

**Figure 5.17:** Comparison between the experimental data and TRNSYS predictions for September 2 (a) Temperatures (b) Thermal and electrical output

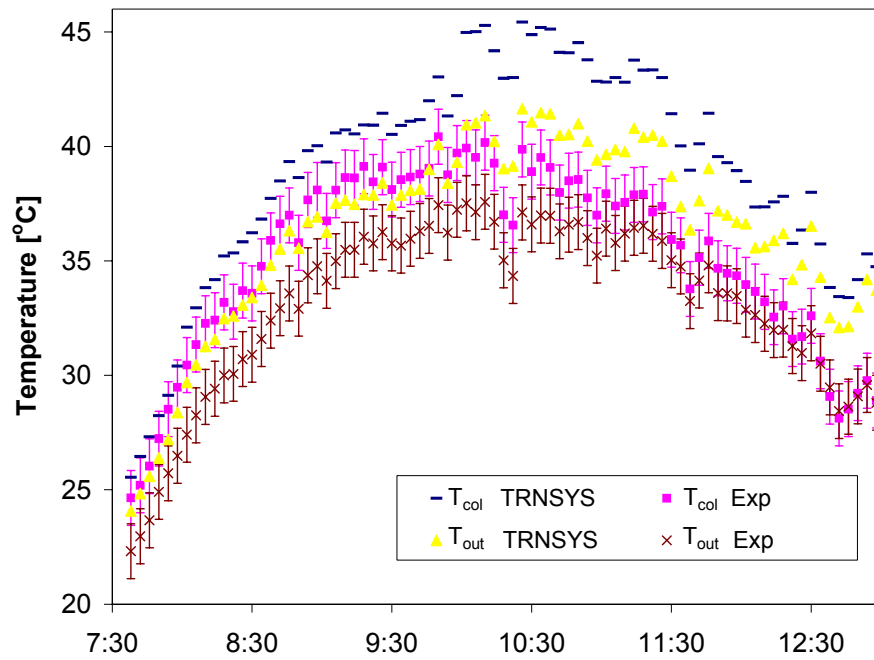


(a)

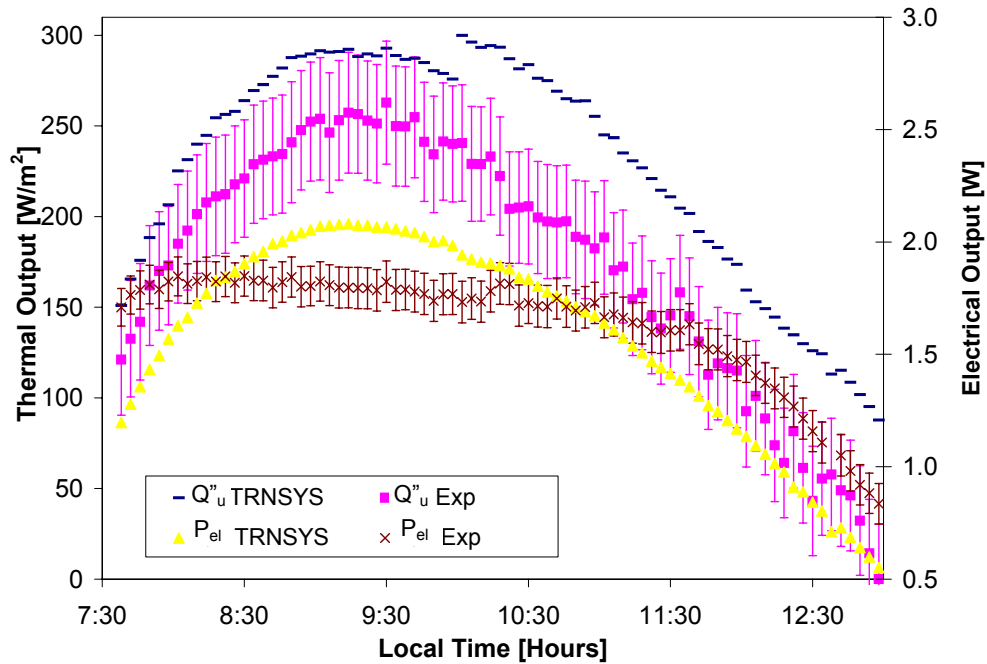


(b)

**Figure 5.18:** Comparison between the experimental data and TRNSYS predictions for September 6 (a) Temperatures (b) Electrical output



(a)



(b)

**Figure 5.19:** Comparison between the experimental data and TRNSYS predictions for September 8 (a) Temperatures (b) Thermal and electrical output

### 5.3.5 Discussion

In Figures 5.16 to 5.19 (a), it can be seen that the surface and outlet temperature curves of the TRNSYS model and the experiment follow the same trend. Although the TRNSYS model predicts a higher surface and outlet temperature, the difference between the curves is relatively constant. The root-mean-square error (RMSE) for both temperatures were calculated and shown in Table 5.4. The RMSE is defined as

$$\text{RMSE} = \left[ \frac{1}{N} \sum_{x=1}^N (T_{\text{pred},x} - T_{\text{exp},x})^2 \right]^{\frac{1}{2}}$$

where  $N$  is the number of observations,  $T_{\text{pred},x}$  is the  $x^{\text{th}}$  predicted temperature and  $T_{\text{exp},x}$  is the  $x^{\text{th}}$  temperature measured experimentally.

**Table 5.4:** RMSE of the collector surface and outlet temperatures predicted by TRNSYS

Date	RMSE	
	$T_{\text{out}}$ [ $^{\circ}\text{C}$ ]	$T_{\text{col,avg}}$ [ $^{\circ}\text{C}$ ]
Sep-01	2.3	3.4
Sep-02	2.7	3.4
Sep-06	-	2.1
Sep-08	3.3	4.2

From Table 5.4 and Figure 5.18 (a) it can be observed that the predictions of the collector temperature were the closest to the experimental results on September 6, when the fan was turned off. This shows that the method used to calculate the amount of solar energy absorbed by the panel is accurate and is not a source of error. For the days when the fan was on, the RMSE of the collector outlet and surface temperature were the smallest on September 1<sup>st</sup>. As mentioned in Section 5.2.1, the wind was blowing from the south-east on that day, while it was generally blowing from west to east on the other days. The models to obtain the wind heat transfer coefficient of UTCs are all based on the assumption that the wind is perpendicular to the normal of the plate (crosswind). Thus, the fact that the wind was the closest to being parallel to the east wall on September 1<sup>st</sup> can explain

why the model predictions were better for that day. With this observation, it was decided to examine if using the wind velocity measured on the roof in correlations requiring the free stream velocity was problematic.

To investigate this possible source of error, TRNSYS simulations were performed with the parameters and inputs indicated in Table 5.3, but using the local wind velocity in front of the wall instead of the wind speed measured on the roof. In order to obtain this local wind speed, correlations developed by Emmel et al. (2007) from CFD analysis on a low-rise building were used. These correlations provided an estimate of the local wind velocity at a distance of 1 m from the wall,  $V_{wind,loc}$ , from the wind free stream velocity measured 10 m above the ground,  $V_{wind,10}$ . Equation 5.8 is for windward conditions when the wind blows at an angle of  $45^\circ$  on the wall, while Equation 5.9 is for leeward conditions where the angle between the wind direction and the normal to the wall is  $180^\circ$ .

$$V_{wind,loc} = 0.57V_{wind,10} + 0.05 \quad (5.8)$$

$$V_{wind,loc} = 0.32V_{wind,10} \quad (5.9)$$

The local wind speed was estimated with Equation 5.8 for September 1<sup>st</sup>, because the wind was generally blowing south-east for that day and for the other days, it was calculated with Equation 5.9. In all cases,  $V_{wind,10}$  was taken as the wind measured on the BEG Hut roof. Table 5.5 presents the RMSE calculated with the new simulation results.

**Table 5.5:** RMSE of the collector surface and outlet temperatures predicted by TRNSYS with the local wind speed as input

Date	RMSE	
	$T_{out}$ [ $^\circ\text{C}$ ]	$T_{col,avg}$ [ $^\circ\text{C}$ ]
Sep-01	3.0	5.0
Sep-02	4.1	6.4
Sep-06	-	8.4
Sep-08	4.8	7.1

By comparing Tables 5.4 and 5.5, it can be observed that using the local wind speed instead of the roof wind velocity increased significantly the difference between the model predictions and the experimental results. This was not surprising, because the local wind speed of a wall with a leeward wind is about a third than the wind velocity measured on the roof (Equation 5.9). Therefore, using  $V_{wind,loc}$  in the TRNSYS simulation decreased significantly the wind heat losses and the model over predicted even more the experimental results. The validity of the model is not compromised by this information, however, because this local wind speed is not equivalent to a crosswind speed, which is the type of wind assumed in the  $h_{wind}$  correlation.

Another issue associated with the wind predictions is that the models to obtain the wind heat transfer coefficient of UTCs are all based on the assumption of the presence of a laminar boundary layer at the panel surface. With the wind being leeward for most of the days, it is probable that local recirculation was occurring at the front of the east wall, inducing turbulence. As observed by Fleck et al. (2002), with the presence of turbulence on the wall where a UTC is mounted, it is unlikely that a laminar boundary layer can develop over the collector. Moreover, recirculation zones at the front of the collector induce hot spots on the collector which decrease the collector efficiency. Thus, the TRNSYS model might have been overpredicted the temperature measurements because the laminar boundary layer assumption was not respected.

In order to verify if the wind heat transfer coefficient estimated with the STRL correlation was still being under predicted, different  $h_{wind}$  were investigated to see if better results could be obtained. Two expressions were found in the literature that could be used to estimate a value of  $h_{wind}$  on a building facade with a leeward wind. The first one was developed by Loveday and Taki (1996) and is given as

$$h_{wind} = 16.25V_{wind,loc}^{0.503} \quad (5.10)$$

where  $V_{wind,loc}$  is a function of  $V_{wind,11}$ , the wind measured 11 m above the ground,

$$V_{wind,loc} = 0.2V_{wind,11} - 0.1$$

The other one is suggested in ASHRAE (1975) and corresponds to

$$h_{wind} = 18.6 * V_{wind,loc}^{0.605} \quad (5.11)$$

where  $V_{wind,loc}$  is obtained from the wind measured 10 m above the ground,  $V_{wind,10}$ .

$$V_{wind,loc} = 0.05V_{wind,10} + 0.3$$

The wind heat transfer coefficients at different wind speeds estimated with the correlations of ASHRAE and Loveday and Taki were compared to the  $h_{wind}$  obtained with the expression used in Maurer's UTC model (Equation 2.12 with  $C_f$  fixed to a value of 5), the  $h_{wind}$  predicted by the STRL model (Equation 3.32) and the  $h_{wind}$  used in the SWift99 software (Equations 3.30 and 3.31). For the correlations using the suction velocity as a variable, a value of 0.02 m/s was used. The results are shown in Figure 5.20. As it can be observed the highest heat transfer coefficient at wind speeds greater than 1.5 m/s is predicted by the STRL model used in TRNSYS. This concludes that in theory the STRL model should have predicted the most accurate results, since a lower  $h_{wind}$  would result in a greater collector temperature. Since the turbulent boundary layer is likely to increase the wind convective heat transfer coefficient, it shows that further research developing an  $h_{wind}$  correlation is required. In addition, none of the  $h_{wind}$  models take into account the trapezoidal corrugated shape of the collector.

Another explanation to the TRNSYS model temperature over prediction is the fact that the model assumes uniform suction and an isothermal panel, whereas these two conditions were not observed during the experiment. The non-homogeneous suction prevented the maximum heat to be extracted from the panel, creating a non-uniform temperature along the absorber plate resulting in higher radiation losses to the surroundings. Therefore, with the panel possibly not working at its optimal performance, it is not surprising that the temperatures estimated by the TRNSYS model were slightly higher than the ones measured on the prototype.

As a direct consequence of the higher collector outlet temperature, the useful thermal output calculated by the TRNSYS model was always greater than

that obtained experimentally, even though the curve trends were very similar. In fact, the difference between the two curves varied between  $50 \text{ W/m}^2\text{panel}$  and  $100 \text{ W/m}^2\text{panel}$ , as shown in Figures 5.16 to 5.19 (b). From these plots, it can also be observed that the predicted maximum electrical power curve was the closest to the experimental results on September 6. On the other days, when the fan was turned on, the power estimated by the model was generally higher between 7:30 and 10:30. Within this period, the trends of the experimental and predicted curves were also quite different. The TRNSYS curves corresponded to a dome with a peak coinciding with the highest measurement of solar radiation, while the experimental data points followed a trend similar to a descending plateau. The experimental results did not show a peak on September 6 either, but the measured values were much closer to what was predicted.

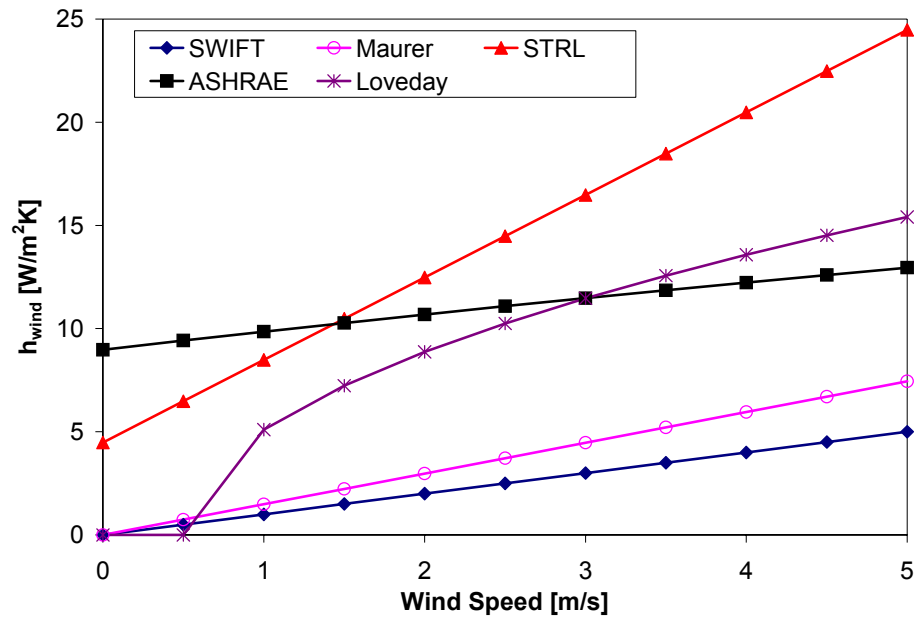


**Figure 5.20:** Variation of the wind heat transfer coefficient with the wind speed for different correlations

The reason why the TRNSYS results were closer to the experimental measurements on the day with zero flow is because the PV cells layout consisted of solar

cells mainly connected in parallel. The maximum power point current and voltage temperature coefficients for the full-size solar cells used in the panel construction were of  $0 \text{ \%}/^{\circ}\text{C}$  and  $-0.45\%/^{\circ}\text{C}$ , respectively. Once the PV cells were cut and connected together, these coefficients changed, but the solar cells voltage at maximum power point should have remained much more sensitive to a change in temperature than the current. When suction occurred at the collector surface, the temperature on the panel was not uniform. Thus, each series of cells was at a particular temperature thereby operating at a different voltage. With the series of cells connected in parallel, the voltage of the whole PV cells layout was brought down to the voltage produced by the series of cells at the highest temperature. This resulted in the reduction of the power measured. On September 6, the collector was closer to being isothermal, and consequently, the voltage generated by each series of cells were more similar and the power measured was predicted better by the PV/Thermal UTC model.

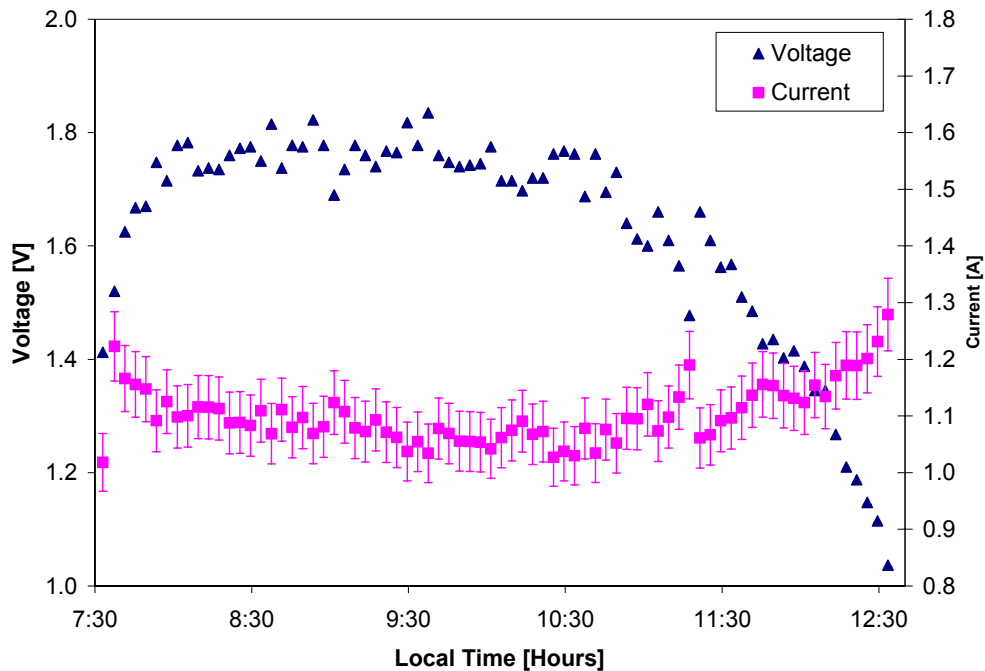


**Figure 5.21:** Variation of the current and voltage recorded on September 1

A possible explanation for the absence of a peak of power on the experimental curve at the point of maximum solar radiation can be found in Figure 5.21 where the voltage and current recorded on September 1<sup>st</sup> are plotted. This figure shows that the trend of the voltage measured was as expected. Between 7:45 and 9:30, the voltage remained constant despite the increase of solar radiation, because of the rise of the cells temperature. The current, on the other hand, was expected to vary only with the irradiance, since the current temperature coefficient of the full size solar cells at maximum power point was of 0%/°C. From Figure 5.21, it can be seen that not only the current seemed to be influenced by the cells temperature, but a greater current was measured at lower irradiance. An assumption for these unexpected measurements can be that even though the cells were electrically insulated from the panel, a portion of the current might have started leaking to the plate when the collector reached a certain temperature. Unfortunately, during the maximum power point tracking, the current was not directly calculated. Thus, the possible anomaly related to this variable was not noticed in the three weeks of the testing.

# Chapter 6

## Conclusions and Recommendations

### 6.1 Conclusions

A TRNSYS model was developed to predict the heat output and electricity produced by a PV/Thermal unglazed transpired collector of corrugated shape. The model was based on an existing UTC component, but was modified to account for the wind effects, the corrugated shape of the plate and the fact that PV cells could be directly mounted on the panel. By comparing the thermal predictions of the PV/Thermal UTC component with no PV cells to the ones of the original UTC model, it was found that accounting for the wind heat losses was the change that had the most significant impact on the overall collector performance. Two configurations were considered in the development of the model. In the first configuration, the cells were mounted only on the top surfaces of the corrugations, while in the second configuration, the cells could be present on every surface of the collector. TRNSYS simulations showed that mounting PV cells according to the first configuration would be a more cost-effective design because it prevented the solar cells from being shaded by the collector. With such a configuration, the addition of PV cells was estimated to decrease the thermal energy savings by 5.9%, but 13.6% were expected to be recovered in the production of electricity.

In order to validate the model, a 2.6 m<sup>2</sup> prototype of a PV/Thermal UTC was built and mounted outdoors on the east facing wall of the University of Waterloo BEG Hut. For a period of three weeks, the performance of the PV/Thermal collector at different air suction rates was studied by recording the collector surface and outlet temperatures as well as the PV cells electrical output. Results showed that when the fan was turned on, the PV cells were kept at a lower temperature and that consequently, the electrical conversion efficiency was better. At 75 m<sup>3</sup>/h·m<sup>2</sup>, an increase of 10% in the electrical power production was observed compared to the case where the fan was turned off. The experiment also showed that at zero flow, the back surface temperature rise of the panel on which the PV cells were mounted was 9°C higher than at a flowrate of 55 m<sup>3</sup>/h·m<sup>2</sup>, and 14°C higher than at 75 m<sup>3</sup>/h·m<sup>2</sup>. Thus, it was concluded that more electrical power could potentially be produced at higher suction rates. As for the collector thermal performance, the experimental results were as expected: greater temperature rise was measured at lower air suction rates and higher thermal efficiencies were obtained at greater air flow rates and lower wind speeds. Both the air temperature rise and collector thermal efficiencies were found to be lower than expected. This could be attributed to the non-uniform suction preventing the maximum heat of being extracted from the panel and to the higher wind heat losses due to the small panel area.

TRNSYS simulations were performed with the PV/Thermal UTC component using the prototype properties and the weather data of some experimental days as parameters and inputs. The collector surface and outlet temperatures measured and predicted by TRNSYS were found to follow similar trends. The temperatures estimated by the model were, however, always a little higher than that obtained experimentally, even after having modified the wind heat transfer correlation to account for the small area of the collector. Several explanations were formulated to justify the deviation between the measured and experimental results. First, the wind heat loss coefficient used in the model did not take the wind direction and trapezoidal corrugated shape of the collector into account. Second, two main assumptions in the model were not respected during the experiment: the suction was non-uniform and the panel was not isothermal. As a result, the thermal output was generally over predicted by the model by approximately 50 W/m<sup>2</sup>*panel* to 100

$W/m^2$  panel. At zero flow, the electrical power estimated by TRNSYS was found to be very similar to that measured on the PV/Thermal collector. On the days where the fan was on, the non-uniform temperature of each series of cells connected in parallel caused a drop in the panel voltage measured. This resulted in lowering the power produced by the prototype and an over prediction in the amount of electricity estimated by the model.

## 6.2 Recommendations

- The correlations to estimate the wind heat transfer coefficient on UTCs have not been adapted yet to panels with trapezoidal corrugated shapes. Furthermore, they do not take the effect of wind direction into account. As noticed in this project, the wind plays a significant role in the performance of UTCs and PV/Thermal UTCs. Thus, there is a need to study more in depth the effect of wind speed and wind direction on transpired collectors with their actual shape, that is trapezoidal corrugated shapes.
- In the experiment performed, it was not possible to evaluate the effect of the PV cells on the UTC thermal performance. Thus, it is recommended that if a similar prototype is built in the future, more PV cells be mounted on the collector surface. Following the same idea, it is strongly suggested that for outdoor testing, the PV/Thermal collector be monitored at the same time as a PV module of equivalent power and a stand-alone UTC of same area, for reference purposes. Furthermore, if resources are available, it would also be very interesting to compare the performance of a PV/Thermal UTC with PV cells mounted directly on the absorber plate to one with a PV Module mounted on the front of the UTC.
- The prototype built for the experiment could not be used in real applications. The reason being that in order to leave the perforations uncovered, the crystalline cells mounted on the panel were left without any cover. This is of course, not recommended because not only could the cells have been easily broken at any moment, but serious problems regarding dust collection

started being noticed after the three weeks of testing. Moreover, if the panel had not been protected on rainy days, the performance of the cells would have seriously been affected. Consequently, it would be interesting to build a prototype less fragile that could be used in the long-term. To build such a collector, paint-on or flexible solar cells would have to be used. These types of cells are, however, not as efficient as crystalline solar cells and do not depend as much on temperature. Thus, the effect of the UTC on the cells would probably not be as noticeable. To avoid the electrical performance of a PV/Thermal collector to be affected by the non-uniform cooling of the cells, it is also strongly recommended that the PV cells on the collector be mounted in series as much as possible.

- Finally, a better model, such as the 5-Parameter model, could be used in the PV/Thermal UTC model to provide a more accurate estimation of the electricity produced by the PV cells. These types of models, however, require much more information regarding the solar cells properties and this is why a simple model was preferred in this study.

# Appendix A

## Method for Calculating the View Factors

The view factors between two surfaces are calculated using Hottel's String Rule for 2D enclosures. This rule states that the view factor between a surface 1 and a surface 2,  $F_{1-2}$ , can be calculated using the following expression (Siegel & Howell, 1992).

$$F_{1-2} = \frac{\text{Sum of crossed strings} - \text{Sum of uncrossed strings}}{2L_1} \quad (\text{A.1})$$

For example, for the enclosure shown in Figure A.1, the view factor  $F_{1-2}$  corresponds to

$$F_{1-2} = \frac{(AC - BD) - (BC + AD)}{2L_1} \quad (\text{A.2})$$

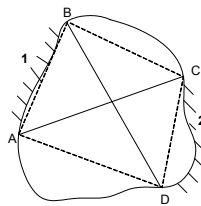


**Figure A.1:** 2D Enclosure for Hottel's String Rule

Six expressions were developed from the Hottel's String Rule to obtain all the view factors needed in the calculation of the absorbed solar radiation. The first expression obtained is used to calculate the view factor between two surfaces with a common edge and separated by an angle  $\alpha$  (Figure A.2).

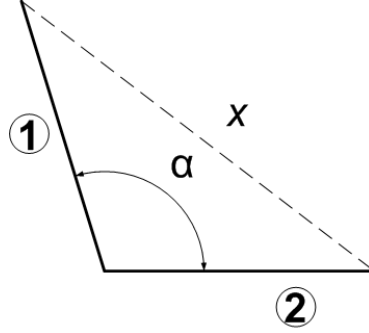


**Figure A.2:** Schematic diagram of surfaces 1 and 2 in the calculation of view factor 1

For surfaces 1 and 2 in Figure A.2, Equation A.1 can be written as

$$F_{1-2} = \frac{(L_1 + L_2) - x}{2L_1} \quad (\text{A.3})$$

where  $x$  can be expressed from the cosine law as

$$x^2 = L_1^2 + L_2^2 - 2L_1L_2 \cos \alpha \quad (\text{A.4})$$

Using Equation A.4 in Equation A.3 and taking  $AF = \frac{L_2}{L_1}$ ,  $F_{1-2}$  can be simplified as

$$F_{1-2} = \frac{AF + 1 - \sqrt{1 + AF^2 - 2AF \cos \alpha}}{2} \quad (\text{A.5})$$

The second expression developed is used to calculate the view factor between two surfaces separated by an angle  $\alpha$  that do not have a common edge (Figure A.3).

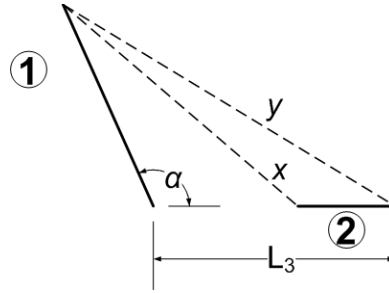


**Figure A.3:** Schematic diagram of surfaces 1 and 2 in the calculation of view factor 2

From Figure A.3, Equation A.1 can be expressed as

$$F_{1-2} = \frac{(L_3 + x) - (L_3 - L_2 + y)}{2L_1} = \frac{x - y + L_2}{2L_1} \quad (\text{A.6})$$

where  $L_3$  is considered to be a known variable and  $x$  and  $y$  correspond to

$$\begin{aligned} x^2 &= (L_3 - L_2)^2 + L_1^2 - 2L_1(L_3 - L_2) \cos \alpha \\ y^2 &= L_3^2 + L_1^2 - 2L_1L_3 \cos \alpha \end{aligned}$$

The third expression is used to calculate the view factor between two areas of same length that face each other as shown in Figure A.4.

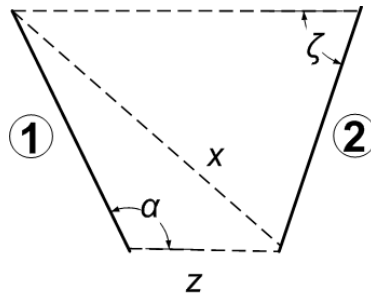


**Figure A.4:** Schematic diagram of surfaces 1 and 2 in the calculation of view factor 3

From Figure A.4, the view factor between surfaces 1 and 2 can be expressed as

$$F_{1-2} = \frac{2x - z - y}{2L_1} \quad (\text{A.7})$$

where  $z$  is considered to be a known variable and  $x$  and  $y$  are given as

$$\begin{aligned} x^2 &= z^2 + L_1^2 - 2L_1z \cos \alpha \\ y^2 &= L_1^2 + x^2 - 2xL_1 \cos (\alpha - \zeta) \end{aligned} \quad (\text{A.8})$$

In Equation A.8,  $\zeta$  is obtained from the sine law.

$$\frac{x}{\sin \alpha} = \frac{L_1}{\sin \zeta} \Rightarrow \zeta = \sin^{-1} \left( \frac{L_1 \sin \alpha}{x} \right)$$

The fourth expression is used to calculate the view factor between two areas of different length facing each other as shown in Figure A.5.

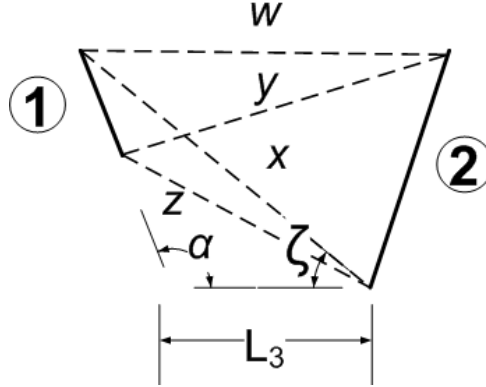


**Figure A.5:** Schematic diagram of surfaces 1 and 2 in the calculation of view factor 4

According to this Figure, the view factor between surface 1 and surface 2 can be expressed as

$$F_{1-2} = \frac{x + y - w - z}{2L_1} \quad (\text{A.9})$$

Considering  $\alpha$  and  $L_3$  to be known variables,  $z$ ,  $x$ ,  $w$  and  $y$  can be found from the cosine law.

$$\begin{aligned}
 z^2 &= (L_2 - L_1)^2 + L_3^2 - 2(L_2 - L_1)L_3 \cos \alpha \\
 x^2 &= L_2^2 + L_3^2 - 2L_2L_3 \cos \alpha \\
 w^2 &= L_2^2 + x^2 - 2L_2x \cos(x - \zeta) \\
 y^2 &= w^2 + L_1^2 - 2wL_1 \cos(180 - \alpha)
 \end{aligned} \tag{A.10}$$

In Equation A.10, the angle  $\zeta$  is given as

$$\frac{x}{\sin \alpha} = \frac{L_2}{\sin \zeta} \Rightarrow \zeta = \sin^{-1} \left( \frac{L_2 \sin \alpha}{x} \right)$$

The fifth expression is to calculate the view factor between two surfaces as shown in Figure A.6.

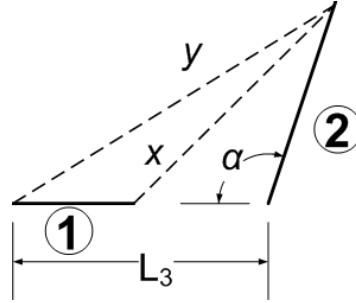


**Figure A.6:** Schematic diagram of surfaces 1 and 2 in the calculation of view factor 5

The view factor between surface 1 and surface 2 is given as

$$F_{1-2} = \frac{x + L_3 - ((L_3 - L_1) + y)}{2L_1} = \frac{x + L_1 - y}{2L_1}$$

where  $L_3$  is a known variable and  $x$  and  $y$  correspond to

$$\begin{aligned}
 x^2 &= (L_3 - L_1)^2 + L_2^2 - 2L_2(L_3 - L_1) \cos \alpha \\
 y^2 &= L_2^2 + L_3^2 - 2L_2L_3 \cos \alpha
 \end{aligned}$$

The sixth expression is to evaluate the view factor between two surfaces of different length facing each other as demonstrated in Figure A.7.

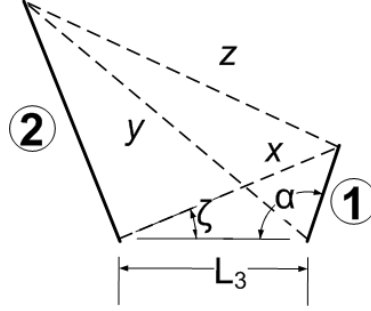


**Figure A.7:** Schematic diagram of surfaces 1 and 2 in the calculation of view factor 6

According to this figure,  $F_{1-2}$  can be expressed as

$$F_{1-2} = \frac{x + y - z - L_3}{2L_1} \quad (\text{A.11})$$

In Equation A.11,  $L_3$  is known and  $x$ ,  $y$  and  $z$  are given as

$$\begin{aligned} x^2 &= L_3^2 + L_1^2 - 2L_3L_1 \cos \alpha \\ y^2 &= L_3^2 + L_2^2 - 2L_3L_2 \cos \alpha \\ z^2 &= x^2 + L_2^2 - 2xL_2 \cos (\alpha - \zeta) \end{aligned}$$

where

$$\zeta = \sin^{-1} \left( \frac{L_1 \sin \alpha}{x} \right)$$

# Appendix B

## Method for Calculating the Shaded Portion

In order to find the shaded portion of a surface  $i$ ,  $P_{sh,i}$ , a two-step method is followed. The first step consists of identifying the shading case by comparing the comparison angle  $\theta_c$  to each one of the 5 shading cases. This comparison angle is the projection of the sun incidence angle on the cross-section plane of the surface on which the collector is mounted. The method used to find  $\theta_c$  is based on the work of Lee, Chung and Park (1987) assuming a surface of slope  $\beta_{col}$  mounted with an azimuth angle  $\gamma_{col}$  as shown in Figure B.1. The orientation of the surface relative to the cardinal points can be expressed with three unit vectors  $\vec{U}_{1,col}$ ,  $\vec{U}_{2,col}$  and  $\vec{U}_{3,col}$  defined as

$$\begin{aligned}\vec{U}_{1,col} &= -\cos \gamma_{col} \vec{i} + \sin \gamma_{col} \vec{j} \\ \vec{U}_{2,col} &= -\sin \gamma_{col} \cos \beta_{col} \vec{i} - \cos \beta_{col} \cos \gamma_{col} \vec{j} + \sin \beta_{col} \vec{k} \\ \vec{U}_{3,col} &= \vec{U}_{1,col} \times \vec{U}_{2,col} = \sin \gamma_{col} \sin \beta_{col} \vec{i} + \sin \beta_{col} \cos \gamma_{col} \vec{j} + \cos \beta_{col} \vec{k}\end{aligned}$$

The sun ray is represented by the vector  $\vec{S}$  and corresponds to

$$\vec{S} = \cos \alpha_s \sin \gamma_s \vec{i} + \cos \alpha_s \cos \gamma_s \vec{j} + \sin \alpha_s \vec{k}$$

By projection the vector  $\vec{S}$  on the  $(\vec{U}_{1,col}, \vec{U}_{3,col})$  plane, the comparison angle  $\theta_c$  is obtained.

$$\tan \theta_c = \left( \frac{\vec{S} \cdot \vec{U}_{3,col}}{\vec{S} \cdot \vec{U}_{1,col}} \right)$$

$$\tan \theta_c = \frac{\cos \alpha_s \sin \beta_{col} (\sin \gamma_s \sin \gamma_{col} + \cos \gamma_s \cos \gamma_{col}) + \sin \alpha_s \cos \beta_{col}}{\cos \alpha_s (\cos \gamma_s \sin \gamma_{col} - \cos \gamma_{col} \sin \gamma_s)}$$

$\theta_c$  is measured from the vector  $\vec{U}_{1,col}$  and is between  $-180^\circ$  and  $180^\circ$ , thus

$$\text{when } \vec{S} \cdot \vec{U}_{1,col} < 0 \text{ and } \vec{S} \cdot \vec{U}_{3,col} \geq 0 \implies \theta_c = \pi - \theta_c$$

$$\text{when } \vec{S} \cdot \vec{U}_{1,col} < 0 \text{ and } \vec{S} \cdot \vec{U}_{3,col} < 0 \implies \theta_c = \theta_c - \pi$$

$$\text{when } \vec{S} \cdot \vec{U}_{1,col} \geq 0 \text{ and } \vec{S} \cdot \vec{U}_{3,col} < 0 \implies \theta_c = -\theta_c$$

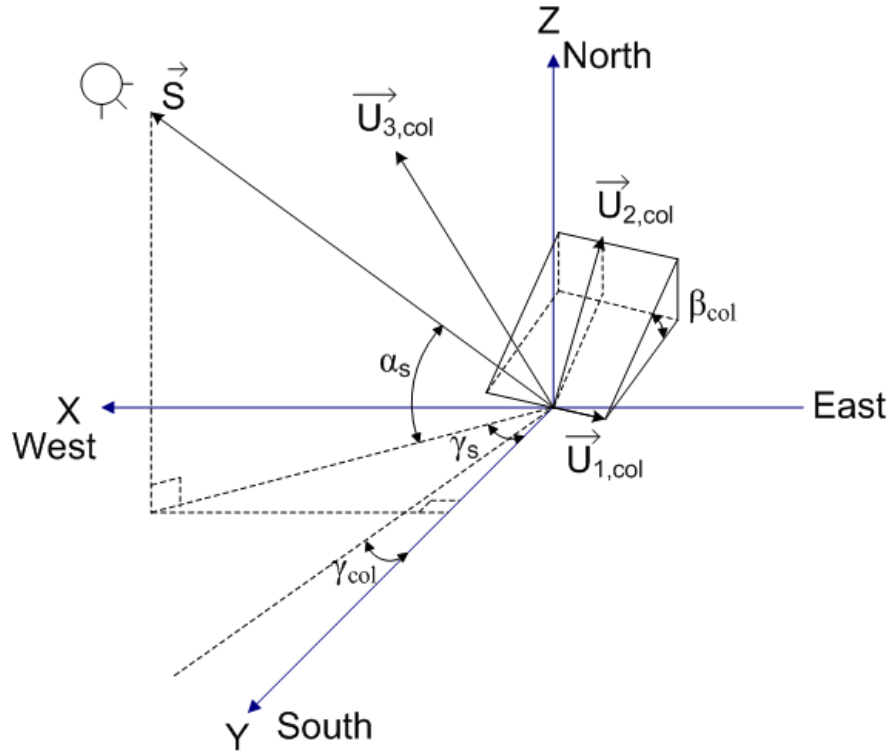


**Figure B.1:** Sun's position relative to the solar collector

There are 5 different shading cases, each delimited by a minimum and a maximum angle that are function of the dimensions of the collector as shown in Figure B.2.

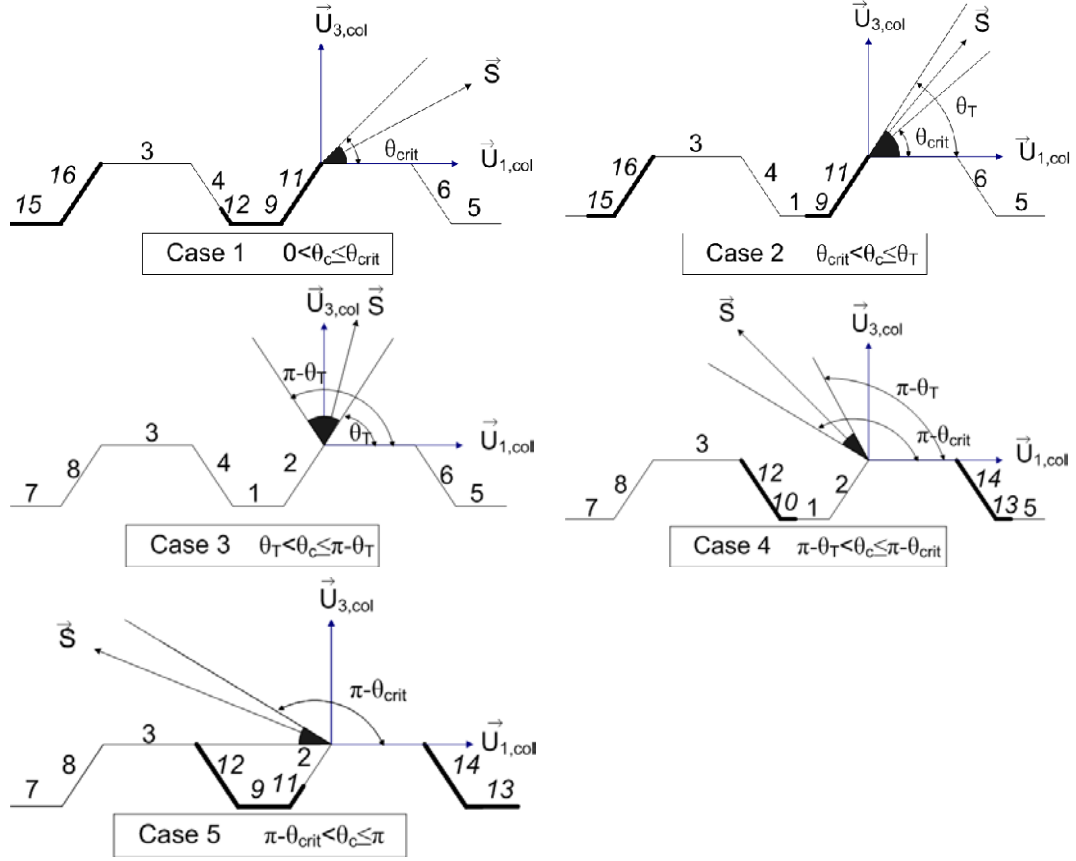


**Figure B.2:** Minimum and maximum angle delimiting the 5 shading cases

The second step consists of calculating the shaded portion of each surface by using the geometric variables of the collector. Defining the critical angle  $\theta_{crit}$  as

$$\theta_{crit} = \tan^{-1}\left(\frac{h_T}{d - a + \left(\frac{a-b}{2}\right)}\right) \quad (\text{B.1})$$

the shaded portion of each surface can be expressed

for case 1 as

$$P_{sh,4} = \frac{D_g \sin(\theta_{crit} - \theta_c)}{t_T \sin(\theta_c + \theta_T)} \quad (\text{B.2})$$

for case 2 as

$$P_{sh,1} = \frac{h_T - (\frac{a-b}{2})\tan\theta_c}{(d-a)\tan\theta_c} \quad (\text{B.3})$$

$$P_{sh,7} = \frac{h_T - (\frac{a-b}{2})\tan\theta_c}{W_{end}\tan\theta_c} \quad (\text{B.4})$$

for case 4 as

$$P_{sh,1} = \frac{h_T - (\frac{a-b}{2})\tan(\pi - \theta_c)}{(d-a)\tan(\pi - \theta_c)} \quad (\text{B.5})$$

$$P_{sh,1} = \frac{h_T - (\frac{a-b}{2})\tan(\pi - \theta_c)}{W_{end}\tan(\pi - \theta_c)} \quad (\text{B.6})$$

and for case 5 as

$$P_{sh,2} = \frac{D_g \sin(\theta_{crit} + \theta_c - \pi)}{t_T \sin(\pi - \theta_c + \theta_T)} \quad (\text{B.7})$$

# Appendix C

## PV/Thermal Collector Model

### Fortran Code

```

SUBROUTINE TYPE250 (TIME,XIN,OUT,T,DTDT,PAR,INFO,ICNTRL,*)
C*****
C Object: NewPV/Thermal UTC
C Simulation Studio Model: Type250
C
C Author: David Summers, 1995 (UTC model)
C Editor: Veronique Delisle, 2007 (PV/Thermal UTC model)
C       Changes were made to account for the wind effects,
C       the corrugated shape of the plate (absorbed solar
C       energy) and the fact that PV cells are mounted
C       on the absorber plate
C Last modified: November 19, 2007
C
C This models predicts the thermal and electrical performance of a
C PV/Thermal Collector unglazed transpired collector with PV cells
C mounted directly on the absorber plate. The absorber plate has a
C trapezoidal corrugated shape. In Mode 1, the collector
C is solved as a stand-alone UTC. In Mode 2, the PV cells can be
C mounted only on the top surfaces of the corrugation. In Mode 3,
C the PV cells can be mounted on every surface of the collector.
C ***
C *** Model Parameters
C ***
C       Length of the base of the trapezoid      m [0;+Inf]
C       Length of the top of the trapezoid      m [0;+Inf]
C       Ribs height                             m [0;+Inf]
C       Plate porosity                          - [0;1]
C       Hole pitch                              m [0;+Inf]
C       Plate length                            m [0;+Inf]
C       Distance between 2 corrugations         m [0;+Inf]
C       Plate width                             m [0;+Inf]
C       Absorbance of the wall/roof on which the collector is mounted - [0;1]
C       Gap between the corrugated plate and the wall m [0;+Inf]
C       Back of the collector emissivity        - [0;1]
C       Wall emissivity                        - [0;1]
C       Collector thickness - [0;+Inf]

```

```

C Panel absorptance - [0;1]
C Collector surface emissivity - [0;1]
C Overall loss coefficient of the building wall kJ/hr.m^2.K [0;+Inf]
C PV Mode - [1;3]
C Efficiency modifier-Temperature - [-Inf;+Inf]
C PV efficiency at reference conditions - [0;1]
C PV cell reference temperatureC [-Inf;+Inf]
C PV absorptance-transmittance product - [0;1]
C PV emissivity - [0;1]
C Bypass collector in the symmer [1:yes,0:NO] - [0;1]
C Bypass temperatureC [-Inf;+Inf]
C PV cells glazing refraction index - [0;+Inf]
C PV cells galzing extinction coefficient m^-1 [0;+Inf]
C PV cells glazing thickness m [0;+Inf]
C Proportion of PV cells on the surface at the top of the corrugation- [0;1]
C Proportion of PV cells on the surface at the bottom of the corr. [0;1]
C Proportion of PV cells on the surface on the sides of the grooves - [0;1]
C ***
C *** Model Inputs
C ***
C Beam radiation on the collector surface kJ/hr.m^2 [-Inf;+Inf]
C Sky diffuse radiation on the collector surface kJ/hr.m^2 [-Inf;+Inf]
C Ground reflected diffuse on the collector surface kJ/hr.m^2 [-Inf;+Inf]
C Horizontal beam radiation kJ/hr.m^2 [-Inf;+Inf]
C Incidence angle on the horizontal surface degrees [-Inf;+Inf]
C Solar azimuth angledegrees [-Inf;+Inf]
C Wind velocity m/s [-Inf;+Inf]
C Ambient temperature C [-Inf;+Inf]
C Ambient pressure Pa [-Inf;+Inf]
C Incidence angle on the collector surface degrees [-Inf;+Inf]
C Building temperature C [-Inf;+Inf]
C Sky temperature C [-Inf;+Inf]
C Minimum air flow rate through the collector kg/hr [-Inf;+Inf]
C Maximum air flow rate through collector kg/hr [-Inf;+Inf]
C Collector slope degrees [-Inf;+Inf]
C Azimuth angle degrees [-Inf;+Inf]
C Gound reflectance - [-Inf;+Inf]
C Total horizontal radiation kJ/hr.m^2 [-Inf;+Inf]
C Horizontal diffuse radiation kJ/hr.m^2 [-Inf;+Inf]
C Temperature of the air that needs to be supplied to the building[-Inf;+Inf]
C ***
C *** Model Outputs
C ***
C Collector surface temperatureC [-Inf;+Inf]
C Plenum temperature C [-Inf;+Inf]
C Mixed temperature C [-Inf;+Inf]
C Collector outlet temperature C [-Inf;+Inf]
C Mass fraction of outside air - [-Inf;+Inf]
C Mass fraction of recirculated air - [-Inf;+Inf]
C Mass flow rate of air through the collector kg/hr [-Inf;+Inf]
C Collector heat exchange effectiveness - [-Inf;+Inf]
C Collector thermal efficiency - [-Inf;+Inf]
C Collector electrical efficiency - [-Inf;+Inf]
C PV cells efficiency - [-Inf;+Inf]
C Collector useful energy W [-Inf;+Inf]
C Maximum electrical power output W [-Inf;+Inf]
C Reduced wall heat losses W [-Inf;+Inf]
C Collector is bypassed: NO=0, YES=1 - [0;1]
C Absorbed solar energy W/m^2 [-Inf;+Inf]
C*****
C TRNSYS access functions (allow to access TIME etc.)
USE TrnsysConstants

```

```

USE TrnsysFunctions
C-----
C REQUIRED BY THE MULTI-DLL VERSION OF TRNSYS
!DEC$ATTRIBUTES DLLEXPORT :: TYPE250 !SET THE CORRECT TYPE NUMBER HERE
C-----
C TRNSYS DECLARATIONS
IMPLICIT NONE !REQUIRES THE USER TO DEFINE ALL VARIABLES BEFORE USING THEM

      DOUBLE PRECISION XIN,OUT,TIME,PAR,STORED,T,DTDT
      INTEGER*4 INFO(15)
      INTEGER*4 NP,NI,NOUT,ND
      INTEGER*4 NPAR,NIN,NDER
      INTEGER*4 IUNIT,ITYPE
      INTEGER*4 ICNTRL
      INTEGER*4 NSTORED
      CHARACTER*3 OCHECK,YCHECK
C-----
C USER DECLARATIONS - SET THE MAXIMUM NUMBER OF PARAMETERS (NP), INPUTS (NI),
C OUTPUTS (NOUT), AND DERIVATIVES (ND) THAT MAY BE SUPPLIED FOR THIS TYPE
PARAMETER (NP=30,NI=20,NOUT=16,ND=0,NSTORED=0)
C-----
C REQUIRED TRNSYS DIMENSIONS
DIMENSION XIN(NI),OUT(NOUT),PAR(NP),YCHECK(NI),OCHECK(NOUT),
          1 STORED(NSTORED),T(ND),DTDT(ND)
INTEGER NITEMS
C-----
C COMMON BLOCK DEFINITIONS
C Common variables
COMMON/PVT/a,b,h_trap,d,pitch,length,dist,width
COMMON/PVT/hp,e_back,e_wall,th,Uwall,EffT,EffRef,Tref
COMMON/PVT/PPV,Uwind,Tamb,Tblg,Tsup,hfilm
COMMON/PVT/Flow,Gam,t_trap,ThetaT,Por,rho_amb,visc_amb
COMMON/PVT/AreaW,k_amb,ecol,Trad,L,cp_amb,Area_cs
COMMON/PVT/QBsurf,QDsurf,Qsurf,Psh,Area,AlphaB,AlphaDcoll
COMMON/PVT/PVOn,SHCASE,nb_corr,PVMode
C-----
C ADD DECLARATIONS AND DEFINITIONS FOR THE USER-VARIABLES HERE
C PARAMETERS
DOUBLE PRECISION a,b,h_trap,d,pitch,length,dist,width,AlphaW
DOUBLE PRECISION hp,e_back,e_wall,th,AlphaPl,e_coll,Uwall
DOUBLE PRECISION EffT,EffRef,Tref,TauAlfPV,e_pv,Tbypass
DOUBLE PRECISION Kgl,Lgl,ngl
DOUBLE PRECISION PPV
C INPUTS
DOUBLE PRECISION GbW,GdW,GgW,GbH
DOUBLE PRECISION ThetaZ,GammaS,Uwind,Tamb,Patm,ThetabW
DOUBLE PRECISION Tblg,Tsky,MinFlow,MFlow,betaW,GammaW
DOUBLE PRECISION GrndRef,Gh,GdH,Tsup
C INTERNAL AND COMMON VARIABLES
DOUBLE PRECISION Gb,Gd,Gg,GamMIN,Theta,Beta,lowg,hig,oldg,difg
DOUBLE PRECISION t_trap,ThetaT,diag,Por,rho_amb,Gam
DOUBLE PRECISION T_comp,T_crit,Trad,visc_amb,Flow,ThetaEnd,k_amb
DOUBLE PRECISION Gamma,Thetar,Tau_a,TauC,Thetar_0,Tau_0
DOUBLE PRECISION Thetard,Thetarg,Tau_ad,Tau_ag,Taud,Taug,hrad_wc
DOUBLE PRECISION prop_sh,Area,L,PS
DOUBLE PRECISION AlphaDcoll,AlphaB,cp_amb,Wend,ecol,Area_cs
DOUBLE PRECISION Tground,AreaW,Zeta,FB,FD
DOUBLE PRECISION mx_dd,ma_augmdd,ma_augmdb,mx_db,ma_augmdg,mx_dg
DOUBLE PRECISION Jdb,Gdb,Jdd,Gdd,Jdg,Gdg,Rb
DOUBLE PRECISION QBsurf,QDsurf,Qsurf,Psh
DOUBLE PRECISION RhoB,RhoGcoll,AlphaG,SsU1,SsU2,AlphaS
DOUBLE PRECISION RhoDColl,ThetadW,ThetagW

```

```

DOUBLE PRECISION EffPV, QE, EffEI, EffTh, QradW, PropPV
DOUBLE PRECISION hfilm, Tsa, QredW, Qpot, Tmix, FCS, FCG
DOUBLE PRECISION Time0, TFINAL, DELT
C PVTrcSOLVE Variables
DOUBLE PRECISION Tcol, Tplen, Qrad_cs, Qrad_wc, Twall
DOUBLE PRECISION Qconv_wa, Qwind, Qconv_ca, Qcond_wT, Qabs
DOUBLE PRECISION Tout, Vs, Qu, effhx, hwall_UTC
C CONSTANTS
DOUBLE PRECISION PI, Rair, SB, G

INTEGER*4 PVmode, BypTemp
INTEGER*4 nb_surf, Bypass, PVSurf, PVOOn
INTEGER*4 i, j, K, nb_case, N, NbJ, SHCASE, FPASS, nb_corr, COUNT

PARAMETER (nb_case=5, nbJ=11, nb_surf=8)

DIMENSION PPV(nb_surf)
DIMENSION Gamma(nbJ), Theta(nbJ), Beta(nbJ), Gd(nbJ), Gg(nbJ), Rb(nbJ)
DIMENSION mx_dd(nbJ), Jdd(NbJ), Jdg(NbJ), mx_dg(nbJ), Gdg(nb_surf)
DIMENSION Gb(nb_surf), Psh(nb_surf), Area(nb_surf)
DIMENSION RhoB(nb_surf), RhoGcoll(nb_surf), PVSurf(nb_surf)
DIMENSION RhoDColl(nb_surf*2), L(nb_surf*2), Jdb(nb_surf*2)
DIMENSION mx_db(nb_surf*2), ma_augmdb((nb_surf*2), ((nb_surf*2)+1))
DIMENSION Gdb(nb_surf*2), FB((nb_surf*2), (nb_surf*2))
DIMENSION prop_sh(nb_surf, (nb_case+1)), Gdd(nb_surf)
DIMENSION PS(nb_surf), QBSurf(nb_surf), QDsurf(nb_surf)
DIMENSION Qsurf(nb_surf), PVOOn(nb_surf), AlphaG(nb_surf)
DIMENSION ma_augmdd(nbJ, (nbJ+1)), ma_augmdg(nbJ, (nbJ+1))
DIMENSION FD(NbJ, NbJ), AlphaB(nb_surf), AlphaDcoll(nb_surf)
DIMENSION Thetar(nb_surf), Tau_a(nb_surf), TauC(nb_surf)
-----
C DATA STATEMENTS
C DATA PI/3.141592654/, Rair/0.2870/, g/9.8/
DATA YCHECK/'IR1','IR1','IR1','IR1','DG1','DG1','VE1','TE1',
& 'PR3','DG1','TE1','TE1','MF1','MF1','DG1','DG1','DM1',
& 'IR1','IR1','TE1'/
DATA OCHECK/'TE1','TE1','TE1','TE1','DM1','DM1','MF1','DM1',
& 'DM1','DM1','DM1','PW2','PW2','PW2','DM1','IR2'/
-----
C TRNSYS FUNCTIONS
C TIME0=getSimulationStartTime()
C TFINAL=getSimulationStopTime()
C DELT=getSimulationTimeStep()
-----
C SET THE VERSION INFORMATION FOR TRNSYS
IF(INFO(7).EQ.-2) THEN
INFO(12)=16
RETURN 1
ENDIF
-----
C DO ALL THE VERY LAST CALL OF THE SIMULATION MANIPULATIONS HERE
IF (INFO(8).EQ.-1) THEN
RETURN 1
ENDIF
-----
C PERFORM ANY 'AFTER-ITERATION' MANIPULATIONS THAT ARE REQUIRED HERE
IF (INFO(13).GT.0) THEN
RETURN 1
ENDIF
-----
C DO ALL THE VERY FIRST CALL OF THE SIMULATION MANIPULATIONS HERE
IF (INFO(7).EQ.-1) THEN

```

```

C   SET SOME INFO ARRAY VARIABLES TO TELL THE TRNSYS ENGINE HOW THIS TYPE IS TO WORK
      IUNIT=INFO(1)
      ITYPE=INFO(2)
      INFO(6)=NOUT
      INFO(9)=1
      INFO(10)=0      !STORAGE FOR VERSION 16 HAS BEEN CHANGED

C   SET THE REQUIRED NUMBER OF INPUTS, PARAMETERS AND DERIVATIVES THAT THE USER
      SHOULD SUPPLY IN THE INPUT FILE
      NIN=NI
      NPAR=NP
      NDER=ND

C   CALL THE TYPE CHECK SUBROUTINE TO COMPARE WHAT THIS COMPONENT REQUIRES TO
      WHAT IS SUPPLIED IN
C   THE TRNSYS INPUT FILE
      CALL TYPECK(1,INFO,NIN,NPAR,NDER)
      CALL RCHECK(INFO,YCHECK,OCHECK)
C   RETURN TO THE CALLING PROGRAM
      RETURN 1
      ENDIF
C-----
C   DO ALL OF THE INITIAL TIMESTEP MANIPULATIONS HERE
      IF (TIME .LT.(TIME0+DELT/2.D0)) THEN

C   SET THE UNIT NUMBER FOR FUTURE CALLS
      IUNIT=INFO(1)
      ITYPE=INFO(2)

C   Read the values of the parameters in sequential order
      a=PAR(1)
      b=PAR(2)
      h_trap=PAR(3)
      Por=PAR(4)
      pitch=PAR(5)
      length=PAR(6)
      dist=PAR(7)
      width=PAR(8)
      AlphaW=PAR(9)
      hp=PAR(10)
      e_back=PAR(11)
      e_wall=PAR(12)
      th=PAR(13)
      AlphaPl=PAR(14)
      e_coll=PAR(15)
      Uwall=PAR(16)
      PVMode=PAR(17)
      EffT=PAR(18)
      EffRef=PAR(19)
      Tref=PAR(20)
      TauAlfPV=PAR(21)
      e_PV=PAR(22)
      BypTemp=PAR(23)
      Tbypass=PAR(24)
      ngl=PAR(25)
      kgl=PAR(26)
      Lgl=PAR(27)
      PPV(3)=PAR(28)
      PPV(1)=PAR(29)
      PPV(2)=PAR(30)

```

C CHECK THE PARAMETERS FOR PROBLEMS AND RETURN FROM THE SUBROUTINE IF AN ERROR IS FOUND

```
IF(a.LE.0) CALL TYPECK(-4,INFO,0,1,0)
IF(b.GE.a) CALL TYPECK(-4,INFO,0,2,0)
IF(b.LE.0) CALL TYPECK(-4,INFO,0,2,0)
IF(h_trap.LE.0) CALL TYPECK(-4,INFO,0,3,0)
IF(Por.LE.0) CALL TYPECK(-4,INFO,0,4,0)
IF(pitch.LE.0) CALL TYPECK(-4,INFO,0,5,0)
IF(length.LE.0.OR.length.LE.a.OR
& length.LE.b) CALL TYPECK(-4,INFO,0,6,0)
IF(a.GE.dist.OR.dist.LE.0) CALL TYPECK(-4,INFO,0,7,0)
IF(width.LE.dist.OR.width.LE.0) CALL TYPECK(-4,INFO,0,8,0)
IF(AlphaW.LE.0.OR.AlphaW.GT.1)CALL TYPECK(-4,INFO,0,9,0)
IF(hp.LE.0)CALL TYPECK(-4,INFO,0,10,0)
IF(e_back.LT.0.OR.e_back.GT.1) CALL TYPECK(-4,INFO,0,11,0)
IF(e_wall.LT.0.OR.e_wall.GT.1) CALL TYPECK(-4,INFO,0,12,0)
IF(th.LE.0) CALL TYPECK(-4,INFO,0,13,0)
IF(AlphaPl.LE.0.OR.AlphaPl.GE.1) CALL TYPECK(-4,INFO,0,14,0)
IF(e_coll.LT.0.OR.e_coll.GT.1) CALL TYPECK(-4,INFO,0,15,0)
IF(Uwall.LE.0) CALL TYPECK(-4,INFO,0,16,0)
IF(PVMode.LT.1.OR.PVMode.GT.3) CALL TYPECK(-4,INFO,0,17,0)
IF(EffRef.LE.0.OR.EffRef.GT.1) CALL TYPECK(-4,INFO,0,19,0)
IF(TauAlfPV.LT.0.OR.TauAlfPV.GT.1) CALL TYPECK(-4,INFO,21,0)
IF(e_PV.LE.0.OR.e_PV.GT.1) CALL TYPECK(-4,INFO,22,0)
IF(BypTemp.LT.0.OR.BypTemp.GT.1)CALL TYPECK(-4,INFO,24,0)
IF(PPV(3).LT.0.OR.PPV(3).GT.1)CALL TYPECK(-4,INFO,28,0)
IF(PPV(1).LT.0.OR.PPV(1).GT.1)CALL TYPECK(-4,INFO,29,0)
IF(PPV(2).LT.0.OR.PPV(2).GT.1)CALL TYPECK(-4,INFO,30,0)
```

RETURN 1  
ENDIF

C-----  
C RE-READ IN THE VALUES OF THE PARAMETERS IN SEQUENTIAL ORDER  
IF(INFO(1).NE.IUNIT) THEN

C RESET THE UNIT NUMBER  
IUNIT=INFO(1)  
ITYPE=INFO(2)

```
a=PAR(1)
b=PAR(2)
h_trap=PAR(3)
Por=PAR(4)
pitch=PAR(5)
length=PAR(6)
dist=PAR(7)
width=PAR(8)
AlphaW=PAR(9)
hp=PAR(10)
e_back=PAR(11)
e_wall=PAR(12)
th=PAR(13)
AlphaPl=PAR(14)
e_coll=PAR(15)
Uwall=PAR(16)
PVMode=PAR(17)
EffT=PAR(18)
EffRef=PAR(19)
Tref=PAR(20)
TauAlfPV=PAR(21)
e_PV=PAR(22)
BypTemp=PAR(23)
```

```

Tbypass=PAR(24)
  ngl=PAR(25)
  kgl=PAR(26)
  Lgl=PAR(27)
  PPV(3)=PAR(28)
  PPV(1)=PAR(29)
  PPV(2)=PAR(30)
ENDIF

C  RETRIEVE THE CURRENT VALUES OF THE INPUTS TO THIS MODEL FROM THE XIN ARRAY
  GbW=XIN(1)
  GdW=XIN(2)
  GgW=XIN(3)
  GbH=XIN(4)
  ThetaZ=XIN(5)
  GammaS=XIN(6)
  Uwind=XIN(7)
  Tamb=XIN(8)
  Patm=XIN(9)
  ThetabW=XIN(10)
  Tblg=XIN(11)
  Tsky=XIN(12)
  MinFlow=XIN(13)
  MFlow=XIN(14)
  BetaW=XIN(15)
  GammaW=XIN(16)
  GrndRef=XIN(17)
  Gh=XIN(18)
  GdH=XIN(19)
  Tsup=XIN(20)

C  CHECK THE INPUTS FOR PROBLEMS
IF(Uwind.LT.0.) CALL TYPECK(-3,INFO,7,0,0)
IF(Patm.LT.0.) CALL TYPECK(-3,INFO,9,0,0)
  IF(MinFlow.LT.0)CALL TYPECK(-3,INFO,13,0,0)
  IF(MFlow.LT.0)CALL TYPECK(-3,INFO,14,0,0)
  IF(MinFlow.GT.MFlow)CALL TYPECK(-3,INFO,14,0,0)
  IF(GrndRef.GT.1)CALL TYPECK(-3,INFO,17,0,0)

  IF(ErrorFound()) RETURN 1

C  SET THE PROPORTION OF PV CELLS ON EACH SURFACE
DO i=1,nb_surf
  PVsurf(i)=0
ENDDO

IF (PVMODE.EQ.1)THEN
  DO i=1,nb_surf
    PPV(i)=0.0
    PVsurf(i)=0
  ENDDO
ELSE IF (PVMODE.EQ.2)THEN
  DO i=1,nb_surf
    IF (i.EQ.3) THEN
      PPV(i)=PPV(i)
      PVsurf(i)=1
    ELSE
      PPV(i)=0.0
      PVsurf(i)=0
    ENDIF
  ENDDO
ELSE

```

```

DO i=1,nb_surf
    IF (i.LE.4)THEN
        PPV(i)=PPV(i)
        PVsurf(i)=1
    ELSE
        PPV(i)=0.0
        PVsurf(i)=0
    ENDIF
ENDDO
ENDIF

IF (MFlow.LE.0.0)THEN
    GamMIN=0.0
ELSE
    GamMIN=MinFlow/MFlow
ENDIF
C   CALCULATE DIAMETER WITH THE RELATION OF Van Decker
D=((4*POR*Pitch*Pitch)/PI)**0.5
*****
C   SET CONSTANTS VALUE
SB=(5.67e-8)*3.6 !Stefan Boltzmann constant [kJ/hr*m2*K4]

C   MODIFY AND CONVERT PARAMETERS & INPUTS
Uwind=Uwind*3600 !Convert m/s in m/h
Tamb=Tamb+273.15
Tsup=Tsup+273.15
Tb1g=Tb1g+273.15
Tsky=Tsky+273.15
Tground=Tamb

C   SET FILM COEFFICIENT TO 15 W/m2 C [ENERMODAL, 1994]
hfilm=15.0*3.6 !Film heat transfer coefficient [kJ/hm2C]

C   CALCULATE TRAD
FCS=(1-COSD(BetaW))/2.0
FCG=(1-COSD(BetaW))/2.0
Trad=((Tground**4)*FCG)+((Tsky**4)*FCS)**0.25

C   CALCULATE TOTAL RADIATION ON THE COLLECTOR SURFACE
QradW=Gbw+GdW+GgW

C   IF NIGHTTIME, THE COLLECTOR IS AUTOMATICALLY BYPASSED
Bypass=0
IF(QradW.LT.1.0)THEN
    Bypass=1
    GO TO 110
ENDIF

C   IF SUMMER, BYPASS COLLECTOR WHEN THE BYPASS OPTION IS SET TO 1
IF (Tamb.GT.(Tbypass+273.15))THEN
    IF(BypTemp.GE.1)THEN
        Bypass=1
    ELSE
        Bypass=0
    ENDIF
ELSE
    Bypass=0
ENDIF

110 CONTINUE
*****
C   CALCULATE PV/THERMAL COLLECTOR GEOMETRIC CONSTANTS AND

```

```

C      AREA FOR EACH SURFACE INCLUDING HOLES
*****
t_trap=sqrt((h_trap**2)+(((a-b)/2)**2))![m]
ThetaT=asin(h_trap/t_trap) ![rad]
ThetaEnd=ATAN(h_trap/(((a-b)/2)+Wend))
diag=(((dist-((a+b)/2))**2)+(h_trap**2))**0.5
nb_corr=AINT((width+dist-a)/dist)
Wend=(width-a-(dist*nb_corr)+dist)/2

i=1
DO i=1,nb_surf
    Area(i)=0.0
ENDDO

Area(1)=(dist-a)*length
Area(2)=t_trap*length
Area(3)=b*length
Area(4)=Area(2)
Area(5)=Wend*length
Area(6)=Area(2)
Area(7)=Area(5)
Area(8)=Area(2)

AreaW=width*length
Area_cs=(width*hp)+(nb_corr*h_trap*((a+b)/2))
*****
C      CALCULATE AIR PROPERTIES AT AMBIENT TEMPERATURE WITH IDEAL GAS LAW
C      AND SUTHERLAND LAW
*****
rho_amb=(Patm*0.001)/(Rair*Tamb) ![kg/m3]
visc_amb=(((1.71e-5)*(Tamb/273)**1.5)*((273+110.4)/
& (Tamb+110.4)))**3600 ![kg/mh]
cp_amb=(28.11+(0.001967*Tamb)+(0.4802e-5*Tamb*Tamb)-
& (1.966e-9*Tamb*Tamb*Tamb))*(1/28.97) ![kJ/kgK]
k_amb=(((2.414e-2)*(Tamb/273)**1.5)*((273+194.4)/
& (Tamb+194.4)))**3.6 ![kJ/mC]

Flow=Mflow/rho_amb ![m3/hr]
*****
C      CALCULATE SOLAR ANGLES AND IRRADIATION FOR EACH SURFACE
*****
DO i=1,NbJ
    Gamma(i)=0.0
    Beta(i)=0.0
    Theta(i)=0.0
    Rb(i)=0.0
    Gg(i)=0.0
    Gd(i)=0.0
ENDDO

C      AZIMUTH ANGLE (Gamma)
DO i=1,9,2
    Gamma(i)=GammaW ![deg]
ENDDO

Gamma(2)=GammaW+ACOSD(SIND(BetaW)*COS(ThetaT)) ![deg]
Gamma(4)=GammaW-ACOSD(SIND(BetaW)*COS(ThetaT)) ![deg]
Gamma(6)=Gamma(4)
Gamma(8)=Gamma(2)
Gamma(10)=GammaW+ACOSD(SIND(BetaW)*COS(ThetaEnd)) ![deg]
Gamma(11)=GammaW-ACOSD(SIND(BetaW)*COS(ThetaEnd)) ![deg]

```

```

DO i=1,NbJ
    IF(Gamma(i).GT.180)THEN
        Gamma(i)=Gamma(i)-360.0
    ELSE IF(Gamma(i).LT.(-1.0*180.0))THEN
        Gamma(i)=Gamma(i)+360.0
    ENDIF
ENDDO

C    SLOPE (Beta)
DO i=1,9,2
    Beta(i)=BetaW
ENDDO

DO i=2,8,2
    Beta(i)=ACOSD(COS(ThetaT)*COSD(BetaW)) ![deg]
ENDDO
Beta(10)=ACOSD(COS(ThetaEnd)*COSD(BetaW))    ![deg]
Beta(11)=ACOSD(COS(ThetaEnd)*COSD(BetaW))

C    INCIDENCE ANGLE (Theta)
DO i=1,NbJ
    Theta(i)=ACOSD((COSD(ThetaZ)*COSD(Beta(i)))+
    & (SIND(ThetaZ)*SIND(Beta(i))*COSD(GammaS-Gamma(i))))    !DEG
ENDDO

C    SKIP THIS STEP WHEN NO RADIATION ON THE COLLECTOR
IF (QradW.LE.(1.0)) GO TO 150

C    CALCULATE RATIO OF BEAM RADIATION (Rb)
DO i=1,NbJ
    IF(COSD(ThetaZ).LE.0.001)THEN
        Rb(i)=COSD(Theta(i))/0.001
    ELSE
        Rb(i)=(MAX(0.0,(COSD(Theta(i)))))/(COSD(ThetaZ))
    ENDIF
ENDDO

C    BEAM RADIATION ON EACH SURFACE (Gb)-ONLY FOR REAL SURFACES
DO i=1,nb_surf
    Gb(i)=Rb(i)*GbH
ENDDO

C    GROUND REFLECTED RADIATION ON EVERY FICTITIOUS SURFACE (Gg)
C    SKY DIFFUSE RADIATION ON EVERY FICTITIOUS SURFACE (Gd)
C    ISOTROPIC MODEL
Gg(9)=GgW
Gd(9)=GdW
DO i=10,11
    Gg(i)=0.5*(1-(COSD(Beta(i))))*GrndRef*Gh
    Gd(i)=GdH*(1+((COSD(Beta(i)))/2.0))
ENDDO

DO i=9,11
    IF (Gg(i).LE.0.001)THEN
        Gg(i)=0.0
        Gd(i)=0.0
    ENDIF
ENDDO
GO TO 160

150 CONTINUE
DO i=1,Nb_surf

```

```

Gb(i)=0.0
      Gd(i)=0.0
      Gg(i)=0.0
      ENDDO
160  CONTINUE
*****
C    CALCULATE SOLAR OPTICAL PROPERTIES FOR EACH SURFACE
*****
      DO i=1,nb_surf
          AlphaB(i)=0.0
          AlphaG(i)=0.0
          RhoB(i)=0.0
          RhoGcoll(i)=0.0

          Thetar(i)=0.0
          Tau_a(i)=0.0
          TauC(i)=0.0
      ENDDO

C    EFFECTIVE SKY DIFFUSE AND GROUND REFLECTED ANGLES [DUFFIE AND BECKMAN, 1991]
ThetadW=59.68-(0.1388*BetaW)+(0.001497*BetaW*BetaW)
ThetaGW=90.0-(0.5788*BetaW)+(0.002693*BetaW*BetaW)

      IF (Lgl.LE.0.001)GO TO 170

      DO i=1,nb_surf
          Thetar(i)=ASIND(SIND(Theta(i))/ngl)
          Tau_a(i)=exp(-1*Kgl*Lgl/COSD(Thetar(i)))
          TauC(i)=Tau_a(i)*(1-(0.5*(((SIND(Thetar(i)-Theta(i)))**2)/
&          ((SIND(Thetar(i)+Theta(i)))**2))+
&          (((TAND(Thetar(i)-Theta(i)))**2)/
&          ((TAND(Thetar(i)+Theta(i)))**2))))))
      ENDDO

      DO i=1,nb_surf
          Thetar(i)=Thetar(i)
          Tau_a(i)=Tau_a(i)
          TauC(i)=TauC(i)
      ENDDO

      Tau_0=exp(-1*Kgl*Lgl)*(1-(((ngl-1)/(ngl+1))**2)/
&          (1+(((ngl-1)/(ngl+1))**2)))

      Thetard=ASIND(SIND(ThetadW)/ngl)
      Thetarg=ASIND(SIND(ThetagW)/ngl)

      Tau_ad=exp(-1*Kgl*Lgl/COSD(Thetard))
      Tau_ag=exp(-1*Kgl*Lgl/COSD(Thetarg))

      Taud=Tau_ad*(1-(0.5*(((SIND(Thetard-ThetadW))**2)/
&          ((SIND(Thetard+ThetadW))**2))+
&          (((TAND(Thetard-ThetadW))**2)/
&          ((TAND(Thetard+ThetadW))**2))))))
      Taug=Tau_ag*(1-(0.5*(((SIND(Thetarg-ThetagW))**2)/
&          ((SIND(Thetarg+ThetagW))**2))+
&          (((TAND(Thetarg-ThetagW))**2)/
&          ((TAND(Thetarg+ThetagW))**2))))))

      DO i=1,nb_surf

          Rhob(i)=PPV(i)*(1-TauC(i)-(1-Tau_a(i)))+((1-PPV(i))*(1-AlphaPl))

```

```

Rhogcoll(i)=PPV(i)*(1-Taug-(1-Tau_ag))+((1-PPV(i))*(1-AlphaPl))
RhoDcoll(i)=PPV(i)*(1-Taud-(1-Tau_ad))+((1-PPV(i))*(1-AlphaPl))

Alphab(i)=(PPV(i)*(TauC(i)/Tau_0)*TauAlfPV)+((1-PPV(i))*AlphaPl)
Alphadcoll(i)=(PPV(i)*(Taud/Tau_0)*TauAlfPV)+((1-PPV(i))*AlphaPl)

ENDDO

170 CONTINUE
C IF NO GLAZING ON THE PV CELLS, DO NOT TAKE INTO ACCOUNT THE
C EFFECT OF THE INCIDENCE ANGLE
C IF (Lgl.LE.0.001)THEN
DO i=1,nb_surf
Rho(i)=(PPV(i)*(1-TauAlfPV))+((1-PPV(i))*(1-AlphaPl))
Rhogcoll(i)=(PPV(i)*(1-TauAlfPV))+((1-PPV(i))*(1-AlphaPl))
RhoDcoll(i)=(PPV(i)*(1-TauAlfPV))+((1-PPV(i))*(1-AlphaPl))

Alphab(i)=(PPV(i)*TauAlfPV)+((1-PPV(i))*AlphaPl)
Alphadcoll(i)=(PPV(i)*TauAlfPV)+((1-PPV(i))*AlphaPl)
ENDDO
ENDIF

C SET RHOB, RHOD AND RHOG FOR EACH SURFACE
C RHODCOLL(9 TO 16) ARE THE SHADED SURFACES TO CALCULATE THE BEAM DUE TO BEAM
C RADIATION
RhoDcoll(10)=RhoDcoll(1)
RhoDcoll(9)=RhoDcoll(1)

DO i=11,16
RhoDcoll(i)=RhoDcoll(i-nb_surf)
ENDDO

C CALCULATE COLLECTOR EMISSIVITY AS A WEIGHTED AVERAGE OF THE
C PANEL AND PV CELLS EMISSIVITIES
IF (PVMODE.EQ.1)THEN
PropPV=0.0
ecol=e_coll

ELSEIF (PvMode.EQ.2)THEN
PropPV=PPV(3)*Area(3)*Nb_corr/(AreaW)
ecol=((1-PropPV)*e_coll)+(PropPV*e_pv)

ELSE
PropPV=((PPV(1)*Area(1)*(Nb_corr-1))+
& (PPV(3)*Area(3)*Nb_corr)+
& (PPV(2)*Area(2)*(Nb_corr-1)*cos(ThetaT))+
& (PPV(4)*Area(4)*(Nb_corr-1)*cos(ThetaT)))/AreaW
ecol=((1-PropPV)*e_coll)+(PropPV*e_pv)
ENDIF

*****
C FIND SHADING PORTION AND VIEW FACTORS
*****
AlphaS=90.0-ThetaZ ![deg]

C CRITICAL ANGLE T_crit
T_crit=atan(h_trap/(dist-a+((a-b)/2))) ![rad]

C CALCULATE SCALAR PRODUCT S.U1 AND S.U2
SsU1=(-1.0*COsd(GammaW)*COsd(AlphaS)*SIND(GammaS))+
& (COsd(AlphaS)*COsd(GammaS)*SIND(GammaW))
SsU2=(COsd(AlphaS)*SIND(GammaS)*SIND(GammaW)*SIND(BetaW))
& +(COsd(AlphaS)*COsd(GammaS)*COsd(GammaW)*SIND(BetaW))+

```

```

&      (SIND(AlphaS)*COSD(BetaW))
C      AVOID DIVIDING BY ZERO!
      IF (SsU1.EQ.0)THEN
          T_comp=ACOS(ABS(SsU2))
      ELSE
          T_comp=ATAN(ABS(SsU2)/ABS(SsU1))
      ENDIF

      IF(SsU1.LT.0.AND.SsU2.GE.0)THEN
          T_comp=PI-T_comp
      ELSE IF(SsU1.LT.0.AND.SsU2.LT.0)THEN
          T_comp=-1.0*(PI-T_comp)
      ELSE IF(SsU1.GE.0.AND.SsU2.LT.0)THEN
          T_comp=-1.0*T_comp
      ELSE
          T_comp=T_comp
      ENDIF

      DO i=1,nb_surf
          PS(i)=0.0
          DO j=1,(nb_case+1)
              prop_sh(i,j)=2.0
          ENDDO
      ENDDO

      DO i=1,(nb_surf*2)
          L(i)=0.0
          DO j=1,(nb_surf*2)
              FB(i,j)=0.0
          ENDDO
      ENDDO

      SHCASE=0
      FPASS=1
200     CONTINUE
      IF (GbW.GT.0) THEN
C         "CASE 1"
          IF(T_comp.GT.(0.0).AND.T_comp.LE.T_crit)THEN

              SHCASE=1
              !CALCULATE SHADING

              prop_sh(1,1)=1.0
              prop_sh(2,1)=1.0
              prop_sh(4,1)=(diag*sin(T_crit-T_comp))/
&              (t_trap*sin(T_comp+ThetaT))
              prop_sh(3,1)=0.0
              prop_sh(5,1)=0.0
              prop_sh(6,1)=0.0
              prop_sh(8,1)=1.0
              prop_sh(7,1)=1.0

              DO i=1,nb_surf
                  PS(i)=prop_sh(i,1)
              ENDDO

C              CALCULATE length OF EACH SURFACE
              CALL CALCULDIM(PS,DIST,A,T_TRAP,B,Wend,L)

C              CALCULATE RELEVANT SHAPE FACTORS

```

```

CALL CALCULSF2(L(9),L(4),t_trap,(PI-ThetaT),FB(9,4))
CALL CALCULSF6(L(12),L(11),(Dist-a),(PI-ThetaT),FB(12,11))
CALL CALCULSF4(L(4),L(11),(Dist-a),(PI-ThetaT),FB(4,11))
CALL CALCULSF1(L(15),L(16),(PI-ThetaT),FB(15,16))
CALL CALCULSF1(L(9),L(12),(PI-ThetaT),FB(9,12))
CALL CALCULSF1(L(9),L(11),(PI-ThetaT),FB(9,11))
CALL CALCULSF1(L(5),L(6),(PI-ThetaT),FB(5,6))

FB(4,9)=(FB(9,4)*L(9))/(L(4))
FB(11,4)=(FB(4,11)*L(4))/(L(11))
FB(12,9)=(FB(9,12)*L(9))/(L(12))
FB(11,12)=(FB(12,11)*L(12))/(L(11))
FB(11,9)=(FB(9,11)*L(9))/(L(11))
FB(16,15)=(FB(15,16)*L(15))/(L(16))
FB(6,5)=(FB(5,6)*L(5))/(L(6))

C      "CASE 2"
      ELSE IF(T_comp.GT.T_crit.AND.T_comp.LE.ThetaT)THEN

      SHCASE=2
      prop_sh(1,2)=(h_trap-(tan(T_comp)*((a-b)/2)))/
&          ((dist-a)*tan(T_comp))
      prop_sh(2,2)=1.0
      prop_sh(3,2)=0.0
      prop_sh(4,2)=0.0
      prop_sh(5,2)=0.0
      prop_sh(6,2)=0.0
&      prop_sh(7,2)=(h_trap-(tan(T_comp)*((a-b)/2)))/
          (Wend*tan(T_comp))

      IF((prop_sh(7,2)).GT.(1.0))THEN
          prop_sh(7,2)=1.0
      ENDIF
      prop_sh(8,2)=1.0

      DO i=1,nb_surf
          PS(i)=prop_sh(i,2)
      ENDDO

C      CALCULATE length OF EACH SURFACE
      CALL CALCULDIM(PS,DIST,A,T_TRAP,B,Wend,L)

C      CALCULATE RELEVANT SHAPE FACTORS
      CALL CALCULSF1(L(1),L(4),(PI-ThetaT),FB(1,4))
      CALL CALCULSF1(L(9),L(11),(PI-ThetaT),FB(9,11))
      CALL CALCULSF5(L(9),L(4),(Dist-a),(PI-ThetaT),FB(9,4))
      CALL CALCULSF3(L(4),(Dist-a),(PI-ThetaT),FB(4,11))
      CALL CALCULSF5(L(1),L(11),(Dist-a),(PI-ThetaT),FB(1,11))
      CALL CALCULSF1(L(15),L(16),(PI-ThetaT),FB(15,16))
      FB(16,15)=(FB(15,16)*L(15))/(L(16))

      IF((PS(7)).LT.(1.0)) THEN
          CALL CALCULSF5(L(7),L(16),Wend,(PI-ThetaT),FB(7,16))
          FB(16,7)=(FB(7,16)*L(7))/(L(16))
      ENDIF

      CALL CALCULSF1(L(5),L(6),(PI-ThetaT),FB(5,6))

      FB(4,1)=(L(1)*FB(1,4))/(L(4))
      FB(4,9)=(FB(9,4)*L(9))/(L(4))
      FB(11,4)=FB(4,11)

```

```

FB(11,9)=(FB(9,11)*L(9))/(L(11))
      FB(11,1)=(FB(1,11)*L(1))/(L(11))
      FB(6,5)=(FB(5,6)*L(5))/(L(6))

C      "CASE 3"
      ELSE IF(T_comp.GT.ThetaT.AND.T_comp.LE.(PI-ThetaT))THEN
        SHCASE=3

        prop_sh(1,3)=0.0
        prop_sh(2,3)=0.0
        prop_sh(3,3)=0.0
        prop_sh(4,3)=0.0
        prop_sh(5,3)=0.0
        prop_sh(6,3)=0.0
        prop_sh(7,3)=0.0
        prop_sh(8,3)=0.0

        DO i=1,nb_surf
          PS(i)=prop_sh(i,3)
        ENDDO

C      CALCULATE length OF EACH SURFACE
      CALL CALCULDIM(PS,DIST,A,T_TRAP,B,Wend,L)

C      CALCULATE SHAPE FACTOR FOR THE EXISTING SURFACES

      CALL CALCULSF1 (L(1),L(4),(PI-ThetaT),FB(1,4))
      CALL CALCULSF1 (L(1),L(2),(PI-ThetaT),FB(1,2))
      CALL CALCULSF1 (L(7),L(8),(PI-ThetaT),FB(7,8))
      CALL CALCULSF1 (L(5),L(6),(PI-ThetaT),FB(5,6))
      CALL CALCULSF3(L(2),(Dist-a),(PI-ThetaT),FB(2,4))

      FB(2,1)=(FB(1,2)*L(1))/(L(2))
      FB(4,1)=(FB(1,4)*L(1))/(L(4))
      FB(4,2)=FB(2,4)
      FB(8,7)=(FB(7,8)*L(7))/(L(8))
      FB(6,5)=(FB(5,6)*L(5))/(L(6))

C      "CASE 4"
      ELSE IF(T_comp.GT.(PI-ThetaT).AND.T_comp.LE.(PI-T_crit))THEN
        SHCASE=4

        prop_sh(1,4)=(h_trap-(tan(PI-T_comp)*((a-b)/2)))/
&          ((dist-a)*tan(PI-T_comp))

        prop_sh(2,4)=0.0
        prop_sh(3,4)=0.0
        prop_sh(4,4)=1.0
        prop_sh(5,4)=(h_trap-(tan(PI-T_comp)*((a-b)/2)))/
&          (Wend*tan(PI-T_comp))
        IF((prop_sh(5,4)).GT.(1.0))THEN
          prop_sh(5,4)=1.0
        ENDIF

        prop_sh(6,4)=1.0
        prop_sh(7,4)=0.0
        prop_sh(8,4)=0.0

        DO i=1,nb_surf
          PS(i)=prop_sh(i,4)
        ENDDO

```

```

C          CALCULATE length OF EACH SURFACE
          CALL CALCULDIM(PS,DIST,A,T_TRAP,B,Wend,L)

C          CALCULATE RELEVANT SHAPE FACTORS
          CALL CALCULSF1 (L(10),L(12),(PI-ThetaT),FB(10,12))
          CALL CALCULSF1 (L(1),L(2),(PI-ThetaT),FB(1,2))
          CALL CALCULSF1 (L(7),L(8),(PI-ThetaT),FB(7,8))
          CALL CALCULSF1 (L(13),L(14),(PI-ThetaT),FB(13,14))
          CALL CALCULSF5 (L(1),L(12),(Dist-a),(PI-ThetaT),FB(1,12))
          CALL CALCULSF3 (L(12),(Dist-a),(PI-ThetaT),FB(12,2))
          CALL CALCULSF5 (L(10),L(2),(Dist-a),(PI-ThetaT),FB(10,2))

          IF((PS(5)).LT.(1.0)) THEN
          CALL CALCULSF5 (L(5),L(14),Wend,(PI-ThetaT),FB(5,14))
              FB(14,5)=(FB(5,14)*L(5))/(L(14))
          ENDIF

          FB(12,10)=(FB(10,12)*L(10))/(L(12))
          FB(12,1)=(FB(1,12)*L(1))/(L(12))
          FB(2,12)=FB(12,2)
          FB(2,10)=(FB(10,2)*L(10))/(L(2))
          FB(2,1)=(FB(1,2)*L(1))/(L(2))
          FB(8,7)=(FB(7,8)*L(7))/(L(8))
          FB(14,13)=(FB(13,14)*L(13))/(L(14))

C          "CASE 5"
          ELSE IF(T_comp.GT.(PI-T_crit).AND.T_comp.LE.PI)THEN
              SHCASE=5

              prop_sh(1,5)=1.0
              prop_sh(2,5)=(diag*sin(T_comp-PI+T_crit))/
&              (t_trap*sin(PI-T_comp+ThetaT))
              prop_sh(3,5)=0.0
              prop_sh(4,5)=1.0
              prop_sh(6,5)=1.0
              prop_sh(7,5)=0.0
              prop_sh(8,5)=0.0
              prop_sh(5,5)=1.0

              DO i=1,nb_surf
                  PS(i)=prop_sh(i,5)
              ENDDO

C          CALCULATE length OF EACH SURFACE
          CALL CALCULDIM(PS,DIST,A,T_TRAP,B,Wend,L)

C          CALCULATE RELEVANT SHAPE FACTORS
          CALL CALCULSF1 (L(9),L(12),(PI-ThetaT),FB(9,12))
          CALL CALCULSF1 (L(9),L(11),(PI-ThetaT),FB(9,11))
          CALL CALCULSF1 (L(7),L(8),(PI-ThetaT),FB(7,8))
          CALL CALCULSF1 (L(13),L(14),(PI-ThetaT),FB(13,14))
          CALL CALCULSF6 (L(11),L(12),(Dist-a),(PI-ThetaT),FB(11,12))
          CALL CALCULSF4 (L(2),L(12),(Dist-a),(PI-ThetaT),FB(2,12))
          CALL CALCULSF2 (L(9),L(2),t_trap,(PI-ThetaT),FB(9,2))

          IF((PS(5)).LT.(1.0)) THEN
          CALL CALCULSF5 (L(5),L(14),Wend,(PI-ThetaT),FB(5,14))
              FB(14,5)=(FB(5,14)*L(5))/(L(14))
          ENDIF

          FB(12,9)=(FB(9,12)*L(9))/L(12)

```

```

        FB(12,11)=(FB(11,12))*L(11)/L(12)
        FB(12,2)=(FB(2,12))*L(2)/(L(12))
        FB(11,9)=(FB(9,11))*L(9)/(L(11))
        FB(2,9)=(FB(9,2))*L(9)/(L(2))
        FB(8,7)=(FB(7,8))*L(7)/(L(8))
        FB(14,13)=(FB(13,14))*L(13)/(L(14))
    ENDIF

    DO i=1,nb_surf
        prop_sh(i,(nb_case+1))=MIN(prop_sh(i,1),prop_sh(i,2),
&                                     prop_sh(i,3),prop_sh(i,4),prop_sh(i,5))
    ENDDO

ENDIF

DO i=1,nb_surf
    IF(prop_sh(i,(nb_case+1)).GE.2.0)THEN
        prop_sh(i,(nb_case+1))=1.0
    ELSE
        prop_sh(i,(nb_case+1))=prop_sh(i,(nb_case+1))
    ENDIF
ENDDO

IF (FPASS.EQ.2) THEN
    go to 210
ENDIF

C*****
C   CALCULATE ABSORBED SOLAR RADIATION DUE TO BEAM
C*****
C   SET MATRIX MA_AUGMDB
DO i=1,(nb_surf*2)
    mx_db(i)=0.0
    DO j=1,((nb_surf*2)+1)
        ma_augmdb(i,j)=0.0
    ENDDO
ENDDO

DO i=1,(nb_surf*2)
    DO j=1,(nb_surf*2)
        IF(i.eq.j)THEN
            ma_augmdb(i,j)=1.0
        ELSE
            ma_augmdb(i,j)=-1.0*RhoDcoll(i)*FB(i,j)
        ENDIF
    ENDDO
ENDDO

DO i=1,nb_surf
    ma_augmdb(i,17)=RhoB(i)*Gb(i)
ENDDO

CALL SOLVEMATRIX((nb_surf*2),ma_augmdb,mx_db)

DO i=1,(nb_surf*2)
    Jdb(i)=mx_db(i)
ENDDO

C   RE CALCULATE CONFIGURATION FACTORS
FPASS=2
DO i=1,(nb_surf*2)
    DO j=1,(nb_surf*2)

```

```

                FB(i,j)=0.0
                ENDDO
            ENDDO

C      RE CALCULATE SHAPE FACTORS
      GO TO 200
210   CONTINUE
      DO i=1,(nb_surf*2)
          Gdb(i)=0.0
          DO j=1,(nb_surf*2)
              Gdb(i)=Gdb(i)+(FB(i,j)*Jdb(j))
          ENDDO
      ENDDO
C*****
C      CALCULATE ABSORBED SOLAR RADIATION DUE TO SKY DIFFUSE
C      AND GROUND REFLECTED RADIATION
C*****
C      CALCULATE VIEW FACTORS
      FPASS=1
220   CONTINUE

      DO i=1,(NbJ)
          DO j=1,(NbJ)
              FD(i,j)=0.0
          ENDDO
      ENDDO

      CALL CALCULSF1 ((dist-a),t_trap,(PI-ThetaT),FD(1,2))
      FD(2,1)=(FD(1,2)*(dist-a))/(t_trap)
      CALL CALCULSF3(t_trap,(Dist-a),(PI-ThetaT),FD(2,4))
      FD(4,2)=FD(2,4)
      FD(1,4)=FD(1,2)
      FD(4,1)=FD(2,1)

      CALL CALCULSF1((dist-b),t_trap,ThetaT,FD(9,2))
      FD(2,9)=(FD(9,2)*(dist-b))/t_trap
      FD(4,9)=FD(2,9)
      FD(9,2)=0.0

      CALL CALCULSF1 (Wend,t_trap,(PI-ThetaT),FD(5,6))
      FD(6,5)=(FD(5,6)*Wend)/t_trap
      FD(8,7)=FD(6,5)
      FD(7,8)=FD(5,6)
      CALL CALCULSF7 ((Dist-a),(Dist-b),h_trap,FD(1,9))
      FD(7,10)=1-FD(7,8)
      FD(8,10)=1.0-FD(8,7)
      FD(5,11)=FD(7,10)
      FD(6,11)=FD(8,10)

      IF(FPASS.EQ.3)GO TO 240

C      Set matrix ma_augmdd and ma_augmdg
      DO i=1,nbJ
          mx_dd(i)=0.0
          mx_dg(i)=0.0
          DO j=1,(nbJ+1)
              ma_augmdd(i,j)=0.0
              ma_augmdg(i,j)=0.0
          ENDDO
      ENDDO

      DO i=1,nbJ

```

```

DO j=1,nbJ
    IF(i.eq.j)THEN
        ma_augmdd(i,j)=1.0
        ma_augmdg(i,j)=1.0
    ELSE
        IF(i.LE.nb_surf)THEN
            ma_augmdd(i,j)=(-1.0*RhoDcoll(i)*FD(i,j))
            ma_augmdg(i,j)=(-1.0*RhoDcoll(i)*FD(i,j))
        ELSE
            ma_augmdd(i,j)=0.0
            ma_augmdg(i,j)=0.0
        ENDIF
    ENDIF
ENDDO
ENDDO

ma_augmdd(3,12)=RhoDcoll(3)*GdW
ma_augmdd(9,12)=Gd(9)
ma_augmdd(10,12)=Gd(10)
ma_augmdd(11,12)=Gd(11)

ma_augmdg(3,12)=RhoGcoll(3)*GgW
ma_augmdg(9,12)=Gg(9)
ma_augmdg(10,12)=Gg(10)
ma_augmdg(11,12)=Gg(11)

IF (FPASS.eq.2)THEN
    go to 230
ENDIF

CALL SOLVEMATRIX(NbJ,ma_augmdd,mx_dd)
DO i=1,NbJ
    Jdd(i)=mx_dd(i)
ENDDO

C    RE CALCULATE CONFIGURATION FACTORS
FPASS=2
GO TO 220
230 CONTINUE

CALL SOLVEMATRIX(NbJ,ma_augmdG,mx_dG)
DO i=1,NbJ
    Jdg(i)=mx_dg(i)
ENDDO

C    RE CALCULATE CONFIGURATION FACTORS
FPASS=3
GO TO 220
240 CONTINUE

DO i=1,nb_surf
    Gdd(i)=0.0
    Gdg(i)=0.0
ENDDO

DO i=1,nb_surf
    IF(i.EQ.3)THEN
        Gdd(i)=GdW
        Gdg(i)=GgW
    ELSE
        DO j=1,NbJ
            Gdd(i)=Gdd(i)+(FD(i,j)*Jdd(j))

```

```

Gdg(i)=Gdg(i)+(FD(i,j)*Jdg(j))
      ENDDO
    ENDF
  ENDDO
C*****
C   DETERMINE QABS ON EACH TYPE OF SURFACE i
C*****
C   DETERMINE % SHADING
  DO i=1,Nb_surf
    Psh(i)=0.0
    Psh(i)=prop_sh(i,(nb_case+1))
    QBsurf(i)=0.0
    QDsurf(i)=0.0
    Qsurf(i)=0.0
  ENDDO

  IF(QradW.GT.(1.0))THEN

C   FIND DIFFUSE AND BEAM PORTION OF THE TOTAL ABSORBED
C   SOLAR RADIATION
  DO i=1,Nb_surf
    QBsurf(i)=(1-Por)*Area(i)*AlphaB(i)*Gb(i)*(1-Psh(i))

    IF(i.EQ.1)THEN
      IF(SHCASE.EQ.4)THEN
        QDsurf(i)=(1-Por)*AlphaDcoll(i)*Area(i)*(Gdd(i)
&          +Gdg(i)+(Gdb(i)*(1-Psh(i)))+
&          (Gdb(i+9)*Psh(i)))
      ELSE
        QDsurf(i)=(1-Por)*AlphaDcoll(i)*Area(i)*(Gdd(i)
&          +Gdg(i)+(Gdb(i)*(1-Psh(i)))+
&          (Gdb(i+nb_surf)*Psh(i)))
      ENDF
    ELSE IF(i.EQ.2)THEN
      QDsurf(i)=(1-Por)*AlphaDcoll(i)*Area(i)*(Gdd(i)
&          +Gdg(i)+(Gdb(i)*(1-Psh(i)))+
&          (Gdb(i+9)*Psh(i)))
    ELSE IF(i.EQ.3)THEN
      QDsurf(i)=(1-Por)*AlphaDcoll(i)*Area(i)*
&          (Gdd(i)+Gdg(i))
    ELSE
      QDsurf(i)=(1-Por)*AlphaDcoll(i)*Area(i)*(Gdd(i)+
&          Gdg(i)+(Gdb(i)*(1-Psh(i)))+
&          (Gdb(i+nb_surf)*Psh(i)))
    ENDF
    Qsurf(i)=QBsurf(i)+QDsurf(i)
  ENDDO

  ELSE
    DO N=1,Nb_surf
      QBsurf(i)=0.0
      QDsurf(i)=0.0
      Qsurf(i)=QBsurf(i)+QDsurf(i)
    ENDDO
  ENDF
C*****
C   OPTIMIZE FLOW RATE AND SOLVE SUBROUTINE FOR HEAT FLOWS AND TEMPERATURES
C   In this model, contrary to Summers' (1995), the collector is automatically bypassed
C   at night and both the thermal and electrical output are set to zero.
C   In the summer, however, the user has the choice to enable or disable an option
C   that will automatically open the collector bypass damper if the ambient
C   temperature becomes greater than a selected bypass temperature, Tbypass.

```

```

C      In such a case, the collector will be solved under bypass conditions, i.e.
C      with a air mass flowrate of zero. If this option is disabled, the mass flowrate of
C      air going through the collector (m) will be set to (mmin). In winter time,
C      during the day, if at the minimum flowrate, the mixed temperature is found
C      to be lower than Tsup, then the mass flowrate is set to mmin. If for the lowest
C      and highest value of Gamma, the mixed temperature is found to be higher
C      than Tsup, then the flowrate in the collector is also set to mmin, unless
C      the summer bypass option was enabled by the user. In any other cases,
C      the mass flowrate, m, that minimizes the auxiliary heat required, i.e.
C      when Tmix=Tsup, is determined using the bisection method.
C*****
C      SET THE FIRST GAMMA TO THE MINIMUM GAMMA
      Gam=GamMIN
      IF(bypass.GE.1)THEN
        Gam=0.0
      ENDIF

C      CALL SUBOURINTE
      CALL PVTtrcSOLVE(Tcol,Tplen,Qrad_cs,Qrad_wc,Twall,
&                      Qconv_wa,Qwind,Qconv_ca,Qcond_wT,Qabs,
&                      Qu,Tout,effhx,Vs,hwall_UTC)

C      CALCULATE TMIX
      Tmix=((Gam*Tout)+((1-Gam)*(Tb1g)))

C      EXIT IF COLLECTOR IS BYPASSED
      IF (Bypass.GE.1) THEN
        Tmix=(GamMIN*Tamb)+((1-GamMIN)*Tb1g)
      GO TO 260
      ENDIF

c      EXIT IF SUMMER AND NO BYPASS
      IF(Tamb.GE.(Tbypass+273.15))GO TO 260

C      WINTER DAYTIME
C      OPTIMIZE FLOW RATE THROUGH COLLECTOR TO MINIMIZE REQUIRED AUXILIARY ENERGY
      IF (Tmix.LT. Tsup)THEN
        GAM=GamMIN
        GO TO 260
      ELSE
C      Tmix>Tsup=>TRY GAM=1
        Gam=1.0
        CALL PVTtrcSOLVE(Tcol,Tplen,Qrad_cs,Qrad_wc,Twall,
&                      Qconv_wa,Qwind,Qconv_ca,Qcond_wT,Qabs,
&                      Qu,Tout,effhx,Vs,hwall_UTC)

        Tmix=((Gam*Tout)+((1-Gam)*(Tb1g)))

        IF(Tmix.LT. Tsup)THEN
C      FIND GAM FOR Tmix=Tsup USING BISSECTION METHOD
          COUNT=0
          lowg=GamMIN
          hig=1.0
          GAM=(lowg+hig)/2.0
250      CONTINUE
          COUNT=COUNT+1
          CALL PVTtrcSOLVE(Tcol,Tplen,Qrad_cs,Qrad_wc,Twall,
&                      Qconv_wa,Qwind,Qconv_ca,Qcond_wT,Qabs,
&                      Qu,Tout,effhx,Vs,hwall_UTC)

          Tmix=((Gam*Tout)+((1-Gam)*(Tb1g)))
          IF(Tmix.LT. Tsup)THEN

```

```

hig=GAM
      ELSE
        lowg=GAM
      ENDIF
      oldg=Gam
      Gam=(lowg+hig)/2.0
      difg=abs(GAM-oldg)
255      IF((difg.gt.0.01).AND.(COUNT.LT.150))GO TO 250
C      ERROR MESSAGE IN CASE IT DOESN'T CONVERGE

      ELSE
C      Tsup IS TOO HOT
      IF (ByTemp.GE.1)THEN
C      SUMMER BYPASS SHOULD HAVE BEEN OPENED BECAUSE Tsup IS TOO HOT
        Gam=0.0
        Bypass=1.0
        CALL PVTtrcSOLVE(Tcol,Tplen,Qrad_cs,
&      Qrad_wc,Twall,
&      Qconv_wa,Qwind,Qconv_ca,Qcond_wT,Qabs,
&      Qu,Tout,effhx,Vs,hwall_UTC)
        Tmix=(GamMIN*Tamb)+((1-GamMIN)*Tb1g)
        GO TO 260
      ELSE
C      NO SUMMER BYPASS AND GAM IS SET TO GAMMIN
        Gam=GamMIN
        CALL PVTtrcSOLVE(Tcol,Tplen,Qrad_cs,
&      Qrad_wc,Twall,
&      Qconv_wa,Qwind,Qconv_ca,Qcond_wT,Qabs,
&      Qu,Tout,effhx,Vs,hwall_UTC)
      ENDIF
    ENDIF
  ENDIF

260  CONTINUE
C*****
C      CALCULATE THE REDUCED WALL HEAT LOSSES, THE ELECTRICITY PRODUCED
C      AND THE THERMAL AND ELECTRICAL EFFICIENCIES
C*****
C      FIND SOL-AIR TEMPERATURE [ASHRAE, 1993]
      Tsa=Tamb+((AlphaW*QradW)/hFilm) ![K]
      Qpot=AreaW*Uwall*(Tb1g-Tsa) ![kJ/hr]
      QredW=Qpot-(AreaW*(1.0/((1.0/Uwall)-(1/hfilm)+(1/hwall_UTC)))*
&      (Tb1g-Tplen))![kJ/hr]
      QE=0.0
      EffPV=0.0

      IF (PVMODE.EQ.1) GO TO 300
      IF (QradW.LT.1.0)GO TO 300

      EffPV=Effref+(EffT*((Tcol-273.15)-Tref))

C      TURN PV OFF ON SURFACES WHERE PV CELLS ARE SHADED
      DO i=1,Nb_surf
        IF((PVsurf(i).GE.0.5).AND.(PSh(i).GT.0.0))THEN
          PVOn(i)=0
        ENDIF
      ENDDO

      IF (PVMODE.EQ.2)THEN
        QE=Qsurf(3)*PPV(3)*EffPV*nb_corr
      ELSE IF (PVMODE.EQ.3)THEN

```

```

IF((PVON(1).LE.0).OR.(PVON(2).LE.0).OR.(PVON(4).LE.0))THEN
C      SHADING, TAKE THE MINIMUM OF THE DIFFUSE RADIATION
      QE=EffPV*(MIN((QDsurf(3)/(Area(3)*AlphaDcoll(3))),
&      (QDsurf(1)/(Area(1)*AlphaDcoll(1))),
&      (QDsurf(2)/(Area(2)*AlphaDcoll(2))),
&      (QDsurf(4)/(Area(4)*AlphaDcoll(4)))))*
&      ((Nb_corr*Area(3)*PPV(3))+
&      ((Nb_corr-1)*(Area(1)*PPV(1)+(Area(2)*PPV(2))+
&      (Area(4)*PPV(4))))
      ELSE
C      NO SHADING, TAKE THE MINIMUM OF THE TOTAL RADIATION
      QE=EffPV*(MIN((QBSurf(3)/(AlphaB(3)*Area(3)))+
&      (QDsurf(3)/(Area(3)*AlphaDcoll(3))),
&      ((QBSurf(1)/(Area(1)*AlphaB(1)))+
&      (QDsurf(1)/(Area(1)*AlphaDcoll(1))),
&      ((QBSurf(2)/(Area(2)*AlphaB(2)))+
&      (QDsurf(2)/(Area(2)*AlphaDcoll(2))),
&      ((QBSurf(4)/(Area(4)*AlphaB(4)))+
&      (QDsurf(4)/(Area(4)*AlphaDcoll(4)))))*
&      ((Nb_corr*Area(3)*PPV(3))+
&      ((Nb_corr-1)*(Area(1)*PPV(1)+Area(2)*PPV(2)+
&      Area(4)*PPV(4))))
      ENDIF
ENDIF
300 CONTINUE

IF (QradW.GT.1.0)THEN
  IF(Qu.GT.1.0)THEN
    Effth=(Qu/(AreaW*QradW))
  ELSE
    Qu=0.0
    Effth=0.0
  ENDIF
  IF(Qe.GT.1.0)THEN
    Effel=QE/(AreaW*QradW)
  ELSE
    Qe=0.0
    Effel=0.0
  ENDIF
ELSE
  Effth=0.0
  Effel=0.0
  effhx=0.0
ENDIF

C      CONVERT TEMPERATURES FROM CELCIUS TO KELVIN
Tcol=Tcol-273.15
Tplen=Tplen-273.15
Tout=Tout-273.15
Tmix=Tmix-273.15
QU=QU*1000/3600
QE=QE*1000/3600
QredW=QredW*1000/3600
Qabs=Qabs*1000/3600/AreaW

350 CONTINUE
C      SET THE OUTPUTS FROM THIS MODEL IN SEQUENTIAL ORDER AND GET OUT
OUT(1)=Tcol      !degC
OUT(2)=Tplen    !degC
OUT(3)=Tmix     !degC
OUT(4)=Tout    !degC
OUT(5)=GAM      !0 TO 1

```

```

OUT(6)=1-GAM  !0 TO 1
  OUT(7)=GAM*MFLOW  !kg/hr
  OUT(8)=effhx
  OUT(9)=Effth
  OUT(10)=Effel
  OUT(11)=EffPV
  OUT(12)=QU  !W
  OUT(13)=QE  !W
  OUT(14)=QredW
  OUT(15)=Bypass
  OUT(16)=Qabs  !W/m2

  RETURN 1
END SUBROUTINE Type250
*****
  SUBROUTINE PVTrcSOLVE (Tcol,Tplen,Qrad_cs,Qrad_wc,Twall,
& Qconv_wa,Qwind,Qconv_ca,Qcond_wT,Qabs,
& Qu,Tout,effhx,Vs,hwall_UTC)
  IMPLICIT NONE
C   Common variables
  COMMON/PVT/a,b,h_trap,d,pitch,length,dist,width
  COMMON/PVT/hp,e_back,e_wall,th,Uwall,EffT,EffRef,Tref
  COMMON/PVT/PPV,Uwind,Tamb,Tblg,Tsup,hfilm
  COMMON/PVT/Flow,Gam,t_trap,ThetaT,Por,rho_amb,visc_amb
  COMMON/PVT/AreaW,k_amb,ecol,Trad,L,cp_amb,Area_cs
  COMMON/PVT/QBsurf,QDsurf,Qsurf,Psh,Area,AlphaB,AlphaDcoll
  COMMON/PVT/PVOn,SHCASE,nb_corr,PVMode

C   COMMON VARIABLES
  DOUBLE PRECISION a,b,h_trap,d,pitch,length,dist,width
  DOUBLE PRECISION hp,e_back,e_wall,th,Uwall,EffT,EffRef,Tref
  DOUBLE PRECISION PPV,Uwind,Tamb,Tblg,Tsup,hfilm
  DOUBLE PRECISION Flow,Gam,t_trap,ThetaT,Por,rho_amb,visc_amb
  DOUBLE PRECISION AreaW,k_amb,ecol,Trad,L,cp_amb,Area_cs
  DOUBLE PRECISION QBsurf,QDsurf,Qsurf,Psh,Area,AlphaB,AlphaDcoll

C   SUBROUTINE VARIABLES
  DOUBLE PRECISION Tcol,Tplen,Qrad_cs,Qrad_wc,Twall
  DOUBLE PRECISION Qconv_wa,Qwind,Qconv_ca,Qcond_wT,Qabs
  DOUBLE PRECISION Tout,Vs,Qu,effhx,hwall_UTC

C   INTERNAL VARIABLES
  DOUBLE PRECISION SB,PR,Rew,Res,Reb,Reh,ef,eb,eh,dif
  DOUBLE PRECISION Ma,Mb,Mx,ResC
  DOUBLE PRECISION hconv_wa,Tsur,Twall_in,diflim,kmax,hwind
  DOUBLE PRECISION ReL,NuL,Rexc
  INTEGER*4 PVOn,SHCASE,nb_corr,PVMode
  INTEGER*4 nb_case,nb_surf
  INTEGER*4 k,neq,i,j,R,N
  INTEGER*4 SPASS

c   COMMON VARIABLES DECLARATION
  PARAMETER (nb_surf=8,nb_case=5,Neq=8)
  DIMENSION QBsurf(Nb_surf),QDsurf(Nb_surf),Qsurf(Nb_surf)
  DIMENSION PPV(Nb_surf),Psh(Nb_surf),Area(Nb_surf)
  DIMENSION AlphaB(Nb_surf),AlphaDcoll(Nb_surf),PVon(Nb_surf)
  DIMENSION L(nb_surf*2),Ma(10,11),Mb(10),Mx(10),ResC(10)

C-----
C   SETTING CONSTANTS
  SB=(5.67e-8)*3.6  !Stefan-Boltzmann constant [kJ/hrm2K4]
  Pr=0.71
  diflim=0.01
  kmax=100

  SPASS=1

```

```

100    CONTINUE
      IF (SPASS.GT.1)GO TO 160

C      SET Vs
      Vs=(Flow*Gam)/AreaW          !m/hr
*****
C      CALCULATE hconv,wall-air
*****
C      IF NO FLOW, HCONV_WA=0.1 W/M2C Maurer [2004]
      IF (Vs.LE.0.01)THEN
          hconv_wa=0.36    ![kJ/m2 h C]
          GO TO 110
      ENDIF

      ReL=(rho_amb*((AreaW*Vs)/Area_cs)*0.5*length)/(visc_amb)
      Rexc=500000

c      Verify if the flow is laminar or if there is transition
      IF (ReL.LE.Rexc)THEN
          !Laminar
          NuL=0.664*(ReL**0.5)*(Pr**0.33333333)
      ELSE IF (ReL.GT.Rexc)THEN
          !Transition
          NuL=((0.037*(ReL**0.8))-871)*(Pr**0.3333333)
      ENDIF
      hconv_wa=(k_amb*NuL)/length    ![kJ/m2 h C]
110    CONTINUE
*****
C      CALCULATE HEAT EXCHANGER EFFECTIVENESS (Van Decker and Hollands, 2001)
C      Assume: Asymptotic region (Boundary layer thickness is invariant)
C      Convection at the back comes only from the back of the hole
*****
      IF (Vs.GT.0.01)THEN
          Rew=Uwind*pitch*rho_amb/visc_amb
          Res=Vs*pitch*rho_amb/visc_amb
          Reb=Vs*pitch*rho_amb/(visc_amb*Por)
          Reh=Vs*D*rho_amb/(visc_amb*Por)

          ef=1-(1/(1+((1/Res)*max(17.7,(0.708*(Rew**0.5))))))
          eb=1-(1.0/(1+(3.4*(Reb**(-0.33333333))))))
          eh=1-exp((-0.0204*(pitch/D))-(20.62*th/(Reh*D)))
          effhx=1-((1-ef)*(1-eb)*(1-eh))

      ELSE
          effhx=1.0
      ENDIF
*****
C      CALCULATE HWINN
*****
      IF(Vs.GT.(0.01))THEN
C      SWIFT SOFTWARE CORRELATION (TO USE)
          hwind=MIN((0.02*(Uwind/Vs)),(2.8+(3.0*
&      (Uwind/3600))))    ![W/m2K]
C      STRL MODEL (FOR SMALL PANEL)
c      hwind=6+(4*Uwind/3600)-(76*Vs/3600)

      ELSE
          hwind=(2.8+(3.0*((Uwind)/3600)))    ![W/m2K]
c      hwind=6+(4*Uwind/3600)
      ENDIF
*****
C      SOLVE SIMULTANEOUS EQUATIONS FOR UNKNOWN TEMPERATURES AND HEAT FLOWS
C      [A][X]=[B]

```

\*\*\*\*\*

```

Tsur=Trad
Twall_in=Tblg

C   SET MATRIX Ma
C   SET A VALUE OF Tcol AND Twall TO START
Tcol=Tamb+20
Twall=Tamb+10

DO i=1,10
  Mx(i)=0.0
  DO j=1,11
    Ma(i,j)=0.0
  ENDDO
ENDDO

C   SET EQUATION 1 :effhx
Ma(1,1)=-1.0*effhx
Ma(1,2)=1.0
Ma(1,11)=Tamb*(1.0-effhx)

C   SET EQUATION 2:Qrad,col-sur
Ma(2,3)=-1.0
Ma(2,1)=SB*(Tcol+Tsur)*((Tcol**2)+
&      (Tsur**2))*(1-Por)*(ecol*AreaW)

Ma(2,11)=SB*(Tcol+Tsur)*((Tcol**2)+(Tsur**2))*
&      (1-Por)*Tsur*(ecol*AreaW)

C   SET EQUATION 3: Qrad,wall-col
Ma(3,1)=(SB*AreaW*((Twall**2)+(Tcol**2))*
&      (Twall+Tcol)/
&      (((1-e_wall)/e_wall)+
&      ((1-e_back)/e_back)+1.0)
Ma(3,4)=1.0
Ma(3,9)=(-1.0*SB*AreaW*((Twall**2)+(Tcol**2))*
&      (Twall+Tcol)/
&      (((1-e_wall)/e_wall)+
&      ((1-e_back)/e_back)+1.0)

C   SET EQUATION 4:Qconv,wall-air
Ma(4,5)=1.0
Ma(4,9)=-1.0*hconv_wa*AreaW
Ma(4,2)=hconv_wa*AreaW

C   SET EQUATION 5:      Qconv,col-amb
Ma(5,6)=1.0
Ma(5,1)=-1.0*hwind*3.6*AreaW
Ma(5,11)=-1.0*hwind*3.6*AreaW*Tamb

C   SET EQUATION 6:      Qconv,col-air
Ma(6,7)=1.0
Ma(6,2)=-1.0*rho_amb*Vs*cp_amb*AreaW
Ma(6,11)=-1.0*rho_amb*Vs*cp_amb*AreaW*Tamb

C   SET EQUATION 7 :Qabs+Qrad_wc-Qconv_ca-Qwind-Qrad_cs=0
Ma(7,8)=1.0
Ma(7,4)=1.0
Ma(7,7)=-1.0
Ma(7,6)=-1.0
Ma(7,3)=-1.0

```

```

C      SET EQUATION 8: Qabs=(1-EffPV)*Qsurf
      MA(8,8)=1.0
      IF (PvMode.EQ.1)THEN
          Ma(8,11)=(Qsurf(5)+Qsurf(6)+Qsurf(7)+Qsurf(8)+
&                (Qsurf(3)*Nb_corr)+
&                ((Qsurf(1)+Qsurf(2)+Qsurf(4))*(Nb_corr-1)))

      ELSE IF (PvMode.EQ.2)THEN
          Ma(8,1)=Qsurf(3)*EffT*Nb_corr*PPV(3)
          Ma(8,11)=Qsurf(5)+Qsurf(6)+Qsurf(7)+Qsurf(8)+
&                ((Qsurf(1)+Qsurf(2)+Qsurf(4))*(Nb_corr-1))+
&                (Qsurf(3)*Nb_corr*(1-(PPV(3)*EffRef)+
&                (PPV(3)*EffT*(Tref+273.15))))

      ELSE IF (PvMode.EQ.3)THEN
          Ma(8,1)=EffT*(Nb_corr*Qsurf(3)*PPV(3)+
&                ((Nb_corr-1)*(Qsurf(1)*PPV(1)+Qsurf(2)*
&                PPV(2)+Qsurf(4)*PPV(4)))
          Ma(8,11)=Qsurf(5)+Qsurf(6)+Qsurf(7)+Qsurf(8)+
&                (Qsurf(1)*(Nb_corr-1)*(1-(PPV(1)*EffRef)+
&                (PPV(1)*(Tref+273.15)*EffT)))+
&                (Qsurf(2)*(Nb_corr-1)*(1-(PPV(2)*EffRef)+
&                (PPV(2)*(Tref+273.15)*EffT)))+
&                (Qsurf(4)*(Nb_corr-1)*(1-(PPV(4)*EffRef)+
&                (PPV(4)*(Tref+273.15)*EffT)))+
&                (Qsurf(3)*Nb_corr*(1-(PPV(3)*EffRef)+
&                (PPV(3)*(Tref+273.15)*EffT)))

      ENDIF

C      SET EQUATION 9:      Qconv,wall-air+Qrad,wall-col-Qcond_wall=0
      Ma(9,5)=1.0
      Ma(9,4)=1.0
      Ma(9,10)=-1.0

C      SET EQUATION 10:Qcond_wallT
      Ma(10,10)=1.0
      Ma(10,9)=(1.0/((1.0/Uwall)-(1.0/hfilm)))*AreaW
      Ma(10,11)=(1.0/((1.0/Uwall)-(1.0/hfilm)))*AreaW*Twall_in
      *****
C      START ITERATION
      *****
      k=0
130     CONTINUE
      k=k+1

      CALL SOLVEMATRIX(10,Ma,Mx)
      Tcol=Mx(1)
      Twall=Mx(9)

150     CONTINUE
      SPASS=SPASS+1
C      RECALCULATE CONFIGURATION FACTORS

160     CONTINUE
      DO i=1,10
          DO j=1,11
              Ma(i,j)=0.0
          ENDDO
      ENDDO

C      SET EQUATION 1 :effhx
      Ma(1,1)=-1.0*effhx

```

```

Ma(1,2)=1.0
Ma(1,11)=Tamb*(1.0-effhx)

C   SET EQUATION 2:Qrad,col-sur
Ma(2,3)=-1.0
Ma(2,1)=SB*(Tcol+Tsur)*((Tcol**2)+
&      (Tsur**2))*(1-Por)*(ecol*AreaW)

Ma(2,11)=SB*(Tcol+Tsur)*((Tcol**2)+(Tsur**2))*
&      (1-Por)*Tsur*(ecol*AreaW)

C   SET EQUATION 3: Qrad,wall-col
Ma(3,1)=(SB*AreaW*((Twall**2)+(Tcol**2))*
&      (Twall+Tcol)/
&      (((1-e_wall)/e_wall)+
&      ((1-e_back)/e_back)+1.0)
Ma(3,4)=1.0
Ma(3,9)=(-1.0*SB*AreaW*((Twall**2)+(Tcol**2))*
&      (Twall+Tcol)/
&      (((1-e_wall)/e_wall)+
&      ((1-e_back)/e_back)+1.0)

C   SET EQUATION 4:Qconv,wall-air
Ma(4,5)=1.0
Ma(4,9)=-1.0*hconv_wa*AreaW
Ma(4,2)=hconv_wa*AreaW

C   SET EQUATION 5:      Qconv,col-amb
Ma(5,6)=1.0
Ma(5,1)=-1.0*hwind*3.6*AreaW
Ma(5,11)=-1.0*hwind*3.6*AreaW*Tamb

C   SET EQUATION 6:      Qconv,col-air
Ma(6,7)=1.0
Ma(6,2)=-1.0*rho_amb*Vs*cp_amb*AreaW
Ma(6,11)=-1.0*rho_amb*Vs*cp_amb*AreaW*Tamb

C   SET EQUATION 7 :Qabs+Qrad_wc-Qconv_ca-Qwind-Qrad_cs=0
Ma(7,8)=1.0
Ma(7,4)=1.0
Ma(7,7)=-1.0
Ma(7,6)=-1.0
Ma(7,3)=-1.0

C   SET EQUATION 8: Qabs=(1-EffPV)*Qsurf
MA(8,8)=1.0
IF (PvMode.EQ.1)THEN
    Ma(8,11)=(Qsurf(5)+Qsurf(6)+Qsurf(7)+Qsurf(8)+
&      (Qsurf(3)*Nb_corr)+
&      ((Qsurf(1)+Qsurf(2)+Qsurf(4))*(Nb_corr-1)))
ELSE IF (PvMode.EQ.2)THEN
    Ma(8,1)=Qsurf(3)*EffT*Nb_corr*PPV(3)
    Ma(8,11)=Qsurf(5)+Qsurf(6)+Qsurf(7)+Qsurf(8)+
&      ((Qsurf(1)+Qsurf(2)+Qsurf(4))*(Nb_corr-1))+
&      (Qsurf(3)*Nb_corr*(1-(PPV(3)*EffRef)+
&      (PPV(3)*EffT*(Tref+273.15))))
ELSE IF (PvMode.EQ.3)THEN
    Ma(8,1)=EffT*((Nb_corr*Qsurf(3)*PPV(3))+
&      ((Nb_corr-1)*(Qsurf(1)*PPV(1)+Qsurf(2)*
&      PPV(2)+Qsurf(4)*PPV(4))))

```

```

Ma(8,11)=Qsurf(5)+Qsurf(6)+Qsurf(7)+Qsurf(8)+
&          (Qsurf(1)*(Nb_corr-1)*(1-(PPV(1)*EffRef)+
&          (PPV(1)*(Tref+273.15)*EffT)))+
&          (Qsurf(2)*(Nb_corr-1)*(1-(PPV(2)*EffRef)+
&          (PPV(2)*(Tref+273.15)*EffT)))+
&          (Qsurf(4)*(Nb_corr-1)*(1-(PPV(4)*EffRef)+
&          (PPV(4)*(Tref+273.15)*EffT)))+
&          (Qsurf(3)*Nb_corr*(1-(PPV(3)*EffRef)+
&          (PPV(3)*(Tref+273.15)*EffT)))
      ENDIF

C      SET EQUATION 9: Qconv,wall-air+Qrad,wall-col-Qcond_wall=0
      Ma(9,5)=1.0
      Ma(9,4)=1.0
      Ma(9,10)=-1.0

C      SET EQUATION 10:Qcond_wallT
      Ma(10,10)=1.0
      Ma(10,9)=(1.0/((1.0/Uwall)-(1.0/hfilm)))*AreaW
      Ma(10,11)=(1.0/((1.0/Uwall)-(1.0/hfilm)))*AreaW*Twall_in
*****
C      CALCULATE RESIDUAL
*****
      DO i=1,10
          Mb(i)=0.0
          DO j=1,10
              Mb(i)=Mb(i)+((Ma(i,j))*(Mx(j)))
          ENDDO
      ENDDO

      dif=0.0
      DO i=1,10
          ResC(i)=0.0
          ResC(i)=Mb(i)-Ma(i,11)
          dif=dif+ABS(ResC(i))
      ENDDO

C      VERIFY IF CONVERGENCE IS OBTAINED
C      IF NOT, REPEAT NEW Tcol AND Twall
      IF (dif.gt.diflim.and.k.lt.kmax) go to 130

C      CONVERGENCE IS OBTAINED
      Tcol=Mx(1)
      Tplen=Mx(2)
      Qrad_cs=Mx(3)
      Qrad_wc=Mx(4)
      Qconv_wa=Mx(5)
      Qwind=Mx(6)
      Qconv_ca=Mx(7)
      Qabs=Mx(8)
      Twall=Mx(9)
      Qcond_wT=Mx(10)

C      CALCULATE Tout
      IF(Vs.GT.0.01)THEN
          Tout=Tamb+((Qconv_wa+Qconv_ca)/(rho_amb*Vs*AreaW*cp_amb))
      ELSE
          Tout=Tamb
      ENDIF
      Qu=rho_amb*Vs*cp_amb*AreaW*(Tout-Tamb)

400    CONTINUE

```

```

Tcol=Tcol
  Tplen=Tplen
  Qrad_cs=Qrad_cs
  Qrad_wc=Qrad_wc
  Twall=Twall
  Qconv_wa=Qconv_wa
  Qwind=Qwind
  Qconv_ca=Qconv_ca
  Qcond_wT=Qcond_wT
  Qabs=Qabs
  Qu=Qu
  Tout=Tout
  effhx=effhx
  Vs=Vs
  hwall_UTC=((SB*((Twall**2)+(Tcol**2))*(Twall+Tcol))/
&          (((1-e_wall)/e_wall)+((1-e_back)/e_back)+1.0))+hconv_wa
&
  RETURN
  END
*****
C  SUBROUTINE CALCULDIM
*****
  SUBROUTINE  CALCULDIM(PS,DIST,A,T_TRAP,B,L_END,L)
  IMPLICIT NONE
  DOUBLE PRECISION PS,L
  DOUBLE PRECISION DIST,A,T_TRAP,B,L_END
  PARAMETER NBSURF=8
  DIMENSION PS(NBSURF)
  DIMENSION L(NBSURF*2)

  L(1)=(dist-a)*(1.0-PS(1))
  L(2)=t_trap*(1.0-PS(2))
  L(3)=b
  L(4)=t_trap*(1.0-PS(4))
  L(5)=L_end*(1.0-PS(5))
  L(6)=t_trap*(1.0-PS(6))
  L(7)=L_end*(1.0-PS(7))
  L(8)=t_trap*(1.0-PS(8))
  L(9)=(dist-a)*PS(1)
  L(10)=(dist-a)*PS(1)
  L(11)=t_trap*PS(2)
  L(12)=t_trap*(PS(4))
  L(13)=L_end*PS(5)
  L(14)=t_trap*PS(6)
  L(15)=L_end*PS(7)
  L(16)=t_trap*PS(8)

  END
*****
C  SUBROUTINE CALCULSF1
*****
  SUBROUTINE CALCULSF1 (LENGTH1,LENGTH2,ALPHA,F12)
  IMPLICIT NONE
  DOUBLE PRECISION AF,PI,LENGTH1,LENGTH2,F12
  DOUBLE PRECISION ALPHA

  PI=3.141592654
  AF=LENGTH2/LENGTH1
  F12=(AF+1-(((AF*AF)+1-(2*AF*(COS(ALPHA))))**0.5))/2

  END
*****

```

```

C      SUBROUTINE CALCULSF2
*****
      SUBROUTINE CALCULSF2 (LENGTH1,LENGTH2,LENGTH3,ALPHA,F12)
      IMPLICIT NONE
      DOUBLE PRECISION LENGTH1,LENGTH2,F12,X,Y,PI
      DOUBLE PRECISION LENGTH3,ALPHA
      PI=3.141592654

      X=((LENGTH1**2)+((LENGTH3-LENGTH2)**2)-
&      (2*LENGTH1*(LENGTH3-LENGTH2)*COS(ALPHA)))*0.5
      Y=((LENGTH1**2)+(LENGTH3**2)-
&      (2*LENGTH1*LENGTH3*COS(ALPHA)))*0.5

      F12=(X+LENGTH2-Y)/(2*LENGTH1)

      END
*****
C      SUBROUTINE CALCULSF3
*****
      SUBROUTINE CALCULSF3(LENGTH1,LENGTH2,ALPHA,F12)
      IMPLICIT NONE
      DOUBLE PRECISION LENGTH1,LENGTH2,F12,X,Y,PI
      DOUBLE PRECISION ALPHA,ZETA
      PI=3.141592654

      X=((LENGTH1**2)+(LENGTH2**2)-
&      (2*LENGTH1*LENGTH2*COS(ALPHA)))*0.5
      ZETA=ASIN((SIN(ALPHA)*LENGTH1)/X)
      Y=((LENGTH1**2)+(X**2)-
&      (2*LENGTH1*X*COS(ALPHA-ZETA)))*0.5

      F12=((2.0*X)-Y-LENGTH2)/(2*LENGTH1)
      END
*****
C      SUBROUTINE CALCULSF4
*****
      SUBROUTINE CALCULSF4(LENGTH1,LENGTH2,LENGTH3,ALPHA,F12)
      IMPLICIT NONE
      DOUBLE PRECISION LENGTH1,LENGTH2,LENGTH3,F12,X,Y,Z,W,PI
      DOUBLE PRECISION ALPHA,ZETA
      PI=3.141592654

      X=((LENGTH2**2)+(LENGTH3**2)-
&      (2*LENGTH2*LENGTH3*COS(ALPHA)))*0.5
      Z=((LENGTH2-LENGTH1)**2)+(LENGTH3**2)-
&      (2*(LENGTH2-LENGTH1)*(LENGTH3)*COS(ALPHA)))*0.5
      ZETA=ASIN((LENGTH2*SIN(ALPHA))/X)
      W=((LENGTH2**2)+(X**2)-
&      (2*LENGTH2*X*COS(ALPHA-ZETA)))*0.5
      Y=((W**2)+(LENGTH1**2)-(2*W*LENGTH1*COS(PI-ALPHA)))*0.5

      F12=(X+Y-W-Z)/(2*LENGTH1)
      END
*****
C      SUBROUTINE CALCULSF5
*****
      SUBROUTINE CALCULSF5(LENGTH1,LENGTH2,LENGTH3,ALPHA,F12)
      IMPLICIT NONE
      DOUBLE PRECISION LENGTH1,LENGTH2,LENGTH3,F12,X,Y,PI
      DOUBLE PRECISION ALPHA
      PI=3.141592654

```

```

X=((LENGTH2**2)+((LENGTH3-LENGTH1)**2)-
& (2*LENGTH2*(LENGTH3-LENGTH1)*COS(ALPHA)))**0.5
Y=((LENGTH2**2)+(LENGTH3**2)-
& (2*LENGTH3*LENGTH2*COS(ALPHA)))**0.5

F12=(X+LENGTH1-Y)/(2*LENGTH1)
END
*****
C SUBROUTINE CALCULSF6
*****
SUBROUTINE CALCULSF6(LENGTH1,LENGTH2,LENGTH3,ALPHA,F12)
IMPLICIT NONE
DOUBLE PRECISION LENGTH1,LENGTH2,LENGTH3,F12,PI
DOUBLE PRECISION ALPHA,X,Y,Z,ZETA
PI=3.141592654

X=((LENGTH3**2)+(LENGTH1**2)-(2*LENGTH3*LENGTH1*
& COS(ALPHA)))**0.5
Y=((LENGTH3**2)+(LENGTH2**2)-(2*LENGTH3*LENGTH2*
& COS(ALPHA)))**0.5
ZETA=ASIN((LENGTH1*sin(ALPHA))/X)
Z=((X**2)+(LENGTH2**2)-(2*X*LENGTH2*
& COS(ALPHA-ZETA)))**0.5
F12=(X+Y-Z-LENGTH3)/(2*LENGTH1)
END
*****
C SUBROUTINE CALCULSF7
*****
SUBROUTINE CALCULSF7(LENGTH1,LENGTH2,LENGTH3,F12)
IMPLICIT NONE
DOUBLE PRECISION LENGTH1,LENGTH2,LENGTH3,F12
DOUBLE PRECISION ALPHA,X,Y

ALPHA=ATAN(LENGTH3/((LENGTH2-LENGTH1)/2.0))
X=((LENGTH3**2)+((LENGTH2-LENGTH1)/2.0)**2.0)**0.5

Y=((LENGTH2**2)+(X**2)-(2*LENGTH2*X*
& COS(ALPHA)))**0.5

F12=((2.0*Y)-(2.0*X))/(2*LENGTH1)
END
*****
C SUBROUTINE USED TO SOLVE MATRIX BY THE ELIMINATION METHOD
C SUPPLEMENTED BY A SEARCH FOR THE LARGEST PIVOTAL ELEMENT AT EACH STAGE
C [WRIGHT J., VISION]
*****
SUBROUTINE SOLVEMATRIX(N,A,XSOL)
IMPLICIT NONE

INTEGER N
DOUBLE PRECISION A(N,(N+2))
DOUBLE PRECISION XSOL(N)
DOUBLE PRECISION CMAX,TEMP,C,Y,D
DOUBLE PRECISION ABS
INTEGER NM1,NP1,NP2,I,J,L,LP,NOS,NI,NJ

NM1=N-1
NP1=N+1
NP2=N+2

```

```

DO I=1,N
    A(I,NP2)=0.0
    ! DO 1 J=1,NP1      ! TODO ?
    END DO

    DO I=1,N
        DO J=1,NP1
            A(I,NP2)=A(I,NP2)+A(I,J)
        END DO
    END DO
    DO L=1,N-1
        CMAX=A(L,L)
        LP=L+1
        NOS=L

        DO I=LP,N
            IF(ABS(CMAX).LT.ABS(A(I,L)))THEN
                CMAX=A(I,L)
                NOS=I
            ENDIF
        END DO
    ! SWAP ROWS
    IF (NOS.NE.L) THEN
        DO J=1,NP2
            TEMP=A(L,J)
            A(L,J)=A(NOS,J)
            A(NOS,J)=TEMP
        END DO
    END IF

    DO I=LP,N
        C=0.0
        Y=-A(I,L)/A(L,L)
        DO J=L,NP2
            A(I,J)=A(I,J)+Y*A(L,J)
        END DO
        DO J=L,NP1
            C=C+A(I,J)
        END DO
    END DO
END DO
! NOW BACKSUBSTITUTE
XSOL(N)=A(N,NP1)/A(N,N)
DO I=1,NM1
    NI=N-I
    D=0.0
    DO J=1,I
        NJ=N+1-J
        D=D+A(NI,NJ)*XSOL(NJ)
    END DO
    XSOL(NI)=(A(NI,NP1)-D)/A(NI,NI)
END DO
END

```

# Appendix D

## Pressure Drop Calculation

The total pressure drop,  $\Delta P_{tot}$ , needed to be overcome by the fan corresponds to the summation of the different pressure drops occurring in the flow line.

$$\Delta P_T = \Delta P_{col} + \Delta P_{buoy} + \Delta P_{acc} + \Delta P_{f,plen} + \Delta P_{f,duct} + \Delta P_{f,elbow} \quad (D.1)$$

In Equation D.1,  $\Delta P_{col}$  is the pressure drop through the collector surface,  $\Delta P_{buoy}$  is the buoyancy pressure drop,  $\Delta P_{acc}$  is the pressure drop due to the acceleration of the air, and  $\Delta P_{f,plen}$ ,  $\Delta P_{f,duct}$  and  $\Delta P_{f,elbow}$  represent the friction pressure drop in the plenum, in the duct and in the elbow, respectively.

The pressure drop through the collector is given by Kutscher (1994) as

$$\Delta P_{col} = \frac{\rho_{avg} V_s^2 \zeta}{2} \quad (D.2)$$

where the dimensionless variable  $\zeta$  corresponds to

$$\zeta = 6.82 \text{Re}_D^{-0.236} \left[ \frac{1 - \sigma}{\sigma} \right]^2 \quad (D.3)$$

and  $\text{Re}_D$  is defined as

$$\text{Re}_D = \frac{V_s D}{\sigma \nu_{avg}} \quad (D.4)$$

Assuming the average kinematic viscosity,  $\nu_{avg}$ , to be 0.0000159 m<sup>2</sup>/s, and a collector of 0.25% porosity with perforations having an equivalent diameter of 0.00079 m,  $Re_D$  and  $\zeta$  at a suction velocity of 0.02 m/s correspond to

$$Re_D = \frac{0.02 \frac{\text{m}}{\text{s}} * 0.00079 \text{m}}{0.0025 * 0.0000159 \frac{\text{m}^2}{\text{s}}} = 438.9 \quad (\text{D.5})$$

$$\zeta = 6.82(438.9^{-0.236}) \left[ \frac{1 - 0.0025}{0.0025} \right]^2 = 258.3 \times 10^3 \quad (\text{D.6})$$

Assuming air to be an ideal gas, the air density can be obtained from the ideal gas law.

$$\rho = \frac{P}{RT} \quad (\text{D.7})$$

In Equation D.7,  $R$  is the gas constant for air. Considering a pressure of 101.325 kPa, an ambient temperature of 20°C and a collector outlet temperature of 40°C, the air density at the average temperature in the plenum can be calculated as follows using Equation D.7.

$$\rho_{avg} = \frac{101.325 \text{ kPa}}{0.287 \frac{\text{kJ}}{\text{kg} \cdot \text{K}} * \left( \frac{293 + 313}{2} \right) \text{K}} = 1.17 \text{ kg/m}^3 \quad (\text{D.8})$$

Using the results from Equations D.6 and D.8 in Equation D.2, the pressure drop through the collector can be calculated.

$$\Delta P_{col} = \frac{1.17 \frac{\text{kg}}{\text{m}^3} * (0.02 \frac{\text{m}}{\text{s}})^2 * 258.3 * 10^3}{2} = 65.3 \text{ Pa} \quad (\text{D.9})$$

The acceleration pressure drop  $\Delta P_{acc}$  is given as

$$\Delta P_{acc} = \frac{\rho_{avg} V_{fan,out}^2}{2} \quad (\text{D.10})$$

where  $V_{fan,out}$  is the air velocity at the fan outlet expressed as

$$V_{fan,out} = \frac{\dot{V}_{max}}{A_{duct}} \quad (\text{D.11})$$

The panel has a width of 1.05 m and a length of 2.5 m. Thus, the maximum volumetric flowrate  $\dot{V}_{\max}$  corresponds to

$$\dot{V}_{\max} = 0.02 \frac{\text{m}}{\text{s}} * \frac{3600 \text{ s}}{\text{h}} * 1.05 \text{ m} * 2.5 \text{ m} = 196 \frac{\text{m}^3}{\text{h}} \quad (\text{D.12})$$

Using Equation D.12 in Equation D.13, the air velocity at the outlet of the fan for a duct with a diameter of 0.152 m is

$$V_{fan,out} = \frac{196 \frac{\text{m}^3}{\text{h}} * \frac{1 \text{ h}}{3600 \text{ s}}}{\frac{\pi * (0.152 \text{ m})^2}{4}} = 3 \frac{\text{m}}{\text{s}} \quad (\text{D.13})$$

Using the result from Equation D.13 in Equation D.10, the acceleration pressure drop can be obtained.

$$\Delta P_{acc} = \frac{1.17 \text{ kg/m}^3 * (3 \text{ m/s})^2}{2} = 5.2 \text{ Pa} \quad (\text{D.14})$$

The buoyancy pressure drop is expressed as

$$\Delta P_{buoy} = \frac{(\rho_{out} - \rho_{amb}) g L}{2} \quad (\text{D.15})$$

Using Equation D.7 to obtain  $\rho_{out}$  and  $\rho_{amb}$ ,  $\Delta P_{buoy}$  can be calculated.

$$\Delta P_{buoy} = \frac{(1.13 - 1.20) \text{ kg/m}^3 * 9.8 \text{ m/s}^2 * 2.5 \text{ m}}{2} = -0.9 \text{ Pa} \quad (\text{D.16})$$

The pressure drop components  $\Delta P_{f,plen}$  and  $\Delta P_{f,duct}$  of Equation D.1 can both be obtained with the following general equation.

$$\Delta P_f = f L \frac{\rho_{avg} V_{avg}^2}{2 D_h} \quad (\text{D.17})$$

where  $D_h$  is the hydraulic diameter. The friction factor,  $f$ , is given by the formula

of Swamee-Jain (Swamee & Jain, 1976) as

$$f = \frac{0.25}{\left[ \log_{10} \left( \frac{5.74}{Re^{0.9}} + \frac{\epsilon}{3.7D} \right)^2 \right]} \quad (D.18)$$

where  $\epsilon$  is the surface roughness. For the plenum, the average velocity and hydraulic diameter correspond to

$$V_{plen,avg} = \frac{1}{2} \frac{\dot{V}_{max}}{A_{plen}} = \frac{1}{2} \left( \frac{196 \frac{m^3}{h} * \frac{1 h}{3600 s}}{1.05 m * 0.14 m} \right) = 0.19 \frac{m}{s}$$

$$D_{h,plen} = 4 \frac{1.05 m * 0.14 m}{(2 * 0.14 m + 2 * 1.05 m)} = 0.25 m$$

Taking the roughness of galvanized steel to be 0.09 mm, the plenum friction factor and total pressure drop can be calculated.

$$f_{plen} = 0.25 * \left[ \log_{10} \left( \frac{5.74}{\left( \frac{0.19 m/s * 2.5 m}{0.0000159 m^2/s} \right)^{0.9} + \frac{0.0009 m}{3.7 * 0.25 m}} \right) \right]^{-2} = 0.024$$

$$\Delta P_{f,plen} = 0.024 * 2.5 m * \frac{1.17 kg/m^3 * (0.19 m/s)^2}{2 * 0.25 m} = 0.01 Pa \quad (D.19)$$

The roughness of the ABS pipe is 0.03 mm. Thus, the duct friction factor and frictional losses correspond to

$$f_{duct} = 0.25 * \left[ \log_{10} \left( \frac{5.74}{\left( \frac{3 m/s * 0.152 m}{0.0000159 m^2/s} \right)^{0.9} + \frac{0.0009 m}{3.7 * 0.152 m}} \right) \right]^{-2} = 0.024$$

$$\Delta P_{f,duct} = 0.024 * 2.3 m * \frac{1.13 kg/m^3 * (3 m/s)^2}{2 * 0.1524 m} = 1.8 Pa \quad (D.20)$$

The pressure drop due to the elbow is a function of the velocity pressure  $P_v$  and is expressed as

$$\Delta P_{f,elbow} = C_o P_v = C_o \left( \frac{V_{avg}}{1.414} \right)^2$$

For a 90° elbow with a diameter of 0.152 m and a ratio r/d of 1.5,  $C_o$  corresponds to 0.14 according to ASHRAE (2005). Thus,  $\Delta P_{f,elbow}$  is given as

$$\Delta P_{f,elbow} = 0.14 * \left( \frac{3 \text{ m/s}}{1.414} \right)^2 = 0.7 \text{ Pa} \quad (\text{D.21})$$

Using the results from Equations D.9, D.14, D.16 and D.19 to D.21, the total pressure drop of the system can be estimated to be 72 Pa.

# Appendix E

## Experimental Data

### E.1 Weather Data from the Roof Hut

Table E.1 presents the experimental data recorded hourly by the BEG Hut data logger and used as inputs in the TRNSYS simulations. The wind speed, wind direction and relative humidity (HR) were measured on the BEG Hut roof and the building temperature was recorded in the Hut.

**Table E.1:** Weather data measured by the BEG Hut data logger

Date	Time [h]	V <sub>wind</sub> [m/s]	Wind Direction [°]	T <sub>blg</sub> [°C]	HR [%]
29/08/2007	8:00	2.952	295.1	19.81	77.37
29/08/2007	9:00	3.609	293.1	20.02	73.20
29/08/2007	10:00	3.715	292.8	20.34	66.60
29/08/2007	11:00	3.584	294.1	20.64	60.58
29/08/2007	12:00	4.109	299.4	20.83	55.71
31/08/2007	7:00	0.687	296.3	20.05	88.80
31/08/2007	8:00	0.705	293.9	20.24	74.49
31/08/2007	9:00	1.486	266.4	20.02	62.79
31/08/2007	10:00	1.890	252.5	20.05	51.77
31/08/2007	11:00	2.466	207.2	20.08	43.93
31/08/2007	12:00	2.863	193.9	20.40	39.43
31/08/2007	13:00	3.082	272.3	20.50	39.69
01/09/2007	7:00	1.425	110.7	20.13	82.90
01/09/2007	8:00	1.930	135.8	20.05	76.09
01/09/2007	9:00	2.112	165.6	20.13	69.17
01/09/2007	10:00	2.118	132.0	20.10	59.72
01/09/2007	11:00	1.982	167.5	20.18	51.70
01/09/2007	12:00	2.152	159.9	20.26	44.28
01/09/2007	13:00	1.885	198.6	20.34	42.72

Date	Time [h]	V <sub>wind</sub> [m/s]	Wind Direction [°]	T <sub>blg</sub> [°C]	HR [%]
02/09/2007	7:00	0.477	170.3	20.13	78.80
02/09/2007	8:00	0.980	257.6	20.29	68.20
02/09/2007	9:00	1.933	283.4	20.13	58.54
02/09/2007	10:00	2.958	305.8	20.18	54.24
02/09/2007	11:00	2.687	314.5	20.13	53.01
02/09/2007	12:00	2.450	304.6	20.13	48.92
02/09/2007	13:00	2.695	286.4	20.18	46.76
06/09/2007	7:00	0.242	184.3	20.24	87.60
06/09/2007	8:00	0.926	232.3	20.29	77.82
06/09/2007	9:00	2.486	281.1	20.18	67.60
06/09/2007	10:00	3.129	284.3	20.34	57.86
06/09/2007	11:00	3.900	288.0	20.24	45.61
06/09/2007	12:00	3.968	289.4	20.00	37.18
06/09/2007	13:00	5.093	296.0	20.13	33.82
06/09/2007	14:00	4.881	296.7	20.26	30.24
08/09/2007	7:00	2.161	320.5	20.05	60.86
08/09/2007	8:00	2.522	323.6	20.08	221.80
08/09/2007	9:00	2.038	289.3	20.00	402.70
08/09/2007	10:00	2.134	253.2	20.02	555.90
08/09/2007	11:00	1.152	269.1	19.89	677.90
08/09/2007	12:00	1.291	229.8	19.89	745.70
08/09/2007	13:00	1.695	286.3	20.29	704.00
02/09/2007	7:00	0.477	170.3	20.13	78.80
02/09/2007	8:00	0.980	257.6	20.29	68.20
02/09/2007	9:00	1.933	283.4	20.13	58.54
02/09/2007	10:00	2.958	305.8	20.18	54.24
02/09/2007	11:00	2.687	314.5	20.13	53.01
02/09/2007	12:00	2.450	304.6	20.13	48.92
02/09/2007	13:00	2.695	286.4	20.18	46.76
06/09/2007	7:00	0.242	184.3	20.24	87.60
06/09/2007	8:00	0.926	232.3	20.29	77.82
06/09/2007	9:00	2.486	281.1	20.18	67.60
06/09/2007	10:00	3.129	284.3	20.34	57.86
06/09/2007	11:00	3.900	288.0	20.24	45.61
06/09/2007	12:00	3.968	289.4	20.00	37.18
06/09/2007	13:00	5.093	296.0	20.13	33.82
06/09/2007	14:00	4.881	296.7	20.26	30.24
08/09/2007	7:00	2.161	320.5	20.05	60.86
08/09/2007	8:00	2.522	323.6	20.08	221.80
08/09/2007	9:00	2.038	289.3	20.00	402.70
08/09/2007	10:00	2.134	253.2	20.02	555.90
08/09/2007	11:00	1.152	269.1	19.89	677.90
08/09/2007	12:00	1.291	229.8	19.89	745.70
08/09/2007	13:00	1.695	286.3	20.29	704.00

## E.2 Experimental Data

Tables E.2 to E.7 present the data recorded during the experiment at a time step of one minute as well as some calculated values.

Table E.2: Experimental Data for August 29

Time [h]	T <sub>wall</sub> [°C]	T <sub>col,1</sub> [°C]	T <sub>col,2</sub> [°C]	T <sub>col,3</sub> [°C]	T <sub>col,4</sub> [°C]	T <sub>out</sub> [°C]	T <sub>amb</sub> [°C]	G <sub>T,col</sub> [W/m <sup>2</sup> ]	Flow Rate [m <sup>3</sup> /h m <sup>2</sup> ]	P <sub>el</sub> [W]	Q'' <sub>u</sub> [W/m <sup>2</sup> ]	Eff <sub>th</sub> %	Eff <sub>PV</sub> %
8:41	26.1	33.3	31.2	37.2	34.4	30.7	23.9	550.0	73.05	1.75	160.8	29.2	4.54
8:42	26.4	33.6	31.4	37.3	34.4	31.1	24.0	550.5	74.05	1.75	171.2	31.1	4.53
8:43	26.5	33.7	31.4	37.5	34.6	31.2	24.1	555.2	74.24	1.75	172.2	31.0	4.50
8:44	26.7	34.6	32.0	38.6	35.4	31.6	24.4	559.2	73.55	1.73	173.5	31.0	4.42
8:45	27.0	35.0	32.5	39.1	35.7	32.1	24.5	564.0	73.39	1.75	181.5	32.2	4.41
8:46	27.2	35.2	32.8	39.3	36.0	32.5	24.7	571.8	73.66	1.75	185.1	32.4	4.37
8:47	27.4	35.4	32.8	39.3	35.9	32.6	25.0	572.8	74.03	1.76	183.4	32.0	4.39
8:48	27.6	35.5	32.9	39.5	36.1	32.8	25.2	573.7	74.52	1.75	183.2	31.9	4.34
8:49	27.8	35.6	33.3	39.8	36.4	33.0	25.1	575.6	74.50	1.74	188.8	32.8	4.30
8:50	28.0	35.4	33.1	39.4	36.2	33.0	25.1	577.9	74.07	1.75	188.0	32.5	4.31
8:51	28.1	35.3	33.1	39.4	36.3	32.9	25.2	580.6	74.67	1.75	187.2	32.3	4.29
8:52	28.2	35.5	33.3	39.7	36.6	33.1	25.3	581.4	73.78	1.76	186.2	32.0	4.31
8:53	28.4	36.1	33.8	40.5	37.1	33.5	25.4	586.8	73.99	1.74	193.9	33.0	4.22
8:54	28.6	36.3	33.7	40.5	37.1	33.7	25.5	588.9	74.37	1.74	196.5	33.4	4.22
8:55	28.7	36.3	33.9	40.4	37.0	33.8	25.4	589.7	74.03	1.75	199.8	33.9	4.23
8:56	28.8	36.1	33.7	40.0	36.8	33.7	25.5	590.8	74.28	1.75	195.8	33.1	4.22
8:57	29.0	36.7	34.2	40.9	37.5	34.0	25.9	593.3	73.07	1.74	190.7	32.1	4.18
8:58	29.2	36.9	34.3	41.0	37.6	34.2	26.0	595.1	73.71	1.75	195.1	32.8	4.19
8:59	29.3	36.7	34.3	40.9	37.5	34.3	25.9	597.5	74.08	1.74	199.7	33.4	4.16
9:00	29.5	36.7	34.3	40.5	37.3	34.3	25.8	596.5	73.89	1.74	200.8	33.7	4.15
9:01	29.5	36.5	34.3	40.3	37.2	34.2	26.0	600.9	74.48	1.77	197.9	32.9	4.20
9:02	29.6	36.6	34.3	40.4	37.3	34.2	25.9	601.4	73.77	1.76	196.7	32.7	4.18
9:03	29.9	36.7	34.4	40.3	37.3	34.4	26.1	604.5	73.95	1.76	196.5	32.5	4.16
9:04	29.8	36.8	34.4	40.5	37.3	34.4	26.1	604.3	73.63	1.75	194.9	32.3	4.13
9:05	29.9	36.6	34.4	40.3	37.2	34.4	26.1	603.1	74.09	1.75	196.5	32.6	4.13
9:06	30.0	36.6	34.5	40.3	37.3	34.4	26.1	604.5	74.06	1.75	199.0	32.9	4.13
9:07	30.2	36.6	34.5	40.5	37.5	34.5	26.1	608.1	74.11	1.77	198.4	32.6	4.14
9:08	30.2	36.9	34.9	41.0	37.8	34.7	26.2	609.0	73.67	1.74	200.8	33.0	4.09
9:09	30.3	37.2	34.9	41.3	37.9	34.8	26.2	612.1	73.99	1.77	203.9	33.3	4.11
9:10	30.5	37.2	34.9	41.0	37.8	34.9	26.5	613.8	74.20	1.75	201.1	32.8	4.06
9:11	30.6	37.3	34.9	41.1	37.9	34.9	26.5	614.7	73.73	1.77	198.0	32.2	4.11
9:12	30.7	37.5	35.3	41.5	38.3	35.1	26.5	615.6	73.31	1.76	202.7	32.9	4.08
9:13	30.8	37.5	35.1	41.4	38.2	35.1	26.5	614.2	73.80	1.76	205.3	33.4	4.09
9:14	30.9	37.5	34.9	41.0	37.7	35.2	26.6	611.4	73.94	1.78	203.2	33.2	4.15
9:15	30.9	36.9	34.7	40.4	37.4	34.9	26.4	604.9	73.76	1.77	202.5	33.5	4.17
9:16	31.0	37.0	35.0	40.6	37.6	34.9	26.2	611.5	73.40	1.78	204.1	33.4	4.15
9:17	31.0	37.0	34.8	40.4	37.4	34.9	26.2	613.8	73.80	1.77	206.5	33.6	4.12
9:18	31.1	36.9	35.0	40.6	37.7	34.9	26.4	618.9	73.55	1.75	200.6	32.4	4.03
9:19	31.1	36.8	34.8	40.3	37.5	34.8	26.4	623.2	73.83	1.75	200.6	32.2	4.00
9:20	31.1	36.5	34.5	39.9	37.2	34.6	26.4	623.3	73.92	1.75	196.5	31.5	4.01
9:21	31.2	36.8	34.8	40.4	37.5	34.7	26.5	625.2	73.48	1.75	194.9	31.2	3.99
9:22	31.3	37.6	35.5	41.6	38.5	35.1	26.8	628.7	72.27	1.76	193.5	30.8	3.99
9:23	31.5	38.1	35.8	42.3	38.9	35.6	26.9	631.4	73.11	1.76	202.9	32.1	3.97
9:24	31.6	38.2	35.6	42.1	38.7	35.8	27.0	631.5	73.51	1.76	206.0	32.6	3.96
9:25	31.7	38.5	35.8	42.2	38.7	36.0	27.2	632.1	73.05	1.72	204.1	32.3	3.87
9:26	31.8	38.4	36.0	42.2	39.0	36.0	27.5	634.9	73.23	1.73	199.2	31.4	3.88
9:27	31.9	38.6	36.0	42.3	38.9	36.1	27.6	637.8	73.07	1.75	197.9	31.0	3.90
9:28	32.0	38.7	36.1	42.5	39.1	36.2	27.9	637.7	72.28	1.74	190.3	29.8	3.89
9:29	32.2	39.3	36.9	43.7	40.0	36.5	27.9	639.6	72.63	1.73	199.8	31.2	3.86
9:30	32.3	39.0	36.6	43.2	39.5	36.7	27.7	636.5	73.70	1.72	209.6	32.9	3.85
9:31	32.3	38.4	36.0	42.1	38.9	36.3	27.5	637.7	74.29	1.75	207.7	32.6	3.91
9:32	32.4	38.6	36.3	42.3	39.2	36.3	27.6	639.4	73.69	1.73	204.8	32.0	3.85
9:33	32.5	38.9	36.4	42.8	39.5	36.5	27.8	640.9	73.92	1.75	206.8	32.3	3.90
9:34	32.6	39.2	36.7	43.3	39.8	36.7	28.0	638.8	73.79	1.75	204.3	32.0	3.91
9:35	32.7	39.1	36.8	43.3	39.8	36.8	27.9	641.5	74.03	1.73	209.5	32.7	3.85
9:36	32.7	38.8	36.4	42.9	39.4	36.7	27.7	638.9	74.65	1.75	212.8	33.3	3.90
9:37	32.7	38.1	36.0	42.0	38.9	36.3	27.6	637.3	74.49	1.75	206.2	32.4	3.91
9:38	32.8	38.6	36.4	42.4	39.2	36.3	27.7	637.6	74.10	1.76	205.5	32.2	3.93
9:39	32.9	38.8	36.5	42.5	39.2	36.5	27.9	640.9	73.57	1.74	201.1	31.4	3.88
9:40	32.9	38.8	36.5	42.5	39.3	36.6	28.0	642.2	75.01	1.75	206.6	32.2	3.88
9:41	33.0	38.7	36.3	42.5	39.1	36.6	28.1	641.9	75.19	1.74	203.3	31.7	3.87

Time [h]	T <sub>wall</sub> [°C]	T <sub>col,1</sub> [°C]	T <sub>col,2</sub> [°C]	T <sub>col,3</sub> [°C]	T <sub>col,4</sub> [°C]	T <sub>out</sub> [°C]	T <sub>amb</sub> [°C]	G <sub>T,col</sub> [W/m <sup>2</sup> ]	Flow Rate [m <sup>3</sup> /h m <sup>2</sup> ]	P <sub>el</sub> [W]	Q'' <sub>u</sub> [W/m <sup>2</sup> ]	Eff <sub>th</sub> %	Eff <sub>PV</sub> %
9:42	33.0	38.6	36.3	42.2	39.0	36.5	28.2	639.4	75.42	1.74	201.0	31.4	3.89
9:43	33.0	38.3	36.1	41.7	38.7	36.4	28.2	636.3	74.94	1.73	195.2	30.7	3.87
9:44	33.1	38.6	36.3	42.2	39.1	36.5	28.3	634.4	74.07	1.73	194.1	30.6	3.88
9:45	33.2	38.8	36.3	42.2	39.0	36.7	28.4	633.4	74.66	1.73	196.5	31.0	3.90
9:46	33.2	38.4	36.3	42.1	39.1	36.5	28.2	634.4	73.96	1.74	196.1	30.9	3.90
9:47	33.2	38.6	36.4	42.3	39.1	36.5	28.2	632.6	74.17	1.72	198.5	31.4	3.87
9:48	33.3	38.8	36.6	42.6	39.5	36.6	28.3	632.9	73.16	1.73	194.5	30.7	3.89
9:49	33.4	38.9	36.6	42.5	39.4	36.7	28.2	631.7	73.76	1.72	200.9	31.8	3.88
9:50	33.4	39.0	36.5	42.5	39.3	36.8	28.3	637.6	73.40	1.73	197.4	31.0	3.86
9:51	33.5	39.4	36.6	42.7	39.3	37.0	28.6	636.8	73.35	1.73	195.1	30.6	3.87
9:52	33.6	39.6	37.2	43.5	40.0	37.2	28.9	638.2	75.19	1.74	199.1	31.2	3.89
9:53	33.7	39.4	37.2	43.4	40.0	37.2	28.7	639.1	76.54	1.74	209.2	32.7	3.89
9:54	33.8	39.5	37.2	43.6	40.2	37.3	28.7	639.2	76.57	1.73	210.1	32.9	3.85
9:55	33.9	39.5	37.0	43.2	39.8	37.4	29.1	639.1	76.29	1.71	202.3	31.7	3.82
9:56	33.9	39.0	36.6	42.5	39.3	37.1	28.8	637.9	76.23	1.73	201.0	31.5	3.86
9:57	33.9	38.8	36.5	42.1	39.1	36.8	28.8	639.0	76.72	1.72	198.1	31.0	3.84
9:58	33.9	39.0	36.8	42.6	39.5	36.9	29.0	638.8	76.07	1.72	192.5	30.1	3.84
9:59	34.0	39.2	37.1	42.9	39.8	37.2	29.1	633.3	76.08	1.72	196.9	31.1	3.87
10:00	34.1	39.2	37.0	42.9	39.9	37.2	29.1	634.5	76.53	1.70	196.9	31.0	3.83
10:01	34.1	39.4	37.2	43.1	40.1	37.3	29.2	635.9	75.97	1.69	195.6	30.8	3.79
10:02	34.1	39.5	37.0	42.8	39.7	37.4	29.2	630.0	75.96	1.69	198.6	31.5	3.82
10:03	34.2	39.4	37.2	43.0	39.8	37.4	29.5	626.0	76.00	1.71	191.2	30.5	3.91
10:04	34.3	39.8	37.4	43.5	40.2	37.5	29.7	631.2	75.46	1.70	187.0	29.6	3.85
10:05	34.4	40.1	37.7	43.9	40.5	37.8	30.2	630.0	75.71	1.70	183.1	29.1	3.84
10:06	34.5	40.4	37.8	44.3	40.6	38.0	30.2	630.0	75.64	1.71	187.6	29.8	3.87
10:07	34.6	39.9	37.6	43.8	40.3	37.9	30.0	624.7	76.69	1.72	193.0	30.9	3.93
10:08	34.6	39.9	37.7	44.0	40.6	37.7	29.8	626.8	75.57	1.72	192.3	30.7	3.91
10:09	34.7	40.1	37.6	44.2	40.6	37.9	30.0	625.4	76.14	1.68	192.4	30.8	3.84
10:10	34.6	39.9	37.3	43.3	39.8	37.8	29.7	625.9	76.33	1.68	195.0	31.2	3.84
10:11	34.6	39.5	37.5	43.2	39.9	37.6	29.6	622.1	75.88	1.68	193.0	31.0	3.86
10:12	34.7	39.5	37.4	43.2	40.0	37.6	29.7	620.0	75.93	1.68	192.4	31.0	3.87
10:13	34.8	40.1	37.9	44.1	40.6	37.9	30.4	620.3	75.38	1.69	180.4	29.1	3.89
10:14	34.9	40.4	38.0	44.2	40.8	38.2	30.6	615.8	75.54	1.71	182.5	29.6	3.96
10:15	35.0	40.7	38.3	44.8	41.2	38.3	30.8	616.7	75.70	1.69	182.2	29.5	3.91
10:16	35.1	40.8	38.2	44.9	41.1	38.5	30.7	612.6	75.81	1.69	187.8	30.7	3.94
10:17	35.1	40.5	38.1	44.6	40.9	38.4	30.7	616.7	76.01	1.69	187.1	30.3	3.92
10:18	35.1	40.1	37.7	44.1	40.5	38.1	30.4	615.4	76.31	1.69	187.2	30.4	3.91
10:19	35.1	40.5	37.8	44.6	41.0	38.1	30.5	615.2	75.41	1.68	182.5	29.7	3.91
10:20	35.2	40.6	37.9	44.6	40.9	38.3	30.8	609.5	75.41	1.67	179.1	29.4	3.91
10:21	35.2	40.3	38.0	44.4	40.9	38.3	30.6	610.1	75.89	1.69	183.7	30.1	3.96
10:22	35.3	40.7	38.2	44.5	41.0	38.5	30.8	608.2	75.39	1.68	183.8	30.2	3.95
10:23	35.4	40.7	38.3	44.7	41.1	38.5	31.0	606.1	75.75	1.70	180.2	29.7	3.99
10:24	35.5	40.8	38.2	44.6	40.8	38.6	31.1	602.9	75.92	1.68	180.6	30.0	3.98
10:25	35.4	39.9	37.5	43.3	39.9	38.1	30.4	601.9	77.39	1.67	188.8	31.4	3.96
10:26	35.4	39.7	37.7	43.4	40.3	37.9	30.5	603.6	76.78	1.68	181.7	30.1	3.98
10:27	35.4	39.6	37.6	43.3	40.2	37.9	30.4	600.4	76.66	1.69	182.4	30.4	4.01
10:28	35.3	39.6	37.6	43.3	40.3	37.8	30.4	598.3	75.97	1.69	179.1	29.9	4.02
10:29	35.4	40.2	37.8	43.9	40.5	38.1	30.7	598.6	76.83	1.68	180.8	30.2	3.99
10:30	35.5	40.2	37.9	44.1	40.6	38.1	30.6	596.8	76.41	1.67	184.0	30.8	3.99
10:31	35.5	40.0	37.9	44.1	40.6	38.2	30.5	595.1	76.56	1.67	188.1	31.6	4.01
10:32	35.5	40.1	37.9	44.0	40.6	38.2	30.7	595.0	77.08	1.67	183.9	30.9	4.01
10:33	35.6	40.3	38.1	44.3	40.8	38.3	30.9	595.5	77.83	1.69	181.7	30.5	4.05
10:34	35.6	40.5	38.0	44.4	40.9	38.4	31.0	593.6	76.74	1.67	179.5	30.2	4.01
10:35	35.7	40.6	38.2	44.5	40.8	38.5	31.2	591.6	77.06	1.67	178.5	30.2	4.03
10:36	35.7	40.2	37.7	43.6	40.2	38.4	31.3	587.1	77.51	1.69	174.3	29.7	4.10
10:37	35.7	39.9	37.7	43.3	40.2	38.2	31.3	589.1	77.49	1.68	168.0	28.5	4.06
10:38	35.7	40.3	38.1	44.1	40.9	38.4	31.4	588.4	76.70	1.66	169.2	28.8	4.02
10:39	35.8	40.7	38.4	44.4	41.1	38.6	31.6	589.5	76.09	1.68	168.2	28.5	4.05
10:40	35.9	40.3	38.1	44.1	40.8	38.5	31.3	587.3	77.50	1.68	177.7	30.3	4.08
10:41	35.9	40.3	38.1	44.4	41.0	38.4	31.2	584.8	77.17	1.67	178.6	30.5	4.07
10:42	35.9	40.6	38.1	44.6	41.0	38.5	31.4	584.8	77.18	1.68	174.8	29.9	4.09
10:43	35.8	40.1	37.8	43.6	40.3	38.3	31.5	579.6	77.57	1.65	166.8	28.8	4.07
10:44	35.8	39.5	37.5	43.0	39.9	38.0	31.1	579.9	77.68	1.68	169.4	29.2	4.14

Time [h]	T <sub>wall</sub> [°C]	T <sub>col,1</sub> [°C]	T <sub>col,2</sub> [°C]	T <sub>col,3</sub> [°C]	T <sub>col,4</sub> [°C]	T <sub>out</sub> [°C]	T <sub>amb</sub> [°C]	G <sub>T,col</sub> [W/m <sup>2</sup> ]	Flow Rate [m <sup>3</sup> /h m <sup>2</sup> ]	P <sub>el</sub> [W]	Q'' <sub>u</sub> [W/m <sup>2</sup> ]	Eff <sub>th</sub> %	Eff <sub>PV</sub> %
10:45	35.3	37.5	35.7	40.0	37.4	36.3	32.7	410.5	76.39	1.68	88.1	21.5	5.84
10:46	35.8	39.5	37.4	43.1	40.1	37.9	31.0	576.0	77.08	1.66	167.6	29.1	4.12
10:47	35.8	39.8	37.6	43.4	40.3	38.0	31.3	572.8	76.41	1.67	162.4	28.4	4.16
10:48	35.8	39.6	37.5	43.0	39.8	38.0	31.4	571.1	76.98	1.66	161.2	28.2	4.14
10:49	35.8	39.6	37.5	43.1	40.1	37.9	31.3	571.3	77.18	1.66	163.1	28.5	4.14
10:50	35.8	39.9	37.7	43.3	40.2	38.0	31.4	570.3	76.38	1.63	159.9	28.0	4.07
10:51	35.9	39.9	37.6	43.1	40.1	38.1	31.6	567.0	76.28	1.64	158.2	27.9	4.13
10:52	35.9	40.0	37.6	43.2	40.0	38.2	31.7	566.7	76.11	1.64	157.7	27.8	4.14
10:53	35.9	40.2	37.9	43.7	40.5	38.3	32.1	566.7	75.48	1.65	147.7	26.1	4.15
10:54	36.1	40.5	38.4	44.4	41.0	38.6	32.5	566.1	75.88	1.64	146.2	25.8	4.13
10:55	36.1	40.4	38.1	43.9	40.6	38.6	32.0	565.4	76.09	1.63	159.2	28.2	4.12
10:56	36.0	40.0	37.7	43.1	40.0	38.3	31.9	561.1	76.56	1.65	156.4	27.9	4.18
10:57	36.0	39.8	37.7	43.1	40.1	38.1	31.9	557.3	76.37	1.63	151.4	27.2	4.17
10:58	36.0	39.9	37.9	43.4	40.4	38.2	31.9	552.3	75.99	1.63	152.5	27.6	4.21
10:59	36.0	39.9	37.8	43.4	40.1	38.2	31.7	550.1	76.33	1.62	157.5	28.6	4.19
11:00	36.0	39.7	37.7	43.2	40.1	38.1	31.6	550.2	76.02	1.62	156.2	28.4	4.20
11:01	36.1	39.9	38.0	43.5	40.4	38.3	32.0	544.4	75.67	1.61	151.4	27.8	4.21
11:02	36.2	40.1	38.1	43.7	40.5	38.4	32.2	544.5	76.15	1.61	149.5	27.5	4.22
11:03	36.2	40.3	38.2	44.1	40.7	38.5	32.2	540.9	76.03	1.60	151.0	27.9	4.23
11:04	36.3	40.7	38.4	44.4	41.1	38.7	32.7	540.0	76.06	1.60	145.6	27.0	4.22
11:05	36.4	40.8	38.5	44.3	41.0	38.9	33.1	537.1	75.52	1.60	138.7	25.8	4.24
11:06	36.4	40.4	38.2	43.9	40.5	38.7	32.6	534.0	76.26	1.60	146.3	27.4	4.28
11:07	36.3	40.3	38.0	43.9	40.5	38.5	32.7	535.1	76.64	1.62	141.0	26.4	4.31
11:08	36.3	40.6	38.2	44.4	40.8	38.6	33.1	528.7	76.20	1.60	133.6	25.3	4.32
11:09	36.4	40.6	38.2	43.9	40.5	38.8	33.4	528.0	75.73	1.61	128.5	24.3	4.35
11:10	36.4	40.4	38.0	43.8	40.5	38.7	33.5	522.7	75.74	1.60	124.7	23.9	4.37
11:11	36.4	40.3	38.0	43.7	40.4	38.5	33.3	526.1	76.53	1.61	127.7	24.3	4.37
11:12	36.4	40.3	38.0	43.7	40.3	38.6	33.3	524.0	75.81	1.61	125.9	24.0	4.39
11:13	36.4	39.9	37.9	43.2	40.1	38.4	32.9	519.0	76.41	1.60	132.8	25.6	4.41
11:14	36.4	40.2	37.8	43.4	40.1	38.4	33.0	519.1	75.76	1.60	130.3	25.1	4.39
11:15	36.4	39.9	37.7	43.3	40.0	38.3	32.9	516.0	76.10	1.61	129.7	25.1	4.44
11:16	36.3	39.5	37.5	42.8	39.7	38.1	32.5	514.8	75.70	1.60	135.3	26.3	4.42
11:17	36.3	39.6	37.6	43.0	39.9	38.0	32.3	510.4	75.93	1.60	137.8	27.0	4.46
11:18	36.3	39.7	37.5	43.0	39.8	38.1	32.5	506.6	76.32	1.59	135.5	26.7	4.47
11:19	36.2	39.3	37.3	42.6	39.5	37.9	32.5	503.6	77.27	1.60	133.0	26.4	4.53
11:20	36.2	39.7	37.5	43.0	39.8	38.0	32.6	502.6	75.96	1.57	129.5	25.8	4.46
11:21	36.2	39.5	37.2	42.6	39.4	37.9	32.6	501.3	76.78	1.59	130.1	26.0	4.52
11:22	36.2	39.2	37.0	42.0	39.0	37.8	32.7	495.1	75.89	1.59	121.8	24.6	4.59
11:23	36.2	39.2	37.1	42.0	39.2	37.7	32.7	498.2	76.44	1.58	122.5	24.6	4.52
11:24	36.2	39.6	37.4	42.5	39.5	37.9	32.9	495.3	75.72	1.60	121.4	24.5	4.60
11:25	36.2	39.3	37.3	42.1	39.2	37.8	32.7	495.1	76.32	1.57	124.2	25.1	4.51
11:26	36.2	38.9	37.1	41.7	38.9	37.7	32.7	486.2	76.66	1.57	121.9	25.1	4.60
11:27	36.1	38.7	36.9	41.5	38.9	37.5	32.2	478.2	76.68	1.57	128.3	26.8	4.68
11:28	36.4	38.9	37.2	42.0	39.3	37.6	32.5	484.4	76.78	1.55	126.6	26.1	4.55
11:29	36.4	39.2	37.3	42.4	39.5	37.8	32.7	480.4	76.53	1.56	124.2	25.9	4.64
11:30	36.4	39.1	37.2	42.0	39.2	37.8	32.7	477.9	76.70	1.56	122.6	25.6	4.65
11:31	36.3	38.7	36.8	41.2	38.5	37.5	32.7	466.6	76.92	1.53	116.7	25.0	4.69
11:32	36.3	38.8	36.8	41.4	38.6	37.5	33.0	461.8	76.66	1.53	108.6	23.5	4.73
11:33	36.2	38.8	36.8	41.3	38.7	37.5	33.4	464.5	76.92	1.53	99.8	21.5	4.70
11:34	36.3	38.9	36.9	41.5	38.8	37.6	33.0	467.9	76.81	1.53	111.7	23.9	4.66
11:35	36.3	38.9	36.9	41.5	38.8	37.5	33.0	465.6	76.72	1.54	110.0	23.6	4.71
11:36	36.3	38.9	36.9	41.5	38.8	37.5	33.0	463.5	76.64	1.55	110.1	23.8	4.77
11:37	36.3	38.9	36.9	41.6	38.8	37.5	33.0	461.9	76.57	1.54	110.1	23.8	4.74
11:38	36.3	38.9	37.0	41.6	38.8	37.5	33.0	460.8	76.57	1.52	110.0	23.9	4.72
11:39	36.2	38.9	37.0	41.6	38.8	37.5	33.0	460.2	76.50	1.52	109.7	23.8	4.71
11:40	36.2	38.8	36.9	41.6	38.8	37.5	33.0	459.8	76.50	1.51	109.4	23.8	4.70
11:41	36.2	38.8	36.9	41.5	38.7	37.4	33.0	459.1	76.46	1.51	109.1	23.8	4.70
11:42	36.2	38.7	36.9	41.5	38.7	37.4	32.9	458.2	76.45	1.51	109.2	23.8	4.69
11:43	36.1	38.7	36.9	41.6	38.7	37.4	32.9	457.3	76.42	1.52	108.8	23.8	4.73
11:44	36.1	38.7	36.8	41.6	38.7	37.4	33.0	456.4	76.42	1.55	108.0	23.7	4.86
11:45	35.8	38.3	36.3	40.9	38.0	37.1	33.3	440.2	77.06	1.44	95.1	21.6	4.66

Table E.3: Experimental data for August 31

Time [h]	T <sub>wall</sub> [°C]	T <sub>col,1</sub> [°C]	T <sub>col,2</sub> [°C]	T <sub>col,3</sub> [°C]	T <sub>col,4</sub> [°C]	T <sub>out</sub> [°C]	T <sub>amb</sub> [°C]	G <sub>T,col</sub> [W/m <sup>2</sup> ]	Flow Rate [m <sup>3</sup> /h m <sup>2</sup> ]	P <sub>el</sub> [W]	Q <sup>u</sup> [W/m <sup>2</sup> ]	Eff <sub>th</sub> %	Eff <sub>PV</sub> %
7:36	16.6	24.5	21.8	28.9	25.2	22.2	13.3	542.6	72.12	1.92	215.8	39.8	5.05
7:37	16.7	24.9	21.8	29.0	25.4	22.3	13.3	548.2	71.77	1.95	217.1	39.6	5.06
7:38	16.8	25.3	22.0	28.8	25.6	22.6	13.3	554.2	72.01	1.94	225.8	40.7	4.99
7:39	16.9	25.5	22.1	29.0	25.7	22.8	13.3	559.4	71.86	1.95	229.6	41.0	4.97
7:40	17.0	25.9	22.4	29.3	26.0	23.1	13.3	564.9	72.08	1.94	234.9	41.6	4.89
7:41	17.2	26.1	22.7	29.5	26.2	23.3	13.3	570.0	71.99	1.92	242.8	42.6	4.81
7:42	17.3	26.3	22.8	29.6	26.3	23.5	13.2	575.2	71.85	1.93	247.5	43.0	4.80
7:43	17.4	26.5	22.8	29.7	26.3	23.6	13.2	580.2	72.19	1.94	250.8	43.2	4.76
7:44	17.6	26.5	22.8	30.1	26.5	23.6	13.3	585.8	71.61	1.95	248.3	42.4	4.74
7:45	17.7	26.8	23.2	30.4	26.9	23.9	13.3	591.1	71.47	1.93	253.3	42.9	4.66
7:46	17.9	26.7	23.2	30.4	26.9	24.0	13.3	596.0	72.29	1.93	256.9	43.1	4.61
7:47	18.0	26.8	23.4	30.9	27.2	24.1	13.5	600.3	71.54	1.93	251.7	41.9	4.58
7:48	18.2	27.1	23.6	31.1	27.4	24.3	13.6	604.4	71.16	1.94	254.5	42.1	4.58
7:49	18.3	27.3	23.9	31.5	27.6	24.5	13.8	608.6	70.83	1.92	252.2	41.4	4.51
7:50	18.5	27.7	24.0	31.7	27.8	24.8	14.0	613.6	70.87	1.92	255.4	41.6	4.46
7:51	18.7	28.1	24.3	31.7	28.0	25.1	14.0	617.3	71.73	1.94	265.2	43.0	4.48
7:52	18.9	28.3	24.4	32.0	28.3	25.3	14.2	623.4	71.48	1.93	263.4	42.3	4.42
7:53	19.1	28.6	24.8	32.3	28.6	25.6	14.3	628.1	71.16	1.92	267.1	42.5	4.36
7:54	19.2	28.8	24.9	32.3	28.6	25.7	14.2	632.0	71.29	1.92	272.5	43.1	4.34
7:55	19.4	28.5	24.9	32.6	28.7	25.6	14.4	635.7	71.93	1.92	267.6	42.1	4.31
7:56	19.6	29.1	25.2	32.9	29.1	26.0	14.6	639.9	71.05	1.94	268.2	41.9	4.33
7:57	19.8	29.1	25.5	33.4	29.3	26.1	14.8	643.9	71.53	1.92	268.7	41.7	4.26
7:58	20.0	28.8	25.4	33.6	29.2	26.1	14.8	646.9	71.96	1.93	268.2	41.5	4.25
7:59	20.1	29.5	25.6	33.8	29.6	26.4	14.9	651.2	70.86	1.91	270.9	41.6	4.19
8:00	20.4	30.0	25.9	33.8	29.7	26.8	15.0	655.1	71.41	1.93	279.6	42.7	4.20
8:01	20.5	30.1	26.0	34.0	30.0	26.9	15.1	658.7	71.81	1.91	281.2	42.7	4.14
8:02	20.7	30.5	26.3	34.1	30.1	27.2	15.0	661.7	72.07	1.91	290.1	43.8	4.12
8:03	20.9	30.4	26.3	34.2	30.2	27.2	15.1	664.8	71.90	1.90	288.7	43.4	4.08
8:04	21.1	30.7	26.7	34.2	30.2	27.5	15.3	668.1	71.36	1.91	287.3	43.0	4.07
8:05	21.3	30.8	26.6	33.9	30.1	27.6	15.0	671.1	72.10	1.91	298.7	44.5	4.07
8:06	21.4	30.7	26.6	34.2	30.3	27.5	15.0	672.9	72.03	1.89	297.2	44.2	4.01
8:07	21.6	31.1	26.9	34.6	30.7	27.8	15.2	675.0	71.84	1.90	298.7	44.3	4.02
8:08	21.8	31.0	26.9	34.3	30.4	27.9	15.2	678.3	71.34	1.91	297.3	43.8	4.02
8:09	21.9	30.9	26.8	34.4	30.5	27.9	15.4	682.3	72.53	1.90	299.0	43.8	3.98
8:10	22.0	31.3	27.2	34.9	30.9	28.1	15.6	685.0	71.56	1.89	295.8	43.2	3.94
8:11	22.2	31.3	27.1	35.1	31.0	28.2	15.5	687.0	71.84	1.89	300.9	43.8	3.93
8:12	22.3	31.5	27.4	35.9	31.5	28.3	15.9	690.3	71.56	1.88	293.8	42.6	3.89
8:13	22.5	31.7	27.6	36.4	31.7	28.6	16.2	692.9	71.66	1.89	291.1	42.0	3.89
8:14	22.7	32.3	27.9	36.4	31.8	28.9	16.3	695.3	71.65	1.88	295.8	42.5	3.86
8:15	22.9	32.3	27.9	35.7	31.6	29.0	16.0	698.7	72.33	1.90	309.0	44.2	3.87
8:16	23.0	32.4	28.0	35.9	31.8	29.1	15.9	700.8	71.82	1.89	311.2	44.4	3.85
8:17	23.2	32.5	28.3	36.6	32.2	29.2	16.3	703.4	72.26	1.88	307.1	43.7	3.81
8:18	23.3	32.0	28.2	36.8	32.1	29.1	16.4	705.6	72.54	1.89	303.1	43.0	3.81
8:19	23.5	32.2	28.2	36.8	32.3	29.2	16.5	707.1	71.51	1.89	298.7	42.2	3.81
8:20	23.6	33.0	28.7	37.2	32.7	29.6	16.7	709.3	71.18	1.87	302.5	42.7	3.77
8:21	23.8	32.6	28.8	37.3	32.9	29.6	16.7	711.2	71.53	1.87	302.6	42.6	3.75
8:22	23.9	33.0	28.7	37.3	32.9	29.8	16.8	714.0	71.91	1.88	307.7	43.1	3.76
8:23	24.0	32.7	28.8	37.4	32.7	29.8	16.8	715.7	71.88	1.87	307.1	42.9	3.73
8:24	24.2	32.7	29.2	37.5	33.1	29.8	16.5	717.6	71.80	1.89	312.0	43.5	3.76
8:25	24.3	33.7	29.5	37.9	33.6	30.3	16.9	719.8	70.38	1.87	309.3	43.0	3.71
8:26	24.6	33.8	30.0	37.9	33.7	30.6	17.2	721.9	71.12	1.87	311.0	43.1	3.70
8:27	24.7	33.2	30.0	38.2	33.8	30.3	16.9	723.6	71.56	1.87	313.0	43.2	3.69
8:28	24.8	33.2	30.1	38.3	34.0	30.4	16.8	725.4	71.12	1.88	316.1	43.6	3.69
8:29	25.0	33.2	30.2	38.4	34.0	30.5	17.3	728.4	71.15	1.87	306.7	42.1	3.66
8:30	25.1	33.1	29.7	38.4	33.8	30.4	17.2	729.5	71.80	1.87	311.1	42.7	3.66
8:31	25.3	34.2	30.1	38.9	34.3	30.9	17.4	731.3	70.85	1.85	312.5	42.7	3.61
8:32	25.5	34.7	30.3	39.1	34.4	31.4	17.9	733.5	70.65	1.85	309.0	42.1	3.60
8:33	25.7	34.8	30.4	39.1	34.5	31.5	18.0	734.6	71.15	1.85	312.4	42.5	3.60
8:34	25.8	34.9	30.4	39.3	34.7	31.6	18.3	736.7	73.87	1.84	318.2	43.2	3.57
8:35	26.0	35.0	30.4	39.1	34.6	31.7	18.5	738.9	74.14	1.85	317.6	43.0	3.58
8:36	26.2	35.5	30.8	39.5	34.9	32.0	18.7	740.0	73.26	1.84	317.1	42.9	3.54
8:37	26.3	35.3	30.7	39.4	35.0	32.0	18.7	740.8	73.33	1.85	318.2	42.9	3.57
8:38	26.4	35.1	30.5	39.6	35.2	31.9	18.8	742.8	76.14	1.85	325.8	43.9	3.55
8:39	26.6	35.2	31.0	39.9	35.2	32.1	19.0	743.8	75.82	1.84	321.6	43.2	3.53

Time [h]	T <sub>wall</sub> [°C]	T <sub>col,1</sub> [°C]	T <sub>col,2</sub> [°C]	T <sub>col,3</sub> [°C]	T <sub>col,4</sub> [°C]	T <sub>out</sub> [°C]	T <sub>amb</sub> [°C]	G <sub>T,col</sub> [W/m <sup>2</sup> ]	Flow Rate [m <sup>3</sup> /h·m <sup>2</sup> ]	P <sub>el</sub> [W]	Q'' <sub>u</sub> [W/m <sup>2</sup> ]	Eff <sub>th</sub> %	Eff <sub>PV</sub> %
8:40	26.7	34.8	30.6	39.7	35.0	31.9	18.9	745.1	76.63	1.86	324.5	43.6	3.55
8:41	26.8	35.0	30.5	39.2	34.6	31.9	18.6	746.2	75.97	1.87	327.8	43.9	3.58
8:42	26.9	35.5	30.9	39.2	35.1	32.2	18.7	747.7	75.72	1.85	332.4	44.5	3.52
8:43	27.0	35.1	30.8	39.2	34.9	32.1	18.7	749.4	77.08	1.86	337.1	45.0	3.55
8:44	27.1	34.7	31.4	39.7	35.3	31.9	18.7	750.3	75.97	1.86	326.5	43.5	3.54
8:45	27.2	34.4	31.1	39.6	35.2	31.8	18.5	752.0	76.29	1.87	331.3	44.1	3.54
8:46	27.2	34.7	31.0	40.2	35.4	31.9	18.9	753.0	75.95	1.85	322.2	42.8	3.50
8:47	27.5	35.6	31.6	40.9	35.8	32.5	19.4	753.9	75.49	1.84	320.8	42.6	3.49
8:48	27.7	36.2	31.9	40.7	35.9	33.0	19.6	754.8	75.40	1.83	326.6	43.3	3.45
8:49	27.8	36.6	31.8	40.5	35.8	33.2	19.6	754.5	76.09	1.83	334.4	44.3	3.46
8:50	27.9	36.4	31.7	40.6	35.7	33.2	19.8	755.5	76.14	1.83	328.9	43.5	3.46
8:51	28.0	36.5	31.7	40.3	35.6	33.2	19.8	755.8	75.33	1.83	327.9	43.4	3.45
8:52	28.1	36.4	31.7	40.7	36.0	33.2	19.9	757.2	75.66	1.83	325.3	43.0	3.44
8:53	28.3	36.7	32.0	41.0	36.1	33.4	20.0	758.4	75.74	1.83	328.7	43.3	3.45
8:54	28.4	36.4	32.0	40.8	36.0	33.4	20.2	758.8	76.79	1.83	326.7	43.1	3.43
8:55	28.5	36.5	32.2	41.0	36.2	33.4	20.2	759.7	75.76	1.84	323.6	42.6	3.45
8:56	28.6	36.4	32.0	40.7	35.9	33.4	20.3	761.0	75.54	1.84	322.0	42.3	3.45
8:57	28.6	36.8	32.2	41.0	36.3	33.6	20.1	761.5	74.84	1.83	327.5	43.0	3.43
8:58	28.7	36.7	32.1	40.7	36.3	33.6	20.0	760.6	76.06	1.83	333.8	43.9	3.44
8:59	28.8	37.1	32.4	41.1	36.4	33.8	20.2	760.6	74.97	1.83	331.0	43.5	3.43
9:00	29.0	36.9	32.5	41.6	36.5	33.8	20.6	761.3	75.61	1.81	323.0	42.4	3.40
9:01	29.2	37.4	32.8	41.8	36.9	34.2	20.8	762.4	75.26	1.82	325.4	42.7	3.40
9:02	29.3	37.1	32.9	42.0	37.0	34.1	21.1	763.8	75.45	1.81	318.1	41.6	3.38
9:03	29.4	37.4	32.9	42.3	37.2	34.3	21.4	764.6	75.55	1.80	315.2	41.2	3.36
9:04	29.5	37.6	32.9	42.1	37.0	34.4	21.4	763.8	75.21	1.81	317.2	41.5	3.39
9:05	29.6	37.7	33.0	41.6	36.9	34.5	20.8	762.8	75.20	1.83	332.6	43.6	3.41
9:06	29.7	37.4	33.5	41.5	37.1	34.4	20.8	762.6	74.78	1.83	328.3	43.0	3.42
9:07	29.7	36.8	32.7	41.5	37.1	34.0	20.6	762.5	76.26	1.82	329.8	43.3	3.40
9:08	29.9	37.8	33.1	41.8	37.2	34.6	20.8	762.3	74.44	1.81	329.4	43.2	3.38
9:09	30.0	38.1	33.4	41.6	37.3	34.8	20.8	762.0	74.52	1.83	337.1	44.2	3.42
9:10	30.0	37.6	33.2	41.5	37.1	34.6	20.9	761.4	75.40	182.97	332.4	43.7	342.77
9:11	30.1	37.5	33.2	41.9	37.3	34.5	21.3	760.3	75.33	1.82	322.8	42.5	3.42
9:12	30.2	37.7	33.4	42.1	37.5	34.8	21.4	759.3	74.85	1.79	323.2	42.6	3.36
9:13	30.4	37.8	33.1	41.5	36.9	34.8	21.2	759.1	75.08	1.81	329.5	43.4	3.41
9:14	30.4	37.4	32.9	41.5	36.8	34.6	21.0	758.0	75.43	1.82	330.5	43.6	3.43
9:15	30.5	37.2	33.4	42.0	37.3	34.6	21.0	756.9	74.92	1.81	328.6	43.4	3.42
9:16	30.5	37.4	33.1	41.8	36.9	34.7	21.3	756.6	74.82	1.81	323.3	42.7	3.41
9:17	30.6	37.7	33.2	41.6	36.8	34.8	21.2	757.6	74.72	1.82	327.7	43.3	3.42
9:18	30.7	37.9	33.4	41.9	37.2	34.9	21.2	757.1	74.95	1.80	331.1	43.7	3.39
9:19	30.8	38.0	33.5	42.0	37.2	35.0	21.9	757.1	76.03	1.79	321.5	42.5	3.38
9:20	30.9	37.9	33.4	42.0	37.3	35.0	22.1	756.4	76.43	1.79	316.8	41.9	3.38
9:21	31.1	38.3	33.8	41.9	37.4	35.2	21.9	754.8	76.17	1.80	325.6	43.1	3.40
9:22	31.1	37.8	33.5	41.9	37.4	35.0	22.2	755.3	76.16	1.79	315.6	41.8	3.39
9:23	31.2	38.0	33.6	42.0	37.2	35.1	22.5	754.6	76.24	1.80	310.5	41.1	3.40
9:24	31.3	38.1	33.7	42.0	37.4	35.2	22.7	754.1	76.09	1.80	307.1	40.7	3.41
9:25	31.3	38.4	33.8	42.1	37.4	35.4	22.6	754.0	76.02	1.80	313.2	41.5	3.40
9:26	31.4	38.5	34.1	42.4	37.6	35.4	22.7	752.2	75.72	1.79	311.1	41.4	3.40
9:27	31.5	38.4	34.0	42.2	37.6	35.4	22.5	750.4	76.22	1.78	315.7	42.1	3.39
9:28	31.6	38.5	34.0	42.1	37.5	35.5	22.7	750.1	76.39	1.79	316.2	42.2	3.40
9:29	31.7	38.6	34.0	42.0	37.7	35.6	22.4	750.8	76.10	1.80	323.2	43.0	3.43
9:30	31.7	38.3	33.8	42.1	37.7	35.5	22.5	749.7	76.33	1.79	319.0	42.6	3.40
9:31	31.7	38.5	34.1	42.3	37.8	35.6	22.7	750.0	75.80	1.78	313.2	41.8	3.38
9:32	31.8	38.4	33.9	41.8	37.5	35.5	22.5	747.3	76.27	1.80	320.2	42.9	3.43
9:33	31.8	38.1	33.8	41.2	37.3	35.3	22.3	745.9	76.10	1.80	320.0	42.9	3.44
9:34	31.8	37.6	33.6	40.6	36.6	35.0	21.8	746.0	76.07	1.82	323.6	43.4	3.48
9:35	31.8	37.5	33.4	41.3	37.0	34.9	22.1	745.6	75.57	1.80	311.7	41.8	3.44
9:36	31.8	38.0	33.7	40.9	37.0	35.2	22.2	744.5	75.54	1.80	315.0	42.3	3.44
9:37	31.8	37.3	33.3	40.3	36.5	34.9	22.1	743.1	75.80	1.82	311.6	41.9	3.49
9:38	31.8	37.3	33.3	41.0	36.8	34.8	22.1	742.4	75.56	1.81	309.3	41.7	3.47
9:39	31.9	37.8	33.7	41.5	37.1	35.1	22.2	740.7	75.00	1.80	312.6	42.2	3.46
9:40	31.9	36.8	33.6	41.4	37.0	34.7	22.2	742.0	76.59	1.84	308.1	41.5	3.54
9:41	31.8	36.0	33.2	41.0	37.0	34.2	21.7	741.9	77.23	1.85	310.6	41.9	3.57
9:42	31.7	36.2	33.0	41.1	37.2	34.2	21.9	741.8	75.35	1.81	300.1	40.5	3.49
9:43	31.9	37.8	33.8	41.8	37.7	35.0	22.7	741.3	74.56	1.79	296.3	40.0	3.44
9:44	32.1	38.2	34.1	42.0	37.8	35.4	23.3	739.7	75.09	1.78	292.4	39.5	3.44
9:45	32.2	38.6	34.3	42.0	37.8	35.7	23.3	738.4	75.01	1.79	298.3	40.4	3.46
9:46	32.3	38.3	34.1	42.1	37.7	35.6	23.3	737.3	75.39	1.78	296.7	40.3	3.44
9:47	32.3	38.5	34.3	41.7	37.6	35.7	23.4	738.1	74.79	1.80	295.5	40.0	3.47
9:48	32.4	38.3	34.1	41.5	37.5	35.6	23.2	737.6	75.36	1.81	300.4	40.7	3.51

Time [h]	T <sub>wall</sub> [°C]	T <sub>col,1</sub> [°C]	T <sub>col,2</sub> [°C]	T <sub>col,3</sub> [°C]	T <sub>col,4</sub> [°C]	T <sub>out</sub> [°C]	T <sub>amb</sub> [°C]	G <sub>T,col</sub> [W/m <sup>2</sup> ]	Flow Rate [m <sup>3</sup> /h·m <sup>2</sup> ]	P <sub>el</sub> [W]	Q'' <sub>u</sub> [W/m <sup>2</sup> ]	Eff <sub>th</sub> %	Eff <sub>PV</sub> %
9:49	32.5	38.3	34.2	41.6	37.5	35.6	23.3	735.3	75.40	1.79	299.8	40.8	3.47
9:50	32.4	38.0	34.2	42.0	37.7	35.4	23.4	733.5	76.34	1.79	296.2	40.4	3.49
9:51	32.5	37.8	34.5	42.5	37.8	35.4	23.5	731.4	76.03	1.79	289.6	39.6	3.50
9:52	32.5	37.0	33.4	41.0	36.7	35.0	23.2	730.2	76.98	1.82	292.3	40.0	3.55
9:53	32.5	37.3	33.7	41.5	37.0	35.1	23.5	728.7	75.40	1.81	280.0	38.4	3.54
9:54	32.5	37.1	33.5	41.1	36.8	34.9	23.4	726.5	77.17	1.81	286.1	39.4	3.56
9:55	32.4	36.5	33.4	41.2	36.8	34.6	23.0	725.8	76.79	1.84	287.9	39.7	3.61
9:56	32.4	36.5	33.5	41.4	37.0	34.6	22.9	724.5	77.07	1.84	292.0	40.3	3.62
9:57	32.4	37.1	33.5	41.6	37.2	34.9	23.2	722.5	75.45	1.80	285.2	39.5	3.55
9:58	32.5	37.5	33.8	42.0	37.4	35.1	23.6	721.3	76.16	1.79	284.0	39.4	3.54
9:59	32.7	38.3	34.3	42.1	37.6	35.6	23.9	720.2	76.59	1.79	289.0	40.1	3.54
10:00	32.7	37.9	34.0	41.6	37.2	35.5	24.0	718.8	76.54	1.79	284.5	39.6	3.55
10:01	32.7	37.3	33.8	41.8	37.2	35.2	24.1	716.6	77.41	1.80	274.7	38.3	3.59
10:02	32.7	36.8	33.4	41.6	36.9	34.9	23.7	715.2	77.45	1.80	279.7	39.1	3.59
10:03	32.6	36.6	33.4	41.3	36.8	34.7	23.4	713.2	77.75	1.80	285.3	40.0	3.59
10:04	32.6	36.3	33.5	40.8	36.7	34.6	23.2	712.0	76.39	1.83	281.3	39.5	3.67
10:05	32.6	36.5	33.6	41.2	37.1	34.6	23.3	711.7	75.71	1.81	276.0	38.8	3.63
10:06	32.7	37.4	34.2	42.2	37.9	35.2	24.0	710.5	73.96	1.77	266.4	37.5	3.56
10:07	32.9	38.6	34.5	42.4	38.0	35.8	24.5	708.0	74.00	1.76	269.9	38.1	3.55
10:08	33.1	38.8	34.4	42.4	37.9	36.0	24.5	704.7	75.16	1.78	278.8	39.6	3.60
10:09	33.1	38.4	34.1	41.9	37.5	35.8	24.3	701.3	77.37	1.78	287.3	41.0	3.62
10:10	33.0	37.8	33.9	41.4	37.1	35.5	24.4	700.4	78.60	1.78	281.0	40.1	3.63
10:11	32.9	36.6	33.3	40.7	36.5	34.9	24.0	700.0	78.55	1.78	276.4	39.5	3.63
10:12	32.9	37.1	33.5	40.7	36.6	35.0	23.7	698.6	75.31	1.79	273.2	39.1	3.65
10:13	32.9	36.7	33.2	40.9	36.8	34.8	23.8	695.8	76.69	1.79	272.8	39.2	3.67
10:14	32.9	37.0	33.3	40.9	36.7	34.9	23.7	694.0	75.96	1.80	274.5	39.6	3.69
10:15	33.0	37.6	33.8	41.7	37.3	35.2	24.3	692.0	75.02	1.77	264.2	38.2	3.66
10:16	33.1	37.8	34.1	41.5	37.3	35.5	24.6	688.9	75.07	1.77	263.7	38.3	3.67
10:17	33.1	37.7	34.2	41.2	37.3	35.4	24.8	686.3	75.19	1.78	256.7	37.4	3.69
10:18	33.1	37.8	34.0	40.7	37.1	35.4	24.7	686.8	75.46	1.78	261.8	38.1	3.70
10:19	33.1	37.6	34.1	40.8	37.2	35.4	24.5	685.0	75.22	1.78	263.1	38.4	3.70
10:20	33.2	37.8	34.1	40.8	37.0	35.4	24.6	682.9	74.46	1.76	258.6	37.9	3.68
10:21	33.1	37.7	34.0	40.6	37.0	35.3	24.6	680.6	74.81	1.77	258.8	38.0	3.72
10:22	33.1	37.4	33.9	40.7	37.0	35.2	24.7	678.9	75.25	1.78	256.5	37.8	3.74
10:23	33.2	37.3	33.8	41.0	36.8	35.3	24.8	676.0	75.64	1.78	255.5	37.8	3.75
10:24	33.1	37.1	33.6	41.0	37.0	35.1	24.2	674.6	75.44	1.77	262.8	39.0	3.73
10:25	33.2	37.9	34.1	41.4	37.5	35.5	24.7	672.7	74.45	1.75	258.1	38.4	3.71
10:26	33.3	38.0	34.2	41.2	37.2	35.6	25.1	669.2	74.59	1.77	253.8	37.9	3.77
10:27	33.2	37.1	33.6	40.7	36.5	35.1	25.3	666.8	76.23	1.77	240.9	36.1	3.78
10:28	33.2	37.3	33.8	41.3	37.0	35.2	25.4	666.9	74.54	1.77	233.8	35.1	3.78
10:29	33.3	37.8	33.9	41.1	36.9	35.5	25.3	665.2	75.02	1.76	246.2	37.0	3.77
10:30	33.2	37.1	33.6	40.9	36.6	35.1	25.1	662.7	76.06	1.78	247.0	37.3	3.83
10:31	33.3	37.6	33.9	41.0	37.1	35.4	25.0	661.1	74.38	1.77	249.9	37.8	3.82
10:32	33.3	37.3	33.6	40.0	36.4	35.1	24.5	658.9	75.21	1.77	257.2	39.0	3.83
10:33	33.2	36.8	33.4	40.1	36.4	34.9	24.3	655.7	75.63	1.77	257.3	39.2	3.85
10:34	33.3	37.6	34.0	41.4	37.3	35.3	25.2	653.6	74.65	1.75	241.8	37.0	3.82
10:35	33.2	36.8	33.7	41.1	36.8	35.1	24.8	651.1	74.91	1.76	247.0	37.9	3.86
10:36	33.2	36.4	33.2	40.2	36.4	34.7	24.7	649.7	76.24	1.76	245.9	37.9	3.87
10:37	33.2	37.2	33.8	41.0	37.1	35.1	25.3	647.5	73.90	1.75	234.6	36.2	3.85
10:38	33.3	37.6	33.9	40.6	36.9	35.3	25.3	644.6	75.03	1.75	242.4	37.6	3.87
10:39	33.4	37.1	33.8	40.0	36.4	35.2	25.4	643.6	75.70	1.75	239.1	37.1	3.88
10:40	33.2	35.9	33.3	39.6	35.9	34.4	25.2	640.8	76.70	1.78	226.8	35.4	3.97
10:41	33.2	35.8	33.0	39.7	36.0	34.2	25.1	638.4	75.47	1.77	223.0	34.9	3.95
10:42	33.2	36.4	33.1	39.5	35.9	34.5	25.0	635.1	74.04	1.76	227.1	35.8	3.96
10:43	33.2	36.7	33.2	40.2	36.3	34.7	25.4	633.2	73.20	1.74	221.2	34.9	3.92
10:44	33.2	37.0	33.5	40.1	36.2	34.9	25.3	630.9	73.95	1.74	228.3	36.2	3.94
10:45	33.2	36.7	33.2	39.9	36.1	34.7	25.4	627.0	74.61	1.75	225.3	35.9	3.98
10:46	33.2	36.1	33.1	39.7	36.0	34.4	25.3	623.3	76.79	1.75	225.3	36.1	3.99
10:47	33.1	35.5	33.0	39.5	35.8	34.0	25.0	621.5	76.06	1.76	222.6	35.8	4.03
10:48	33.1	36.0	33.1	40.2	36.1	34.3	25.4	619.7	75.29	1.75	215.8	34.8	4.03
10:49	33.0	35.4	32.6	39.1	35.2	34.0	24.8	615.9	75.46	1.75	223.6	36.3	4.05
10:50	32.9	35.1	32.5	39.3	35.5	33.7	24.9	615.3	75.30	1.76	214.6	34.9	4.07
10:51	32.8	34.4	32.1	38.4	34.8	33.3	24.5	613.8	76.44	1.79	217.9	35.5	4.16
10:52	32.7	34.2	31.9	38.1	34.7	33.2	24.3	611.4	75.88	1.79	219.2	35.8	4.18
10:53	32.5	33.0	31.0	36.6	33.6	32.4	23.8	607.9	76.93	1.82	213.7	35.2	4.28
10:54	32.3	32.8	30.9	36.5	33.7	32.1	23.5	606.3	75.90	1.81	212.3	35.0	4.27
10:55	32.3	33.9	31.5	37.7	34.5	32.7	24.2	605.1	73.84	1.78	204.8	33.8	4.20
10:56	32.5	35.1	32.3	38.5	35.1	33.4	24.9	604.1	73.56	1.72	201.1	33.3	4.06
10:57	32.5	35.4	32.5	38.9	35.4	33.6	25.4	602.0	74.15	1.74	196.1	32.6	4.13

Time [h]	T <sub>wall</sub> [°C]	T <sub>col,1</sub> [°C]	T <sub>col,2</sub> [°C]	T <sub>col,3</sub> [°C]	T <sub>col,4</sub> [°C]	T <sub>out</sub> [°C]	T <sub>amb</sub> [°C]	G <sub>T,col</sub> [W/m <sup>2</sup> ]	Flow Rate [m <sup>3</sup> /h·m <sup>2</sup> ]	P <sub>el</sub> [W]	Q'' <sub>u</sub> [W/m <sup>2</sup> ]	Eff <sub>th</sub> %	Eff <sub>PV</sub> %
10:58	32.5	35.4	32.5	39.0	35.5	33.7	25.7	599.4	75.34	1.74	195.8	32.7	4.13
10:59	32.7	36.0	32.8	39.4	35.7	34.1	25.8	595.9	75.46	1.75	203.1	34.1	4.19
11:00	32.7	35.9	32.7	39.2	35.4	34.1	25.8	591.6	76.04	1.73	202.9	34.3	4.18
11:01	32.6	35.3	32.4	39.0	35.2	33.7	25.6	589.7	76.13	1.72	198.2	33.6	4.16
11:02	32.5	33.7	31.3	37.5	33.8	32.8	24.9	585.9	78.05	1.76	200.0	34.1	4.28
11:03	32.3	32.9	30.9	36.7	33.6	32.1	24.2	583.5	77.29	1.78	199.9	34.3	4.36
11:04	32.2	33.2	31.0	36.8	33.8	32.2	24.1	581.8	76.71	1.76	202.8	34.9	4.30
11:05	32.1	32.8	30.8	36.5	33.4	32.0	23.9	579.0	76.69	1.77	201.8	34.9	4.37
11:06	32.1	33.6	31.4	37.1	34.1	32.3	24.6	577.1	75.78	1.76	190.4	33.0	4.35
11:07	32.1	33.5	31.4	37.2	34.0	32.4	24.8	574.4	76.35	1.78	189.6	33.0	4.41
11:08	32.1	33.3	31.3	37.0	33.9	32.3	24.7	572.0	77.13	1.75	190.2	33.3	4.36
11:09	32.0	33.2	31.2	37.0	33.9	32.3	24.6	569.1	76.22	1.76	189.8	33.3	4.42
11:10	31.9	32.4	30.5	36.0	33.1	31.7	24.2	565.5	76.50	1.76	187.9	33.2	4.43
11:11	31.8	32.2	31.1	36.7	33.8	32.0	24.4	562.4	74.72	1.73	185.2	32.9	4.38
11:12	31.9	34.0	31.5	37.3	34.1	32.5	25.3	558.9	75.02	1.74	175.1	31.3	4.44
11:13	32.0	34.7	31.9	37.7	34.5	32.9	25.7	555.0	73.99	1.72	172.0	31.0	4.42
11:14	32.1	34.9	31.9	37.4	34.4	33.1	25.7	553.8	74.48	1.70	177.8	32.1	4.39
11:15	32.1	34.6	31.8	36.7	34.0	32.9	25.5	551.5	74.68	1.72	178.8	32.4	4.45
11:16	32.1	34.4	31.7	36.9	34.0	32.9	25.7	550.0	75.58	1.71	176.6	32.1	4.43
11:17	32.1	34.0	31.5	37.3	34.1	32.7	25.7	547.5	75.55	1.72	170.3	31.1	4.47
11:18	32.0	33.8	31.6	37.5	34.2	32.6	25.9	545.2	75.97	1.71	164.5	30.2	4.46
11:19	31.9	33.6	31.4	37.3	33.9	32.5	25.7	541.4	75.47	1.71	166.7	30.8	4.51
11:20	31.9	33.9	31.3	37.4	33.9	32.6	25.5	538.0	74.51	1.70	171.9	32.0	4.52
11:21	31.8	33.2	30.8	36.4	33.1	32.2	25.1	532.9	75.50	1.70	172.3	32.3	4.56
11:22	31.8	33.4	30.9	36.6	33.2	32.2	25.5	530.6	75.01	1.70	162.9	30.7	4.58
11:23	31.7	33.7	31.2	37.1	33.7	32.3	26.2	528.5	73.96	1.70	146.5	27.7	4.60
11:24	31.7	34.0	31.3	37.1	33.6	32.4	26.5	525.1	74.10	1.69	143.8	27.4	4.60
11:25	31.7	33.9	31.2	36.3	33.2	32.5	26.0	520.8	74.79	1.70	156.6	30.1	4.64
11:26	31.7	33.8	31.1	36.5	33.6	32.4	25.8	517.5	74.78	1.70	160.2	31.0	4.70
11:27	31.8	33.9	31.1	36.8	33.8	32.4	25.9	514.5	75.16	1.67	158.3	30.8	4.64
11:28	31.7	32.9	30.8	36.3	33.2	31.9	25.6	512.0	75.95	1.71	157.5	30.8	4.75
11:29	31.5	32.1	30.1	35.5	32.4	31.4	24.8	510.1	76.17	1.71	162.3	31.8	4.78
11:30	31.4	32.3	30.1	35.5	32.5	31.3	24.9	507.5	75.77	1.70	158.0	31.1	4.78
11:31	31.3	32.3	30.2	35.6	32.6	31.4	25.2	504.1	74.51	1.71	150.8	29.9	4.83
11:32	31.4	32.7	30.5	36.0	32.9	31.7	25.5	501.8	74.20	1.69	149.1	29.7	4.81
11:33	31.2	31.4	29.5	34.7	31.7	31.0	24.9	497.8	76.43	1.72	152.8	30.7	4.93
11:34	30.9	30.0	28.4	33.0	30.5	29.9	24.1	493.5	76.49	1.74	146.3	29.6	5.02
11:35	30.9	30.7	29.0	33.8	31.4	30.1	24.5	490.7	74.74	1.71	137.4	28.0	4.97
11:36	30.9	31.7	29.5	34.5	31.9	30.6	25.0	488.1	73.95	1.69	137.5	28.2	4.95
11:37	30.9	32.0	29.7	34.8	32.0	30.9	25.3	484.6	74.18	1.66	136.6	28.2	4.90
11:38	30.9	31.8	29.7	34.7	31.9	30.9	25.2	481.3	74.87	1.67	139.2	28.9	4.95
11:39	30.8	31.4	29.5	34.4	31.7	30.7	24.9	478.8	74.74	1.67	140.9	29.4	4.98
11:40	30.8	31.0	29.3	34.1	31.3	30.5	24.7	476.0	75.09	1.66	141.1	29.6	4.98
11:41	30.5	29.6	28.1	32.5	30.1	29.5	24.1	472.2	75.59	1.69	132.8	28.1	5.10
11:42	30.4	29.9	28.5	33.1	30.6	29.5	24.2	469.4	74.01	1.66	128.0	27.3	5.04
11:43	30.4	31.0	29.1	34.3	31.4	30.1	24.9	465.6	73.51	1.63	125.3	26.9	5.00
11:44	30.5	31.9	29.7	34.8	32.0	30.7	25.5	463.2	73.46	1.62	124.7	26.9	4.99
11:45	30.5	31.6	29.6	35.0	32.1	30.7	25.7	459.8	74.53	1.61	122.5	26.6	5.00
11:46	30.5	31.0	29.2	34.2	31.4	30.4	25.3	456.6	75.26	1.65	124.1	27.2	5.14
11:47	30.5	31.1	29.2	34.2	31.6	30.3	25.5	454.2	75.51	1.61	119.3	26.3	5.07
11:48	30.4	30.1	28.4	33.0	30.2	29.7	24.8	449.2	76.03	1.67	122.9	27.4	5.30
11:49	30.2	29.7	28.1	32.4	30.2	29.3	24.5	445.2	75.07	1.65	118.6	26.6	5.28
11:50	30.1	30.2	28.4	32.9	30.6	29.6	24.8	442.6	74.86	1.62	117.1	26.5	5.21
11:51	30.1	30.4	28.8	33.5	31.0	29.7	25.1	440.0	74.72	1.60	113.7	25.8	5.17
11:52	30.1	30.6	28.9	33.5	30.9	29.9	25.4	437.3	74.40	1.59	109.7	25.1	5.20
11:53	30.1	30.4	28.7	33.3	30.8	29.8	25.4	434.7	74.53	1.58	108.5	25.0	5.19
11:54	30.2	31.5	29.4	34.2	31.6	30.4	26.3	431.2	73.65	1.56	100.4	23.3	5.15
11:55	30.2	31.2	29.1	33.9	31.0	30.3	26.5	424.3	74.40	1.56	93.2	22.0	5.24
11:56	30.2	31.1	29.0	33.7	30.9	30.1	26.6	420.0	74.75	1.55	87.6	20.9	5.28
11:57	30.1	31.1	29.0	33.5	30.8	30.1	26.3	418.5	74.02	1.56	92.4	22.1	5.31
11:58	30.1	31.2	29.0	33.3	30.9	30.1	26.0	415.2	74.56	1.54	100.7	24.2	5.30
11:59	30.1	30.9	28.8	33.0	30.6	29.9	25.8	392.7	74.68	1.54	100.5	25.6	5.60
12:00	29.9	29.6	27.8	31.9	29.3	29.2	25.4	372.2	76.45	1.56	95.1	25.6	5.99
12:01	29.7	28.7	27.2	31.2	28.8	28.5	24.6	406.2	76.71	1.57	99.0	24.4	5.52
12:02	29.5	27.8	26.5	30.1	28.0	27.9	23.9	400.8	76.19	1.57	101.2	25.3	5.58
12:03	29.4	28.5	27.0	31.0	28.9	28.1	24.1	398.7	74.36	1.52	100.1	25.1	5.44
12:04	29.4	29.7	27.9	32.3	29.8	28.9	25.1	396.3	74.18	1.51	92.5	23.3	5.43
12:05	29.5	30.2	28.5	32.9	30.2	29.3	25.5	393.0	73.51	1.49	92.6	23.6	5.40
12:06	29.6	30.9	28.9	33.0	30.6	29.8	26.3	389.8	73.29	1.47	83.5	21.4	5.37

Time [h]	T <sub>wall</sub> [°C]	T <sub>col,1</sub> [°C]	T <sub>col,2</sub> [°C]	T <sub>col,3</sub> [°C]	T <sub>col,4</sub> [°C]	T <sub>out</sub> [°C]	T <sub>amb</sub> [°C]	G <sub>T,col</sub> [W/m <sup>2</sup> ]	Flow Rate [m <sup>3</sup> /h·m <sup>2</sup> ]	P <sub>el</sub> [W]	Q'' <sub>u</sub> [W/m <sup>2</sup> ]	Eff <sub>th</sub> %	Eff <sub>PV</sub> %
12:07	29.7	31.2	29.1	33.8	31.0	30.0	27.0	384.3	73.47	1.46	72.6	18.9	5.42
12:08	29.8	31.5	29.2	34.0	31.2	30.2	27.4	382.1	74.31	1.44	68.1	17.8	5.39
12:09	29.8	31.4	29.0	33.7	30.8	30.3	27.1	324.6	74.44	1.43	76.6	23.6	6.29
12:10	29.6	29.6	27.2	30.8	27.9	29.0	25.6	285.8	75.95	1.45	86.2	30.2	7.24
12:11	29.4	30.0	27.9	31.7	29.4	29.0	26.0	372.8	74.46	1.45	73.3	19.6	5.53
12:12	29.5	30.4	28.2	32.3	29.8	29.3	26.2	368.6	74.11	1.43	75.3	20.4	5.54
12:13	29.4	29.9	27.8	31.6	29.3	29.1	25.8	364.8	74.86	1.43	79.3	21.7	5.59
12:14	29.3	29.4	27.6	31.4	29.0	28.8	25.7	362.5	75.20	1.45	77.5	21.4	5.69
12:15	29.2	28.6	27.2	30.8	28.7	28.4	25.2	363.8	74.97	1.44	78.7	21.6	5.66
12:16	29.1	29.5	27.6	31.5	29.2	28.7	25.6	359.8	73.37	1.42	74.7	20.8	5.61
12:17	29.1	29.7	27.8	31.5	29.4	28.9	25.9	350.2	74.18	1.40	72.6	20.7	5.72
12:18	29.0	29.1	27.3	31.0	28.9	28.5	25.8	348.3	74.29	1.38	66.6	19.1	5.66
12:19	29.0	29.3	27.5	31.4	29.1	28.6	25.7	327.1	74.13	1.36	69.4	21.2	5.94
12:20	29.0	29.4	27.4	31.2	28.9	28.6	25.9	336.5	74.63	1.36	67.6	20.1	5.78
12:21	28.9	29.4	27.4	31.2	28.9	28.6	25.9	331.9	74.46	1.35	65.5	19.7	5.80
12:22	28.9	28.9	27.1	30.9	28.6	28.3	26.0	328.5	74.74	1.34	56.1	17.1	5.82
12:23	28.8	29.1	27.1	30.8	28.5	28.4	26.2	324.5	73.77	1.31	53.4	16.5	5.77
12:24	28.7	28.8	27.0	30.6	28.4	28.2	25.9	322.9	74.73	1.31	57.0	17.7	5.77
12:25	28.6	28.1	26.5	30.2	28.0	27.7	25.3	319.2	75.45	1.31	60.9	19.1	5.86
12:26	28.4	27.4	26.0	29.4	27.3	27.3	24.8	314.8	76.27	1.31	63.9	20.3	5.93
12:27	28.2	26.4	25.1	28.2	26.3	26.6	23.8	310.5	76.49	1.31	69.7	22.5	6.04
12:28	28.1	26.3	25.0	28.0	26.3	26.3	23.5	306.6	75.91	1.29	71.5	23.3	5.99
12:29	27.9	25.3	24.2	26.7	25.2	25.7	23.1	302.0	76.24	1.31	67.3	22.3	6.18
12:30	27.8	26.2	25.1	28.0	26.4	26.1	23.9	299.4	73.89	1.26	53.9	18.0	5.98
12:31	27.8	27.3	25.7	29.2	27.1	26.8	25.0	296.2	72.94	1.23	44.2	14.9	5.92
12:32	27.9	27.9	26.2	29.9	27.7	27.2	25.6	293.8	72.95	1.22	39.1	13.3	5.90
12:33	27.9	27.8	26.2	29.9	27.6	27.4	25.7	291.0	74.26	1.21	40.5	13.9	5.91
12:34	27.8	27.2	25.8	29.2	27.2	27.0	25.3	286.7	74.41	1.20	42.4	14.8	5.98
12:35	27.7	26.7	25.4	28.5	26.5	26.7	24.8	281.1	74.38	1.20	47.2	16.8	6.11
12:36	27.6	26.4	25.1	28.2	26.3	26.4	24.5	276.7	73.97	1.18	45.0	16.3	6.11
12:37	27.5	26.3	25.1	28.1	26.3	26.2	24.3	272.7	74.35	1.16	47.5	17.4	6.09
12:38	27.6	27.2	25.8	29.2	27.1	26.8	25.2	269.6	72.70	1.13	38.4	14.3	6.00
12:39	27.7	27.9	26.2	29.5	27.5	27.2	25.6	265.9	72.28	1.12	38.0	14.3	5.98
12:40	27.8	28.3	26.5	29.9	27.9	27.5	26.3	262.5	72.78	1.10	30.9	11.8	5.96
12:41	27.7	28.1	26.2	29.4	27.4	27.4	26.3	257.8	72.92	1.09	25.9	10.0	6.02
12:42	27.6	27.5	25.8	28.8	26.9	27.0	25.9	253.8	72.58	1.09	26.6	10.5	6.12
12:43	27.6	27.6	26.1	28.8	27.1	27.0	26.1	253.0	72.67	1.07	21.2	8.4	6.05
12:44	27.6	27.5	25.9	28.9	27.1	27.0	26.1	251.1	72.22	1.07	20.0	8.0	6.08
12:45	27.6	27.4	25.8	28.8	26.9	26.9	26.0	248.6	72.84	1.06	23.1	9.3	6.10
12:46	27.5	27.3	25.7	28.5	26.8	26.8	25.8	243.9	72.79	1.04	24.5	10.1	6.07
12:47	27.4	26.7	25.2	27.8	26.1	26.4	25.3	238.4	73.52	1.03	26.2	11.0	6.17
12:48	27.3	26.9	25.3	28.0	26.3	26.4	25.6	236.2	73.14	1.02	20.2	8.6	6.18
12:49	27.3	26.6	25.1	27.8	26.0	26.2	25.7	232.6	73.59	1.02	13.2	5.7	6.24
12:50	27.2	26.2	24.8	27.4	25.7	26.0	25.4	228.3	73.57	1.00	14.2	6.2	6.23
12:51	27.2	26.5	25.1	27.8	26.0	26.1	25.6	225.6	73.88	0.98	12.9	5.7	6.21
12:52	27.1	26.3	24.9	27.7	25.9	26.0	25.6	222.0	74.87	0.97	10.8	4.9	6.26
12:53	27.0	26.0	24.7	27.4	25.7	25.8	25.3	218.9	73.96	0.97	11.4	5.2	6.33
12:54	27.0	26.6	25.1	27.9	26.1	26.2	25.9	216.1	73.57	0.95	6.6	3.1	6.26
12:55	27.0	26.4	24.9	27.7	25.9	26.1	25.8	213.5	74.14	0.95	6.9	3.2	6.33
12:56	26.9	25.9	24.5	27.3	25.4	25.7	25.5	209.2	74.73	0.94	5.0	2.4	6.42
12:57	26.7	25.6	24.1	26.8	24.9	25.4	25.0	201.5	75.16	0.91	10.8	5.4	6.46
12:58	26.6	25.5	24.1	26.5	24.9	25.3	25.0	194.8	74.43	0.89	8.7	4.4	6.51
12:59	26.6	25.4	24.1	26.5	24.9	25.2	25.2	189.2	74.73	0.86	1.9	1.0	6.50
13:00	26.5	25.3	24.0	26.5	24.9	25.1	25.2	184.6	73.41	0.85	-0.6	-0.3	6.58

Table E.4: Experimental data for September 1

Time [h]	T <sub>wall</sub> [°C]	T <sub>col,1</sub> [°C]	T <sub>col,2</sub> [°C]	T <sub>col,3</sub> [°C]	T <sub>col,4</sub> [°C]	T <sub>out</sub> [°C]	T <sub>amb</sub> [°C]	G <sub>T,col</sub> [W/m <sup>2</sup> ]	Flow Rate [m <sup>3</sup> /h·m <sup>2</sup> ]	P <sub>el</sub> [W]	Q'' <sub>u</sub> [W/m <sup>2</sup> ]	Eff <sub>th</sub> %	Eff <sub>PV</sub> %
7:32	13.1	16.4	15.4	18.2	17.0	15.6	11.8	339.0	81.60	1.81	108.3	31.9	7.63
7:33	13.3	17.7	16.6	20.1	18.7	16.5	11.9	355.9	80.49	1.82	127.2	35.7	7.28
7:34	13.4	17.9	16.7	20.2	18.5	16.8	12.0	283.9	81.73	1.83	135.6	47.8	9.12
7:35	13.4	17.2	16.1	19.2	17.9	16.3	12.0	368.6	82.19	1.86	121.8	33.0	7.19
7:36	13.6	18.4	17.2	21.0	19.6	17.1	12.3	423.7	80.06	1.86	131.8	31.1	6.26
7:37	13.8	19.2	17.8	22.1	20.4	17.8	12.3	406.8	80.05	1.84	149.3	36.7	6.44
7:38	14.0	19.6	18.1	22.5	20.7	18.1	12.4	428.0	80.93	1.85	159.1	37.2	6.18

Time [h]	T <sub>wall</sub> [°C]	T <sub>col,1</sub> [°C]	T <sub>col,2</sub> [°C]	T <sub>col,3</sub> [°C]	T <sub>col,4</sub> [°C]	T <sub>out</sub> [°C]	T <sub>amb</sub> [°C]	G <sub>T,col</sub> [W/m <sup>2</sup> ]	Flow Rate [m <sup>3</sup> /h·m <sup>2</sup> ]	P <sub>el</sub> [W]	Q'' <sub>u</sub> [W/m <sup>2</sup> ]	Eff <sub>th</sub> %	Eff <sub>PV</sub> %
7:39	14.2	20.1	18.4	23.1	21.2	18.5	12.5	444.9	81.03	1.87	166.1	37.3	6.00
7:40	14.4	20.5	18.8	23.7	21.6	18.8	12.6	457.6	80.74	1.88	171.9	37.6	5.85
7:41	14.6	20.9	19.1	24.2	22.2	19.2	12.8	470.3	80.64	1.89	176.1	37.4	5.72
7:42	14.8	21.3	19.5	24.6	22.3	19.5	12.9	474.6	80.53	1.90	181.2	38.2	5.70
7:43	15.0	21.2	19.4	24.3	22.2	19.5	13.1	483.1	81.92	1.91	179.6	37.2	5.65
7:44	15.2	21.6	19.7	24.8	22.6	19.8	13.3	491.5	81.40	1.91	180.7	36.8	5.53
7:45	15.3	21.6	19.7	24.9	22.6	19.9	13.3	500.0	81.82	1.93	183.6	36.7	5.51
7:46	15.5	21.7	19.9	25.1	22.8	20.1	13.3	504.2	81.07	1.92	187.6	37.2	5.44
7:47	15.7	22.0	20.1	25.4	23.1	20.3	13.3	512.7	80.75	1.93	192.2	37.5	5.36
7:48	15.8	22.5	20.5	26.0	23.7	20.6	13.3	521.2	81.23	1.92	201.4	38.6	5.26
7:49	16.0	23.1	20.9	26.7	24.2	21.0	13.4	525.4	80.55	1.91	209.8	39.9	5.18
7:50	16.2	23.7	21.4	27.5	24.7	21.5	13.6	525.4	80.27	1.90	215.3	41.0	5.16
7:51	16.5	23.5	21.3	27.2	24.5	21.6	13.7	529.7	81.09	1.93	216.3	40.8	5.20
7:52	16.6	23.8	21.7	27.7	24.9	21.7	13.6	533.9	80.54	1.91	220.7	41.3	5.09
7:53	16.8	24.3	22.0	28.3	25.3	22.1	13.6	538.1	80.25	1.90	231.0	42.9	5.03
7:54	17.0	24.5	22.2	28.4	25.5	22.3	13.8	542.4	81.30	1.90	234.4	43.2	5.00
7:55	17.2	24.5	22.2	28.4	25.6	22.4	13.9	550.8	80.73	1.91	233.3	42.3	4.95
7:56	17.4	24.8	22.5	28.8	25.8	22.7	13.7	555.1	80.59	1.91	242.5	43.7	4.91
7:57	17.5	24.8	22.5	28.6	25.8	22.7	13.8	563.6	80.61	1.91	241.9	42.9	4.84
7:58	17.7	25.0	22.7	28.8	26.0	22.9	13.9	576.3	81.06	1.95	245.6	42.6	4.82
7:59	17.8	25.3	22.8	29.2	26.4	23.1	14.0	580.5	80.31	1.94	244.8	42.2	4.76
8:00	18.0	25.3	23.0	29.3	26.4	23.2	14.1	580.5	80.35	1.93	246.9	42.5	4.75
8:01	18.3	25.7	23.3	29.8	26.8	23.5	14.2	589.0	80.63	1.94	252.2	42.8	4.70
8:02	18.4	25.6	23.3	29.5	26.6	23.6	14.3	589.0	81.45	1.96	254.7	43.2	4.76
8:03	18.5	25.1	22.8	28.8	26.0	23.3	14.5	589.0	81.18	1.95	240.4	40.8	4.73
8:04	18.6	25.3	22.8	29.0	26.3	23.3	14.4	593.2	81.56	1.95	242.7	40.9	4.68
8:05	18.8	25.8	23.4	29.7	26.9	23.7	14.4	597.5	80.26	1.96	249.8	41.8	4.67
8:06	18.9	25.7	23.5	29.6	26.8	23.7	14.5	601.7	81.09	1.97	250.7	41.7	4.66
8:07	19.0	25.8	23.5	29.7	27.0	23.8	14.7	605.9	81.10	1.96	248.8	41.1	4.61
8:08	19.2	26.4	23.8	30.5	27.6	24.2	14.5	614.4	80.81	1.95	262.5	42.7	4.53
8:09	19.4	26.8	23.8	30.6	27.5	24.4	14.4	614.4	80.47	1.93	271.4	44.2	4.48
8:10	19.6	27.3	24.3	31.3	28.1	24.8	14.7	614.4	80.17	1.91	271.4	44.2	4.42
8:11	19.8	27.6	24.9	31.7	28.3	25.2	15.2	614.4	80.88	1.94	269.7	43.9	4.50
8:12	19.9	26.9	24.4	30.9	27.8	24.8	15.1	622.9	80.98	1.94	263.0	42.2	4.44
8:13	20.0	27.3	24.4	31.5	28.1	25.0	15.1	627.1	80.62	1.92	266.3	42.5	4.38
8:14	20.2	27.6	24.9	31.8	28.3	25.3	15.2	627.1	81.70	1.93	275.9	44.0	4.38
8:15	20.4	27.6	24.9	31.8	28.5	25.3	15.2	635.6	81.52	1.95	275.5	43.3	4.38
8:16	20.5	27.5	24.8	31.6	28.4	25.3	15.5	635.6	81.52	1.96	268.7	42.3	4.39
8:17	20.6	27.7	25.0	32.0	28.8	25.4	15.5	639.8	80.74	1.93	267.9	41.9	4.29
8:18	20.7	28.4	25.2	32.5	29.1	25.8	15.7	644.1	80.44	1.92	271.9	42.2	4.25
8:19	20.9	28.5	25.7	32.8	29.4	26.1	15.7	648.3	80.50	1.91	277.6	42.8	4.21
8:20	21.1	29.1	25.7	33.3	29.8	26.4	15.9	652.5	80.18	1.89	278.9	42.7	4.13
8:21	21.3	29.5	26.4	34.0	30.2	26.8	16.0	652.5	80.90	1.91	290.4	44.5	4.17
8:22	21.4	29.0	25.9	33.2	29.8	26.5	15.8	656.8	82.26	1.93	294.9	44.9	4.19
8:23	21.5	28.9	25.5	32.9	29.5	26.5	15.6	661.0	82.04	1.92	297.2	45.0	4.14
8:24	21.6	28.8	25.6	33.2	29.4	26.5	15.4	661.0	81.63	1.91	301.5	45.6	4.12
8:25	21.8	29.1	25.7	33.3	29.6	26.6	15.3	665.3	81.66	1.90	308.3	46.3	4.08
8:26	21.9	29.0	26.0	33.3	29.6	26.7	15.3	669.5	81.89	1.95	309.8	46.3	4.16
8:27	21.9	28.8	25.8	33.1	29.6	26.6	15.6	669.5	82.48	1.94	303.6	45.4	4.13
8:28	22.0	29.4	25.7	33.2	29.8	26.8	15.5	673.7	81.32	1.92	307.3	45.6	4.08
8:29	22.2	30.1	26.4	33.7	30.2	27.3	15.6	678.0	80.83	1.93	312.2	46.1	4.05
8:30	22.4	30.0	26.8	34.5	30.7	27.4	16.0	678.0	81.28	1.91	308.9	45.6	4.01
8:31	22.6	30.3	27.1	34.9	31.1	27.7	16.5	682.2	81.34	1.92	301.4	44.2	4.02
8:32	22.7	29.8	26.9	34.4	30.8	27.5	16.4	682.2	82.11	1.93	302.2	44.3	4.04
8:33	22.7	29.3	26.5	33.8	30.2	27.2	16.5	682.2	82.64	1.94	292.6	42.9	4.06
8:34	22.8	29.2	26.4	33.5	30.2	27.1	16.3	682.2	82.01	1.93	295.7	43.3	4.04
8:35	22.9	29.3	26.5	33.7	30.3	27.2	16.2	682.2	81.82	1.95	299.0	43.8	4.08
8:36	23.0	29.4	26.3	33.6	30.3	27.2	16.2	686.4	81.22	1.94	297.3	43.3	4.04
8:37	23.1	30.0	26.7	34.1	30.7	27.6	16.4	686.4	80.92	1.92	300.7	43.8	3.99
8:38	23.2	29.8	26.6	34.0	30.3	27.6	16.1	690.7	81.53	1.94	311.3	45.1	4.01
8:39	23.2	29.4	26.4	33.8	30.3	27.3	15.7	690.7	81.66	1.94	314.3	45.5	4.01
8:40	23.3	29.7	26.4	34.0	30.3	27.5	15.8	690.7	81.49	1.93	314.0	45.5	3.99
8:41	23.5	30.3	26.7	34.4	30.6	27.9	16.0	699.2	81.19	1.92	317.8	45.5	3.92
8:42	23.7	30.7	27.3	34.6	30.9	28.2	16.3	699.2	81.29	1.92	321.1	45.9	3.93
8:43	23.8	30.5	27.3	34.8	31.2	28.2	16.5	699.2	81.90	1.94	318.6	45.6	3.95
8:44	23.9	30.9	27.1	35.0	31.2	28.3	16.5	703.4	81.31	1.91	318.9	45.3	3.86
8:45	24.0	31.1	27.6	35.3	31.5	28.5	16.6	703.4	81.36	1.92	320.5	45.6	3.90
8:46	24.2	31.1	27.9	35.6	31.7	28.6	16.6	703.4	80.99	1.91	320.8	45.6	3.87
8:47	24.3	30.9	27.9	35.5	31.8	28.7	17.0	707.6	81.82	1.93	315.1	44.5	3.90
8:48	24.3	30.1	27.4	34.5	31.1	28.2	17.2	707.6	82.52	1.96	301.0	42.5	3.95
8:49	24.4	30.4	27.6	34.8	31.4	28.3	17.0	711.9	81.53	1.94	304.9	42.8	3.89

Time [h]	T <sub>wall</sub> [°C]	T <sub>col,1</sub> [°C]	T <sub>col,2</sub> [°C]	T <sub>col,3</sub> [°C]	T <sub>col,4</sub> [°C]	T <sub>out</sub> [°C]	T <sub>amb</sub> [°C]	G <sub>T,col</sub> [W/m <sup>2</sup> ]	Flow Rate [m <sup>3</sup> /h·m <sup>2</sup> ]	P <sub>el</sub> [W]	Q <sup>u</sup> [W/m <sup>2</sup> ]	Eff <sub>th</sub> %	Eff <sub>PV</sub> %
8:50	24.5	30.5	27.8	34.8	31.5	28.5	17.2	711.9	81.57	1.95	304.6	42.8	3.90
8:51	24.6	30.6	27.9	35.0	31.7	28.6	17.0	716.1	81.38	1.93	311.1	43.4	3.85
8:52	24.7	30.6	27.7	35.0	31.8	28.6	17.4	716.1	82.21	1.94	303.9	42.4	3.87
8:53	24.7	31.1	28.1	35.7	32.1	28.8	17.4	711.9	81.04	1.93	306.1	43.0	3.87
8:54	24.9	30.9	28.0	35.5	31.8	28.8	17.6	716.1	81.66	1.96	304.1	42.5	3.90
8:55	24.9	30.4	27.5	34.8	31.4	28.5	17.5	716.1	82.58	1.96	299.7	41.8	3.90
8:56	24.9	30.9	27.8	35.5	32.0	28.7	17.4	716.1	81.82	1.91	306.5	42.8	3.81
8:57	25.0	31.3	28.2	35.8	32.2	28.9	17.1	720.3	81.27	1.94	316.8	44.0	3.83
8:58	25.2	31.5	28.1	36.0	32.2	29.1	17.3	720.3	81.53	1.92	318.9	44.3	3.80
8:59	25.3	31.6	28.1	36.0	32.2	29.1	17.2	720.3	81.13	1.91	318.7	44.2	3.78
9:00	25.4	31.6	27.7	35.8	31.8	29.3	17.2	720.3	81.16	1.91	323.2	44.9	3.78
9:01	25.4	31.8	27.7	35.8	31.7	29.3	17.3	724.6	81.58	1.91	321.9	44.4	3.75
9:02	25.5	32.4	28.3	36.5	32.3	29.6	17.5	724.6	81.05	1.87	323.2	44.6	3.68
9:03	25.7	32.4	28.1	35.9	31.8	29.8	17.4	724.6	81.92	1.90	334.0	46.1	3.74
9:04	25.7	31.5	27.6	34.9	31.2	29.3	17.0	720.3	83.21	1.91	335.7	46.6	3.79
9:05	25.6	30.9	27.3	34.5	31.1	28.9	16.9	724.6	82.28	1.94	325.1	44.9	3.82
9:06	25.7	32.2	28.4	36.1	32.8	29.4	17.4	724.6	80.60	1.88	321.3	44.3	3.70
9:07	25.9	32.2	28.4	36.2	32.6	29.7	17.5	728.8	82.10	1.90	329.4	45.2	3.72
9:08	25.9	31.9	28.0	35.9	32.0	29.6	17.4	728.8	81.66	1.92	326.7	44.8	3.76
9:09	26.0	32.0	27.9	35.5	31.8	29.6	17.4	724.6	81.86	1.92	328.1	45.3	3.77
9:10	26.0	31.6	27.8	35.2	31.7	29.4	17.2	724.6	82.62	1.92	332.5	45.9	3.79
9:11	26.1	31.8	28.4	36.3	32.6	29.5	17.3	733.1	81.22	1.90	326.7	44.6	3.70
9:12	26.2	32.2	28.7	37.0	32.9	29.9	17.5	728.8	81.33	1.90	331.2	45.4	3.72
9:13	26.4	32.8	29.2	37.4	33.4	30.2	17.7	733.1	80.79	1.88	330.3	45.1	3.65
9:14	26.4	32.7	29.3	37.4	33.3	30.3	18.1	733.1	81.43	1.87	325.4	44.4	3.64
9:15	26.6	32.6	29.3	37.5	33.3	30.4	18.4	733.1	81.47	1.89	322.9	44.1	3.68
9:16	26.6	32.5	28.9	37.1	32.9	30.3	18.1	733.1	82.06	1.89	328.9	44.9	3.68
9:17	26.7	32.7	29.0	37.2	32.9	30.4	18.0	733.1	81.48	1.90	333.1	45.4	3.69
9:18	26.8	32.8	29.2	37.5	33.3	30.4	18.3	733.1	81.69	1.90	326.4	44.5	3.70
9:19	26.9	32.4	29.0	37.2	33.2	30.3	18.1	733.1	82.06	1.90	330.8	45.1	3.70
9:20	26.9	32.7	29.0	37.1	33.2	30.4	18.0	728.8	81.06	1.92	330.4	45.3	3.75
9:21	27.0	32.7	29.3	36.9	32.9	30.5	18.2	728.8	81.70	1.90	330.5	45.3	3.72
9:22	27.0	32.3	29.3	37.0	33.2	30.4	18.3	728.8	81.67	1.89	323.8	44.4	3.70
9:23	27.2	33.2	29.9	37.9	34.0	30.9	19.0	728.8	80.56	1.85	312.3	42.8	3.63
9:24	27.4	34.4	30.7	38.8	34.6	31.5	19.6	733.1	80.12	1.85	312.8	42.7	3.59
9:25	27.5	34.2	30.5	38.6	34.7	31.6	19.9	737.3	80.96	1.86	310.7	42.1	3.60
9:26	27.6	34.3	30.2	38.0	34.3	31.7	19.7	733.1	81.60	1.90	320.3	43.7	3.70
9:27	27.6	33.2	29.4	37.4	33.3	31.1	19.2	733.1	82.69	1.88	323.8	44.2	3.66
9:28	27.7	33.3	30.0	37.8	33.7	31.0	19.1	733.1	81.64	1.88	320.8	43.8	3.66
9:29	27.8	33.9	30.8	38.7	34.8	31.4	19.2	737.3	80.71	1.87	322.6	43.8	3.63
9:30	28.0	34.1	31.1	38.8	35.0	31.8	19.6	737.3	81.01	1.88	322.9	43.8	3.65
9:31	28.0	33.4	30.6	38.0	34.5	31.4	19.8	737.3	81.73	1.90	310.4	42.1	3.67
9:32	28.0	33.6	30.5	38.3	34.8	31.4	20.1	733.1	81.32	1.89	300.8	41.0	3.68
9:33	28.1	33.8	30.8	38.6	34.8	31.6	20.4	728.8	81.59	1.87	299.2	41.0	3.67
9:34	28.2	33.8	30.1	38.1	34.2	31.5	20.0	728.8	81.56	1.87	306.9	42.1	3.67
9:35	28.3	34.1	30.4	38.7	34.7	31.7	19.9	728.8	80.78	1.85	311.5	42.7	3.62
9:36	28.3	33.9	30.4	38.5	34.5	31.7	19.8	728.8	81.81	1.88	317.6	43.6	3.67
9:37	28.4	33.7	30.5	38.4	34.3	31.6	19.8	724.6	81.79	1.88	315.4	43.5	3.69
9:38	28.3	32.9	29.9	37.4	33.7	31.2	20.1	728.8	82.91	1.93	300.9	41.3	3.77
9:39	28.3	32.4	29.5	36.9	33.5	30.8	20.3	733.1	82.81	1.91	285.4	38.9	3.72
9:40	28.3	32.8	29.8	37.3	33.8	30.9	20.0	728.8	82.02	1.89	293.1	40.2	3.70
9:41	28.4	33.4	30.3	38.1	34.2	31.4	20.0	728.8	80.91	1.87	300.6	41.2	3.67
9:42	28.5	33.2	30.2	37.7	34.0	31.4	20.5	728.8	81.74	1.91	292.1	40.1	3.73
9:43	28.4	33.0	30.1	37.4	34.0	31.2	20.8	724.6	82.70	1.90	280.9	38.8	3.75
9:44	28.4	32.8	29.7	37.4	33.9	31.1	20.3	724.6	81.85	1.89	287.8	39.7	3.71
9:45	28.5	33.6	30.6	38.3	34.6	31.4	20.3	724.6	80.93	1.86	295.3	40.8	3.67
9:46	28.7	34.6	31.2	39.3	35.4	32.1	20.8	724.6	80.68	1.85	296.7	40.9	3.64
9:47	28.8	34.7	31.0	39.3	35.1	32.3	20.9	724.6	81.37	1.86	304.0	42.0	3.67
9:48	28.8	34.2	30.3	38.4	34.3	32.0	20.5	724.6	81.89	1.84	308.5	42.6	3.63
9:49	28.9	34.4	30.9	39.0	34.8	32.1	20.8	724.6	81.30	1.86	299.8	41.4	3.65
9:50	29.0	34.9	31.6	39.9	35.5	32.4	21.4	724.6	80.36	1.82	288.1	39.8	3.58
9:51	29.2	35.4	31.8	40.1	35.9	32.8	21.7	724.6	81.48	1.82	292.6	40.4	3.58
9:52	29.3	35.4	31.5	40.0	35.6	32.8	21.8	720.3	81.92	1.82	293.8	40.8	3.61
9:53	29.3	34.9	31.4	39.6	35.3	32.7	21.5	720.3	81.67	1.82	299.2	41.5	3.61
9:54	29.4	35.2	31.2	39.2	35.1	32.8	21.1	716.1	80.66	1.84	305.7	42.7	3.67
9:55	29.5	35.6	31.6	39.2	35.8	33.0	21.4	711.9	80.71	1.83	305.4	42.9	3.67
9:56	29.5	35.1	31.0	38.6	35.0	32.8	21.2	711.9	80.86	1.84	304.6	42.8	3.68
9:57	29.6	35.2	31.2	39.2	35.4	32.8	21.3	711.9	81.91	1.85	306.6	43.1	3.70
9:58	29.6	35.2	31.3	39.6	35.4	32.8	21.6	707.6	81.91	1.82	298.6	42.2	3.68
9:59	29.6	34.2	30.4	38.6	34.3	32.4	21.2	707.6	83.24	1.83	302.8	42.8	3.70
10:00	29.5	34.3	30.7	38.8	34.4	32.2	21.1	707.6	82.17	1.84	298.8	42.2	3.70

Time [h]	T <sub>wall</sub> [°C]	T <sub>col,1</sub> [°C]	T <sub>col,2</sub> [°C]	T <sub>col,3</sub> [°C]	T <sub>col,4</sub> [°C]	T <sub>out</sub> [°C]	T <sub>amb</sub> [°C]	G <sub>T,col</sub> [W/m <sup>2</sup> ]	Flow Rate [m <sup>3</sup> /h·m <sup>2</sup> ]	P <sub>el</sub> [W]	Q' <sub>u</sub> [W/m <sup>2</sup> ]	Eff <sub>th</sub> %	Eff <sub>PV</sub> %
10:01	29.5	34.6	30.9	39.0	34.9	32.4	21.0	707.6	81.38	1.82	302.4	42.7	3.68
10:02	29.7	34.8	30.7	38.6	34.5	32.6	21.0	707.6	81.85	1.85	310.4	43.9	3.72
10:03	29.6	33.7	30.6	38.0	34.1	32.0	21.0	703.4	82.53	1.88	298.9	42.5	3.81
10:04	29.5	34.0	30.5	38.1	34.2	32.0	20.9	703.4	81.90	1.86	297.5	42.3	3.77
10:05	29.8	35.3	31.7	39.6	35.5	32.8	21.7	703.4	80.04	1.80	288.4	41.0	3.66
10:06	29.8	34.9	30.8	38.8	34.8	32.7	21.8	699.2	82.08	1.81	291.3	41.7	3.69
10:07	29.9	35.6	31.5	39.5	35.3	33.0	22.2	699.2	80.71	1.80	284.1	40.6	3.68
10:08	30.0	36.1	31.7	40.0	35.7	33.4	22.7	699.2	81.02	1.79	280.6	40.1	3.66
10:09	30.1	35.4	31.1	39.3	34.8	33.1	22.3	699.2	82.60	1.84	288.8	41.3	3.75
10:10	29.9	34.0	30.9	38.3	34.3	32.3	21.7	694.9	83.01	1.86	286.3	41.2	3.83
10:11	29.9	33.9	31.1	38.2	34.6	32.2	21.8	694.9	82.16	1.86	279.7	40.3	3.82
10:12	29.9	33.4	30.5	37.7	34.1	31.9	21.4	694.9	82.08	1.85	282.4	40.6	3.80
10:13	29.9	34.0	31.1	38.1	34.6	32.2	21.8	690.7	82.35	1.86	278.5	40.3	3.85
10:14	29.9	34.2	31.4	38.5	34.9	32.3	21.9	690.7	80.95	1.85	274.5	39.7	3.81
10:15	30.1	34.7	31.8	39.2	35.5	32.7	22.5	690.7	81.26	1.81	271.2	39.3	3.75
10:16	30.0	33.7	30.8	38.0	34.4	32.2	22.4	686.4	83.20	1.84	267.7	39.0	3.81
10:17	30.0	33.6	30.5	38.0	34.2	32.1	21.8	686.4	82.12	1.83	274.4	40.0	3.81
10:18	30.0	34.3	31.1	38.8	34.8	32.4	21.9	686.4	81.18	1.83	278.1	40.5	3.79
10:19	30.1	34.1	31.0	38.7	34.7	32.4	21.6	682.2	81.80	1.84	287.1	42.1	3.85
10:20	30.1	34.2	31.1	38.7	34.6	32.4	21.6	682.2	80.56	1.84	285.2	41.8	3.84
10:21	30.1	34.3	31.5	38.7	35.0	32.5	21.9	682.2	81.00	1.83	280.5	41.1	3.83
10:22	30.2	33.9	31.1	38.3	34.7	32.4	22.3	678.0	82.62	1.85	272.0	40.1	3.89
10:23	30.0	33.4	30.6	37.9	34.2	32.1	21.9	678.0	82.12	1.85	273.3	40.3	3.89
10:24	30.1	33.8	30.7	38.2	34.5	32.1	21.8	673.7	81.30	1.82	272.4	40.4	3.86
10:25	30.2	34.4	30.9	38.8	34.7	32.5	22.2	673.7	81.41	1.81	272.1	40.4	3.84
10:26	30.3	35.4	31.2	39.0	34.9	32.9	22.5	669.5	80.70	1.79	274.1	40.9	3.81
10:27	30.4	35.6	31.8	39.3	35.2	33.2	22.8	669.5	81.59	1.81	274.3	41.0	3.85
10:28	30.5	35.2	31.5	38.9	35.0	33.0	22.8	665.3	81.96	1.82	273.0	41.0	3.90
10:29	30.4	34.1	31.0	38.1	34.5	32.4	22.1	665.3	83.03	1.84	277.4	41.7	3.94
10:30	30.4	34.0	31.2	38.2	34.6	32.3	22.3	665.3	82.38	1.83	268.1	40.3	3.91
10:31	30.3	33.4	30.4	37.6	34.0	32.0	22.4	665.3	82.51	1.85	257.4	38.7	3.96
10:32	30.3	34.0	30.8	38.2	34.5	32.2	22.5	665.3	81.33	1.82	256.5	38.5	3.91
10:33	30.4	34.2	31.0	38.5	34.8	32.4	22.9	661.0	81.81	1.82	253.2	38.3	3.92
10:34	30.4	34.0	30.9	38.3	34.5	32.3	22.8	661.0	81.98	1.80	254.9	38.6	3.88
10:35	30.4	33.9	30.6	38.3	34.2	32.3	22.6	656.8	82.19	1.82	259.3	39.5	3.94
10:36	30.3	33.8	30.3	37.8	33.8	32.2	22.5	656.8	82.77	1.80	262.1	39.9	3.91
10:37	30.3	34.7	30.8	38.5	34.5	32.5	23.0	652.5	80.80	1.80	252.1	38.6	3.94
10:38	30.4	34.9	30.9	38.5	34.4	32.8	22.9	652.5	81.69	1.81	261.9	40.1	3.95
10:39	30.4	33.9	30.3	37.3	33.6	32.2	22.3	648.3	82.79	1.85	267.8	41.3	4.07
10:40	30.3	33.3	29.9	36.5	33.1	31.8	22.1	644.1	82.47	1.83	262.8	40.8	4.05
10:41	30.2	32.9	29.8	36.5	33.0	31.6	22.1	644.1	82.00	1.81	254.8	39.6	4.02
10:42	30.2	33.3	30.4	37.3	33.7	31.8	22.3	644.1	80.80	1.82	250.9	39.0	4.03
10:43	30.2	32.9	30.5	37.1	33.6	31.7	22.3	639.8	82.02	1.82	251.8	39.4	4.07
10:44	30.1	32.8	30.0	36.9	33.3	31.5	22.1	639.8	81.36	1.82	252.3	39.4	4.05
10:45	30.1	33.3	29.9	37.0	33.2	31.7	22.1	635.6	80.99	1.82	255.0	40.1	4.09
10:46	30.1	33.3	30.4	37.3	33.5	31.8	22.6	635.6	81.24	1.81	245.8	38.7	4.07
10:47	30.1	32.5	30.0	36.3	33.0	31.4	22.4	631.4	81.96	1.84	242.1	38.4	4.15
10:48	30.1	32.9	29.8	36.5	33.1	31.5	22.3	631.4	81.56	1.82	246.8	39.1	4.10
10:49	30.1	33.3	30.5	37.3	33.8	31.8	22.6	627.1	80.81	1.82	242.5	38.7	4.15
10:50	30.2	33.1	30.4	37.2	33.6	31.7	22.4	627.1	81.20	1.81	247.7	39.5	4.11
10:51	30.1	32.9	29.6	36.4	33.1	31.5	22.3	622.9	81.55	1.82	245.7	39.5	4.17
10:52	30.1	33.5	30.5	37.6	34.0	31.7	22.7	622.9	81.21	1.81	241.6	38.8	4.14
10:53	30.2	33.5	30.4	37.5	33.8	31.9	23.0	618.6	80.85	1.79	237.4	38.4	4.13
10:54	30.2	33.2	30.4	37.2	33.4	31.8	22.9	614.4	81.44	1.78	237.4	38.6	4.14
10:55	30.2	33.0	30.2	36.8	33.1	31.6	22.5	614.4	81.79	1.80	243.1	39.6	4.19
10:56	30.2	33.7	30.6	37.6	33.9	31.9	23.3	610.2	80.64	1.77	226.5	37.1	4.15
10:57	30.3	34.5	30.9	37.6	34.1	32.4	23.7	610.2	80.55	1.76	227.3	37.2	4.12
10:58	30.4	34.2	31.2	37.9	34.1	32.3	24.0	605.9	80.53	1.76	218.6	36.1	4.13
10:59	30.4	34.1	31.4	38.1	34.6	32.4	24.4	605.9	80.97	1.77	212.3	35.0	4.17
11:00	30.4	33.7	30.5	37.3	33.7	32.2	24.1	601.7	81.95	1.77	217.7	36.2	4.20
11:01	30.3	32.7	29.8	36.5	32.9	31.6	23.2	597.5	82.42	1.80	228.8	38.3	4.30
11:02	30.1	32.3	29.4	36.0	32.6	31.2	22.5	597.5	81.89	1.79	233.0	39.0	4.27
11:03	30.1	32.9	29.9	36.6	33.1	31.4	22.9	593.2	80.90	1.78	224.3	37.8	4.27
11:04	30.2	33.0	30.5	36.9	33.3	31.6	23.5	593.2	80.75	1.78	214.4	36.1	4.29
11:05	30.2	33.2	30.6	37.4	33.8	31.7	23.8	589.0	81.19	1.77	209.9	35.6	4.28
11:06	30.2	33.0	30.5	37.2	33.5	31.6	23.8	589.0	81.59	1.77	208.3	35.4	4.28
11:07	30.1	32.2	29.8	36.0	32.8	31.3	23.2	584.7	82.93	1.80	217.7	37.2	4.39
11:08	30.1	32.3	29.7	36.1	32.8	31.1	23.1	580.5	81.66	1.79	215.8	37.2	4.39
11:09	30.2	33.2	30.4	37.2	33.6	31.5	23.7	580.5	80.95	1.77	207.3	35.7	4.34
11:10	30.3	33.3	30.5	37.5	33.8	31.8	24.1	576.3	81.63	1.76	206.2	35.8	4.35
11:11	30.3	33.6	30.8	37.6	33.7	31.9	24.2	572.0	80.64	1.76	202.8	35.5	4.38

Time [h]	T <sub>wall</sub> [°C]	T <sub>col,1</sub> [°C]	T <sub>col,2</sub> [°C]	T <sub>col,3</sub> [°C]	T <sub>col,4</sub> [°C]	T <sub>out</sub> [°C]	T <sub>amb</sub> [°C]	G <sub>T,col</sub> [W/m <sup>2</sup> ]	Flow Rate [m <sup>3</sup> /h·m <sup>2</sup> ]	P <sub>el</sub> [W]	Q'' <sub>u</sub> [W/m <sup>2</sup> ]	Eff <sub>th</sub> %	Eff <sub>PV</sub> %
11:12	30.2	32.3	29.8	35.9	32.4	31.3	23.9	572.0	82.95	1.78	203.1	35.5	4.45
11:13	30.0	31.5	29.2	34.8	32.0	30.7	23.7	567.8	81.96	1.78	187.0	32.9	4.47
11:14	30.0	31.8	29.4	35.5	32.5	30.8	23.6	567.8	82.39	1.78	194.5	34.3	4.47
11:15	30.0	32.4	29.9	36.4	33.2	31.0	24.0	563.6	81.23	1.74	187.3	33.2	4.41
11:16	30.1	32.7	29.8	36.2	32.9	31.4	24.1	559.3	81.73	1.74	193.9	34.7	4.44
11:17	30.1	32.6	29.9	36.1	32.7	31.3	24.0	559.3	80.89	1.75	193.0	34.5	4.47
11:18	30.0	32.0	29.6	35.5	32.4	30.9	24.1	555.1	82.02	1.76	183.0	33.0	4.53
11:19	29.9	31.6	29.3	35.0	32.1	30.6	24.3	550.8	81.74	1.77	170.7	31.0	4.59
11:20	29.9	31.4	29.2	34.8	31.8	30.5	24.3	546.6	81.71	1.78	166.7	30.5	4.64
11:21	29.7	30.7	28.7	34.1	31.3	30.1	23.8	546.6	82.01	1.78	171.1	31.3	4.64
11:22	29.7	31.4	29.1	34.9	31.9	30.5	23.7	542.4	80.87	1.74	178.6	32.9	4.58
11:23	29.8	32.0	29.1	35.3	32.0	30.8	23.6	542.4	80.95	1.74	189.5	34.9	4.56
11:24	29.8	32.3	29.5	35.6	32.2	30.9	23.7	538.1	81.40	1.73	192.8	35.8	4.58
11:25	29.8	32.2	29.8	35.9	32.5	30.8	23.8	533.9	80.96	1.74	186.8	35.0	4.65
11:26	29.9	32.9	30.0	36.4	33.0	31.3	24.1	529.7	80.26	1.72	188.1	35.5	4.63
11:27	30.0	33.6	30.6	37.2	33.8	31.7	25.7	529.7	80.80	1.67	160.5	30.3	4.50
11:28	30.1	33.7	31.1	37.7	34.0	32.0	26.0	525.4	81.69	1.67	160.0	30.5	4.55
11:29	30.2	33.8	30.7	37.0	33.8	32.0	25.6	525.4	81.90	1.67	170.8	32.5	4.54
11:30	30.1	32.6	29.6	35.7	32.5	31.4	24.8	521.2	82.76	1.71	176.8	33.9	4.69
11:31	30.0	31.6	28.8	34.7	31.6	30.6	23.9	516.9	82.95	1.74	181.8	35.2	4.80
11:32	29.8	30.9	28.3	34.1	31.0	30.2	23.5	512.7	82.64	1.72	182.7	35.6	4.79
11:33	29.7	30.9	28.7	34.0	30.9	30.0	23.5	512.7	81.35	1.75	172.7	33.7	4.87
11:34	29.7	31.3	29.2	34.8	31.7	30.3	24.0	512.7	80.82	1.68	167.4	32.7	4.68
11:35	29.7	32.0	29.3	35.6	32.1	30.7	24.5	508.5	80.72	1.69	163.0	32.1	4.74
11:36	29.7	31.4	28.7	34.8	31.2	30.4	23.9	504.2	82.29	1.70	175.8	34.9	4.82
11:37	29.6	31.5	28.6	34.4	31.3	30.3	23.5	500.0	82.05	1.67	183.7	36.7	4.78
11:38	29.6	32.1	29.3	35.2	32.0	30.6	24.1	495.8	80.29	1.67	170.9	34.5	4.80
11:39	29.6	31.5	29.0	34.8	31.5	30.5	24.2	491.5	81.48	1.66	166.3	33.8	4.81
11:40	29.6	31.6	29.2	34.8	31.6	30.4	24.5	487.3	81.46	1.68	157.5	32.3	4.92
11:41	29.5	30.7	28.6	33.9	30.9	30.0	24.3	487.3	82.17	1.71	154.7	31.7	5.00
11:42	29.3	29.8	28.0	32.8	30.2	29.4	24.2	483.1	82.42	1.68	140.0	29.0	4.97
11:43	29.2	30.1	28.2	33.1	30.4	29.4	24.2	483.1	81.61	1.68	140.2	29.0	4.96
11:44	29.2	30.3	28.3	33.5	30.7	29.5	24.1	478.8	81.44	1.66	145.0	30.3	4.93
11:45	29.3	31.2	28.8	34.3	31.5	30.0	24.7	474.6	81.17	1.67	141.3	29.8	5.00
11:46	29.3	31.2	28.8	34.4	31.3	30.1	25.3	470.3	82.22	1.65	131.7	28.0	5.00
11:47	29.2	30.4	28.3	33.5	30.7	29.6	24.8	466.1	82.70	1.63	132.4	28.4	4.98
11:48	29.2	30.8	28.7	33.9	31.0	29.8	24.9	466.1	81.73	1.63	131.9	28.3	4.99
11:49	29.2	30.7	28.2	33.8	30.8	29.8	24.7	461.9	82.11	1.70	136.0	29.5	5.26
11:50	29.1	30.7	28.2	33.7	30.5	29.7	24.6	461.9	81.68	1.63	136.2	29.5	5.05
11:51	29.1	30.9	27.8	33.4	30.1	29.7	24.4	457.6	81.48	1.65	142.5	31.1	5.14
11:52	29.1	30.6	27.8	33.5	30.5	29.5	24.6	453.4	82.45	1.59	132.7	29.3	5.01
11:53	29.1	31.0	28.1	34.0	30.6	29.7	25.2	449.2	81.48	1.61	119.7	26.7	5.10
11:54	29.1	31.2	28.4	34.1	30.8	29.9	25.7	444.9	81.53	1.59	112.8	25.3	5.09
11:55	29.1	30.9	28.5	33.9	30.8	29.9	25.8	440.7	81.75	1.58	110.3	25.0	5.13
11:56	29.0	30.3	28.1	33.1	30.1	29.6	25.5	436.4	82.47	1.59	109.3	25.0	5.20
11:57	28.9	29.2	27.3	31.8	29.3	28.8	24.7	436.4	83.09	1.62	113.1	25.9	5.29
11:58	28.8	29.2	27.4	32.1	29.6	28.7	24.5	432.2	82.25	1.60	116.1	26.9	5.27
11:59	28.7	29.6	27.5	32.5	29.9	28.9	24.5	428.0	81.68	1.59	119.8	28.0	5.31
12:00	28.7	29.9	27.7	32.8	29.9	29.0	24.8	428.0	81.72	1.57	113.9	26.6	5.24
12:01	28.8	30.3	27.8	33.4	30.3	29.3	25.4	423.7	81.37	1.56	103.1	24.3	5.24
12:02	28.9	31.1	28.3	33.8	30.8	29.7	25.6	423.7	81.49	1.55	111.7	26.4	5.22
12:03	28.8	30.1	27.7	32.9	29.9	29.3	25.1	419.5	83.23	1.55	116.7	27.8	5.28
12:04	28.7	29.8	27.6	32.7	29.7	29.0	24.9	415.3	82.33	1.56	111.4	26.8	5.35
12:05	28.6	29.4	27.3	32.2	29.2	28.8	24.8	411.0	83.28	1.55	110.1	26.8	5.38
12:06	28.4	28.7	26.8	31.3	28.7	28.3	24.1	406.8	82.75	1.55	115.0	28.3	5.45
12:07	28.3	28.8	26.8	31.2	28.7	28.2	24.2	406.8	81.50	1.54	109.0	26.8	5.40
12:08	28.4	29.5	27.5	32.2	29.4	28.7	25.1	402.5	81.41	1.54	95.3	23.7	5.46
12:09	28.3	28.7	26.9	31.2	28.8	28.3	24.9	398.3	82.13	1.54	93.5	23.5	5.50
12:10	28.3	29.1	27.1	31.8	29.3	28.4	25.0	398.3	81.55	1.52	91.5	23.0	5.44
12:11	28.3	29.5	27.4	32.4	29.5	28.7	25.5	394.1	81.41	1.49	84.2	21.4	5.41
12:12	28.3	28.7	26.9	31.4	28.7	28.3	25.1	389.8	83.34	1.51	88.6	22.7	5.52
12:13	28.2	28.5	26.7	31.2	28.5	28.0	24.9	385.6	82.06	1.50	86.2	22.3	5.54
12:14	28.2	29.4	27.2	32.1	29.3	28.5	25.7	381.4	81.17	1.47	75.2	19.7	5.52
12:15	28.3	30.0	27.7	32.9	29.9	29.0	26.6	377.1	81.49	1.45	64.6	17.1	5.49
12:16	28.4	30.1	27.9	33.0	30.0	29.1	27.1	372.9	81.32	1.45	52.6	14.1	5.53
12:17	28.4	30.2	27.8	32.7	29.9	29.2	27.2	368.6	81.15	1.44	52.8	14.3	5.58
12:18	28.5	30.3	27.8	32.3	29.8	29.2	26.9	364.4	81.36	1.45	62.5	17.2	5.66
12:19	28.4	29.7	27.3	31.9	29.1	28.8	26.8	360.2	82.07	1.42	54.0	15.0	5.63
12:20	28.2	28.8	26.6	31.1	28.4	28.3	26.4	355.9	82.73	1.43	52.0	14.6	5.72
12:21	28.1	28.5	26.5	30.9	28.2	28.0	25.8	355.9	82.46	1.41	61.5	17.3	5.67
12:22	28.0	28.4	26.6	30.9	28.3	27.9	25.5	351.7	82.02	1.41	65.0	18.5	5.70

Time [h]	T <sub>wall</sub> [°C]	T <sub>col,1</sub> [°C]	T <sub>col,2</sub> [°C]	T <sub>col,3</sub> [°C]	T <sub>col,4</sub> [°C]	T <sub>out</sub> [°C]	T <sub>amb</sub> [°C]	G <sub>T,col</sub> [W/m <sup>2</sup> ]	Flow Rate [m <sup>3</sup> /h·m <sup>2</sup> ]	P <sub>el</sub> [W]	Q'' <sub>u</sub> [W/m <sup>2</sup> ]	Eff <sub>th</sub> %	Eff <sub>PV</sub> %
12:23	27.9	28.3	26.4	30.8	28.2	27.8	25.6	347.5	81.99	1.40	60.9	17.5	5.73
12:24	28.0	28.7	26.6	31.2	28.5	28.1	25.6	347.5	81.45	1.38	65.6	18.9	5.65
12:25	28.0	29.0	26.6	31.1	28.4	28.2	25.5	343.2	81.90	1.37	72.9	21.3	5.71
12:26	27.9	28.4	26.2	30.7	28.0	27.9	25.3	339.0	82.22	1.39	70.3	20.7	5.83
12:27	27.8	28.1	26.1	30.4	27.7	27.6	24.9	339.0	82.56	1.37	75.9	22.4	5.78
12:28	27.8	28.0	26.2	30.3	27.8	27.6	24.8	334.7	81.92	1.38	73.9	22.1	5.87
12:29	27.7	27.5	25.7	29.6	27.3	27.3	24.7	330.5	82.66	1.38	71.1	21.5	5.94
12:30	27.5	26.7	25.2	28.6	26.6	26.7	24.2	330.5	82.92	1.38	69.2	21.0	5.95
12:31	27.4	26.8	25.3	28.7	26.8	26.7	24.2	326.3	82.50	1.36	67.0	20.5	5.93
12:32	27.3	27.0	25.4	29.0	27.1	26.8	24.4	322.0	81.92	1.33	64.3	20.0	5.88
12:33	27.2	26.6	24.9	28.4	26.4	26.5	24.0	313.6	82.85	1.33	68.4	21.8	6.06
12:34	27.1	26.4	24.7	28.3	26.3	26.2	23.8	309.3	82.17	1.32	66.0	21.3	6.07
12:35	27.0	27.0	25.0	29.2	26.8	26.4	24.4	309.3	81.21	1.28	55.4	17.9	5.92
12:36	27.1	27.2	25.2	29.4	26.9	26.7	25.0	305.1	81.48	1.27	43.7	14.3	5.95
12:37	27.0	27.6	25.4	29.5	27.1	26.9	25.0	300.8	81.73	1.26	50.8	16.9	5.98
12:38	27.1	27.4	25.3	29.3	27.2	26.8	24.4	296.6	81.91	1.26	63.8	21.5	6.04
12:39	27.1	27.5	25.3	29.5	27.2	26.9	24.8	292.4	81.74	1.21	56.0	19.2	5.91
12:40	27.0	27.3	25.3	29.3	26.9	26.7	25.0	292.4	82.31	1.24	47.1	16.1	6.03
12:41	27.0	27.1	25.1	28.7	26.6	26.6	24.4	288.1	81.46	1.25	59.4	20.6	6.17
12:42	26.9	26.7	24.8	28.0	26.1	26.2	23.4	220.3	81.97	1.19	76.8	34.8	7.70
12:43	26.7	25.4	23.6	26.3	24.3	25.4	22.7	194.9	82.94	1.25	74.8	38.4	9.14
12:44	26.6	25.6	24.2	27.0	25.2	25.4	23.4	245.8	81.95	1.25	54.5	22.2	7.23
12:45	26.5	25.4	24.1	26.7	25.1	25.3	23.6	283.9	81.91	1.23	47.6	16.8	6.20
12:46	26.5	25.9	24.6	27.5	25.9	25.7	24.0	279.7	81.01	1.21	45.4	16.2	6.19
12:47	26.4	25.9	24.5	27.5	25.7	25.7	24.1	275.4	81.82	1.20	42.3	15.4	6.19
12:48	26.4	25.8	24.4	27.4	25.6	25.6	23.9	271.2	81.40	1.17	46.5	17.1	6.16
12:49	26.3	25.4	23.9	26.9	25.2	25.3	23.9	266.9	82.52	1.17	39.2	14.7	6.23
12:50	26.2	25.3	23.9	26.9	25.1	25.2	23.8	266.9	82.30	1.17	38.5	14.4	6.24
12:51	26.1	25.1	23.7	26.5	24.9	25.1	23.8	266.9	82.06	1.19	34.6	13.0	6.34

Table E.5: Experimental data for September 2

Time [h]	T <sub>wall</sub> [°C]	T <sub>col,1</sub> [°C]	T <sub>col,2</sub> [°C]	T <sub>col,3</sub> [°C]	T <sub>col,4</sub> [°C]	T <sub>out</sub> [°C]	T <sub>amb</sub> [°C]	G <sub>T,col</sub> [W/m <sup>2</sup> ]	Flow Rate [m <sup>3</sup> /h·m <sup>2</sup> ]	P <sub>el</sub> [W]	Q'' <sub>u</sub> [W/m <sup>2</sup> ]	Eff <sub>th</sub> %	Eff <sub>PV</sub> %
7:33	14.2	20.5	18.5	23.7	21.2	18.6	11.9	416.6	70.73	1.81	162.7	39.1	6.20
7:34	14.5	20.8	19.1	24.3	21.7	19.0	11.9	421.7	71.14	1.81	171.7	40.7	6.12
7:35	14.7	21.0	19.3	24.4	22.0	19.2	11.9	431.1	71.33	1.82	177.9	41.3	6.03
7:36	14.8	21.1	19.0	24.5	22.1	19.3	12.0	441.6	70.76	1.83	175.7	39.8	5.92
7:37	14.9	21.6	19.2	24.8	22.2	19.5	12.1	449.6	71.10	1.84	180.2	40.1	5.83
7:38	15.1	21.8	19.5	25.2	22.6	19.8	12.2	454.4	70.71	1.84	182.9	40.3	5.79
7:39	15.2	22.2	19.5	25.6	22.8	20.0	12.4	458.7	70.64	1.84	183.1	39.9	5.72
7:40	15.4	22.9	19.8	26.0	23.2	20.4	12.7	466.6	71.01	1.84	184.3	39.5	5.63
7:41	15.6	23.0	20.2	26.4	23.5	20.6	12.9	475.5	70.71	1.85	184.6	38.8	5.56
7:42	15.8	23.3	20.3	26.7	23.6	20.9	13.0	483.4	70.67	1.86	188.8	39.1	5.50
7:43	16.0	23.5	20.7	27.2	24.0	21.1	13.1	492.6	71.26	1.87	195.1	39.6	5.42
7:44	16.2	23.7	21.0	27.4	24.3	21.4	13.1	499.3	70.93	1.87	198.1	39.7	5.35
7:45	16.3	24.1	20.9	27.7	24.5	21.6	13.2	504.9	70.45	1.86	199.3	39.5	5.25
7:46	16.5	24.9	21.5	28.0	24.9	22.1	13.3	509.3	70.13	1.87	208.0	40.8	5.25
7:47	16.7	24.7	21.5	28.2	25.1	22.2	13.5	511.7	70.32	1.87	207.1	40.5	5.21
7:48	17.0	24.9	21.9	28.7	25.3	22.4	13.6	517.5	70.55	1.87	208.6	40.3	5.15
7:49	17.1	25.1	22.0	29.0	25.5	22.6	13.7	522.5	70.35	1.86	209.3	40.1	5.09
7:50	17.3	25.6	22.1	29.2	25.8	22.9	13.8	527.6	70.13	1.87	213.4	40.4	5.06
7:51	17.5	26.0	22.3	29.2	25.9	23.2	14.0	531.4	71.37	1.87	218.9	41.2	5.03
7:52	17.7	25.9	22.4	29.4	26.0	23.2	14.2	534.4	72.67	1.87	220.5	41.3	4.98
7:53	17.8	26.0	22.4	29.8	26.2	23.3	14.3	538.8	71.63	1.88	217.1	40.3	4.98
7:54	18.0	26.2	22.7	30.0	26.4	23.5	14.4	544.6	71.58	1.87	218.2	40.1	4.91
7:55	18.2	26.5	23.1	30.4	26.7	23.8	14.6	549.4	71.71	1.88	221.1	40.3	4.88
7:56	18.4	26.5	23.4	30.6	26.9	23.9	14.7	550.8	71.67	1.87	221.7	40.2	4.84
7:57	18.7	26.7	23.4	30.9	27.1	24.2	14.8	553.7	72.06	1.87	226.5	40.9	4.81
7:58	18.8	26.8	23.6	31.0	27.2	24.3	15.0	559.8	72.45	1.87	226.2	40.4	4.77
7:59	19.0	27.4	23.7	30.8	27.5	24.6	15.0	565.6	71.70	1.88	229.1	40.5	4.74
8:00	19.2	27.6	23.9	31.1	27.6	24.8	15.2	572.3	72.07	1.88	230.8	40.3	4.69
8:01	19.4	27.8	24.2	31.6	27.8	24.9	15.3	577.3	72.02	1.87	231.5	40.1	4.62
8:02	19.7	27.9	24.8	32.0	28.1	25.2	15.5	579.9	71.96	1.88	234.3	40.4	4.63
8:03	19.8	27.9	24.4	31.9	28.1	25.2	15.4	580.3	72.01	1.87	234.4	40.4	4.60
8:04	19.9	28.4	24.4	32.1	28.3	25.4	15.6	581.8	71.58	1.87	234.7	40.3	4.58
8:05	20.1	28.6	24.6	32.0	28.4	25.6	15.6	586.9	72.21	1.87	241.5	41.1	4.55
8:06	20.3	29.3	25.4	31.9	28.7	26.1	15.5	591.9	70.84	1.89	250.6	42.3	4.56
8:07	20.5	29.2	25.4	31.7	28.8	26.2	15.2	594.7	72.28	1.89	263.7	44.3	4.54

Time [h]	T <sub>wall</sub> [°C]	T <sub>col,1</sub> [°C]	T <sub>col,2</sub> [°C]	T <sub>col,3</sub> [°C]	T <sub>col,4</sub> [°C]	T <sub>out</sub> [°C]	T <sub>amb</sub> [°C]	G <sub>T,col</sub> [W/m <sup>2</sup> ]	Flow Rate [m <sup>3</sup> /h·m <sup>2</sup> ]	P <sub>el</sub> [W]	Q <sup>u</sup> [W/m <sup>2</sup> ]	Eff <sub>th</sub> %	Eff <sub>PV</sub> %
8:08	20.7	29.3	25.6	31.9	29.0	26.3	15.3	596.1	71.91	1.88	262.7	44.1	4.51
8:09	20.8	29.5	25.7	31.8	29.1	26.4	15.4	599.9	71.38	1.89	262.6	43.8	4.50
8:10	21.0	29.5	25.9	31.7	29.2	26.5	15.3	602.2	71.89	1.89	268.0	44.5	4.49
8:11	21.1	29.4	26.0	31.6	29.2	26.6	15.3	605.0	72.08	1.90	270.3	44.7	4.48
8:12	21.0	29.3	26.1	31.6	29.2	26.6	15.2	605.0	72.02	1.89	272.7	45.1	4.47
8:13	21.2	29.5	26.2	31.7	29.5	26.7	15.3	608.1	71.76	1.89	272.9	44.9	4.44
8:14	21.3	29.6	26.2	32.0	29.5	26.8	15.4	612.0	72.16	1.89	273.8	44.7	4.41
8:15	21.4	29.6	26.2	32.0	29.6	26.8	15.4	619.3	72.04	1.91	273.1	44.1	4.40
8:16	21.5	29.7	26.1	32.6	29.8	26.9	15.7	627.7	71.91	1.90	266.6	42.5	4.31
8:17	21.7	30.0	26.4	32.8	29.9	27.1	15.7	628.5	72.47	1.90	273.6	43.5	4.30
8:18	21.9	30.2	26.7	32.8	30.2	27.3	15.8	630.0	71.55	1.90	274.4	43.6	4.31
8:19	22.0	30.1	26.9	32.6	30.3	27.4	15.6	630.5	71.62	1.90	280.3	44.5	4.29
8:20	22.2	30.5	27.2	32.9	30.5	27.7	15.7	633.4	71.97	1.90	284.5	44.9	4.27
8:21	22.3	30.7	27.4	33.1	30.7	27.9	15.8	636.1	71.51	1.89	284.9	44.8	4.25
8:22	22.4	30.5	27.2	32.9	30.6	27.8	15.9	638.4	71.69	1.89	282.2	44.2	4.22
8:23	22.6	30.7	27.5	33.1	30.7	28.0	15.8	639.8	71.36	1.89	286.9	44.8	4.22
8:24	22.8	30.6	27.6	33.0	30.9	28.1	15.8	642.8	71.51	1.91	290.9	45.3	4.23
8:25	23.0	31.1	27.9	33.4	31.2	28.3	15.8	646.5	71.54	1.90	294.7	45.6	4.18
8:26	23.1	31.4	28.1	33.7	31.4	28.5	16.0	649.5	71.00	1.89	294.4	45.3	4.14
8:27	23.3	31.6	28.2	33.8	31.5	28.7	16.2	652.1	71.84	1.89	297.1	45.6	4.14
8:28	23.5	31.8	28.5	34.1	31.8	28.9	16.5	653.4	71.38	1.89	292.0	44.7	4.13
8:29	23.6	31.9	28.4	34.7	32.1	29.0	16.8	654.4	71.03	1.88	287.5	43.9	4.09
8:30	23.7	32.3	28.4	35.3	32.2	29.2	17.0	656.2	71.98	1.87	289.5	44.1	4.06
8:31	23.9	32.6	28.6	35.8	32.4	29.4	17.2	658.1	71.45	1.86	288.0	43.8	4.03
8:32	24.0	32.6	28.8	36.0	32.5	29.6	17.4	661.9	72.28	1.86	290.7	43.9	4.01
8:33	24.2	32.8	29.1	35.8	32.6	29.8	17.4	664.4	71.37	1.86	289.5	43.6	4.00
8:34	24.3	32.7	28.8	35.9	32.8	29.7	17.5	666.6	72.58	1.86	290.9	43.6	3.98
8:35	24.4	32.8	28.9	36.3	32.8	29.8	17.7	668.4	71.73	1.86	285.3	42.7	3.96
8:36	24.7	33.2	29.4	36.0	32.8	30.1	17.6	669.4	71.55	1.88	292.9	43.8	4.00
8:37	24.8	33.3	29.5	36.0	33.1	30.2	17.7	672.1	71.77	1.87	295.9	44.0	3.96
8:38	25.0	33.6	29.7	36.1	33.3	30.4	17.8	674.0	71.76	1.87	297.4	44.1	3.96
8:39	25.1	33.8	29.8	36.5	33.6	30.5	17.9	675.3	72.83	1.86	303.0	44.9	3.93
8:40	25.3	33.9	30.0	36.6	33.6	30.7	18.0	676.6	72.98	1.87	303.4	44.8	3.93
8:41	25.4	34.0	29.9	37.0	33.7	30.8	18.3	676.3	74.17	1.85	304.9	45.1	3.90
8:42	25.6	34.1	30.2	36.8	33.8	31.0	18.5	674.2	73.63	1.86	301.0	44.7	3.94
8:43	25.8	34.2	30.2	36.8	33.8	31.0	18.5	672.5	74.16	1.86	303.6	45.1	3.94
8:44	25.9	34.2	30.3	36.9	33.9	31.1	18.7	669.7	74.06	1.85	301.3	45.0	3.93
8:45	26.0	34.0	30.2	36.8	33.7	31.1	18.7	663.2	74.50	1.86	301.8	45.5	4.00
8:46	26.1	34.1	30.2	36.6	33.6	31.1	18.6	665.1	74.18	1.85	302.9	45.5	3.96
8:47	26.2	34.0	30.3	36.4	33.5	31.1	18.6	667.3	75.23	1.87	307.3	46.0	3.99
8:48	26.3	33.8	30.1	36.2	33.5	31.0	18.5	669.4	75.04	1.86	306.4	45.8	3.95
8:49	26.4	33.9	30.1	36.6	33.6	31.0	18.7	674.0	75.63	1.86	305.8	45.4	3.93
8:50	26.5	34.2	30.4	37.2	34.1	31.3	18.9	677.9	74.84	1.85	303.1	44.7	3.88
8:51	26.6	34.5	30.9	37.1	34.3	31.6	19.1	686.3	74.74	1.86	305.7	44.5	3.87
8:52	26.8	34.6	31.0	37.1	34.6	31.7	19.1	691.4	75.25	1.87	310.8	44.9	3.85
8:53	26.9	34.5	31.1	36.9	34.6	31.7	19.0	693.9	74.96	1.86	312.3	45.0	3.83
8:54	27.0	34.8	31.2	37.4	34.8	31.9	19.0	692.8	75.02	1.85	314.2	45.4	3.82
8:55	27.1	35.1	31.4	37.8	35.0	32.0	19.4	695.3	74.50	1.84	307.0	44.2	3.77
8:56	27.3	35.4	31.5	38.4	35.2	32.3	19.6	694.3	74.52	1.84	307.5	44.3	3.78
8:57	27.5	35.6	31.8	38.2	35.3	32.5	19.8	696.0	74.98	1.84	310.2	44.6	3.78
8:58	27.5	34.8	31.4	37.3	35.0	32.2	19.6	698.6	74.88	1.85	308.0	44.1	3.77
8:59	27.6	35.6	31.9	38.4	35.7	32.6	19.9	703.0	73.91	1.84	304.5	43.3	3.73
9:00	27.8	35.8	32.1	38.9	36.0	32.8	20.1	706.3	73.49	1.84	303.5	43.0	3.72
9:01	27.9	36.0	32.5	38.7	36.1	33.0	20.3	707.7	74.15	1.85	307.6	43.5	3.72
9:02	28.1	35.5	32.2	38.2	35.9	32.9	20.1	708.1	74.22	1.86	310.2	43.8	3.74
9:03	28.1	35.6	32.2	38.5	36.2	32.9	20.3	709.4	73.52	1.84	302.3	42.6	3.71
9:04	28.2	36.0	32.3	39.2	36.3	33.1	20.5	710.6	73.71	1.83	302.7	42.6	3.67
9:05	28.3	36.0	32.3	39.9	36.4	33.2	20.9	710.7	75.45	1.83	301.8	42.5	3.67
9:06	28.5	36.5	32.7	40.2	36.7	33.5	21.1	711.3	74.45	1.82	301.8	42.4	3.66
9:07	28.7	37.0	33.1	40.0	36.8	33.8	21.2	713.6	74.74	1.82	306.2	42.9	3.64
9:08	28.8	37.0	32.9	40.2	37.0	33.8	21.6	714.8	75.54	1.81	300.9	42.1	3.61
9:09	29.0	37.2	33.3	39.9	37.0	34.1	21.5	715.2	74.85	1.82	306.5	42.8	3.63
9:10	29.1	37.0	33.1	40.1	37.0	34.0	21.6	715.2	75.45	1.83	301.4	42.1	3.64
9:11	29.1	37.2	33.5	40.0	36.9	34.1	21.9	715.0	74.88	1.83	296.8	41.5	3.64
9:12	29.3	36.9	33.3	39.7	37.0	34.1	21.5	715.4	75.56	1.83	307.3	42.9	3.65
9:13	29.3	36.1	32.8	39.6	36.6	33.6	21.8	714.1	76.33	1.83	293.1	41.0	3.66
9:14	29.4	36.7	33.1	40.0	36.8	33.9	22.1	712.4	75.65	1.83	290.0	40.7	3.66
9:15	29.6	37.0	33.4	39.8	37.0	34.2	22.0	710.8	75.70	1.83	300.0	42.2	3.67
9:16	29.7	36.9	33.7	40.6	37.5	34.1	22.4	712.0	75.84	1.81	287.7	40.4	3.63
9:17	29.8	37.2	33.9	41.2	37.7	34.4	22.8	714.0	75.48	1.81	285.1	39.9	3.62
9:18	30.0	37.8	34.0	41.0	37.8	34.8	22.7	713.7	75.75	1.81	295.7	41.4	3.61

Time [h]	T <sub>wall</sub> [°C]	T <sub>col,1</sub> [°C]	T <sub>col,2</sub> [°C]	T <sub>col,3</sub> [°C]	T <sub>col,4</sub> [°C]	T <sub>out</sub> [°C]	T <sub>amb</sub> [°C]	G <sub>T,col</sub> [W/m <sup>2</sup> ]	Flow Rate [m <sup>3</sup> /h·m <sup>2</sup> ]	P <sub>el</sub> [W]	Q <sup>u</sup> [W/m <sup>2</sup> ]	Eff <sub>th</sub> %	Eff <sub>PV</sub> %
9:19	30.0	37.6	33.9	40.8	37.8	34.7	22.7	713.0	75.96	1.80	294.8	41.3	3.60
9:20	30.1	37.0	33.4	39.6	37.1	34.5	22.2	710.4	76.56	1.84	304.3	42.8	3.69
9:21	30.2	36.9	33.9	40.4	37.5	34.4	22.6	710.6	75.43	1.81	288.5	40.6	3.63
9:22	30.3	37.0	34.3	41.2	37.6	34.6	23.0	710.9	75.64	1.82	282.6	39.8	3.65
9:23	30.4	37.1	34.1	41.1	37.6	34.6	23.3	711.1	76.52	1.81	279.6	39.3	3.64
9:24	30.4	37.1	33.6	40.6	37.4	34.6	23.3	709.4	76.37	1.83	280.4	39.5	3.67
9:25	30.6	37.5	34.1	41.0	37.5	34.8	23.5	708.0	76.21	1.80	278.8	39.4	3.62
9:26	30.6	37.2	33.9	41.0	37.6	34.7	23.5	707.6	76.73	1.80	279.1	39.4	3.63
9:27	30.7	37.1	33.7	40.3	37.2	34.6	23.2	707.4	76.64	1.81	282.1	39.9	3.64
9:28	30.7	36.7	33.2	39.6	36.6	34.2	22.9	705.3	77.02	1.83	282.9	40.1	3.70
9:29	30.7	36.3	33.1	39.6	36.7	34.0	22.6	704.2	76.76	1.83	283.3	40.2	3.72
9:30	30.7	36.1	32.7	38.9	36.2	33.8	22.3	702.8	76.88	1.85	287.7	40.9	3.76
9:31	30.7	36.2	33.0	39.4	36.4	33.9	22.4	701.6	76.03	1.82	282.0	40.2	3.70
9:32	30.8	36.3	33.0	39.6	36.6	33.9	22.7	700.9	76.32	1.83	279.2	39.8	3.73
9:33	30.8	36.6	33.8	40.5	37.1	34.2	23.2	699.4	75.67	1.83	270.8	38.7	3.72
9:34	30.9	36.4	33.6	40.3	37.0	34.1	23.4	700.0	76.27	1.80	264.7	37.8	3.67
9:35	30.9	36.8	34.2	40.9	37.3	34.5	24.0	699.7	75.57	1.81	258.0	36.9	3.68
9:36	31.0	37.0	34.0	40.6	37.3	34.6	24.1	699.1	75.59	1.82	257.2	36.8	3.72
9:37	31.0	36.3	33.0	39.2	36.5	34.2	23.1	696.4	76.51	1.84	275.0	39.5	3.76
9:38	31.0	36.1	32.9	38.5	36.1	34.0	22.8	694.5	76.09	1.84	276.3	39.8	3.78
9:39	31.0	36.0	33.0	38.8	36.2	33.8	23.0	696.4	76.06	1.82	267.8	38.5	3.73
9:40	31.1	36.7	33.9	40.4	37.3	34.4	23.9	699.3	74.62	1.82	253.9	36.3	3.71
9:41	31.2	37.0	34.2	41.0	37.3	34.7	24.2	699.4	75.88	1.81	256.3	36.6	3.70
9:42	31.3	36.9	34.1	40.8	37.3	34.7	24.4	698.1	75.71	1.80	250.3	35.9	3.68
9:43	31.3	36.8	33.9	40.7	37.2	34.6	24.8	695.9	76.27	1.81	241.7	34.7	3.72
9:44	31.3	36.8	34.0	40.7	37.3	34.6	24.6	694.8	75.55	1.80	243.7	35.1	3.70
9:45	31.4	36.4	33.8	40.2	36.7	34.4	24.6	693.2	76.02	1.82	241.7	34.9	3.75
9:46	31.3	36.0	33.3	39.5	36.5	34.0	24.5	693.4	76.11	1.83	233.3	33.7	3.77
9:47	31.3	36.6	33.9	40.4	37.2	34.4	24.4	695.6	74.88	1.81	243.4	35.0	3.70
9:48	31.5	37.0	34.3	40.8	37.3	34.7	24.5	696.4	74.93	1.80	248.8	35.7	3.68
9:49	31.6	37.1	34.4	41.1	37.6	34.9	24.7	694.7	75.23	1.80	248.7	35.8	3.70
9:50	31.7	37.4	34.6	41.4	37.9	35.1	25.0	692.8	74.84	1.77	244.6	35.3	3.65
9:51	31.7	37.5	34.3	40.9	37.4	35.1	24.7	689.9	74.93	1.79	253.0	36.7	3.71
9:52	31.7	37.0	34.3	40.9	37.3	34.9	24.5	688.4	75.83	1.81	254.4	37.0	3.76
9:53	31.8	36.8	34.2	40.9	37.3	34.8	24.4	687.4	75.58	1.79	254.3	37.0	3.71
9:54	31.8	37.0	34.3	41.1	37.6	34.9	24.2	686.5	75.24	1.80	259.3	37.8	3.73
9:55	31.9	37.3	34.7	41.2	37.8	35.2	24.8	687.5	75.47	1.78	251.3	36.6	3.70
9:56	32.0	37.2	34.4	41.3	37.7	35.2	25.1	688.8	75.22	1.79	243.6	35.4	3.71
9:57	32.3	38.1	34.7	41.6	38.1	35.6	25.2	687.7	74.91	1.79	252.0	36.6	3.71
9:58	32.5	38.5	35.5	42.7	38.9	36.0	25.7	686.8	75.51	1.78	250.1	36.4	3.70
9:59	32.6	38.9	35.1	42.5	38.7	36.2	25.7	685.0	75.98	1.77	256.2	37.4	3.68
10:00	32.7	38.8	35.1	41.6	38.4	36.2	25.5	683.8	75.73	1.78	260.4	38.1	3.71
10:01	32.7	38.6	35.3	42.3	38.8	36.2	25.7	683.8	75.85	1.78	256.1	37.5	3.71
10:02	32.8	38.8	35.5	42.7	38.8	36.3	26.3	684.8	76.09	1.77	245.8	35.9	3.69
10:03	32.9	38.3	35.0	41.8	38.4	36.0	26.3	684.5	76.18	1.77	239.5	35.0	3.68
10:04	32.9	38.3	34.8	41.3	38.1	35.9	25.7	680.9	76.10	1.78	250.4	36.8	3.74
10:05	32.9	38.3	35.0	41.4	38.2	36.0	26.0	679.8	75.32	1.78	242.0	35.6	3.75
10:06	32.9	38.2	34.9	41.7	38.1	35.9	26.2	677.5	75.99	1.78	237.7	35.1	3.75
10:07	33.0	38.3	34.8	41.5	37.9	35.9	25.9	674.3	76.11	1.78	244.1	36.2	3.76
10:08	33.0	37.9	35.1	41.2	37.9	35.8	26.1	672.6	76.47	1.80	237.9	35.4	3.82
10:09	33.0	38.1	35.0	41.4	38.0	35.9	26.6	673.2	75.51	1.78	226.9	33.7	3.78
10:10	33.1	38.5	35.4	42.1	38.6	36.2	27.0	671.3	75.12	1.77	222.2	33.1	3.76
10:11	33.2	38.7	35.6	42.1	38.6	36.4	27.2	669.7	75.59	1.76	224.8	33.6	3.75
10:12	33.2	38.3	35.5	42.0	38.4	36.2	27.2	670.7	76.27	1.77	220.6	32.9	3.77
10:13	33.2	38.1	35.5	42.0	38.4	36.0	26.9	670.7	76.34	1.79	224.7	33.5	3.81
10:14	33.3	38.2	35.6	42.1	38.4	36.1	26.9	668.6	75.99	1.78	225.2	33.7	3.79
10:15	33.2	37.5	35.0	41.3	37.8	35.7	27.0	667.7	76.64	1.78	214.6	32.1	3.80
10:16	33.2	37.5	34.9	41.1	37.7	35.6	26.9	665.9	75.76	1.78	213.4	32.1	3.80
10:17	33.2	37.4	35.0	41.1	37.8	35.6	26.8	666.8	75.75	1.78	214.4	32.2	3.81
10:18	33.2	37.5	35.1	41.2	37.8	35.7	27.0	668.4	76.07	1.77	214.7	32.1	3.77
10:19	33.3	37.8	35.4	41.6	38.2	35.8	26.9	666.1	75.79	1.77	219.4	32.9	3.79
10:20	33.3	37.6	34.9	41.3	37.7	35.7	26.9	661.9	76.28	1.76	217.3	32.8	3.79
10:21	33.3	37.9	35.2	41.5	38.0	35.9	27.2	660.4	75.23	1.76	211.3	32.0	3.80
10:22	33.3	37.6	35.1	41.2	37.6	35.7	27.1	657.8	75.67	1.77	209.8	31.9	3.83
10:23	33.2	37.0	34.5	40.7	37.2	35.3	26.9	656.4	76.92	1.78	207.6	31.6	3.86
10:24	33.1	36.5	34.1	39.9	36.7	35.0	26.6	654.2	76.32	1.80	205.4	31.4	3.92
10:25	33.1	36.9	34.3	40.5	37.2	35.1	26.7	651.6	75.58	1.76	205.9	31.6	3.85
10:26	33.2	37.3	34.5	40.6	37.3	35.3	26.6	648.6	76.04	1.76	215.0	33.2	3.88
10:27	33.2	36.8	33.9	39.8	36.8	35.0	26.0	645.5	75.95	1.78	223.1	34.6	3.93
10:28	33.2	37.3	34.5	40.5	37.3	35.4	26.2	644.6	74.92	1.76	222.1	34.5	3.89
10:29	33.3	37.5	35.0	41.1	37.8	35.6	26.7	645.0	75.56	1.76	215.9	33.5	3.90

Time [h]	T <sub>wall</sub> [°C]	T <sub>col,1</sub> [°C]	T <sub>col,2</sub> [°C]	T <sub>col,3</sub> [°C]	T <sub>col,4</sub> [°C]	T <sub>out</sub> [°C]	T <sub>amb</sub> [°C]	G <sub>T,col</sub> [W/m <sup>2</sup> ]	Flow Rate [m <sup>3</sup> /h·m <sup>2</sup> ]	P <sub>el</sub> [W]	Q <sup>u</sup> [W/m <sup>2</sup> ]	Eff <sub>th</sub> %	Eff <sub>pv</sub> %
10:30	33.3	37.3	34.9	40.8	37.5	35.5	26.8	643.8	75.74	1.77	212.6	33.0	3.92
10:31	33.2	36.6	34.5	39.9	37.0	35.1	26.8	643.9	75.12	1.78	202.4	31.4	3.93
10:32	33.2	36.8	34.6	40.1	37.2	35.2	26.9	644.5	75.55	1.76	204.4	31.7	3.89
10:33	33.1	37.0	34.7	40.5	37.5	35.3	27.1	643.1	74.99	1.75	197.4	30.7	3.88
10:34	33.1	37.8	35.3	41.5	38.1	35.7	27.5	639.9	74.74	1.75	197.0	30.8	3.90
10:35	33.1	37.5	35.1	41.3	37.7	35.6	27.3	635.7	75.27	1.74	202.3	31.8	3.90
10:36	33.1	37.2	34.8	40.7	37.3	35.4	27.2	634.0	75.66	1.77	201.7	31.8	3.98
10:37	33.1	36.9	34.5	40.2	37.1	35.2	27.3	633.6	75.43	1.75	193.5	30.5	3.95
10:38	33.1	37.0	34.5	40.4	37.2	35.3	27.4	632.3	75.24	1.76	191.7	30.3	3.97
10:39	33.1	36.9	34.1	40.1	36.8	35.2	27.1	628.5	75.52	1.76	197.9	31.5	3.99
10:40	33.2	37.4	34.6	41.2	37.7	35.4	27.4	623.2	74.53	1.71	191.5	30.7	3.92
10:41	33.3	38.0	35.3	41.8	38.1	35.8	28.0	621.9	74.32	1.72	186.6	30.0	3.94
10:42	33.4	38.2	35.4	41.9	38.2	36.1	28.2	619.9	74.25	1.73	187.7	30.3	3.98
10:43	33.4	37.7	35.0	41.1	37.5	35.9	28.1	617.3	75.55	1.74	190.6	30.9	4.02
10:44	33.4	37.2	34.9	40.7	37.4	35.6	27.5	615.6	75.63	1.75	198.0	32.2	4.06
10:45	33.3	36.8	34.2	40.1	36.8	35.3	27.2	614.3	75.86	1.75	196.2	31.9	4.05
10:46	33.2	36.5	33.8	39.6	36.4	35.0	27.3	613.3	75.90	1.74	190.0	31.0	4.06
10:47	33.2	36.9	34.1	39.7	36.5	35.1	27.1	610.0	74.67	1.72	192.6	31.6	4.02
10:48	33.2	36.6	34.1	39.6	36.5	35.0	27.4	605.8	75.41	1.70	185.3	30.6	4.00
10:49	33.2	36.6	34.0	39.6	36.5	35.0	27.5	603.2	75.09	1.74	182.4	30.2	4.12
10:50	33.2	36.4	34.0	39.4	36.4	34.9	27.7	602.6	74.60	1.76	174.1	28.9	4.16
10:51	33.2	36.7	34.4	40.1	37.1	35.1	27.8	600.9	74.77	1.74	176.8	29.4	4.12
10:52	33.3	37.1	34.7	40.5	37.2	35.3	28.0	598.1	74.84	1.72	176.9	29.6	4.10
10:53	33.4	37.3	35.0	41.0	37.6	35.6	28.2	595.9	74.93	1.71	178.6	30.0	4.09
10:54	33.4	37.4	34.6	41.2	37.6	35.5	28.4	592.7	75.52	1.70	172.5	29.1	4.09
10:55	33.4	37.5	34.4	40.8	37.1	35.6	28.2	589.5	75.28	1.71	178.8	30.3	4.13
10:56	33.4	37.6	34.3	40.7	37.3	35.6	28.2	586.0	75.24	1.70	180.2	30.8	4.13
10:57	33.6	38.2	34.8	41.1	37.6	36.0	28.5	583.9	74.30	1.70	180.6	30.9	4.15
10:58	33.6	37.9	34.6	40.8	37.2	35.9	28.6	582.2	76.41	1.70	181.1	31.1	4.16
10:59	33.6	37.4	34.3	40.4	36.8	35.6	28.8	580.5	76.93	1.69	168.5	29.0	4.16
11:00	33.4	36.8	33.9	40.2	36.6	35.2	28.5	577.0	77.44	1.71	167.0	28.9	4.22
11:01	33.5	36.7	34.0	39.9	36.4	35.1	28.3	573.2	76.04	1.71	167.4	29.2	4.25
11:02	33.4	36.2	34.0	39.4	36.2	34.8	27.9	569.8	76.75	1.71	172.4	30.3	4.27
11:03	33.3	35.7	33.6	38.8	35.9	34.5	27.5	566.4	76.96	1.71	173.3	30.6	4.31
11:04	33.3	35.7	33.1	38.4	35.5	34.4	27.1	563.5	76.47	1.72	180.6	32.1	4.35
11:05	33.2	35.6	33.0	38.2	35.6	34.2	26.7	560.6	76.25	1.71	185.4	33.1	4.36
11:06	33.2	36.1	33.9	39.3	36.3	34.6	27.6	557.5	75.37	1.70	170.7	30.6	4.35
11:07	33.3	36.7	34.1	40.2	36.8	35.0	28.0	555.9	75.61	1.67	170.1	30.6	4.29
11:08	33.3	36.7	34.1	39.9	36.4	35.0	28.3	553.3	75.92	1.69	164.3	29.7	4.37
11:09	33.3	35.9	33.6	38.9	35.8	34.6	28.1	550.2	76.81	1.69	162.0	29.5	4.39
11:10	33.2	36.2	33.6	39.5	36.2	34.7	28.1	547.7	76.80	1.68	162.8	29.7	4.38
11:11	33.2	36.3	33.3	39.0	35.6	34.7	27.9	545.4	75.47	1.68	164.9	30.2	4.40
11:12	33.2	36.0	33.0	38.7	35.3	34.5	27.9	543.2	75.46	1.68	162.0	29.8	4.40
11:13	33.2	36.4	33.5	39.2	35.8	34.6	28.0	541.7	75.39	1.67	162.8	30.0	4.41
11:14	33.2	36.2	33.5	39.4	36.0	34.7	28.1	539.3	75.83	1.67	160.9	29.8	4.42
11:15	33.2	36.7	33.8	39.9	36.4	35.0	28.3	535.6	75.30	1.66	162.6	30.4	4.41
11:16	33.3	36.6	34.2	40.1	36.7	35.0	29.0	531.7	75.79	1.64	146.5	27.6	4.41
11:17	33.2	36.2	33.9	39.7	36.3	34.8	28.7	525.6	76.07	1.65	149.6	28.5	4.47
11:18	33.2	36.0	33.8	39.3	35.9	34.6	28.6	523.5	76.22	1.66	148.8	28.4	4.53
11:19	33.2	35.5	33.3	38.6	35.5	34.3	28.3	516.7	76.70	1.66	149.2	28.9	4.57
11:20	33.1	35.2	33.0	38.4	35.3	34.0	28.0	513.8	76.01	1.66	148.1	28.8	4.62
11:21	33.1	35.3	33.2	38.2	35.3	34.1	28.0	510.7	75.73	1.66	149.3	29.2	4.65
11:22	33.0	35.3	33.1	38.2	35.3	34.1	28.4	508.2	75.56	1.65	139.9	27.5	4.63
11:23	33.0	35.3	33.0	37.9	35.0	34.1	28.6	506.7	76.58	1.65	134.7	26.6	4.63
11:24	32.9	35.2	33.0	38.1	35.1	34.0	28.7	504.4	75.90	1.63	129.3	25.6	4.61
11:25	33.0	35.4	33.3	38.6	35.5	34.1	28.4	501.4	76.10	1.63	141.7	28.3	4.65
11:26	33.0	35.5	33.2	38.7	35.5	34.2	28.5	497.9	75.75	1.63	138.7	27.9	4.67
11:27	33.0	35.3	33.1	38.4	35.3	34.0	28.2	495.9	75.90	1.65	144.7	29.2	4.74
11:28	32.9	35.2	33.0	38.0	35.1	33.9	28.5	493.2	76.43	1.64	135.3	27.4	4.73
11:29	32.9	34.9	32.7	37.4	34.6	33.7	28.4	489.7	76.42	1.64	131.7	26.9	4.77
11:30	32.9	35.0	32.8	37.9	35.1	33.8	28.3	488.2	76.37	1.63	137.1	28.1	4.75
11:31	32.9	35.3	32.5	37.8	34.8	33.8	27.9	485.9	76.42	1.63	146.2	30.1	4.79
11:32	32.8	34.9	32.1	37.1	34.4	33.6	27.5	482.4	76.50	1.63	150.9	31.3	4.83
11:33	32.8	34.8	32.3	37.2	34.6	33.5	27.4	479.7	75.91	1.63	152.3	31.7	4.84
11:34	32.7	34.7	32.5	37.4	34.7	33.5	27.8	478.8	76.29	1.62	141.1	29.5	4.82
11:35	32.6	34.3	32.3	37.0	34.2	33.3	28.0	477.2	76.05	1.63	130.8	27.4	4.87
11:36	32.6	34.2	32.3	37.1	34.3	33.2	27.9	475.8	75.95	1.62	129.1	27.1	4.85
11:37	32.6	34.4	32.3	37.0	34.2	33.2	28.1	472.7	76.08	1.61	127.2	26.9	4.86
11:38	32.5	33.7	31.8	36.5	33.8	32.9	28.0	467.1	76.32	1.61	121.0	25.9	4.92
11:39	32.5	34.1	31.8	36.8	34.1	33.0	28.1	462.2	75.92	1.60	119.2	25.8	4.95
11:40	32.5	34.1	32.1	36.9	34.0	33.0	28.2	461.2	76.29	1.61	119.0	25.8	4.98

Time [h]	T <sub>wall</sub> [°C]	T <sub>col,1</sub> [°C]	T <sub>col,2</sub> [°C]	T <sub>col,3</sub> [°C]	T <sub>col,4</sub> [°C]	T <sub>out</sub> [°C]	T <sub>amb</sub> [°C]	G <sub>T,col</sub> [W/m <sup>2</sup> ]	Flow Rate [m <sup>3</sup> /h·m <sup>2</sup> ]	P <sub>el</sub> [W]	Q <sup>u</sup> [W/m <sup>2</sup> ]	Eff <sub>th</sub> %	Eff <sub>pv</sub> %
11:41	32.4	34.0	31.8	36.8	34.0	32.9	28.1	461.1	76.37	1.61	121.6	26.4	4.97
11:42	32.4	34.2	32.0	37.0	34.2	33.1	28.6	458.7	75.84	1.59	111.0	24.2	4.95
11:43	32.4	34.4	32.0	37.1	34.1	33.2	28.7	456.3	77.14	1.59	112.2	24.6	4.98
11:44	32.3	34.3	32.0	36.8	34.0	33.1	28.8	452.6	75.47	1.59	107.1	23.7	5.01
11:45	32.4	34.2	32.1	36.9	34.1	33.1	28.7	450.5	75.91	1.59	109.0	24.2	5.03
11:46	32.3	34.1	31.8	36.5	33.7	33.0	28.8	449.2	75.76	1.59	102.0	22.7	5.05
11:47	32.4	34.2	32.1	36.8	34.0	33.1	29.2	448.0	76.16	1.57	97.2	21.7	4.99
11:48	32.4	34.6	32.5	37.3	34.4	33.3	29.4	447.0	76.01	1.57	95.0	21.3	4.99
11:49	32.4	34.3	32.3	37.2	34.3	33.2	29.3	443.2	75.79	1.56	95.9	21.6	5.02
11:50	32.3	33.9	31.8	36.7	33.7	32.9	28.9	440.3	76.11	1.56	99.9	22.7	5.06
11:51	32.3	34.0	31.8	36.4	33.6	32.9	28.7	436.5	76.29	1.56	103.9	23.8	5.10
11:52	32.2	33.8	31.6	36.0	33.4	32.8	28.6	433.9	76.42	1.56	103.2	23.8	5.12
11:53	32.2	33.7	31.6	36.0	33.4	32.7	29.0	431.0	76.07	1.54	92.2	21.4	5.08
11:54	32.2	33.9	31.6	36.3	33.6	32.8	29.1	428.2	76.27	1.52	91.5	21.4	5.08
11:55	32.2	33.9	31.6	36.3	33.5	32.8	29.1	424.8	75.76	1.52	90.1	21.2	5.12
11:56	32.1	33.9	31.9	36.3	33.6	32.8	29.2	422.7	75.42	1.51	87.6	20.7	5.11
11:57	32.2	34.1	31.8	36.6	33.8	32.9	29.2	420.9	75.88	1.52	92.1	21.9	5.16
11:58	32.1	34.2	31.7	36.6	33.8	32.9	29.0	419.9	76.19	1.54	96.0	22.9	5.22
11:59	32.1	34.1	31.7	36.5	33.6	32.8	29.2	422.3	75.84	1.54	90.3	21.4	5.19
12:00	32.0	33.5	31.0	35.5	32.8	32.4	28.4	420.4	77.08	1.50	101.6	24.2	5.09
12:01	32.0	33.2	31.0	35.3	32.8	32.2	28.2	406.8	75.92	1.50	98.3	24.2	5.25
12:02	32.0	33.5	31.4	35.8	33.1	32.4	28.8	412.7	75.17	1.53	89.6	21.7	5.28
12:03	32.0	33.7	31.9	36.4	33.7	32.7	29.2	410.0	75.35	1.49	84.7	20.7	5.20
12:04	32.0	33.7	31.5	36.3	33.7	32.6	29.2	423.8	75.93	1.48	86.3	20.4	4.98
12:05	32.0	34.1	31.6	36.7	33.7	32.9	29.3	398.0	75.86	1.42	87.1	21.9	5.10
12:06	32.0	34.0	31.7	36.4	33.6	32.8	29.3	404.1	75.27	1.46	85.5	21.2	5.15
12:07	32.0	33.6	31.5	35.9	33.0	32.6	29.2	368.0	76.26	1.52	85.3	23.2	5.89
12:08	31.8	32.7	30.9	35.1	32.4	32.0	28.8	382.9	76.11	1.43	80.6	21.0	5.32
12:09	31.7	32.4	30.6	34.6	32.0	31.8	28.6	363.4	76.78	1.44	79.9	22.0	5.66
12:10	31.7	32.5	30.5	34.5	32.0	31.8	28.6	357.4	75.86	1.41	79.7	22.3	5.61
12:11	31.6	31.9	29.8	33.7	31.4	31.3	28.0	355.2	76.52	1.40	82.2	23.1	5.61
12:12	31.5	32.3	30.6	34.6	32.2	31.5	28.2	369.6	75.30	1.44	83.1	22.5	5.55
12:13	31.5	32.4	30.3	34.5	32.1	31.5	27.8	368.1	75.53	1.43	90.8	24.7	5.55
12:14	31.5	32.5	30.7	34.9	32.3	31.7	28.1	360.5	74.95	1.41	86.5	24.0	5.60
12:15	31.4	32.0	30.1	33.7	31.2	31.3	28.2	318.2	76.47	1.35	78.7	24.7	6.06
12:16	31.2	31.5	29.8	33.4	31.1	31.0	28.3	343.9	76.43	1.42	66.9	19.5	5.87
12:17	31.2	31.9	30.1	34.4	31.9	31.2	29.1	352.5	75.65	1.38	51.7	14.7	5.60
12:18	31.3	32.5	30.4	34.8	32.2	31.5	29.2	348.4	75.28	1.38	57.4	16.5	5.64
12:19	31.3	32.5	30.6	34.9	32.2	31.6	29.4	344.8	75.68	1.38	56.1	16.3	5.70
12:20	31.3	32.5	30.5	35.0	32.3	31.6	29.2	341.5	75.45	1.36	59.1	17.3	5.69
12:21	31.2	31.9	29.8	34.2	31.5	31.2	28.8	337.7	76.69	1.36	60.9	18.0	5.75
12:22	31.0	31.5	29.7	33.7	31.2	30.9	28.4	333.8	76.14	1.36	62.0	18.6	5.82
12:23	31.1	31.7	30.1	34.0	31.7	31.1	28.5	331.1	75.43	1.34	62.0	18.7	5.77
12:24	31.0	31.7	29.6	33.4	30.9	30.9	28.4	325.9	75.98	1.33	62.9	19.3	5.84
12:25	31.0	31.6	29.8	33.6	31.2	30.8	28.4	322.9	75.87	1.32	61.5	19.0	5.82
12:26	31.0	31.8	30.0	34.0	31.6	31.0	28.8	320.2	75.15	1.30	54.7	17.1	5.77
12:27	31.0	31.9	30.1	34.0	31.6	31.2	29.1	317.5	75.39	1.29	49.8	15.7	5.79
12:28	30.9	31.5	29.6	33.2	30.9	30.8	28.8	313.4	76.35	1.29	49.7	15.9	5.89
12:29	30.8	31.2	29.6	32.9	30.8	30.6	29.0	311.3	76.17	1.28	41.5	13.3	5.87
12:30	30.8	31.0	29.5	33.1	30.9	30.5	28.8	309.7	76.64	1.28	42.7	13.8	5.89
12:31	30.7	30.9	29.4	32.9	30.7	30.5	28.6	306.0	75.75	1.27	47.8	15.6	5.92
12:32	30.7	31.0	29.5	32.9	30.8	30.5	28.7	301.9	76.07	1.24	45.2	15.0	5.88
12:33	30.6	31.0	29.4	32.7	30.6	30.5	28.9	297.2	75.63	1.23	38.9	13.1	59.42
12:34	30.6	30.9	29.2	32.7	30.5	30.4	28.9	293.5	75.80	1.22	36.7	12.5	5.95
12:35	30.4	30.6	28.9	32.4	30.3	30.1	28.7	289.0	76.09	1.21	36.0	12.5	5.98
12:36	30.4	30.6	28.7	32.3	30.1	30.0	28.5	284.8	75.83	1.20	39.3	13.8	6.01
12:37	30.4	30.5	28.7	32.2	30.0	29.9	28.3	280.7	75.91	1.18	40.3	14.4	6.01
12:38	30.3	30.2	28.4	31.9	29.7	29.7	28.4	277.0	75.85	1.18	32.2	11.6	6.08
12:39	30.2	30.4	28.6	32.1	30.0	29.8	28.5	273.5	75.32	1.16	32.3	11.8	6.06
12:40	30.2	30.3	28.6	32.0	29.8	29.8	29.0	269.5	75.75	1.15	19.5	7.2	6.09
12:41	30.1	30.2	28.4	32.1	29.7	29.7	29.2	266.6	75.83	1.14	12.1	4.6	6.09
12:42	30.1	30.3	28.4	32.3	29.7	29.8	29.1	263.3	75.87	1.13	16.9	6.4	6.11
12:43	30.1	30.2	28.4	31.8	29.5	29.7	28.6	260.3	75.83	1.12	26.1	10.0	6.15
12:44	30.0	30.2	28.5	31.8	29.7	29.6	29.2	258.0	76.25	1.11	10.1	3.9	6.14
12:45	30.0	30.0	28.3	31.9	29.6	29.5	29.5	254.7	75.59	1.09	1.9	0.8	6.13
12:46	29.9	29.9	28.2	31.7	29.4	29.5	29.3	251.4	76.37	1.09	4.5	1.8	6.17
12:47	29.8	29.7	28.1	31.3	29.1	29.3	28.9	248.6	76.18	1.08	10.1	4.1	6.22
12:48	29.7	29.5	28.1	31.2	29.3	29.2	28.6	246.7	75.82	1.08	14.8	6.0	6.23
12:49	29.7	29.8	28.3	31.4	29.5	29.4	28.9	243.8	76.23	1.07	12.4	5.1	6.28
12:50	29.8	29.8	28.4	31.4	29.5	29.4	29.1	240.0	75.97	1.06	8.4	3.5	6.30
12:51	29.8	29.8	28.4	31.4	29.5	29.4	29.0	236.4	75.89	1.05	10.6	4.5	6.36

Time [h]	T <sub>wall</sub> [°C]	T <sub>col,1</sub> [°C]	T <sub>col,2</sub> [°C]	T <sub>col,3</sub> [°C]	T <sub>col,4</sub> [°C]	T <sub>out</sub> [°C]	T <sub>amb</sub> [°C]	G <sub>T,col</sub> [W/m <sup>2</sup> ]	Flow Rate [m <sup>3</sup> /h m <sup>2</sup> ]	P <sub>el</sub> [W]	Q <sub>u</sub> [W/m <sup>2</sup> ]	Eff <sub>th</sub> %	Eff <sub>PV</sub> %
12:52	29.7	30.0	28.5	31.5	29.6	29.5	29.3	232.0	75.77	1.02	4.3	1.8	6.30
12:53	29.7	29.7	28.2	31.1	29.1	29.3	29.4	226.6	76.05	1.01	-2.3	-1.0	6.36
12:54	29.6	29.2	27.5	30.5	28.5	28.9	28.8	222.7	76.99	1.00	1.4	0.6	6.42
12:55	29.4	28.8	27.0	30.2	28.0	28.5	28.2	220.3	76.59	1.00	6.8	3.1	6.45
12:56	29.4	28.9	27.3	30.4	28.3	28.6	28.2	218.4	76.31	1.00	10.0	4.6	6.54
12:57	29.4	28.8	27.1	30.1	28.0	28.5	27.9	215.4	75.79	0.99	13.1	6.1	6.58
12:58	29.3	29.1	27.7	30.6	28.7	28.7	28.5	213.8	74.68	0.98	4.7	2.2	6.52

Table E.6: Experimental data for September 6

Time [h]	T <sub>wall</sub> [°C]	T <sub>col,1</sub> [°C]	T <sub>col,2</sub> [°C]	T <sub>col,3</sub> [°C]	T <sub>col,4</sub> [°C]	T <sub>amb</sub> [°C]	G <sub>T,col</sub> [W/m <sup>2</sup> ]	P <sub>el</sub> [W]	Eff <sub>PV</sub> %
7:34	15.5	23.1	24.1	23.3	26.4	15.4	242.3	1.19	6.99
7:35	15.8	23.6	24.7	23.9	27.1	15.4	250.4	1.23	7.00
7:36	16.0	24.0	25.1	24.4	27.6	15.7	256.8	1.25	6.93
7:37	16.3	24.5	25.7	24.9	28.1	15.8	263.4	1.26	6.80
7:38	16.5	24.9	26.0	25.3	28.5	15.9	269.5	1.28	6.77
7:39	16.7	25.3	26.4	25.5	28.9	15.9	276.5	1.29	6.66
7:40	17.0	25.8	27.0	26.1	29.5	15.9	283.3	1.30	6.54
7:41	17.2	26.4	27.6	26.5	30.1	15.8	288.1	1.31	6.51
7:42	17.4	26.9	27.9	27.1	30.8	15.8	294.7	1.33	6.44
7:43	17.7	27.3	28.5	27.6	31.3	15.8	301.9	1.35	6.38
7:44	17.9	27.8	28.9	27.9	31.7	16.0	308.6	1.36	6.27
7:45	18.2	28.2	29.5	28.5	32.3	16.1	315.2	1.37	6.18
7:46	18.5	28.7	30.0	29.0	32.9	16.3	322.4	1.38	6.10
7:47	18.8	29.1	30.5	29.5	33.3	16.3	328.8	1.39	6.04
7:48	19.1	29.5	30.7	29.7	33.3	16.3	334.5	1.41	6.00
7:49	19.3	29.8	31.2	30.0	34.0	16.4	339.8	1.44	6.02
7:50	19.7	30.4	31.7	30.7	34.6	16.7	344.7	1.43	5.91
7:51	19.8	30.8	32.1	30.8	34.9	16.8	350.4	1.44	5.85
7:52	20.1	31.1	32.4	31.2	35.2	16.7	357.3	1.46	5.82
7:53	20.3	31.3	32.7	31.4	35.4	16.9	364.1	1.47	5.74
7:54	20.7	31.9	33.2	32.0	36.0	17.0	371.8	1.47	5.66
7:55	20.9	32.3	33.5	32.4	36.4	17.0	377.3	1.47	5.57
7:56	21.1	32.6	34.1	32.7	36.9	17.2	383.9	1.49	5.53
7:57	21.4	33.0	34.4	33.3	37.4	17.4	388.4	1.48	5.44
7:58	21.7	33.5	34.8	34.0	37.9	17.5	394.3	1.49	5.38
7:59	22.0	34.0	35.5	34.3	38.2	17.6	401.5	1.50	5.35
8:00	22.2	34.4	35.8	34.5	38.6	17.9	403.8	1.51	5.33
8:01	22.5	34.6	36.0	34.7	38.9	18.2	407.6	1.50	5.23
8:02	22.8	34.9	36.5	35.1	39.1	18.3	411.8	1.52	5.26
8:03	23.1	35.1	36.5	35.3	39.3	18.6	417.0	1.51	5.18
8:04	23.3	35.3	36.8	35.5	39.5	18.8	421.1	1.51	5.12
8:05	23.5	35.6	37.0	35.9	39.8	18.8	424.7	1.53	5.14
8:06	23.8	35.8	37.5	36.2	40.0	19.1	428.5	1.53	5.10
8:07	24.0	36.0	37.5	36.2	40.1	19.3	431.7	1.54	5.10
8:08	24.2	36.1	37.8	36.4	40.4	19.3	436.4	1.52	4.98
8:09	24.5	36.5	37.9	36.6	40.7	19.3	440.5	1.54	4.99
8:10	24.7	36.8	38.2	36.7	40.9	19.6	445.2	1.54	4.93
8:11	25.0	37.1	38.5	37.2	41.4	19.7	449.8	1.54	4.88
8:12	25.2	37.3	38.9	37.4	41.4	20.0	453.8	1.54	4.85
8:13	25.4	37.6	39.2	37.9	41.9	20.1	459.3	1.54	4.79
8:14	25.7	38.0	39.7	38.5	42.5	20.4	464.2	1.54	4.74
8:15	25.9	38.3	40.0	38.7	42.9	20.3	468.1	1.54	4.68
8:16	26.2	38.7	40.3	38.9	43.2	20.3	472.2	1.55	4.67
8:17	26.4	39.1	40.5	39.4	43.4	20.6	476.6	1.55	4.63

Time [h]	T <sub>wall</sub> [°C]	T <sub>col,1</sub> [°C]	T <sub>col,2</sub> [°C]	T <sub>col,3</sub> [°C]	T <sub>col,4</sub> [°C]	T <sub>amb</sub> [°C]	G <sub>T,col</sub> [W/m <sup>2</sup> ]	P <sub>el</sub> [W]	Eff <sub>PV</sub> %
8:18	26.7	39.1	40.8	39.3	43.4	20.8	481.9	1.55	4.60
8:19	26.9	39.4	41.0	39.5	43.8	21.1	485.7	1.55	4.55
8:20	27.1	39.9	41.5	40.2	44.4	21.3	490.1	1.54	4.48
8:21	27.5	40.4	42.1	40.8	44.9	21.2	491.8	1.52	4.41
8:22	27.8	40.9	42.7	41.1	45.5	21.3	494.2	1.53	4.41
8:23	28.1	41.4	42.9	41.5	45.9	21.4	495.7	1.53	4.40
8:24	28.4	41.6	43.2	41.6	45.7	21.3	498.5	1.53	4.38
8:25	28.6	41.8	43.4	41.7	45.9	21.3	504.2	1.53	4.33
8:26	28.8	42.0	43.7	42.0	46.3	21.4	508.4	1.53	4.30
8:27	29.1	42.3	43.9	42.7	46.8	21.5	511.0	1.52	4.23
8:28	29.4	42.7	44.2	42.9	46.8	21.8	514.5	1.53	4.23
8:29	29.6	42.7	44.4	42.9	47.1	22.1	516.2	1.53	4.22
8:30	29.9	43.0	44.7	43.3	47.4	22.0	520.5	1.54	4.22
8:31	30.1	43.1	44.7	43.0	47.1	21.8	521.9	1.53	4.18
8:32	30.3	43.4	44.8	43.2	47.1	21.8	523.8	1.53	4.16
8:33	30.6	43.3	44.9	43.4	47.2	21.8	526.1	1.53	4.15
8:34	30.8	43.8	45.4	43.6	47.7	22.1	528.6	1.52	4.11
8:35	31.0	44.1	45.7	44.1	48.1	22.4	530.8	1.51	4.07
8:36	31.3	44.5	46.1	44.5	48.4	22.5	535.8	1.52	4.04
8:37	31.6	44.8	46.4	44.7	48.8	22.7	538.7	1.51	4.00
8:38	31.8	45.1	46.7	45.1	49.3	23.0	541.2	1.50	3.95
8:39	32.1	45.7	47.3	45.5	49.7	23.1	542.3	1.50	3.93
8:40	32.3	46.0	47.7	45.9	50.2	23.5	545.9	1.49	3.90
8:41	32.6	46.1	47.5	45.8	49.9	23.9	548.7	1.52	3.96
8:42	32.7	45.5	47.1	45.2	49.1	24.2	552.8	1.53	3.96
8:43	32.9	45.7	47.4	45.6	49.6	24.6	556.0	1.52	3.89
8:44	33.1	46.1	47.6	45.9	49.7	24.9	558.9	1.56	3.97
8:45	33.2	45.5	46.8	45.4	48.9	24.3	558.7	1.55	3.96
8:46	33.4	45.5	46.8	45.4	49.1	24.7	560.5	1.54	3.93
8:47	33.5	45.5	46.9	45.3	49.1	24.8	561.3	1.53	3.88
8:48	33.7	46.4	47.9	46.1	50.2	25.3	565.1	1.51	3.80
8:49	34.0	46.7	48.3	46.5	50.3	25.4	568.6	1.52	3.82
8:50	34.2	46.9	48.6	46.4	50.4	25.2	567.9	1.51	3.79
8:51	34.4	47.0	48.7	46.7	50.6	25.5	568.9	1.52	3.81
8:52	34.5	47.0	48.7	46.9	50.7	25.5	572.1	1.52	3.79
8:53	34.6	46.5	47.9	46.3	49.4	24.8	572.2	1.55	3.86
8:54	34.7	46.4	47.7	46.0	49.4	25.1	572.3	1.55	3.87
8:55	34.9	46.1	47.7	46.3	49.4	25.3	575.4	1.54	3.81
8:56	35.0	47.0	48.4	46.9	50.6	25.8	579.0	1.53	3.78
8:57	35.2	47.1	48.6	47.0	50.5	26.2	580.8	1.54	3.78
8:58	35.4	47.4	49.0	47.4	51.3	26.0	581.4	1.51	3.70
8:59	35.6	47.8	49.4	47.7	51.5	25.9	582.2	1.51	3.70
9:00	35.8	48.3	49.9	48.0	51.9	26.3	584.8	1.52	3.70
9:01	36.0	48.3	49.7	47.9	51.4	26.7	587.1	1.51	3.67
9:02	36.1	47.8	49.3	47.5	50.6	26.4	588.1	1.60	3.89
9:03	36.1	46.4	47.4	46.1	48.9	25.3	589.4	1.59	3.85
9:04	36.2	46.8	48.3	46.9	50.7	25.8	592.9	1.53	3.69
9:05	36.5	48.1	49.8	48.3	52.2	26.4	595.2	1.49	3.58
9:06	36.8	48.9	50.5	49.0	52.5	26.6	595.5	1.51	3.61
9:07	37.0	49.0	50.6	49.0	52.6	26.9	596.8	1.52	3.62
9:08	37.1	48.8	50.2	48.6	51.9	27.1	596.5	1.52	3.62
9:09	37.2	48.8	50.5	48.5	51.8	27.2	598.2	1.52	3.63
9:10	37.4	49.2	50.7	48.8	52.2	27.5	600.9	1.54	3.65
9:11	37.5	48.9	50.4	48.8	51.9	27.5	601.8	1.55	3.67
9:12	37.7	49.4	50.9	49.1	52.5	27.3	604.3	1.54	3.63
9:13	37.9	49.2	50.8	49.0	52.1	27.4	606.3	1.52	3.58
9:14	38.1	49.9	51.5	49.6	53.3	27.7	608.0	1.51	3.55
9:15	38.2	49.8	51.5	49.7	53.2	27.8	609.7	1.51	3.54
9:16	38.4	49.8	51.3	49.8	53.2	27.7	610.9	1.52	3.54
9:17	38.5	49.9	51.6	49.9	53.3	27.6	611.3	1.52	3.54

Time [h]	T <sub>wall</sub> [°C]	T <sub>col,1</sub> [°C]	T <sub>col,2</sub> [°C]	T <sub>col,3</sub> [°C]	T <sub>col,4</sub> [°C]	T <sub>amb</sub> [°C]	G <sub>T,col</sub> [W/m <sup>2</sup> ]	P <sub>el</sub> [W]	Eff <sub>PV</sub> %
9:18	38.7	50.2	51.8	50.1	53.6	27.6	613.9	1.52	3.54
9:19	38.9	50.5	51.8	50.7	53.6	27.7	613.1	1.50	3.49
9:20	38.9	49.3	50.6	49.4	52.2	28.0	613.0	1.53	3.57
9:21	38.9	48.6	49.9	48.8	51.5	28.3	613.7	1.54	3.59
9:22	38.9	48.9	50.2	49.1	51.7	28.5	614.9	1.56	3.61
9:23	39.0	49.2	50.5	49.2	52.0	28.3	615.4	1.54	3.58
9:24	39.1	49.3	50.7	49.4	52.5	28.2	616.8	1.52	3.52
9:25	39.3	50.1	51.7	49.9	53.2	28.5	618.5	1.52	3.51
9:26	39.5	50.4	51.8	50.6	53.6	28.8	619.1	1.53	3.53
9:27	39.6	50.4	51.8	50.6	53.6	28.8	618.4	1.52	3.50
9:28	39.8	50.8	52.4	50.7	53.5	28.6	619.4	1.49	3.44
9:29	40.0	51.5	53.0	51.5	54.3	28.6	617.7	1.49	3.43
9:30	40.3	52.1	53.8	51.9	55.2	28.9	619.7	1.46	3.37
9:31	40.5	52.4	54.3	52.2	55.7	29.1	619.3	1.46	3.37
9:32	40.7	52.2	54.1	52.3	55.3	28.8	620.2	1.49	3.42
9:33	40.8	52.6	54.2	52.8	56.1	29.0	619.7	1.45	3.34
9:34	41.1	53.2	54.8	53.2	56.3	29.5	619.9	1.47	3.37
9:35	41.2	52.7	54.5	52.9	55.5	29.1	619.9	1.47	3.39
9:36	41.3	52.0	53.5	52.2	55.0	28.6	619.4	1.53	3.52
9:37	41.4	52.1	53.8	52.3	55.1	28.8	618.5	1.50	3.45
9:38	41.5	51.9	53.5	52.2	54.8	28.5	617.7	1.49	3.43
9:39	41.5	51.6	53.2	51.6	54.3	28.4	618.4	1.50	3.45
9:40	41.6	51.3	52.8	51.3	53.7	28.0	619.3	1.53	3.52
9:41	41.6	51.3	52.8	51.6	54.1	27.8	619.7	1.52	3.50
9:42	41.8	51.5	53.0	52.0	54.6	28.4	619.8	1.49	3.43
9:43	41.9	52.0	53.5	52.1	55.1	29.2	620.3	1.48	3.41
9:44	42.0	51.6	53.0	51.8	54.0	28.7	621.1	1.52	3.49
9:45	42.0	51.3	52.9	51.9	54.6	29.1	620.4	1.50	3.45
9:46	42.0	50.2	51.3	50.2	51.8	27.9	618.0	1.55	3.57
9:47	41.9	49.6	50.8	50.1	52.4	27.7	616.8	1.55	3.58
9:48	42.0	50.7	51.9	51.3	54.0	28.6	619.1	1.52	3.50
9:49	42.1	50.5	51.6	51.0	53.1	28.9	618.1	1.53	3.53
9:50	42.0	49.7	50.9	50.0	52.2	29.4	616.7	1.53	3.53
9:51	42.0	49.8	51.2	50.2	52.5	29.6	618.5	1.53	3.53
9:52	42.1	50.5	52.0	50.7	52.7	29.7	618.6	1.52	3.50
9:53	42.3	50.8	52.3	51.0	53.5	29.8	617.6	1.51	3.49
9:54	42.3	50.5	52.1	50.5	53.2	30.1	617.4	1.55	3.59
9:55	42.5	51.7	53.1	51.8	54.7	30.1	617.7	1.47	3.40
9:56	42.7	52.8	54.3	52.8	55.6	30.7	618.1	1.48	3.41
9:57	42.9	53.4	54.8	53.6	56.5	30.7	617.9	1.45	3.34
9:58	43.1	53.4	54.7	53.6	56.0	30.3	616.3	1.48	3.43
9:59	43.1	52.6	54.1	52.7	55.0	29.7	613.8	1.49	3.47
10:00	43.2	52.5	54.0	52.4	54.9	30.2	613.5	1.49	3.46
10:01	43.3	52.5	54.0	52.7	55.0	30.4	611.6	1.49	3.47
10:02	43.4	52.7	54.2	52.7	55.1	30.3	611.6	1.48	3.44
10:03	43.5	52.8	54.1	53.1	55.3	30.5	609.7	1.48	3.46
10:04	43.5	52.2	53.4	52.4	54.6	30.4	609.5	1.50	3.51
10:05	43.5	52.3	53.7	52.4	54.7	30.4	611.9	1.49	3.48
10:06	43.6	52.5	53.9	52.6	54.5	30.4	611.1	1.50	3.50
10:07	43.6	51.9	52.9	52.1	54.0	29.5	609.2	1.53	3.59
10:08	43.6	50.5	51.7	50.9	52.7	29.2	609.2	1.52	3.57
10:09	43.5	50.2	51.5	50.7	52.3	29.0	610.6	1.54	3.60
10:10	43.5	50.3	51.6	50.8	52.3	29.2	610.5	1.55	3.62
10:11	43.4	50.1	51.1	50.6	52.4	29.5	611.5	1.52	3.56
10:12	43.4	50.2	51.4	50.8	53.0	30.4	610.8	1.54	3.61
10:13	43.5	51.2	52.3	51.7	53.6	30.5	606.5	1.51	3.56
10:14	43.6	52.0	53.1	52.3	54.1	30.8	606.1	1.49	3.51
10:15	43.8	52.3	53.5	52.5	54.2	31.2	605.5	1.48	3.48
10:16	43.9	52.6	53.8	52.6	54.5	31.5	605.9	1.47	3.46
10:17	44.0	52.7	54.0	53.0	54.7	31.8	607.7	1.46	3.42

Time [h]	T <sub>wall</sub> [°C]	T <sub>col,1</sub> [°C]	T <sub>col,2</sub> [°C]	T <sub>col,3</sub> [°C]	T <sub>col,4</sub> [°C]	T <sub>amb</sub> [°C]	G <sub>T,col</sub> [W/m <sup>2</sup> ]	P <sub>el</sub> [W]	Eff <sub>PV</sub> %
10:18	44.0	51.8	52.8	52.0	53.2	30.3	605.8	1.50	3.54
10:19	44.1	52.2	53.4	52.6	54.8	30.8	604.7	1.48	3.48
10:20	44.3	53.3	54.8	53.9	56.3	31.7	603.0	1.45	3.43
10:21	44.4	53.4	54.9	54.0	56.1	32.0	602.5	1.46	3.46
10:22	44.6	53.8	55.2	54.0	56.0	32.3	601.0	1.46	3.45
10:23	44.7	53.7	54.8	54.0	55.5	31.8	601.3	1.49	3.52
10:24	44.7	53.6	54.9	54.0	55.7	31.4	598.7	1.46	3.47
10:25	44.8	53.6	54.9	54.0	55.8	31.7	598.4	1.45	3.47
10:26	44.9	54.0	55.1	53.8	55.7	32.5	596.9	1.46	3.48
10:27	45.1	54.4	55.6	54.3	56.2	32.8	596.0	1.44	3.44
10:28	45.2	54.2	55.5	54.0	55.9	32.9	592.4	1.42	3.41
10:29	45.2	53.2	54.4	53.1	55.0	32.7	589.7	1.44	3.48
10:30	45.2	53.0	54.3	53.2	54.6	31.9	588.1	1.52	3.68
10:31	45.1	52.5	53.5	52.9	54.5	31.2	588.7	1.48	3.58
10:32	45.2	53.0	54.0	53.4	54.7	31.3	588.6	1.47	3.57
10:33	45.2	52.4	53.6	52.8	54.1	31.1	587.6	1.48	3.59
10:34	45.2	52.3	53.6	52.5	53.8	31.1	585.0	1.50	3.66
10:35	45.2	51.7	52.7	52.0	53.0	30.5	580.3	1.50	3.69
10:36	45.1	50.5	51.3	51.2	52.5	29.8	576.6	1.51	3.73
10:37	45.1	50.9	52.0	51.9	53.8	30.8	574.7	1.49	3.70
10:38	45.0	50.5	51.8	51.4	53.4	31.4	571.8	1.49	3.72
10:39	45.0	50.7	51.8	51.6	53.3	31.5	570.9	1.52	3.79
10:40	45.0	51.3	52.5	52.0	53.7	31.6	570.0	1.48	3.71
10:41	45.2	52.3	53.5	53.0	54.6	31.8	565.8	1.45	3.66
10:42	45.4	53.3	54.6	53.6	55.5	32.6	563.9	1.42	3.58
10:43	45.5	53.4	54.5	53.6	55.2	32.9	560.4	1.45	3.68
10:44	45.5	52.3	53.1	52.3	54.0	32.8	560.5	1.48	3.77
10:45	45.4	51.4	52.5	52.0	53.2	32.7	557.0	1.47	3.76
10:46	45.4	51.6	52.5	52.0	53.4	32.2	556.6	1.47	3.76
10:47	45.4	51.7	52.6	52.1	53.6	32.5	557.9	1.44	3.69
10:48	45.4	52.1	53.3	52.5	53.9	32.4	557.8	1.45	3.70
10:49	45.5	51.7	52.7	51.8	53.3	31.9	555.8	1.49	3.82
10:50	45.3	49.9	50.4	49.9	51.6	32.5	552.4	1.51	3.90
10:51	45.2	49.9	50.7	50.3	51.6	32.5	551.0	1.48	3.83
10:52	45.2	50.0	50.3	49.9	51.6	32.6	548.1	1.51	3.93
10:53	45.0	49.2	49.6	49.5	50.9	32.7	545.7	1.51	3.94
10:54	45.0	49.9	50.5	50.5	51.4	32.1	545.6	1.48	3.86
10:55	45.1	50.0	50.8	50.6	51.0	31.7	544.5	1.48	3.87
10:56	45.1	50.6	51.5	51.1	51.9	31.7	546.1	1.48	3.86
10:57	45.2	51.2	52.3	51.5	52.8	32.2	545.8	1.45	3.78
10:58	45.3	51.6	52.6	52.2	53.1	31.9	542.1	1.45	3.81
10:59	45.3	51.4	52.2	52.1	52.8	32.1	540.9	1.45	3.81
11:00	45.4	51.5	52.5	52.2	53.3	33.1	538.8	1.44	3.82
11:01	45.3	50.7	51.3	51.3	52.5	33.6	539.2	1.46	3.87
11:02	45.2	49.5	50.0	49.6	51.2	33.2	536.9	1.48	3.93
11:03	45.1	49.6	50.1	49.9	51.2	33.1	532.5	1.49	3.98
11:04	45.1	49.5	50.3	49.9	51.2	33.2	530.8	1.48	3.98
11:05	45.1	50.5	51.3	51.0	52.0	33.2	529.1	1.46	3.93
11:06	45.3	51.3	52.2	51.9	52.8	33.5	526.8	1.43	3.86
11:07	45.3	51.1	52.2	51.5	52.4	33.6	526.1	1.44	3.91
11:08	45.3	50.9	51.9	51.2	52.2	33.7	525.3	1.46	3.96
11:09	45.4	51.1	52.2	51.2	52.4	33.8	522.7	1.44	3.92
11:10	45.4	50.8	51.9	51.1	52.2	33.7	521.1	1.44	3.94
11:11	45.4	51.1	52.2	51.3	52.4	33.7	519.3	1.44	3.95
11:12	45.4	51.5	52.5	51.7	52.9	34.0	519.4	1.42	3.91
11:13	45.5	51.0	51.8	51.2	52.5	34.0	515.7	1.43	3.94
11:14	45.5	51.2	52.0	51.6	52.5	34.1	516.1	1.44	3.98
11:15	45.5	50.8	51.7	51.5	52.1	34.2	513.8	1.43	3.96
11:16	45.5	51.0	51.7	51.4	52.2	33.9	509.8	1.41	3.94
11:17	45.5	50.3	51.1	50.7	51.3	33.6	506.4	1.43	4.03

Time [h]	T <sub>wall</sub> [°C]	T <sub>col,1</sub> [°C]	T <sub>col,2</sub> [°C]	T <sub>col,3</sub> [°C]	T <sub>col,4</sub> [°C]	T <sub>amb</sub> [°C]	G <sub>T,col</sub> [W/m <sup>2</sup> ]	P <sub>el</sub> [W]	Eff <sub>PV</sub> %
11:18	45.4	49.8	50.5	50.0	50.6	33.1	501.7	1.43	4.05
11:19	45.4	49.8	50.5	49.8	51.0	33.3	504.7	1.44	4.07
11:20	45.3	49.9	50.7	50.3	51.0	33.2	501.0	1.44	4.10
11:21	45.3	49.1	49.4	49.2	50.3	32.7	497.6	1.45	4.14
11:22	45.1	47.5	47.9	47.1	48.7	33.1	495.1	1.48	4.27
11:23	45.1	48.3	49.0	48.5	49.1	33.3	493.0	1.45	4.18
11:24	45.0	48.2	48.5	47.8	49.3	33.2	489.8	1.47	4.28
11:25	44.9	47.9	48.7	48.1	49.5	33.2	486.0	1.44	4.23
11:26	44.9	48.8	49.7	49.3	50.4	33.3	484.3	1.42	4.17
11:27	45.0	48.8	49.2	48.8	50.0	33.7	483.1	1.42	4.19
11:28	44.8	47.4	47.5	46.8	48.5	33.5	481.0	1.46	4.33
11:29	44.7	47.1	47.4	47.2	48.3	33.0	481.4	1.46	4.33
11:30	44.6	47.2	47.7	47.4	48.8	33.4	478.5	1.45	4.33
11:31	44.5	47.3	47.7	47.4	49.0	33.5	473.7	1.43	4.30
11:32	44.5	47.5	48.0	48.1	48.8	33.2	472.9	1.46	4.40
11:33	44.4	46.8	47.0	46.8	48.1	33.0	469.8	1.46	4.44
11:34	44.4	46.7	47.3	47.1	48.2	33.2	468.8	1.45	4.42
11:35	44.4	47.4	47.9	48.2	48.7	33.1	466.5	1.44	4.41
11:36	44.3	47.3	47.7	48.1	48.9	33.1	464.2	1.44	4.42
11:37	44.4	47.4	48.0	48.4	48.8	32.7	462.7	1.43	4.42
11:38	44.4	47.3	47.3	47.6	49.0	33.3	461.8	1.43	4.41
11:39	44.1	46.1	46.2	45.5	47.8	33.8	459.9	1.43	4.45
11:40	44.1	46.9	47.3	47.2	48.1	34.1	457.0	1.42	4.43
11:41	44.2	47.6	48.4	48.1	48.9	34.5	452.7	1.40	4.42
11:42	44.2	47.9	48.4	48.0	48.7	34.4	449.5	1.39	4.42
11:43	44.2	47.0	47.3	47.5	47.3	33.0	445.6	1.45	4.63
11:44	44.1	46.4	46.6	47.0	47.5	32.7	444.4	1.43	4.58
11:45	44.0	46.6	47.1	47.4	48.1	33.5	440.6	1.42	4.59
11:46	44.1	47.0	47.7	47.6	48.2	33.9	439.2	1.39	4.50
11:47	44.1	47.1	47.6	47.3	48.3	34.2	438.4	1.40	4.54
11:48	44.1	47.5	48.2	48.0	48.7	34.3	436.7	1.38	4.50
11:49	44.1	47.6	47.9	47.5	48.5	34.6	435.0	1.37	4.50
11:50	44.0	46.9	47.3	46.9	47.7	34.9	432.7	1.38	4.56
11:51	44.0	47.4	48.0	47.7	48.3	34.9	430.3	1.37	4.54
11:52	44.1	47.4	47.9	47.9	47.9	34.3	426.4	1.39	4.65
11:53	44.0	46.6	47.0	47.1	47.7	33.9	423.5	1.38	4.64
11:54	44.0	46.9	47.4	47.5	48.1	34.1	421.2	1.35	4.58
11:55	43.9	46.4	46.9	47.1	47.8	33.9	417.4	1.37	4.67
11:56	43.8	45.9	45.8	45.7	47.1	34.0	412.6	1.37	4.74
11:57	43.7	45.3	45.2	45.4	46.3	34.4	410.2	1.36	4.73
11:58	43.6	45.5	46.0	46.2	46.8	34.1	404.9	1.36	4.78
11:59	43.6	46.1	46.5	47.1	47.1	33.7	402.0	1.35	4.80
12:00	43.7	46.4	46.8	47.4	47.6	33.9	401.0	1.33	4.74
12:01	43.7	46.8	47.2	47.6	47.7	34.1	397.9	1.35	4.82
12:02	43.7	46.5	46.9	47.3	47.4	33.7	395.4	1.33	4.81
12:03	43.7	46.1	46.6	47.0	46.7	33.6	393.1	1.33	4.83
12:04	43.7	46.2	46.6	47.1	47.2	33.9	389.6	1.32	4.83
12:05	43.6	46.1	46.2	46.9	47.0	34.3	387.0	1.32	4.87
12:06	43.6	45.6	46.0	46.1	46.4	34.0	382.5	1.32	4.91
12:07	43.5	45.6	46.1	46.4	46.5	34.1	378.1	1.30	4.92
12:08	43.5	45.6	46.0	46.1	46.5	34.5	377.2	1.29	4.89
12:09	43.4	45.3	45.6	45.7	46.0	34.8	375.1	1.29	4.91
12:10	43.3	44.6	44.9	45.3	45.4	34.7	371.4	1.29	4.97
12:11	43.2	44.8	45.2	45.3	45.6	34.5	367.6	1.28	4.98
12:12	43.2	45.0	45.2	45.4	45.5	34.4	364.3	1.27	4.99
12:13	43.1	44.2	44.7	45.0	44.9	34.0	360.8	1.28	5.06
12:14	43.0	43.5	43.8	44.2	44.1	33.6	357.2	1.29	5.14
12:15	43.0	43.9	44.3	44.5	44.5	33.8	354.1	1.28	5.14
12:16	42.9	44.2	44.6	45.2	45.3	34.6	352.6	1.25	5.04
12:17	43.0	45.3	45.6	46.1	45.8	34.5	348.6	1.23	5.04

Time [h]	T <sub>wall</sub> [°C]	T <sub>col,1</sub> [°C]	T <sub>col,2</sub> [°C]	T <sub>col,3</sub> [°C]	T <sub>col,4</sub> [°C]	T <sub>amb</sub> [°C]	G <sub>T,col</sub> [W/m <sup>2</sup> ]	P <sub>el</sub> [W]	Eff <sub>PV</sub> %
12:18	42.9	44.3	44.1	44.4	44.8	34.4	343.9	1.25	5.17
12:19	42.8	43.8	43.9	44.4	44.5	34.7	339.9	1.23	5.17
12:20	42.7	43.7	43.7	44.0	44.3	34.6	335.7	1.23	5.21
12:21	42.8	44.0	44.2	44.7	44.5	34.6	334.0	1.22	5.21
12:22	42.7	43.6	43.8	44.2	44.4	34.7	332.8	1.22	5.24
12:23	42.5	43.0	43.3	44.0	43.8	34.6	329.0	1.21	5.23
12:24	42.6	43.7	43.9	44.3	43.7	34.4	325.1	1.19	5.24
12:25	42.5	43.2	43.2	43.6	43.0	33.6	321.1	1.21	5.37
12:26	42.4	41.9	42.2	42.6	42.1	33.1	316.9	1.21	5.45
12:27	42.2	41.7	42.0	42.6	42.7	33.4	314.9	1.20	5.42
12:28	42.2	42.5	43.0	43.8	43.6	33.8	311.7	1.17	5.37
12:29	42.2	42.6	42.9	43.9	43.3	33.3	309.6	1.19	5.47
12:30	42.2	42.5	42.8	43.8	43.5	34.0	307.1	1.16	5.40
12:31	42.1	42.4	42.9	43.7	43.4	34.5	303.8	1.15	5.40
12:32	42.1	43.1	43.3	43.9	43.4	34.9	301.0	1.14	5.40
12:33	42.0	42.8	43.0	43.5	42.6	34.3	297.3	1.15	5.50
12:34	42.0	42.0	42.3	42.9	42.1	33.8	294.1	1.14	5.53
12:35	41.9	42.0	42.2	42.8	41.9	33.3	290.3	1.15	5.63
12:36	41.8	40.9	41.0	41.9	40.6	32.5	285.0	1.14	5.73
12:37	41.6	39.9	40.2	40.7	40.3	32.7	281.1	1.11	5.62
12:38	41.4	40.0	40.6	41.2	40.9	33.6	277.4	1.09	5.63
12:39	41.4	40.9	41.2	42.1	41.2	33.6	275.4	1.10	5.70
12:40	41.3	40.7	41.0	41.6	41.2	34.0	272.3	1.08	5.66
12:41	41.2	39.9	40.6	41.1	40.6	33.6	267.5	1.08	5.75
12:42	41.1	40.2	40.7	41.3	40.7	33.6	265.6	1.07	5.74
12:43	41.1	40.5	40.9	41.5	40.9	33.6	263.1	1.07	5.79
12:44	41.1	40.6	40.9	41.7	41.0	33.7	260.5	1.04	5.71
12:45	41.0	40.3	40.7	41.4	40.6	34.2	256.5	1.04	5.77
12:46	41.0	40.6	40.8	41.6	41.1	34.1	255.3	1.03	5.74
12:47	41.0	41.4	41.7	42.5	41.6	34.6	252.5	1.01	5.70
12:48	41.0	42.1	42.3	42.9	41.9	35.3	249.8	1.00	5.72
12:49	41.1	42.3	42.5	42.8	42.0	35.7	249.6	1.00	5.70
12:50	41.0	41.8	42.0	42.2	41.3	35.6	246.2	1.00	5.77
12:51	40.9	41.2	41.2	41.1	40.8	35.5	240.6	0.98	5.82
12:52	40.7	40.0	40.0	39.6	39.4	35.0	235.9	0.99	5.98
12:53	40.6	39.9	40.1	40.5	39.5	34.4	234.5	0.98	5.96
12:54	40.6	39.8	40.1	40.6	39.3	34.1	229.5	0.97	6.03
12:55	40.5	39.5	39.6	40.1	38.8	33.3	224.9	0.97	6.15
12:56	40.5	39.6	39.8	40.5	39.4	33.5	224.9	0.96	6.06
12:57	40.5	39.5	39.7	40.6	39.1	33.4	220.5	0.96	6.19
12:58	40.1	38.1	38.4	38.6	38.2	33.5	218.5	0.96	6.25
12:59	40.1	38.1	38.5	38.9	37.9	33.1	216.0	0.96	6.31
13:00	39.9	38.3	38.6	38.6	38.2	33.5	211.8	0.93	6.29

Table E.7: Experimental data for September 8

Time [h]	T <sub>wall</sub> [°C]	T <sub>col,1</sub> [°C]	T <sub>col,2</sub> [°C]	T <sub>col,3</sub> [°C]	T <sub>col,4</sub> [°C]	T <sub>out</sub> [°C]	T <sub>amb</sub> [°C]	G <sub>T,col</sub> [W/m <sup>2</sup> ]	Flow Rate [m <sup>3</sup> /h m <sup>2</sup> ]	P <sub>el</sub> [W]	Q <sup>u</sup> [W/m <sup>2</sup> ]	Eff <sub>th</sub> %	Eff <sub>PV</sub> %
7:35	17.9	23.6	22.1	24.8	24.0	21.4	15.1	370.1	51.32	1.67	109.3	29.5	6.43
7:36	18.1	24.0	22.4	25.4	24.4	21.7	15.2	381.0	51.06	1.69	111.5	29.3	6.32
7:37	18.3	24.3	22.7	25.6	24.6	22.0	15.3	385.5	51.39	1.70	116.3	30.2	6.30
7:38	18.4	24.7	23.0	25.9	25.0	22.3	15.3	394.4	51.15	1.71	120.9	30.7	6.18

Time [h]	T <sub>wall</sub> [°C]	T <sub>col,1</sub> [°C]	T <sub>col,2</sub> [°C]	T <sub>col,3</sub> [°C]	T <sub>col,4</sub> [°C]	T <sub>out</sub> [°C]	T <sub>amb</sub> [°C]	G <sub>T,col</sub> [W/m <sup>2</sup> ]	Flow Rate [m <sup>3</sup> /h m <sup>2</sup> ]	P <sub>el</sub> [W]	Q'' <sub>u</sub> [W/m <sup>2</sup> ]	Eff <sub>th</sub> %	Eff <sub>PV</sub> %
7:39	18.6	24.8	23.1	26.4	25.1	22.5	15.4	399.5	51.66	1.70	122.2	30.6	6.08
7:40	18.7	25.0	23.2	26.4	25.3	22.7	15.4	406.1	51.54	1.73	124.5	30.7	6.07
7:41	18.9	25.2	23.4	26.4	25.3	22.9	15.5	414.2	51.64	1.73	128.5	31.0	5.97
7:42	19.0	25.3	23.4	26.7	25.4	23.0	15.6	422.8	53.57	1.76	132.4	31.3	5.95
7:43	19.2	25.4	23.5	26.8	25.5	23.2	15.6	428.5	53.51	1.75	135.4	31.6	5.83
7:44	19.3	25.7	23.7	27.0	25.7	23.3	15.6	433.2	53.90	1.78	138.8	32.0	5.86
7:45	19.4	25.8	23.9	27.2	26.0	23.5	15.7	441.3	53.32	1.77	138.7	31.4	5.73
7:46	19.5	26.1	24.1	27.5	26.4	23.7	15.7	450.2	53.42	1.79	141.7	31.5	5.66
7:47	19.7	26.9	24.8	28.4	27.1	24.2	15.9	457.7	52.47	1.78	144.9	31.7	5.55
7:48	19.9	27.4	25.2	28.8	27.5	24.6	16.0	465.3	53.12	1.79	152.4	32.8	5.48
7:49	20.1	27.7	25.5	29.5	27.8	24.9	16.1	472.5	53.18	1.78	155.0	32.8	5.38
7:50	20.2	27.5	25.2	28.8	27.3	24.9	16.0	477.9	54.71	1.81	161.7	33.8	5.40
7:51	20.4	27.9	25.5	29.3	27.8	25.1	16.0	483.7	54.17	1.81	163.0	33.7	5.34
7:52	20.6	28.1	25.7	29.6	28.0	25.3	16.1	487.9	54.10	1.80	165.7	34.0	5.26
7:53	20.7	28.3	25.8	29.9	28.1	25.4	16.1	493.3	54.26	1.79	167.5	33.9	5.17
7:54	20.8	28.7	26.2	30.5	28.7	25.7	16.3	500.4	54.17	1.79	169.7	33.9	5.10
7:55	21.0	28.7	26.4	30.9	28.9	25.8	16.4	507.1	54.70	1.76	170.8	33.7	4.95
7:56	21.2	28.9	26.6	31.2	29.0	26.0	16.6	514.5	53.83	1.75	168.3	32.7	4.86
7:57	21.3	29.4	27.0	32.0	29.6	26.2	16.8	521.3	53.98	1.81	168.0	32.2	4.96
7:58	21.4	29.4	27.0	31.8	29.6	26.5	16.9	528.0	54.25	1.82	172.7	32.7	4.93
7:59	21.6	30.0	27.3	31.9	30.0	26.8	16.8	535.5	53.73	1.81	177.0	33.0	4.82
8:00	21.8	30.4	27.6	32.0	30.2	27.1	16.9	543.2	53.32	1.84	179.9	33.1	4.82
8:01	22.0	30.7	28.0	32.3	30.5	27.4	17.0	549.6	53.23	1.82	182.9	33.3	4.73
8:02	22.2	30.5	28.0	32.7	30.6	27.4	17.1	551.9	54.15	1.85	184.7	33.5	4.77
8:03	22.4	30.8	28.2	32.8	30.7	27.6	17.1	554.7	53.92	1.84	186.2	33.6	4.74
8:04	22.5	30.6	28.1	32.9	30.7	27.6	17.3	560.3	54.86	1.83	187.1	33.4	4.65
8:05	22.7	31.2	28.4	33.4	31.2	27.9	17.4	563.6	54.25	1.81	187.0	33.2	4.58
8:06	22.8	31.7	28.7	33.5	31.4	28.3	17.5	566.9	54.37	1.81	191.9	33.9	4.57
8:07	23.0	31.5	28.6	33.1	31.3	28.3	17.5	575.1	54.51	1.84	192.5	33.5	4.56
8:08	23.1	31.6	28.7	33.4	31.4	28.4	17.5	582.8	54.60	1.83	194.9	33.4	4.47
8:09	23.3	32.3	29.2	34.0	32.0	28.7	17.6	586.8	54.39	1.82	199.1	33.9	4.43
8:10	23.5	32.6	29.5	34.6	32.3	29.1	17.7	590.8	54.12	1.83	201.0	34.0	4.41
8:11	23.6	32.6	29.5	34.7	32.3	29.1	17.8	595.8	54.65	1.85	202.6	34.0	4.43
8:12	23.8	32.8	29.7	34.2	32.2	29.3	17.7	598.8	54.09	1.85	204.7	34.2	4.41
8:13	23.9	32.7	29.7	34.0	32.2	29.3	17.5	602.6	53.74	1.83	207.0	34.4	4.34
8:14	24.1	32.8	30.0	34.3	32.6	29.4	17.6	606.7	53.49	1.84	207.4	34.2	4.33
8:15	24.2	33.2	30.2	34.6	32.8	29.7	17.6	611.8	53.76	1.85	211.8	34.6	4.32
8:16	24.3	32.8	30.1	34.7	32.6	29.6	17.7	617.3	54.24	1.84	211.0	34.2	4.24
8:17	24.5	33.0	30.1	34.8	32.7	29.7	17.8	625.0	53.97	1.84	209.2	33.5	4.20
8:18	24.7	33.6	30.4	35.3	33.4	30.0	18.1	628.9	54.03	1.82	210.8	33.5	4.14
8:19	24.9	33.7	30.6	35.4	33.1	30.3	18.1	629.5	53.67	1.87	213.2	33.9	4.23
8:20	25.0	33.1	30.2	34.6	32.5	30.0	17.9	627.0	54.48	1.87	215.7	34.4	4.26
8:21	25.1	33.6	30.5	35.0	33.0	30.2	18.0	630.7	53.62	1.83	212.8	33.7	4.14
8:22	25.2	33.2	30.4	34.8	32.7	30.1	18.0	634.8	53.84	1.85	212.0	33.4	4.15
8:23	25.2	33.5	30.6	35.0	33.0	30.1	18.0	638.1	54.09	1.82	215.3	33.7	4.07
8:24	25.4	33.8	30.8	35.3	33.4	30.4	18.1	640.5	53.57	1.84	215.3	33.6	4.10
8:25	25.5	33.9	30.8	35.3	33.5	30.5	18.0	641.3	53.40	1.84	217.2	33.9	4.10
8:26	25.7	34.2	31.2	35.7	33.8	30.7	18.1	644.4	53.09	1.82	217.4	33.7	4.02
8:27	25.8	34.7	31.6	36.0	34.3	31.0	18.3	649.1	52.62	1.92	218.5	33.7	4.21
8:28	25.9	34.7	31.7	36.2	34.2	31.1	18.3	652.9	53.04	1.84	221.7	34.0	4.01
8:29	26.0	34.4	31.5	36.2	34.2	31.0	18.4	656.9	53.00	1.85	218.7	33.3	4.01
8:30	26.1	33.9	31.2	35.5	33.7	30.9	18.2	658.0	53.38	1.85	220.7	33.5	4.01
8:31	26.2	34.0	31.3	35.5	33.8	30.8	18.2	661.4	53.40	1.84	220.3	33.3	3.98
8:32	26.3	34.0	31.4	35.4	33.9	30.9	18.2	665.1	52.72	1.86	218.2	32.8	3.99
8:33	26.4	34.4	31.7	36.0	34.5	31.1	18.3	668.4	52.80	1.84	220.3	33.0	3.93
8:34	26.7	35.2	32.2	36.8	34.9	31.6	18.5	670.6	53.77	1.83	228.5	34.1	3.89
8:35	26.8	35.1	32.2	36.8	34.8	31.7	18.6	672.4	54.03	1.83	231.0	34.4	3.88
8:36	26.8	35.0	32.1	36.8	34.9	31.6	18.6	675.5	54.25	1.85	228.8	33.9	3.91
8:37	27.0	35.5	32.3	37.2	35.3	31.8	18.8	678.6	53.63	1.83	226.7	33.4	3.85
8:38	27.2	36.4	33.1	38.1	36.1	32.4	19.1	681.4	53.64	1.83	230.9	33.9	3.83
8:39	27.4	35.9	32.9	37.6	35.5	32.4	19.2	684.1	57.21	1.83	244.9	35.8	3.81
8:40	27.5	36.0	33.0	37.9	35.9	32.4	19.2	688.8	53.82	1.84	230.4	33.5	3.80
8:41	27.6	36.5	33.2	38.2	36.1	32.7	19.4	693.2	53.48	1.82	231.2	33.3	3.75
8:42	27.7	36.8	33.5	39.4	36.8	32.9	19.5	695.7	53.42	1.80	232.8	33.5	3.68
8:43	28.0	37.8	34.1	40.1	37.3	33.5	20.0	697.0	52.98	1.79	232.2	33.3	3.67
8:44	28.2	37.6	34.0	39.5	37.0	33.6	20.1	698.0	54.48	1.81	238.7	34.2	3.70
8:45	28.3	37.6	34.2	39.7	37.3	33.7	20.2	700.9	54.45	1.79	237.9	33.9	3.64

Time [h]	T <sub>wall</sub> [°C]	T <sub>col,1</sub> [°C]	T <sub>col,2</sub> [°C]	T <sub>col,3</sub> [°C]	T <sub>col,4</sub> [°C]	T <sub>out</sub> [°C]	T <sub>amb</sub> [°C]	G <sub>T,col</sub> [W/m <sup>2</sup> ]	Flow Rate [m <sup>3</sup> /h m <sup>2</sup> ]	P <sub>el</sub> [W]	Q'' <sub>u</sub> [W/m <sup>2</sup> ]	Eff <sub>th</sub> %	Eff <sub>PV</sub> %
8:46	28.4	37.1	34.1	39.7	37.0	33.6	20.2	702.8	54.31	1.82	234.1	33.3	3.70
8:47	28.6	36.9	33.7	38.8	36.2	33.5	19.9	704.5	54.62	1.83	239.1	33.9	3.71
8:48	28.6	36.5	33.3	38.4	36.0	33.2	19.7	706.3	55.22	1.83	241.3	34.2	3.70
8:49	28.7	36.4	33.6	39.0	36.4	33.2	19.7	708.3	55.49	1.83	241.6	34.1	3.69
8:50	28.7	35.7	33.0	38.5	35.9	32.9	19.5	709.4	55.31	1.84	240.6	33.9	3.71
8:51	28.7	36.4	33.2	38.5	36.1	33.1	19.5	711.6	54.80	1.83	241.2	33.9	3.68
8:52	28.9	37.1	34.0	39.8	37.1	33.5	19.9	714.7	54.70	1.80	241.5	33.8	3.60
8:53	29.1	37.8	34.5	40.2	37.4	34.1	20.0	717.1	54.08	1.80	245.7	34.3	3.58
8:54	29.4	38.0	34.7	40.3	37.6	34.4	20.4	717.3	54.80	1.80	247.2	34.5	3.58
8:55	29.6	38.0	34.8	40.4	37.7	34.5	20.7	720.5	55.17	1.80	245.2	34.0	3.57
8:56	29.7	38.3	34.7	40.5	37.9	34.7	20.7	720.8	54.97	1.83	247.4	34.3	3.63
8:57	29.8	38.4	34.7	40.2	37.8	34.7	20.4	721.6	54.73	1.82	251.6	34.9	3.60
8:58	29.7	38.7	35.0	40.6	38.2	34.8	20.4	722.4	54.65	1.80	252.0	34.9	3.56
8:59	29.8	38.7	35.0	40.9	38.1	34.9	20.7	724.1	54.89	1.80	249.9	34.5	3.54
9:00	29.9	38.1	34.4	40.0	37.1	34.6	20.6	724.7	56.39	1.82	255.2	35.2	3.58
9:01	29.9	37.6	34.2	39.1	36.8	34.3	20.3	723.7	55.99	1.83	253.6	35.0	3.60
9:02	30.0	37.3	34.1	38.9	36.6	34.1	20.1	725.8	55.98	1.82	253.5	34.9	3.58
9:03	30.0	37.7	34.3	39.4	37.0	34.3	20.1	727.7	55.01	1.81	251.8	34.6	3.54
9:04	30.1	38.4	35.0	40.7	37.9	34.7	20.6	729.0	55.13	1.80	248.8	34.1	3.53
9:05	30.2	38.3	35.0	40.8	38.0	34.8	21.1	730.5	55.22	1.80	242.9	33.3	3.52
9:06	30.3	38.6	34.9	40.8	38.0	35.0	21.1	731.5	55.18	1.81	245.9	33.6	3.53
9:07	30.5	38.6	34.9	40.6	37.9	35.0	21.2	732.3	54.66	1.81	243.8	33.3	3.53
9:08	30.6	39.1	35.4	41.2	38.5	35.3	21.3	733.0	54.51	1.79	245.7	33.5	3.48
9:09	30.8	39.2	35.5	41.3	38.6	35.5	21.3	733.3	55.13	1.78	250.6	34.2	3.47
9:10	30.9	39.0	35.6	41.4	38.6	35.5	21.2	733.3	55.17	1.80	252.7	34.5	3.50
9:11	31.0	39.2	35.7	41.2	38.7	35.5	21.1	733.9	54.81	1.78	254.0	34.6	3.46
9:12	31.1	39.1	35.7	41.8	38.7	35.6	21.3	733.8	55.53	1.80	255.1	34.8	3.49
9:13	31.2	39.1	35.5	41.4	38.3	35.6	21.3	733.8	55.22	1.81	253.8	34.6	3.52
9:14	31.2	39.0	35.4	41.6	38.5	35.5	21.1	733.8	55.58	1.80	256.9	35.0	3.49
9:15	31.3	39.3	35.6	41.3	38.6	35.7	21.1	733.1	55.14	1.79	257.9	35.2	3.49
9:16	31.4	39.3	35.7	40.9	38.5	35.7	21.4	733.0	54.87	1.79	252.9	34.5	3.49
9:17	31.5	39.5	35.9	41.3	38.6	35.9	21.5	731.5	54.76	1.78	253.2	34.6	3.48
9:18	31.7	39.8	36.1	41.6	39.1	36.1	21.4	732.5	54.46	1.80	256.1	35.0	3.50
9:19	31.8	40.0	36.4	42.0	39.3	36.2	21.7	732.7	54.50	1.77	254.1	34.7	3.44
9:20	31.8	39.2	35.4	40.3	37.8	35.9	21.3	732.5	56.63	1.81	264.2	36.1	3.53
9:21	31.8	38.9	35.6	40.2	38.1	35.6	21.4	732.6	55.24	1.80	251.9	34.4	3.50
9:22	31.9	38.9	35.7	40.7	38.5	35.8	21.4	732.8	55.00	1.79	252.5	34.5	3.49
9:23	32.0	39.9	36.4	42.0	39.3	36.2	21.7	733.3	54.83	1.77	254.8	34.7	3.44
9:24	32.0	38.9	35.6	41.7	38.7	36.0	21.7	732.4	56.13	1.80	258.2	35.3	3.50
9:25	32.1	39.2	35.7	41.8	38.9	35.9	21.9	732.2	55.25	1.78	248.4	33.9	3.47
9:26	32.2	39.8	36.1	41.7	38.8	36.3	22.0	731.6	54.91	1.79	250.8	34.3	3.48
9:27	32.3	39.2	35.8	41.1	38.2	36.1	21.8	729.7	56.29	1.79	257.3	35.3	3.51
9:28	32.2	38.5	35.4	40.7	38.2	35.7	21.8	729.1	55.61	1.79	247.8	34.0	3.50
9:29	32.4	39.3	35.9	41.1	38.6	36.0	21.9	729.5	54.74	1.78	247.8	34.0	3.48
9:30	32.4	38.5	35.3	40.7	38.0	35.8	21.4	728.4	56.88	1.82	262.5	36.0	3.57
9:31	32.4	38.4	35.5	41.3	38.5	35.6	21.8	728.9	56.72	1.79	250.3	34.3	3.50
9:32	32.5	39.3	35.9	41.7	38.8	36.1	22.3	728.6	55.53	1.80	245.4	33.7	3.53
9:33	32.5	38.3	35.4	41.3	38.1	35.8	21.8	727.3	56.46	1.81	252.4	34.7	3.55
9:34	32.5	38.3	35.7	41.7	38.5	35.7	21.7	727.2	55.65	1.79	249.5	34.3	3.50
9:35	32.5	38.6	35.9	42.1	38.6	35.9	21.9	726.4	56.66	1.79	253.7	34.9	3.51
9:36	32.5	38.7	35.8	41.8	38.5	35.9	22.1	726.2	56.03	1.78	246.6	34.0	3.49
9:37	32.6	38.9	35.5	40.9	38.1	35.9	22.0	725.2	56.11	1.82	249.7	34.4	3.58
9:38	32.7	39.1	35.7	41.2	38.7	36.0	21.9	724.3	55.44	1.79	249.3	34.4	3.52
9:39	32.8	39.7	36.3	42.1	39.5	36.3	22.3	723.8	54.59	1.77	244.7	33.8	3.48
9:40	32.9	39.7	36.3	42.5	39.4	36.5	22.7	723.6	55.93	1.76	246.7	34.1	3.47
9:41	32.9	39.6	36.2	42.3	39.2	36.5	22.5	722.4	55.08	1.77	246.7	34.1	3.49
9:42	33.0	39.2	35.6	41.6	38.8	36.3	22.2	721.9	56.17	1.78	254.3	35.2	3.52
9:43	33.0	39.4	35.9	41.9	39.1	36.4	22.3	721.0	55.67	1.77	250.3	34.7	3.51
9:44	33.1	40.3	36.7	42.7	39.8	36.8	22.8	720.7	53.72	1.75	240.2	33.3	3.46
9:45	33.2	40.5	36.9	42.5	39.6	37.0	23.0	719.8	54.08	1.76	241.7	33.6	3.49
9:46	33.2	39.5	36.2	41.8	38.7	36.5	23.0	718.6	55.84	1.77	240.8	33.5	3.51
9:47	33.3	39.7	36.4	42.2	39.2	36.5	23.2	717.7	54.61	1.77	232.7	32.4	3.51
9:48	33.4	40.5	37.0	42.9	39.9	37.0	23.4	717.3	54.23	1.74	234.7	32.7	3.46
9:49	33.5	41.2	37.4	43.9	40.3	37.4	23.9	716.1	53.55	1.73	230.0	32.1	3.46
9:50	33.6	41.0	37.1	43.7	39.9	37.4	24.1	714.5	54.94	1.74	233.9	32.7	3.47
9:51	33.6	40.6	36.9	43.3	39.8	37.2	23.8	714.0	54.52	1.74	232.8	32.6	3.48
9:52	33.6	39.5	36.4	42.6	38.9	36.9	23.1	711.7	55.69	1.80	244.7	34.4	3.61

Time [h]	T <sub>wall</sub> [°C]	T <sub>col,1</sub> [°C]	T <sub>col,2</sub> [°C]	T <sub>col,3</sub> [°C]	T <sub>col,4</sub> [°C]	T <sub>out</sub> [°C]	T <sub>amb</sub> [°C]	G <sub>T,col</sub> [W/m <sup>2</sup> ]	Flow Rate [m <sup>3</sup> /h m <sup>2</sup> ]	P <sub>el</sub> [W]	Q'' <sub>u</sub> [W/m <sup>2</sup> ]	Eff <sub>th</sub> %	Eff <sub>pv</sub> %
9:53	33.5	38.6	36.0	42.1	38.6	36.3	22.5	710.9	55.96	1.78	245.9	34.6	3.57
9:54	33.5	38.7	35.9	41.7	38.7	36.2	22.5	710.1	54.75	1.77	241.0	33.9	3.55
9:55	33.6	39.4	36.5	42.3	39.3	36.5	23.1	708.8	53.59	1.77	229.5	32.4	3.55
9:56	33.7	39.7	36.8	42.4	39.7	36.7	23.5	708.5	53.70	1.75	228.1	32.2	3.52
9:57	33.8	40.6	37.2	42.7	40.0	37.2	23.7	707.3	53.39	1.74	229.2	32.4	3.50
9:58	33.9	40.4	36.9	42.2	39.4	37.2	23.4	705.4	54.48	1.77	239.7	34.0	3.58
9:59	33.9	40.1	36.7	41.9	39.1	37.0	23.4	703.2	54.68	1.76	237.6	33.8	3.56
10:00	33.9	40.0	36.7	42.4	39.4	37.0	23.6	701.0	54.32	1.75	231.9	33.1	3.55
10:01	34.1	40.9	37.5	43.3	40.2	37.5	23.8	700.5	53.34	1.73	232.9	33.3	3.52
10:02	34.2	40.7	37.1	42.5	39.4	37.5	23.7	699.2	54.65	1.73	240.2	34.3	3.53
10:03	34.2	40.6	37.3	42.6	39.8	37.5	23.9	698.0	53.99	1.73	233.1	33.4	3.54
10:04	34.3	40.5	37.1	42.0	39.3	37.4	23.8	695.3	54.39	1.74	235.9	33.9	3.58
10:05	34.2	39.9	36.7	42.1	39.0	37.1	23.8	694.5	54.86	1.75	233.1	33.6	3.58
10:06	34.3	40.0	36.7	42.2	39.2	37.1	23.9	692.8	54.22	1.75	228.7	33.0	3.60
10:07	34.3	40.5	37.1	42.5	39.4	37.4	24.0	692.2	54.11	1.74	230.0	33.2	3.59
10:08	34.3	40.2	36.9	42.6	39.1	37.2	24.2	690.7	55.00	1.74	228.5	33.1	3.59
10:09	34.4	40.4	37.1	43.3	39.8	37.3	24.4	689.8	54.09	1.74	222.7	32.3	3.60
10:10	34.5	40.7	37.2	43.0	39.7	37.6	24.3	688.8	53.89	1.73	228.6	33.2	3.59
10:11	34.5	39.6	36.6	42.2	39.1	37.2	23.8	687.5	56.12	1.76	239.5	34.8	3.64
10:12	34.4	39.5	36.8	43.0	39.5	37.0	23.9	686.6	54.95	1.74	229.4	33.4	3.62
10:13	34.4	39.5	37.0	43.1	39.6	36.9	24.0	685.5	54.09	1.76	222.0	32.4	3.65
10:14	34.3	38.8	36.5	42.6	39.1	36.7	23.4	683.8	54.89	1.78	232.7	34.0	3.72
10:15	34.3	37.9	35.8	41.6	38.1	36.3	23.1	681.5	55.41	1.80	234.8	34.5	3.77
10:16	34.1	36.7	34.7	40.3	37.2	35.5	22.5	678.8	55.85	1.81	233.9	34.5	3.81
10:17	34.0	36.5	34.6	40.3	37.3	35.2	22.6	677.3	54.94	1.81	221.8	32.7	3.81
10:18	33.9	36.3	34.5	40.1	37.1	35.0	22.6	676.0	55.54	1.82	222.0	32.8	3.83
10:19	33.7	35.8	34.1	39.6	36.6	34.7	22.3	674.5	55.34	1.86	219.5	32.5	3.93
10:20	33.6	34.8	33.3	38.6	35.8	34.1	22.1	672.8	55.14	1.88	213.4	31.7	3.98
10:21	33.4	34.6	33.2	38.4	35.7	33.9	21.8	671.5	54.39	1.88	211.6	31.5	3.98
10:22	33.4	36.0	33.8	39.5	36.9	34.3	22.6	670.6	53.73	1.81	203.9	30.4	3.86
10:23	33.6	37.8	35.2	40.9	38.2	35.3	23.3	669.6	52.57	1.77	202.9	30.3	3.78
10:24	33.8	39.2	36.1	41.7	38.8	36.2	24.2	668.4	52.37	1.72	200.6	30.0	3.67
10:25	34.0	39.8	36.5	42.1	39.1	36.7	24.9	666.9	53.24	1.74	200.4	30.0	3.73
10:26	34.2	40.4	37.0	42.6	39.5	37.1	25.1	665.3	53.16	1.72	204.6	30.7	3.68
10:27	34.3	40.7	37.3	43.4	40.1	37.4	25.6	664.3	54.00	1.69	204.1	30.7	3.63
10:28	34.5	40.7	37.1	43.5	40.0	37.5	25.7	662.7	55.19	1.72	207.5	31.3	3.70
10:29	34.4	39.2	36.1	41.9	38.5	36.8	24.6	661.0	56.05	1.77	218.2	33.0	3.83
10:30	34.4	39.1	36.0	42.3	38.2	36.6	24.9	660.4	54.83	1.73	205.2	31.1	3.73
10:31	34.3	38.4	35.8	41.7	38.2	36.3	24.7	657.3	55.57	1.76	206.8	31.5	3.83
10:32	34.3	39.0	36.0	41.7	38.5	36.5	24.9	653.8	54.67	1.73	202.9	31.0	3.77
10:33	34.4	39.3	36.2	41.7	38.6	36.6	25.0	651.3	54.17	1.73	200.8	30.8	3.79
10:34	34.5	39.8	37.0	42.1	39.2	37.0	25.4	649.8	53.72	1.71	199.2	30.7	3.76
10:35	34.5	39.7	36.5	41.5	38.6	37.0	25.3	647.5	54.57	1.73	204.8	31.6	3.80
10:36	34.5	39.3	36.2	41.1	38.3	36.8	25.2	645.1	55.01	1.75	205.0	31.8	3.86
10:37	34.5	39.4	36.3	41.7	38.1	36.8	25.3	643.1	54.64	1.71	200.5	31.2	3.78
10:38	34.6	39.7	36.5	41.7	38.5	37.0	25.7	641.0	54.79	1.71	197.0	30.7	3.81
10:39	34.6	39.7	36.5	41.4	38.4	37.0	25.7	638.3	54.18	1.73	195.4	30.6	3.87
10:40	34.5	38.8	35.8	40.2	37.4	36.5	25.2	635.2	54.08	1.75	196.1	30.9	3.92
10:41	34.5	38.7	35.8	40.3	37.6	36.4	25.0	633.0	53.49	1.75	194.7	30.8	3.93
10:42	34.5	38.5	35.7	40.2	37.5	36.3	24.9	630.6	54.05	1.75	196.5	31.2	3.96
10:43	34.5	38.5	35.8	40.0	37.6	36.2	25.0	629.0	53.22	1.74	191.4	30.4	3.94
10:44	34.5	38.7	36.0	40.1	38.0	36.4	25.0	627.0	53.24	1.73	192.9	30.8	3.95
10:45	34.6	39.1	36.4	40.7	38.4	36.6	25.3	625.1	53.09	1.70	192.1	30.7	3.89
10:46	34.5	38.9	36.2	40.7	38.2	36.6	25.1	622.5	53.86	1.71	197.0	31.6	3.92
10:47	34.6	39.2	36.2	40.9	38.3	36.6	25.3	620.3	53.19	1.72	193.1	31.1	3.94
10:48	34.7	39.5	36.5	41.8	38.5	36.8	25.6	618.9	53.14	1.68	190.0	30.7	3.88
10:49	34.7	39.6	36.6	41.8	38.6	36.9	25.9	616.7	54.70	1.69	191.4	31.0	3.91
10:50	34.7	39.1	36.1	41.2	37.8	36.7	25.9	614.7	54.77	1.70	188.5	30.7	3.93
10:51	34.7	38.7	35.6	40.5	37.6	36.5	25.8	612.1	55.76	1.71	190.6	31.1	3.99
10:52	34.7	38.8	35.9	40.8	38.0	36.5	26.0	610.3	54.55	1.69	182.1	29.8	3.94
10:53	34.7	39.0	36.1	41.2	37.9	36.6	26.4	608.3	54.97	1.70	179.8	29.6	3.98
10:54	34.6	37.9	35.4	40.2	37.5	36.0	25.7	605.3	56.64	1.71	186.9	30.9	4.03
10:55	34.4	36.6	34.7	39.6	36.6	35.4	24.9	603.3	56.24	1.75	189.8	31.5	4.13
10:56	34.2	35.4	33.8	38.5	35.8	34.7	24.1	601.2	55.96	1.74	190.1	31.6	4.14
10:57	34.2	36.8	34.5	39.5	36.7	35.1	24.8	598.4	55.02	1.73	182.2	30.4	4.12
10:58	34.2	36.9	34.6	39.9	36.6	35.2	24.8	595.9	54.43	1.73	182.1	30.6	4.14
10:59	34.2	37.3	34.7	40.1	36.7	35.4	24.8	593.3	54.59	1.70	185.9	31.3	4.09
11:00	34.3	38.3	35.4	40.3	36.8	35.9	25.2	590.0	54.87	1.69	188.4	31.9	4.08
11:01	34.4	39.0	35.7	40.4	38.0	36.3	25.4	587.2	54.40	1.69	190.6	32.5	4.10
11:02	34.5	38.9	35.7	39.9	37.2	36.4	25.7	584.4	54.74	1.66	188.2	32.2	4.06
11:03	34.5	38.7	35.7	39.5	37.3	36.3	25.9	581.6	56.03	1.67	186.9	32.1	4.10

Time [h]	T <sub>wall</sub> [°C]	T <sub>col,1</sub> [°C]	T <sub>col,2</sub> [°C]	T <sub>col,3</sub> [°C]	T <sub>col,4</sub> [°C]	T <sub>out</sub> [°C]	T <sub>amb</sub> [°C]	G <sub>T,col</sub> [W/m <sup>2</sup> ]	Flow Rate [m <sup>3</sup> /h m <sup>2</sup> ]	P <sub>el</sub> [W]	Q'' <sub>u</sub> [W/m <sup>2</sup> ]	Eff <sub>th</sub> %	Eff <sub>PV</sub> %
12:00	32.9	33.9	32.3	36.7	34.0	33.0	27.3	403.0	54.58	1.46	100.2	24.9	5.17
12:01	32.9	34.0	32.2	36.7	33.8	33.0	27.8	399.4	55.17	1.46	93.3	23.4	5.22
12:02	32.8	33.7	32.0	36.4	33.7	32.9	27.7	396.3	55.08	1.47	92.5	23.3	5.28
12:03	32.7	33.1	31.3	35.7	32.8	32.5	27.0	392.1	55.83	1.46	99.6	25.4	5.32
12:04	32.5	32.6	30.7	35.0	32.3	32.1	26.5	387.6	55.47	1.45	100.5	25.9	5.34
12:05	32.5	33.4	31.1	35.4	32.9	32.4	26.5	383.7	55.16	1.43	105.8	27.6	5.33
12:06	32.5	33.9	31.6	35.9	33.2	32.6	26.9	379.9	54.50	1.41	100.9	26.6	5.28
12:07	32.5	34.0	31.5	35.7	33.1	32.8	26.9	376.0	54.89	1.40	104.5	27.8	5.30
12:08	32.5	33.9	31.5	35.9	33.2	32.7	27.3	373.0	55.05	1.39	96.1	25.8	5.30
12:09	32.5	33.5	31.4	35.6	32.9	32.6	27.4	369.5	55.09	1.39	91.6	24.8	5.36
12:10	32.4	33.1	31.1	35.6	33.0	32.3	27.3	366.8	55.38	1.37	88.5	24.1	5.33
12:11	32.5	34.1	31.9	36.1	33.5	32.7	28.1	364.0	53.83	1.36	80.9	22.2	5.31
12:12	32.5	34.0	31.9	35.7	33.2	32.8	28.7	360.4	55.24	1.35	73.4	20.4	5.32
12:13	32.4	33.5	31.3	35.3	32.6	32.5	28.6	356.4	55.15	1.35	71.0	19.9	5.40
12:14	32.2	32.6	30.7	34.8	32.1	32.0	27.9	352.4	55.65	1.35	73.6	20.9	5.46
12:15	32.1	32.2	30.4	34.7	32.0	31.7	27.3	349.2	55.80	1.34	78.5	22.5	5.48
12:16	32.0	32.1	30.3	34.6	31.9	31.6	27.3	342.5	54.74	1.32	76.2	22.2	5.50
12:17	32.0	32.8	30.7	35.0	32.3	31.8	27.7	342.7	54.84	1.32	74.0	21.6	5.51
12:18	32.0	33.1	30.9	35.3	32.7	32.0	28.4	339.8	54.39	1.31	64.0	18.8	5.49
12:19	32.1	33.4	31.2	35.2	32.8	32.2	28.6	335.6	54.37	1.30	63.8	19.0	5.51
12:20	32.0	33.2	30.9	34.8	32.3	32.1	27.8	333.0	55.03	1.28	76.1	22.9	5.46
12:21	32.0	32.7	30.5	34.6	31.9	31.9	27.6	311.7	54.73	1.26	76.3	24.5	5.75
12:22	31.8	31.7	29.9	33.7	31.1	31.3	26.8	313.8	56.14	1.27	81.4	25.9	5.76
12:23	31.6	31.1	29.5	33.3	30.8	30.9	26.4	319.9	55.05	1.26	80.4	25.1	5.61
12:24	31.5	31.2	29.5	33.4	31.0	30.8	26.6	317.6	54.73	1.25	73.8	23.2	5.61
12:25	31.5	31.6	29.6	33.7	31.2	30.9	27.2	313.4	54.62	1.23	66.1	21.1	5.59
12:26	31.5	31.8	29.6	34.0	31.4	31.0	27.5	307.2	54.54	1.21	61.3	19.9	5.64
12:27	31.5	32.2	30.1	34.3	31.8	31.2	28.3	300.5	54.54	1.19	52.0	17.3	5.63
12:28	31.5	32.8	30.6	34.6	32.2	31.6	29.0	293.8	54.26	1.17	46.6	15.9	5.67
12:29	31.6	33.0	30.8	34.7	32.2	31.8	29.1	284.0	54.60	1.12	48.2	17.0	5.65
12:30	31.6	32.9	30.9	34.4	32.2	31.8	29.4	293.7	54.46	1.16	43.1	14.7	5.62
12:31	31.6	32.7	30.6	34.4	31.9	31.7	29.8	289.8	54.83	1.14	34.4	11.9	5.60
12:32	31.5	32.4	30.3	34.2	31.5	31.5	29.4	285.3	55.24	1.13	38.5	13.5	5.66
12:33	31.4	31.4	29.5	33.3	30.6	31.0	28.8	280.5	55.86	1.13	41.2	14.7	5.76
12:34	31.2	30.8	29.0	32.6	30.1	30.5	27.5	277.0	55.97	1.11	55.3	20.0	5.71
12:35	31.1	30.9	29.1	32.6	30.2	30.4	27.2	273.9	55.23	1.11	57.9	21.1	5.78
12:36	31.0	30.8	28.9	32.5	30.1	30.4	27.4	249.4	55.61	1.03	54.5	21.9	5.88
12:37	30.9	30.0	28.3	31.6	29.0	30.0	26.8	239.0	55.97	1.01	58.0	24.3	6.05
12:38	30.7	29.4	27.9	30.7	28.4	29.5	26.3	243.0	55.48	0.97	57.6	23.7	5.85
12:39	30.5	28.9	27.5	30.2	28.3	29.1	26.1	251.0	55.46	1.06	53.6	21.4	6.02
12:40	30.3	28.7	27.4	30.1	28.3	28.9	26.0	251.5	55.00	1.05	52.6	20.9	5.97
12:41	30.2	28.3	27.0	29.8	27.9	28.7	25.8	251.8	55.40	1.07	53.1	21.1	6.03
12:42	30.0	28.0	26.9	29.6	27.9	28.4	25.7	248.6	55.23	1.05	48.9	19.7	6.03
12:43	30.0	28.3	27.2	29.9	28.2	28.5	26.0	244.9	55.08	1.02	45.6	18.6	5.96
12:44	29.9	28.7	27.3	30.2	28.3	28.6	26.2	241.6	54.91	1.01	43.5	18.0	5.96
12:45	29.9	28.9	27.3	30.4	28.3	28.7	26.5	238.0	54.50	0.99	39.3	16.5	5.94
12:46	29.8	28.7	27.2	30.2	28.0	28.6	26.1	233.9	54.48	0.98	46.0	19.7	5.99
12:47	29.7	28.9	27.5	30.5	28.4	28.7	26.5	230.9	54.03	0.96	39.2	17.0	5.96
12:48	29.8	29.3	27.8	30.9	28.7	28.9	27.3	227.5	53.89	0.95	28.3	12.4	5.94
12:49	29.7	29.5	27.6	30.7	28.6	29.0	26.9	220.5	53.77	0.92	37.4	17.0	5.98
12:50	29.7	29.6	27.7	30.9	28.7	29.1	27.3	219.2	54.17	0.92	32.2	14.7	5.98
12:51	29.8	29.9	28.1	31.4	29.3	29.3	28.1	216.7	53.42	0.92	20.0	9.2	6.04
12:52	29.8	30.1	28.2	31.5	29.4	29.4	28.6	212.7	53.37	0.89	14.6	6.9	5.97
12:53	29.8	30.2	28.5	31.4	29.5	29.6	28.9	209.9	54.18	0.88	11.8	5.6	6.01
12:54	29.9	30.1	28.4	31.2	29.4	29.6	28.8	206.1	53.61	0.88	14.2	6.9	6.10
12:55	29.7	29.4	27.8	30.6	28.7	29.2	28.5	202.4	54.45	0.87	12.0	5.9	6.10
12:56	29.6	29.1	27.5	30.5	28.4	28.9	28.4	199.0	54.90	0.86	8.8	4.4	6.19
12:57	29.5	28.8	27.2	30.2	28.1	28.6	28.3	195.5	54.08	0.85	5.9	3.0	6.23
12:58	29.5	29.1	27.6	30.4	28.4	28.8	28.8	189.3	54.31	0.84	0.0	0.0	6.29
12:59	29.4	28.6	27.1	29.8	27.8	28.5	28.2	179.2	54.61	0.80	5.7	3.2	6.39
13:00	29.3	27.9	26.6	29.0	27.2	28.2	27.1	178.1	55.12	0.79	18.3	10.3	6.35

# Appendix F

## Uncertainty Analysis

### F.1 Introduction

The uncertainty of a measured quantity  $v$ ,  $u_v$ , is due to both bias and precision errors. The bias error,  $e_{bias}$ , refers to the accuracy and calibration error of the instrument while the precision error,  $e_{precision}$ , is related to the repeatability of the measurement.

$$u_v = \pm (e_{bias}^2 + e_{precision}^2)^{\frac{1}{2}}$$

This experiment was performed outdoors and only a limited amount of time was available to take measurements. Thus, it was not possible to get the same weather conditions several times and repeat the measurements of the variables to evaluate the precision error. Consequently, only the bias error was considered in the calculation of the uncertainty. The uncertainty for the bias error can be calculated using the method developed by Kline and McClintock (1953) that states that if  $R$  is a linear function of  $n$  independent normally distributed variables known as  $v_i$

$$R = R(v_1, v_2, v_3, \dots, v_n)$$

the uncertainty of  $R$ ,  $\delta R$ , is related to the uncertainties of each variable  $i$ ,  $\delta v_i$  with

the following function, known as the second-power equation.

$$\delta_R = \left[ \left( \frac{\partial R}{\partial v_1} \delta v_1 \right)^2 + \left( \frac{\partial R}{\partial v_2} \delta v_2 \right)^2 + \dots + \left( \frac{\partial R}{\partial v_n} \delta v_n \right)^2 \right]^{\frac{1}{2}} \quad (\text{F.1})$$

This section presents a sample calculation of the uncertainty analysis on a set of measured variables as well as their impact on the uncertainty of the calculated quantities.

## F.2 Measured Quantities

The measured quantities used in the sample calculation of the uncertainty analysis are shown in Table F.1.

**Table F.1:** Values of the measured variables used in the uncertainty analysis

Variable	Value	Variable	Value
$T_{wall}$	34.3°C	$L$	2.49 m
$T_{amb}$	19.2°C	$W$	1.05 m
$T_{col,1}$	40.2°C	$L_{PV}$	102.5 mm
$T_{col,2}$	36.9°C	$W_{PV}$	17.1 mm
$T_{col,3}$	42.5°C	$P_{amb}$	101.826 kPa
$T_{col,4}$	39.3°C	$V_{\dot{V}}$	2.58 V
$T_{out}$	37.2°C	$V_{G_{T,col}}$	1.62 V
$V_{PV}$	1.037 V	$V_{Rsh}$	0.168 V

### F.2.1 PV Cells Dimensions

The width and length of the PV cells bits were stated by the manufacturer to have a tolerance of  $\pm 1$  mm. Thus, the uncertainty on the PV cells width ( $W_{PV}$ )

and length ( $L_{PV}$ ) are given as

$$\frac{\delta L_{PV}}{L_{PV}} = \pm \frac{1 \text{ mm}}{102.5 \text{ mm}} = \pm 0.01 \quad (\text{F.2})$$

$$\frac{\delta W_{PV}}{W_{PV}} = \pm \frac{1 \text{ mm}}{17.1 \text{ mm}} = \pm 0.06 \quad (\text{F.3})$$

## F.2.2 Panel Dimensions

The width and length of the collector were measured with a measuring tape. Taking the error on these measurements to be half of the smallest division of the measuring tape, the uncertainties on the collector width and length correspond to

$$\frac{\delta L}{L} = \pm \frac{0.0005 \text{ m}}{2.49 \text{ m}} = \pm 0.0002 \quad (\text{F.4})$$

$$\frac{\delta W}{W} = \pm \frac{0.0005 \text{ m}}{1.05 \text{ m}} = \pm 0.0005 \quad (\text{F.5})$$

## F.2.3 Barometric Pressure

The barometric pressure was taken from the measurements recorded at the Waterloo Weather Station with a Setra 270 pressure transducer. The accuracy of this instrument was  $\pm 0.2$  mb (Waterloo Weather Station, 2007) and the uncertainty of the ambient pressure corresponds to

$$\delta P_{amb} = \pm 20 \text{ Pa}$$

or

$$\frac{\delta P_{amb}}{P_{amb}} = \pm \frac{20 \text{ Pa}}{101826 \text{ Pa}} = \pm 0.002 \quad (\text{F.6})$$

## F.2.4 Voltage Measurements

The voltage across the PV module was measured with a Fluke 29 multimeter with an accuracy of  $\pm 0.3\%$  while the voltage across the shunt resistance was read from a Omega HHM26 multimeter. The accuracy of this meter in the range of

2.5 V was stated to be  $\pm (0.25\% * \text{Reading} + 1 \text{ digit})$  and its resolution was  $100 \mu\text{V}$ . With this information, the uncertainties on the voltage measurements can be written as

$$\frac{\delta V_{PV}}{V_{PV}} = \pm 0.003 \quad (\text{F.7})$$

$$\frac{\delta V_{Rsh}}{V_{Rsh}} = \frac{\pm (0.0025 * 0.168 \text{ V} + 0.0001\text{V})}{0.168 \text{ V}} = \pm 0.003 \quad (\text{F.8})$$

## F.2.5 Shunt Resistance

The shunt resistance had a value of  $0.1\Omega$  and an accuracy of  $\pm 5\%$ . Therefore, its uncertainty is given as

$$\frac{\delta R_{sh}}{R_{sh}} = \pm 0.05 \quad (\text{F.9})$$

## F.2.6 Irradiance on the East Wall

The total irradiance on the east wall,  $G_{T,col}$ , was obtained from the voltage output of a Eppley pyranometer model 8-48 amplified by a USEA amplifier set to a gain of 200. The voltage signal recorded by the data logger,  $V_{G_{T,col}}$ , was converted in solar radiation units using the following relation.

$$G_{T,col} = \frac{V_{G_{T,col}} [\text{V}]}{200 * 11.8 * 10^{-6} [\text{V}/\text{Wm}^{-2}]}$$

By expressing the uncertainty on the irradiation measurement as the root-sum-square combination of each individual error, the following can be written.

$$\frac{\delta G_{T,col}}{G_{T,col}} = \left[ \left( \frac{\delta V_{PYR}}{V_{PYR}} \right)^2 + \left( \frac{\delta V_{AMP}}{V_{AMP}} \right)^2 + \left( \frac{\delta V_{G_{T,col}}}{V_{G_{T,col}}} \right)^2 \right]^{\frac{1}{2}} \quad (\text{F.10})$$

In Equation F.10,  $\delta V_{PYR}$ ,  $\delta V_{AMP}$ , and  $\delta V_{G_{T,col}}$  are the uncertainties of the pyranometer, amplifier and data logger, respectively. The pyranometer was linear to

within  $\pm 1\%$ . Therefore  $\delta V_{PYR}$  is given as

$$\frac{\delta V_{PYR}}{V_{PYR}} = \pm 0.01 \quad (\text{F.11})$$

From the data logger specifications, the accuracy of the voltage output is given as

$$\delta V_{G_{T,col}} = \pm (0.0001 * V_{G_{T,col}} + 0.00002 * \text{Range}) \quad (\text{F.12})$$

The range selected for the irradiance measurement was -2.5 V to 2.5 V. Using Equation F.12, the uncertainty of  $V_{G_{T,col}}$  corresponds to

$$\frac{\delta V_{G_{T,col}}}{V_{G_{T,col}}} = \pm \left( 0.0001 + \frac{0.00002 * 5 \text{ V}}{1.63 \text{ V}} \right) = \pm 0.000161 \quad (\text{F.13})$$

The amplifier had an output offset voltage of  $\pm 3$  mV. Thus, its uncertainty is given as

$$\frac{\delta V_{AMP}}{V_{AMP}} = \pm \frac{0.003 \text{ V}}{1.63 \text{ V}} = \pm 0.00185 \quad (\text{F.14})$$

Using the results of Equations F.11, F.13 and F.14 into Equation F.10, the total uncertainty on the irradiation measurement corresponds to

$$\frac{\delta G_{T,col}}{G_{T,col}} = \pm [(0.01)^2 + (0.00185)^2 + (0.000161)^2]^{\frac{1}{2}} = \pm 0.01 \quad (\text{F.15})$$

## F.2.7 Standard Volumetric Flowrate Measurement

The standard air volumetric flowrate in the duct,  $\dot{V}_{std}$ , was measured with the Sierra 620S insertion mass flowmeter and transmitted as a DC voltage signal to the Personal Daq/56. The volumetric flowrate at standard conditions was calculated from the data logger voltage output,  $V_{\dot{V}}$ , with the following relation

$$\dot{V}_{std} = \frac{V_{\dot{V}} [\text{V}] * 155 \text{ SCFM}}{5 \text{ V}}$$

The uncertainty on the volumetric flowrate can be expressed as the root-sum-square

combination of each individual error. In this case, the voltage signal of the flowmeter was the same than the voltage output of the data logger. Therefore,  $\delta\dot{V}_{std}$  is given as

$$\frac{\delta\dot{V}_{std}}{\dot{V}_{std}} = \pm \left[ \left( \frac{\delta V_{FM}}{V_{\dot{V}}} \right)^2 + \left( \frac{\delta V_{\dot{V}}}{V_{\dot{V}}} \right)^2 \right]^{\frac{1}{2}} \quad (\text{F.16})$$

where  $\delta V_{FM}$  and  $\delta V_{\dot{V}}$  are the uncertainties of the flowmeter and the data logger, respectively. From the calibration certificate, the accuracy of the flowmeter corresponds to

$$\delta V_{FM} = \pm (0.01 * \text{Full Scale Voltage Output} + 0.005 * V_{\dot{V}}) \quad (\text{F.17})$$

The full scale voltage of the flowmeter was 5 V according to the flowmeter calibration certificate. Therefore, from Equation F.17, the uncertainty on the flowmeter measurement can be written as

$$\frac{\delta V_{FM}}{V_{\dot{V}}} = \pm \left( \frac{0.01 * 5 + 0.005 * V_{\dot{V}}}{V_{\dot{V}}} \right) = \pm \left( \frac{0.01 * 5 + 0.005 * 2.58}{2.58} \right) = \pm 0.024 \quad (\text{F.18})$$

From the data logger specifications, the accuracy of the voltage output is given by

$$\delta V_{\dot{V}} = \pm (0.0001 * V_{\dot{V}} + 0.00002 * \text{Range}) \quad (\text{F.19})$$

The range selected for the irradiance measurement was -5 V to 5 V. Using Equation F.19, the uncertainty of  $V_{\dot{V}}$  can be expressed as

$$\frac{\delta V_{\dot{V}}}{V_{\dot{V}}} = \pm \left( 0.0001 + \frac{0.00002 * 10 \text{ V}}{2.58 \text{ V}} \right) = \pm 0.00018 \quad (\text{F.20})$$

Using the results of Equations F.18 and F.20 into Equation F.16, the total uncertainty on the volumetric flowrate measurement corresponds to

$$\frac{\delta\dot{V}_{std}}{\dot{V}_{std}} = \pm [(0.024)^2 + (0.00018)^2]^{\frac{1}{2}} = \pm 0.024 \quad (\text{F.21})$$

## F.2.8 Temperature Measurements

The temperature measurements were done using Omega type T thermocouples with an accuracy of  $\pm 1^\circ\text{C}$ . For the data logger, the cold junction calibration error and the accuracy for the measurement of type T thermocouples were stated to be  $\pm 0.5^\circ\text{C}$  and  $\pm 0.4^\circ\text{C}$ , respectively. Therefore, the uncertainty of the measured temperatures are given as

$$\begin{aligned}\delta T &= \pm [1^2 + 0.5^2 + 0.4^2]^{\frac{1}{2}} = \pm 1.2^\circ\text{C} \\ \delta T_{wall} &= \delta T_{amb} = \delta T_{out} = \delta T_{col,1} = \pm 1.2^\circ\text{C} \\ \delta T_{col,2} &= \delta T_{col,3} = \delta T_{col,4} = \pm 1.2^\circ\text{C}\end{aligned}\tag{F.22}$$

## F.3 Calculated Quantities

Table F.2 presents the values of the variables calculated with the measured quantities listed in the previous section.

**Table F.2:** Values of the calculated variables used in the uncertainty analysis

Variable	Value	Variable	Value
$A_{PV}$	0.07 m <sup>2</sup>	$\rho$	1.14 kg/m <sup>3</sup>
$A_{col,proj}$	2.61 m <sup>2</sup>	$\dot{V}_{act}$	83.8 ACFM
$P_{el}$	1.74 W	$\dot{V}$	54.55 m <sup>3</sup> /h·m <sup>2</sup>
$T_{rise}$	18.1°C	$\dot{m}$	162.31 kg/h
$T_{rise,b}$	19.4 °C	$\dot{Q}_u$	313.6 W/m <sup>2</sup>
$\eta_{PV}$	3.6 %	$\eta_{th}$	45.7%
$I$	1.68 A		

### F.3.1 PV Cells Area

The total area of the PV cells was calculated with the following equation.

$$A_{PV} = 40 * W_{PV} L_{PV}$$

Using Equation F.1, the uncertainty on the PV cells area can be expressed as

$$\delta A_{PV} = \pm \left[ \left( \frac{\partial A_{PV}}{\partial W_{PV}} \delta W_{PV} \right)^2 + \left( \frac{\partial A_{PV}}{\partial L_{PV}} \delta L_{PV} \right)^2 \right]^{\frac{1}{2}} \quad (\text{F.23})$$

Simplifying Equation F.23, the following relation is obtained.

$$\frac{\delta A_{PV}}{A_{PV}} = \pm \left[ \left( \frac{\delta W_{PV}}{W_{PV}} \right)^2 + \left( \frac{\delta L_{PV}}{L_{PV}} \right)^2 \right]^{\frac{1}{2}} \quad (\text{F.24})$$

Substituting Equations F.2 and F.3 into Equation F.24, the uncertainty on the PV cells area can be calculated.

$$\frac{\delta A_{PV}}{A_{PV}} = \pm [(0.06)^2 + (0.01)^2]^{\frac{1}{2}} = \pm 0.06 \quad (\text{F.25})$$

### F.3.2 Collector Projected Area

The collector projected area was obtained with the following equation.

$$A_{col,proj} = WL$$

The uncertainty on the calculation of the projected area can consequently be expressed as

$$\delta A_{col,proj} = \pm \left[ \left( \frac{\partial A_{col,proj}}{\partial W} \delta W \right)^2 + \left( \frac{\partial A_{col,proj}}{\partial L} \delta L \right)^2 \right]^{\frac{1}{2}} \quad (\text{F.26})$$

Simplifying Equation F.26, a new expression for  $\delta A_{col,proj}$  can be obtained.

$$\frac{\delta A_{col,proj}}{A_{col,proj}} = \pm \left[ \left( \frac{\delta W}{W} \right)^2 + \left( \frac{\delta L}{L} \right)^2 \right]^{\frac{1}{2}} \quad (\text{F.27})$$

Using the results of Equations F.4 and F.5 into Equation F.27,  $\delta A_{col,proj}$  can be

calculated.

$$\frac{\delta A_{col,proj}}{A_{col,proj}} = \pm [(0.0002)^2 + (0.0005)^2]^{\frac{1}{2}} = \pm 0.0005 \quad (\text{F.28})$$

### F.3.3 Maximum Electrical Power

From Ohms law, the current in the circuit is given as

$$I = \frac{V_{Rsh}}{R_{sh}} = V_{Rsh} R_{sh}^{-1}$$

Therefore, the uncertainty associated with the calculation of the current corresponds to

$$\delta I = \pm \left[ \left( \frac{\partial I}{\partial V_{Rsh}} \delta V_{Rsh} \right)^2 + \left( \frac{\partial I}{\partial R_{sh}} \delta R_{sh} \right)^2 \right]^{\frac{1}{2}} \quad (\text{F.29})$$

Simplifying Equation F.29, the uncertainty on the current becomes

$$\frac{\delta I}{I} = \pm \left[ \left( \frac{\delta V_{Rsh}}{V_{Rsh}} \right)^2 + \left( \frac{-\delta R_{sh}}{R_{sh}} \right)^2 \right]^{\frac{1}{2}} \quad (\text{F.30})$$

Substituting the results from Equations F.8 and F.9 into Equation F.30, the uncertainty on the current can be calculated.

$$\frac{\delta I}{I} = \pm [(0.003)^2 + (-0.05)^2]^{\frac{1}{2}} = \pm 0.05 \quad (\text{F.31})$$

From Ohms law, the electrical power generated by the PV cells is expressed as

$$P_{el} = IV_{PV}$$

Thus, the uncertainty on the maximum electrical power is

$$\delta P_{el} = \pm \left[ \left( \frac{\partial P_{el}}{\partial V_{PV}} \delta V_{PV} \right)^2 + \left( \frac{\partial P_{el}}{\partial I} \delta I \right)^2 \right]^{\frac{1}{2}} \quad (\text{F.32})$$

Re-arranging Equation F.32, the uncertainty on the power becomes

$$\frac{\delta P_{el}}{P_{el}} = \pm \left[ \left( \frac{\delta V_{PV}}{V_{PV}} \right)^2 + \left( \frac{\delta I}{I} \right)^2 \right]^{\frac{1}{2}} \quad (\text{F.33})$$

Using the results from Equations F.7 and F.31,  $\delta P_{el}$  corresponds to

$$\frac{\delta P_{el}}{P_{el}} = \pm [(0.003)^2 + (0.05)^2]^{\frac{1}{2}} = \pm 0.05 \quad (\text{F.34})$$

### F.3.4 Air Temperature Rise

The air temperature rise is given as

$$T_{rise} = T_{out} - T_{amb}$$

The uncertainty on  $T_{rise}$  can be obtained from

$$\delta T_{rise} = \pm \left[ \left( \frac{\partial T_{rise}}{\partial T_{out}} \delta T_{out} \right)^2 + \left( \frac{\partial T_{rise}}{\partial T_{amb}} \delta T_{amb} \right)^2 \right]^{\frac{1}{2}} \quad (\text{F.35})$$

Re-arranging Equation F.35,

$$\frac{\delta T_{rise}}{T_{rise}} = \pm \left[ \left( \frac{\delta T_{out}}{T_{rise}} \right)^2 + \left( \frac{-\delta T_{amb}}{T_{rise}} \right)^2 \right]^{\frac{1}{2}} \quad (\text{F.36})$$

Replacing the known variables in Equation F.36,  $\delta T_{rise}$  can be calculated.

$$\frac{\delta T_{rise}}{T_{rise}} = \pm \left[ \left( \frac{1.2^\circ C}{18.1^\circ C} \right)^2 + \left( \frac{-1.2^\circ C}{18.1^\circ C} \right)^2 \right]^{\frac{1}{2}} = 0.094 \quad (\text{F.37})$$

### F.3.5 Upper Panel Temperature Rise

The upper panel temperature rise is given as

$$T_{rise,b} = T_{up,avg} - T_{amb}$$

where  $T_{up,avg}$  is the average temperature measured on the upper panel. The uncertainty for  $T_{rise,b}$  is given as

$$\delta T_{rise,b} = \pm \left[ \left( \frac{\partial T_{rise,b}}{\partial T_{up,avg}} \delta T_{up,avg} \right)^2 + \left( \frac{\partial T_{rise,b}}{\partial T_{amb}} \delta T_{amb} \right)^2 \right]^{\frac{1}{2}} \quad (\text{F.38})$$

Simplifying Equation F.38,

$$\frac{\delta T_{rise,b}}{T_{rise,b}} = \pm \left[ \left( \frac{\delta T_{up,avg}}{T_{rise,b}} \right)^2 + \left( \frac{-\delta T_{amb}}{T_{rise,b}} \right)^2 \right]^{\frac{1}{2}} \quad (\text{F.39})$$

Replacing the variables of Equation F.39 with their respective values, the uncertainty of  $\delta T_{rise,b}$  corresponds to

$$\frac{\delta T_{rise,b}}{T_{rise,b}} = \pm \left[ \left( \frac{1.2^\circ C}{19.4^\circ C} \right)^2 + \left( \frac{-1.2^\circ C}{19.4^\circ C} \right)^2 \right]^{\frac{1}{2}} = \pm 0.087$$

### F.3.6 PV Cells Efficiency

The PV cells efficiency is calculated with the following expression.

$$\eta_{PV} = \frac{P_{el}}{G_{T,col} A_{PV}}$$

Therefore, the uncertainty on the PV cells efficiency can be expressed as

$$\delta \eta_{PV} = \pm \left[ \left( \frac{\partial \eta_{PV}}{\partial G_{T,col}} \delta G_{T,col} \right)^2 + \left( \frac{\partial \eta_{PV}}{\partial P_{el}} \delta P_{el} \right)^2 + \left( \frac{\partial \eta_{PV}}{\partial A_{PV}} \delta A_{PV} \right)^2 \right]^{\frac{1}{2}} \quad (\text{F.40})$$

Simplifying Equation F.40,

$$\frac{\delta\eta_{PV}}{\eta_{PV}} = \pm \left[ \left( \frac{-\delta G_{T,col}}{G_{T,col}} \right)^2 + \left( \frac{\delta P_{el}}{P_{el}} \right)^2 + \left( \frac{-\delta A_{PV}}{A_{PV}} \right)^2 \right]^{\frac{1}{2}} \quad (\text{F.41})$$

Substituting the results from Equations F.15, F.34 and F.25 into Equation F.41, the uncertainty associated with the calculation of the PV cells efficiency corresponds to

$$\frac{\delta\eta_{PV}}{\eta_{PV}} = \pm [(-0.01)^2 + (0.05)^2 + (-0.06)^2]^{\frac{1}{2}} = \pm 0.08$$

### F.3.7 Air Density

The density of air is calculated with the following expression.

$$\rho = \frac{P_{amb}}{RT_{out}}$$

Taking  $R$  to be a constant, the uncertainty on  $\rho$  is given as

$$\delta\rho = \pm \left[ \left( \frac{\partial\rho}{\partial P_{amb}} \delta P_{amb} \right)^2 + \left( \frac{\partial\rho}{\partial T_{out}} \delta T_{out} \right)^2 \right]^{\frac{1}{2}} \quad (\text{F.42})$$

Simplifying F.42,

$$\frac{\delta\rho}{\rho} = \pm \left[ \left( \frac{\delta P_{amb}}{P_{amb}} \right)^2 + \left( -\frac{\delta T_{out}}{T_{out}} \right)^2 \right]^{\frac{1}{2}} \quad (\text{F.43})$$

Using Equations F.6 and F.22, the uncertainty of  $\rho$  corresponds to

$$\frac{\delta\rho}{\rho} = \pm \left[ \left( \frac{20}{101826} \right)^2 + \left( -\frac{1.2}{37.2} \right)^2 \right]^{\frac{1}{2}} = \pm 0.03 \quad (\text{F.44})$$

### F.3.8 Actual Volumetric Flowrate

The actual volumetric flowrate is obtained from the standard volumetric flowrate with the relation

$$\dot{V}_{act} = \dot{V}_{std} * \left[ \frac{P_{std}}{P_{act}} \right] \left[ \frac{T_{act}}{T_{std}} \right] \quad (\text{F.45})$$

In the flowmeter calibration certificate, it is stated that  $P_{std} = 14.7$  psia and  $T_{std} = 530^{\circ}R$ . It has been shown that taking the temperature of the air at the probe insertion point to be equal to the air temperature measured at the collector outlet is a valid assumption, therefore  $T_{act} = T_{out}$ . Taking the pressure in the duct to be the same as the ambient pressure, Equation F.45 can be re-written as

$$\dot{V}_{act} = \dot{V}_{std} * \left[ \frac{P_{std}}{P_{amb}} \right] \left[ \frac{T_{out}}{T_{std}} \right]$$

and the uncertainty on the actual volumetric flowrate can be expressed as

$$\delta\dot{V}_{act} = \pm \left[ \left( \frac{\partial\dot{V}_{act}}{\partial\dot{V}_{std}} \delta\dot{V}_{std} \right)^2 + \left( \frac{\partial\dot{V}_{act}}{\partial P_{amb}} \delta P_{amb} \right)^2 + \left( \frac{\partial\dot{V}_{act}}{\partial T_{out}} \delta T_{out} \right)^2 \right]^{\frac{1}{2}} \quad (\text{F.46})$$

Simplifying Equation F.46, the uncertainty of  $\dot{V}_{act}$  corresponds to

$$\frac{\delta\dot{V}_{act}}{\dot{V}_{act}} = \pm \left[ \left( \frac{\delta\dot{V}_{std}}{\dot{V}_{std}} \right)^2 + \left( \frac{\delta P_{amb}}{P_{amb}} \right)^2 + \left( \frac{\delta T_{out}}{T_{out}} \right)^2 \right]^{\frac{1}{2}} \quad (\text{F.47})$$

Substituting the results from Equations F.21, F.6 and F.22 into Equation F.47,

$$\frac{\delta\dot{V}_{act}}{\dot{V}_{act}} = \pm \left[ (0.024)^2 + \left( \frac{20 \text{ Pa}}{101826 \text{ Pa}} \right)^2 + \left( \frac{1.2 \text{ }^{\circ}C}{37.2 \text{ }^{\circ}C} \right)^2 \right]^{\frac{1}{2}} = \pm 0.03 \quad (\text{F.48})$$

### F.3.9 Volumetric Flowrate per Unit Area

The volumetric flowrate per unit of collector projected area is calculated as follows

$$\dot{V} = \dot{V}_{act}[\text{CFM}] * \frac{0.028317 \text{ [m}^3/\text{min]}}{\text{CFM}} * \frac{60 \text{ min}}{\text{hr}} * \frac{1}{A_{col,proj} \text{ [m}^2]}$$

Thus, the uncertainty on  $\dot{V}$  corresponds to

$$\delta\dot{V} = \pm \left[ \left( \frac{\partial\dot{V}}{\partial\dot{V}_{act}} \delta\dot{V}_{act} \right)^2 + \left( \frac{\partial\dot{V}}{\partial A_{col,proj}} \delta A_{col,proj} \right)^2 \right]^{\frac{1}{2}} \quad (\text{F.49})$$

Simplifying Equation F.49, the following is obtained.

$$\frac{\delta\dot{V}}{\dot{V}} = \pm \left[ \left( \frac{\delta\dot{V}_{act}}{\dot{V}_{act}} \right)^2 + \left( \frac{\delta A_{col,proj}}{A_{col,proj}} \right)^2 \right]^{\frac{1}{2}} \quad (\text{F.50})$$

Using Equations F.48 and F.28 into Equation F.50,  $\delta\dot{V}$  can be calculated.

$$\frac{\delta\dot{V}}{\dot{V}} = \pm [(0.03)^2 + (0.0005)^2]^{\frac{1}{2}} = \pm 0.03$$

### F.3.10 Mass Flowrate

The mass flowrate of the air in the duct is given as

$$\dot{m} = \dot{V}_{act}[\text{CFM}] * \frac{0.028317 \text{ [m}^3/\text{min]}}{\text{CFM}} * \frac{60 \text{ min}}{\text{h}} * \rho \left[ \frac{\text{kg}}{\text{m}^3} \right]$$

The uncertainty on  $\dot{m}$  can therefore be expressed as

$$\delta\dot{m} = \pm \left[ \left( \frac{\partial\dot{m}}{\partial\dot{V}_{act}} \delta\dot{V}_{act} \right)^2 + \left( \frac{\partial\dot{m}}{\partial\rho} \delta\rho \right)^2 \right]^{\frac{1}{2}} \quad (\text{F.51})$$

Simplifying Equation F.51,  $\delta\dot{m}$  corresponds to

$$\frac{\delta\dot{m}}{\dot{m}} = \pm \left[ \left( \frac{\delta\dot{V}_{act}}{\dot{V}_{act}} \right)^2 + \left( \frac{\delta\rho}{\rho} \right)^2 \right]^{\frac{1}{2}} \quad (\text{F.52})$$

Using the results from Equations F.48 and F.44 into Equation F.52, the following is obtained.

$$\frac{\delta\dot{m}}{\dot{m}} = \pm [(0.03)^2 + (0.03)^2]^{\frac{1}{2}} = \pm 0.04 \quad (\text{F.53})$$

### F.3.11 Thermal Output

The thermal output is given as

$$\dot{Q}_u'' = \frac{\dot{m}c_p(T_{out} - T_{amb})}{A_{col,proj}} = \frac{\dot{m}c_p T_{rise}}{A_{col,proj}}$$

Taking  $c_p$  to be a constant and equal to 1005 J/kgK, the uncertainty of  $\dot{Q}_u''$  can be expressed as

$$\delta\dot{Q}_u'' = \pm \left[ \left( \frac{\partial\dot{Q}_u''}{\partial\dot{m}} \delta\dot{m} \right)^2 + \left( \frac{\partial\dot{Q}_u''}{\partial T_{rise}} \delta T_{rise} \right)^2 + \left( \frac{\partial\dot{Q}_u''}{\partial A_{col,proj}} \delta A_{col,proj} \right)^2 \right]^{\frac{1}{2}} \quad (\text{F.54})$$

Simplifying Equation F.54,  $\delta\dot{Q}_u''$  corresponds to

$$\frac{\delta\dot{Q}_u''}{\dot{Q}_u''} = \pm \left[ \left( \frac{\delta\dot{m}}{\dot{m}} \right)^2 + \left( \frac{\delta T_{rise}}{T_{rise}} \right)^2 + \left( \frac{-\delta A_{col,proj}}{A_{col,proj}} \right)^2 \right]^{\frac{1}{2}} \quad (\text{F.55})$$

Using Equations F.53 and F.37 into Equation F.55, the uncertainty of  $\dot{Q}_u''$  can be

calculated.

$$\frac{\delta \dot{Q}_u''}{\dot{Q}_u''} = \pm [(0.04)^2 + (0.094)^2 + (-0.0005)^2]^{\frac{1}{2}} = \pm 0.1 \quad (\text{F.56})$$

### F.3.12 Thermal Efficiency

The collector thermal efficiency is given as

$$\eta_{th} = \frac{\dot{m}c_p(T_{out} - T_{amb})}{G_{T,col}A_{col,proj}} = \frac{\dot{Q}_u}{G_{T,col}A_{col,proj}} = \frac{\dot{Q}_u''}{G_{T,col}}$$

Therefore, the uncertainty of  $\eta_{th}$  corresponds to

$$\delta \eta_{th} = \pm \left[ \left( \frac{\partial \eta_{th}}{\partial \dot{Q}_u''} \delta \dot{Q}_u'' \right)^2 + \left( \frac{\partial \eta_{th}}{\partial G_{T,col}} \delta G_{T,col} \right)^2 \right]^{\frac{1}{2}} \quad (\text{F.57})$$

Equation F.57 can be simplified into

$$\frac{\delta \eta_{th}}{\eta_{th}} = \pm \left[ \left( \frac{\delta \dot{Q}_u''}{\dot{Q}_u''} \right)^2 + \left( \frac{-\delta G_{T,col}}{G_{T,col}} \right)^2 \right]^{\frac{1}{2}} \quad (\text{F.58})$$

Substituting Equations F.56, F.15 and F.28 into Equation F.58, the uncertainty on the thermal efficiency can be obtained.

$$\frac{\delta \eta_{th}}{\eta_{th}} = \pm [(0.1)^2 + (-0.01)^2]^{\frac{1}{2}} = \pm 0.1$$

# Appendix G

## Radiation Converter Component

### Fortran Code

```

SUBROUTINE TYPE202 (TIME,XIN,OUT,T,DTDT,PAR,INFO,ICNTRL,*)
C*****
C Object: 202
C Simulation Studio Model: Type202
C
C TRNSYS Subroutine, RADIATION CONVERTER
C
C This subroutine 'untilts' radiation data measured on the
C tilted surface to the horizontal surface value
C needed for input into the TRNSYS radiation processor.
C
C Original component developed by Ann L. Barrett, 1987
C Modified by Veronique Delisle, 2007
C ***
C *** Model Parameters
C ***
C      n=Day number for beginning simulation          - [0;366]
C      Latitude - [-Inf;+Inf]
C      Collector Slope - [-Inf;+Inf]
C      Ground reflectance - [0;1]
C      Time shift - [-Inf;+Inf]
C      Surface azimuth angle - [-Inf;+Inf]
C ***
C *** Model Inputs
C ***
C      Total radiation on the tilted surface - [-Inf;+Inf]
C      Civil time - [-Inf;+Inf]
C      Advanced Time? Yes=1, No=0
C ***
C *** Model Outputs
C ***
C      Horizontal surface total radiation - [-Inf;+Inf]
C      Horizontal surface diffuse radiation - [-Inf;+Inf]
C      Horizontal surface beam radiation - [-Inf;+Inf]
C      Zenith angle - [-Inf;+Inf]

```

```

C      Tilted beam radiation - [-Inf;+Inf]
C      Tilted diffuse radiation - [-Inf;+Inf]
C      Tilted Ground reflected radiation - [-Inf;+Inf]
C      Solar incidence angle on the tilted surface - [-Inf;+Inf]
C      Solar azimuth angle - [-Inf;+Inf]

C TRNSYS access functions (allow to access TIME etc.)
  USE TrnsysConstants
  USE TrnsysFunctions
C*****
C  REQUIRED BY THE MULTI-DLL VERSION OF TRNSYS
  !DEC$ATTRIBUTES DLLEXPORT :: TYPE202 !SET THE CORRECT TYPE NUMBER HERE
C*****
C TRNSYS DECLARATIONS
  IMPLICIT NONE

      DOUBLE PRECISION XIN,OUT,TIME,PAR,STORED,T,DTDT
      INTEGER*4 INFO(15)
      INTEGER*4 NP,NI,NOUT,ND
      INTEGER*4 NPAR,NIN,NDER
      INTEGER*4 IUNIT,ITYPE,ICNTRL,NSTORED,LUW
      CHARACTER*3 OCHECK
      CHARACTER*3 YCHECK
C*****
C  USER DECLARATIONS - SET THE MAXIMUM NUMBER OF PARAMETERS C (NP), INPUTS (NI),
C  OUTPUTS (NOUT), AND DERIVATIVES (ND) THAT MAY BE SUPPLIED FOR C THIS TYPE
  PARAMETER (NP=6,NI=3,NOUT=9,ND=0,NSTORED=0)
C*****
C  REQUIRED TRNSYS DIMENSIONS
  DIMENSION XIN(NI),OUT(NOUT),PAR(NP),YCHECK(NI),OCHECK(NOUT),
    1 STORED(NSTORED),T(ND),DTDT(ND)
  INTEGER NITEMS
C*****
C  ADD DECLARATIONS AND DEFINITIONS FOR THE USER-VARIABLES C HERE

C  PARAMETERS
  DOUBLE PRECISION DAY,LAT,BETA,RHO,SHIFT,GAMSURF

C  INPUTS
  INTEGER*4 ADVTIME
  DOUBLE PRECISION GtT,CIVILT

C  OUTPUT
  DOUBLE PRECISION GtH,GDH,GBH,THETAZ,GBT,GDT,GGT,THETA

C  OTHER VARIABLES
  DOUBLE PRECISION TIME0,TFINAL,DELT
  DOUBLE PRECISION DEC,COSTH,COSTHZ
  DOUBLE PRECISION RB,KT,GtT2,B,E
  DOUBLE PRECISION SOLTIME,W,W2,GOH,DEL
  DOUBLE PRECISION CHECK,DELHOLD
  DOUBLE PRECISION LOW_KT,HIGH_KT,OLD_KT
  DOUBLE PRECISION C1,C2,C3,GAMSP,GAMS,SINGAMSP,
  DOUBLE PRECISION PI,COSWEW,WEW
  INTEGER*4 J

C  COMMON VARIABLES
  COMMON IUNIT,ITYPE,LUW

C  DATA STATEMENTS
  DATA PI/3.1415927/

```

```

C*****
C   TRNSYS FUNCTIONS
   TIME0=getSimulationStartTime()
   TFINAL=getSimulationStopTime()
   DELT=getSimulationTimeStep()

C   SET THE VERSION INFORMATION FOR TRNSYS
   IF(INFO(7).EQ.-2) THEN
       INFO(12)=16
       RETURN 1
   ENDIF
C*****
C   DO ALL THE VERY LAST CALL OF THE SIMULATION MANIPULATIONS HERE
   IF (INFO(8).EQ.-1) THEN
       RETURN 1
   ENDIF
C*****
C   PERFORM ANY 'AFTER-ITERATION' MANIPULATIONS THAT ARE REQUIRED HERE
C   e.g. save variables to storage array for the next timestep
   IF (INFO(13).GT.0) THEN
       NITEMS=0
C       STORED(1)=... (if NITEMS > 0)
C       CALL setStorageVars(STORED,NITEMS,INFO)
       RETURN 1
   ENDIF
C*****
C   DO ALL THE VERY FIRST CALL OF THE SIMULATION MANIPULATIONS HERE
   IF (INFO(7).EQ.-1) THEN

       IUNIT=INFO(1)
       ITYPE=INFO(2)

C   SET SOME INFO ARRAY VARIABLES TO TELL THE TRNSYS ENGINE HOW THIS TYPE IS TO WORK
   INFO(6)=NOUT
   INFO(9)=1
       INFO(10)=0   !STORAGE FOR VERSION 16 HAS BEEN CHANGED

C   THE TRNSYS INPUT FILE
       CALL TYPECK(1,INFO,NI,NP,ND)

       RETURN 1
   ENDIF
C*****
C   DO ALL OF THE INITIAL TIMESTEP MANIPULATIONS HERE - THERE ARE NO ITERATIONS AT THE
INITIAL TIME
   IF (TIME .LT.(TIME0+DELT/2.D0)) THEN

C   SET THE UNIT NUMBER FOR FUTURE CALLS
       IUNIT=INFO(1)
       ITYPE=INFO(2)
C   SET PARAMETERS AND CONVERT ANGLES TO RADIANS

       DAY = PAR(1)
       LAT = PAR(2)
       BETA = PAR(3)
       RHO = PAR(4)
       SHIFT = PAR(5)
       GAMSURF=PAR(6)

       LAT = LAT*PI/180.0
       BETA = BETA*PI/180.0
       GAMSURF=GAMSURF*PI/180.0

```

```

RETURN 1
  ENDIF
C   RE-READ IN THE VALUES OF THE PARAMETERS IN SEQUENTIAL ORDER
    IF(INFO(1).NE.IUNIT) THEN

c     RESET THE UNIT NUMBER
      IUNIT=INFO(1)
      ITYPE=INFO(2)

      DAY = PAR(1)
      LAT = PAR(2)
      BETA = PAR(3)
      RHO = PAR(4)
      SHIFT = PAR(5)
      GAMSURF=PAR(6)

      LAT = LAT*PI/180.0
      BETA = BETA*PI/180.0
      GAMSURF=GAMSURF*PI/180.0
    ENDIF
C   SET INPUTS

      GiT = XIN(1)
      CIVILT=XIN(2)
      ADVTIME=XIN(3)

      DEL=0.0
      CHECK=0.0
      DELHOLD=0.0
C*****
C   CALCULATE SOLAR ANGLES AND EXTRATERRESTRIAL RADIATION
C   [Duffie and Beckman, 1991]
C*****
      DEC=23.45*SIN(360*(284+DAY)*PI/365/180)*PI/180      !RAD
      B = 360*(DAY-81)/364*PI/180      !RAD
      E=(9.87*SIN(2.*B)-7.53*COS(B)-1.5*SIN(B))/60.      !HR

      IF(ADVTIME.GE.1)THEN
        SOLTIME=CIVILT-1.0+(SHIFT/15.0)+E
      ELSE
        SOLTIME=CIVILT+(SHIFT/15.0)+E
      ENDIF
C*****
C   FOR SMALL TIME STEP HOUR ANGLE IS TAKEN AT THE SOLAR TIME
C   OF THE ACTUAL TIME
C*****
      W = (SOLTIME-12.0)*15.0*PI/180.0      !RAD
      GOH=1367*3.6*(1.0+(0.033*COS(DAY*2.0*PI/365)))*
      & (COS(LAT)*COS(DEC)*COS(W)+SIN(LAT)*SIN(DEC))
C*****
C   CALCULATE SOLAR POSITION ANGLES AND RB
C*****
      COSTH=SIN(DEC)*SIN(LAT)*COS(BETA)-
      & SIN(DEC)*COS(LAT)*SIN(BETA)*COS(GAMSURF)+
      & COS(DEC)*COS(LAT)*COS(BETA)*COS(W)+
      & COS(DEC)*SIN(LAT)*SIN(BETA)*COS(GAMSURF)*COS(W)+
      & COS(DEC)*SIN(BETA)*SIN(GAMSURF)*SIN(W)

      THETA=ACOS(COSTH)*180./PI !DEG
      COSTHZ=COS(LAT)*COS(DEC)*COS(W)+SIN(LAT)*SIN(DEC)
      THETAZ=ACOS(COSTHZ)*180./PI      !DEG

```

```

RB=COSTH/COSTHZ
C*****
C    CALCULATE SOLAR AZIMUTH ANGLE WITH THE FORMULATION OF
C    Braun and Mitchell [1983]
C*****
SINGAMSP=SIN(W)*COS(DEC)/SIN(THETAZ*PI/180.0)
GAMSP=ASIN(SINGAMSP)*180./PI !DEG
COSWEW=TAN(DEC)/TAN(LAT)
WEW=ACOS(COSWEW) !RAD

IF((ABS(W).LT.WEW).OR.(ABS(COSWEW).GT.1))THEN
    C1=1
ELSE
    C1=-1
ENDIF

IF ((LAT*(LAT-DEC)).GE.0) THEN
    C2=1
ELSE
    C2=-1
ENDIF

IF(W.GE.0) THEN
    C3=1
ELSE
    C3=-1
ENDIF
GAMS=(C1*C2*GAMSP)+(C3*0.5*180*(1-(C1*C2)))
C*****
C    EXIT FOR LOW RADIATION, THE CORRECTION IS NEGLIGIBLE
C*****
IF(GOH.LT.10.) THEN
    GtH=GtT
    GOTO 60
ENDIF
C*****
C    EXIT IF THERE IS NO MEASURED RADIATION
C*****
IF (GtT.LE.0.) THEN
    GtH = GtT
    GOTO 60
ENDIF
C*****
C    SOLVE FO KT
C    BEGIN WITH AN ITITIAL GUESS FOR KT OF 0.5 AND GTH=KT*GOH
C    ASSUME INSTANTANEOUS RADIATION CORRESPONDS TO THE
C    RADIATION AVERAGED HOURLY
C*****
J=0
DEL=0.0
LOW_KT=0.0
HIGH_KT=1.0
KT=(LOW_KT+HIGH_KT)/2.0

C    BEGIN THE MAIN ITERATION LOOP
20 CONTINUE
J=J+1
GtH=KT*GOH
C*****
C    USE THE Erbs CORRELATION TO CALCULATE THE HORIZONTAL
C    DIFFUSE COMPONENT
C    CALCULATE CORRESPONDING HORIZONTAL BEAM RADIATION

```

```

C*****
IF(KT.GT.0.8) THEN
  GdH=.165*GtH
ELSE IF(KT.GT.0.22) THEN
  GdH=GtH*(.9511-.1604*KT+4.388*KT*KT-16.638*(KT**3)
& +12.336*(KT**4))
ELSE
  GdH=GtH*(1.-.09*KT)
ENDIF

  GbH=GtH-GdH
C*****
C      OBTAIN A NEW TOTAL TILTED RADIATION AND COMPARE WITH THE
C      INPUT Gt , FIND KT USING THE BISSECTION METHOD
C*****
  GtT2=GbH*RB+GdH*(1.+COS(BETA))/2.+RHO*GtH*(1.-COS(BETA))/2.

  IF(GtT2.LT.GtT)THEN
    LOW_KT=KT
  ELSE
    HIGH_KT=KT
  ENDIF

  OLD_KT=KT
  KT=(LOW_KT+HIGH_KT)/2.0
  DEL=ABS(GtT2-GtT)

C      CONTINUE ITERATIONS
C      CALCULATE A NEW GTH WITH THE NEW KT
  IF(DEL.GT.0.5.AND.J.LT.300)GO TO 20
C      TOO MANY ITERATIONS
  IF(J.GE.200) GOTO 40
C      CONVERGENCE IS OBTAINED
  IF (DEL.LT.1.) GOTO 60
C      EXIT ITERATION IF KT=1, CLEAR DAY
25  GtH=GOH
  GOTO 60
C
40  WRITE(LUW,*)'Radiation converter error at time=',TIME
  WRITE(LUW,*)'Too many iterations'
  GtH=GtT
  GOTO 60
50  WRITE (LUW,*)'Radiation converter error at time =',TIME
  WRITE (LUW,*)'No Convergence'
  GtH = GtT
  GOTO 60
C
60  CONTINUE

  GBT=GbH*RB
  GDT=GdH*((1+COS(BETA))/2.0)
  GGT=GtH*RHO*((1-COS(BETA))/2.0)

  IF(GDH.LT.0)THEN
    GDH=0
  ENDIF

  IF(GtH.LT.0)THEN
    GtH=0
  ENDIF

  IF(GBH.LT.0)THEN

```

```
    GBH=0
    ENDIF

    IF(GBT.LT.0)THEN
        GBT=0
    ENDIF

    IF(GdT.LT.0)THEN
        GdT=0
    ENDIF

    IF(GgT.LT.0)THEN
        GgT=0
    ENDIF

C      Set OUTPUTS
      OUT(1)=GtH
      OUT(2)=GDH
      OUT(3)=GBH
      OUT(4)=THETAZ
      OUT(5)=GBT
      OUT(6)=GDT
      OUT(7)=GGT
      OUT(8)=THETA
      OUT(9)=GamS

      RETURN 1
      END
```

# Bibliography

- [1] Arulanandam, S.J., Hollands, K.G.T., & Brundrett, E. (1999). A CFD Heat Transfer Analysis of the Transpired Solar Collector Under No-Wind Conditions. *Solar Energy* 67(1), 93-100.
- [2] ASHRAE Task Group on Energy Requirements. Subcommittee for Buildings and Coolings Loads. (1975). *Subroutine Algorithms for Heating and Cooling Loads to Determine Building Energy Requirements*. New York: American Society of Heating, Refrigerating and Air-Conditioning Engineers, Inc.
- [3] ASHRAE. (2005). *ASHRAE Handbook-Fundamentals*. Atlanta: American Society of Heating, Refrigerating and Air-Conditioning Engineers, Inc.
- [4] ASTM E891-87. (1987). *Standard Tables for Terrestrial Direct Normal Solar Spectral Irradiance for Air Mass 1.5*. American Society for Testing and Materials.
- [5] ASTM E903-96. (1996). *Standard Test Method for Solar Absorptance, Reflectance, and Transmittance of Materials Using Integrating Spheres*. American Society for Testing and Materials.
- [6] Brandemuehl, M.J., & Beckman, W.A. (1980). Transmission of Diffuse radiation through CPC and Flat Plate Collector Glazings. *Solar Energy* 24(5), 511-513.
- [7] Cao, S., Hollands, K.G.T., & Brundrett, E. (1993). Heat Exchange Effectiveness of Unglazed Transpired-Plate Solar Collector in 2D Flow. *Proceedings of the ISES World Congress, August 23-27, Budapest, Hungary*, 351-366.

- [8] Carpenter, S., Daniels, S., Kemp, S., Kokko, J., & Van Decker, G. (1999). New Tools for Assessing the Performance of Solar Ventilation Air Heating Systems. *Proceedings of the 8th Biannual Conference of Solar Energy in High Latitudes (North sun '99), Incorporating the 25th Annual Conference of the Solar Energy Society of Canada Inc. (SESCI), Edmonton, AB, Canada.*
- [9] Carpenter, S., & Meloche, N. (2002). The Retscreen Model for Simulating the Performance of Solar Air Heating Systems. *Proceedings eSim, September, 11-13.*
- [10] Conservall Engineering inc. (2007). *SolarWall*. Retrieved June, 2007, from <http://www.solarwall.com/home/CaseHistory.aspx>.
- [11] De Soto, W., Klein, S.A., & Beckman, W.A. (2005). Improvement and Validation of a Model for Photovoltaic Array Performance. *Solar Energy* 80(1), 78-88.
- [12] Duffie, J.A., & Beckman, W.A.(1991). *Solar Engineering of Thermal Processes* (Ed.2). New York: John Wiley & Sons, Inc.
- [13] Dymond, C., & Kutscher, C. (1995). Computer Design Model for Transpired Solar Collector Systems. *International Solar Energy Conference* (2), 1165-1174.
- [14] Dymond, C., & Kutscher, C. (1997). Development of a Flow Distribution and Design Model for Transpired Solar Collectors. *Solar Energy* 60(5), 291-300.
- [15] E. Jordan Brookes. (2007). *The E. Jordan Brookes Co., Inc.* Retrieved May, 2007, from <http://www.ejbco.com/index.asp>.
- [16] Emmel, M.G., Abadie, M.O., & Mendes, N. (2007). New External Convective Heat Transfer Coefficient Correlations for Isolated Low-Rise Building. *Energy and Buildings* 39, 335-342.
- [17] Enermodal. (1994). *Performance of the Perforated-Plate/Canopy Solar Wall at GM Canada, Oshawa*. Report prepared for CANMET, Natural Resources Canada, Ottawa.

- [18] Fantech. (2007). *Fantech FG Series*. Retrieved May, 2007, from <http://www.fantech.net/fg.htm>.
- [19] Fleck, B.A., Meier R.M., & Matovic M.D. (2002). A Field Study of the Wind Effects on the Performance of an Unglazed Transpired Solar Collector. *Solar Energy* 73(3), 209-216.
- [20] Gawlik, K.M., & Kutscher C. 2002. Wind Heat Loss from Corrugated, Transpired Solar Collectors. *Transactions of the ASME* 124(3), 256-261.
- [21] Gawlik, G., Christensen C., & Kutscher C. (2005). A Numerical and Experimental Investigation of Low-Conductivity Unglazed, Transpired Solar Air Heaters. *Journal of Solar Energy Engineering Transactions of the ASME* 127(1), 153-155.
- [22] Gogakis, C. (2005). *Theoretical and Experimental Analysis of SolarWall<sup>®</sup> Technology*. MSc Thesis. The University of Reading, UK.
- [23] Golneshan, A.A., & Hollands K.G.T. (1998). Experiments on Forced Convection Heat Transfer from Slotted Transpired Plates. *Proceedings of Canadian Society of Mechanical Engineering Forum 1998, Toronto, Canada* 1, 78–88.
- [24] Golneshan, A.A. (1994). *Forced Convection Heat Transfer From Low Porosity Slotted Transpired Plates*. Ph.D. Thesis. University of Waterloo, Waterloo, Ontario.
- [25] Gunnewiek, L.H. (1994). *An Investigation of the Flow Distribution through Unglazed Transpired-Plate Solar Air Heaters*. MSc Thesis. University of Waterloo, Waterloo, Ontario.
- [26] Gunnewiek, L.H., Brundrett E., & Hollands K.G.T. (1996). Flow Distribution in Unglazed Transpired Plate Solar Air Heaters of Large Area. *Solar Energy* 58 (4-6), 227-237.
- [27] Gunnewiek, L.H., Hollands K.G.T., & Brundrett E. (2002). Effect of Wind on Flow Distribution in Unglazed Transpired-Plate Collectors. *Solar Energy* 72(4), 317-325.

- [28] Hollick, J.C. (1994). Unglazed Solar Wall Air Heaters. *Renewable Energy* 5(1), 415-421.
- [29] Hollick, J.C. (1998). Solar Cogeneration Panels. *Renewable Energy* 15(1-4), 195-200.
- [30] IEC 61215. (2005). *Crystalline Silicon Terrestrial Photovoltaic (PV) Modules- Design Qualification and Type Approval*. International Electrotechnical Commission.
- [31] Incropera, F.P., & DeWitt D.P. (2002). *Fundamentals of Heat and Mass Transfer* (Ed. 5). New York: John Wiley & Sons, Inc.
- [32] IPCC (Intergovernmental Panel on Climate Change). (2007). Retrieved June, 2007, from <http://www.ipcc.ch/pub/spm22-01.pdf>.
- [33] Kline, S.J., & McClintock F.A. (1953). Describing Uncertainties in Single-Sample Experiments. *Mechanical Engineering by ASME* 75(1), 3-8.
- [34] Kutscher, C.F., Christensen C., & Barker G. (1991). Unglazed Transpired Solar Collectors: An Analytical Model and Test Results. *Solar World Congress* 2(2), 1245-1250.
- [35] Kutscher, C.F., Christensen C., & Barker G. (1993). Unglazed Transpired Solar Collectors: Heat Loss Theory. *Journal of Solar Energy Engineering, Transactions of the ASME* 115(3), 182-188.
- [36] Kutscher C.F. (1994). Heat Exchange Effectiveness and Pressure Drop for Air Flow through Perforated Plates with and without Crosswind. *Journal of Heat Transfer, Transactions of the ASME* 116(2), 391-399.
- [37] Lee, J.H, Chung, M., & Park., W.-H. (1987). An Experimental and Theoretical Study on the Corrugated Water-Trickle Collector. *Solar Energy* 38(2), 113-123.
- [38] Leon, M.A., & Kumar, S. (2007). Mathematical Modeling and Thermal Performance Analysis of Unglazed Transpired Solar Collector. *Solar Energy* 81(1), 62-75.

- [39] Liu, B.Y.U., & Jordan, R.C. (1963). A Rational Procedure for Predicting the Long-Term Average Performance of Flat Plate Solar Energy Collectors. *Solar Energy* 7, 53.
- [40] Loveday, D.L., & Taki, A.H. (1996). Convective Heat Transfer Coefficients at a Plane Surface on a Full-Scale Building Facade. *International Journal of Heat and Mass Transfer* 39(8), 1729-1742.
- [41] Maurer, C. (2004). *Field Study and Modeling of an Unglazed Transpired Solar Collector System*. MASC Thesis. North Carolina State University, Raleigh.
- [42] Naveed, A.T., Kang, E.C., & Lee, E.J. (2006). Effect of Unglazed Transpired Collector on the Performance of a Polycrystalline Silicon Photovoltaic Module. *Journal of Solar Engineering, Transactions of the ASME* 128, 349-353.
- [43] Omega Engineering. (2003). USB Data Acquisition Modules for Thermocouples Process Signals. Retrieved March, 2007, <http://www.omega.ca/shop/pptsc.asp?ref=OMB-DAQ55&flag=1>.
- [44] RETScreen International. (2005). *Clean Energy Project Analysis Software, Solar Air Heating Project Model*. Version 3.1.
- [45] Sandnes, B., & Rekstad J. (2002). A Photovoltaic/Thermal (PV/T) Collector with a Polymer Absorber Plate. Experimental Study and Analytical Model. *Solar Energy* 72(1), 63-73.
- [46] SEL (Solar Energy Laboratory). (2005). *TRNSYS 16 – A Transient System Simulation Program*. Version 16. University of Wisconsin, Madison.
- [47] Siegel R., & Howell, J.R. (1992). *Thermal Radiation Heat Transfer* (Ed. 3). Washington: Hemisphere Publishing Corporation.
- [48] Sierra Instruments. (1999). *Sierra Series 620s Fast-Flo<sup>TM</sup> Insertion Mass Flow Meter*. Monterey, California.
- [49] Sparrow, E.M., & Ortiz, C. (1982). Heat Transfer Coefficients for the Upstream Face of a Perforated Plate Positioned Normal to an Oncoming Flow. *International Journal of Heat and Mass Transfer* 25(1), 127-135.

- [50] Statistics Canada. (2006). *Energy Use Data Handbook*. Retrieved June, 2007, from <http://www.oeenrncan.gc.ca/Publications/statistics/handbook06/pdf/handbook06.pdf>.
- [51] Summers, D. (1995). *Thermal Simulation and Economic Assessment of Unglazed Transpired Collector Systems*. MASC Thesis. University of Wisconsin, Madison.
- [52] Surface Optics. (2001). *SOC 400T Directional Reflectometer*. Retrieved November, 2007, from <http://www.surfaceoptics.com/Products/FTIRs/400t.htm>.
- [53] Swamee, P.K., & Jain, A.K. (1976). Explicit equations for pipe-flow problems. *Journal of the Hydraulics Division, ASCE* 102 (5), 657–664.
- [54] SWift99. (2001). *Solarwall International Feasibility Tool*. Version 1.04.
- [55] TESS (Thermal Energy Systems Specialists). 2005. TESS Libraries Version 2.02, Reference Manuals (13 Volumes), Madison, WI., <http://tess-inc.com>.
- [56] Van Decker, G.W.E., Hollands, K.G.T & Brunger, A.P. (2001). Heat Exchange Effectiveness of Unglazed Transpired-Plate Solar Collector in 3D Flow. *Solar Energy* 71(1), 33-45.
- [57] Varian Inc. (2005). *Cary 5000 UV-Vis-NIR spectrophotometer*. Retrieved November, 2007, from [http://www.varianinc.com/cgi-bin/nav?products/spectr/uv/cary5000/cary\\_5000&cid=HFIH](http://www.varianinc.com/cgi-bin/nav?products/spectr/uv/cary5000/cary_5000&cid=HFIH).
- [58] Whitaker, C.M., Townsend, T.U., Wenger, H.J., Iliceto, A., Chimento, G., Paletta, F. (1991). Effects of Irradiance and Other Factors on PV Temperature Coefficients. *Conference Record of the Twenty Second IEEE Photovoltaic Specialists Conference - 1991* 1, 608-613.
- [59] Waterloo Weather Station. (September 2007). *UW Weather Station Data Archives*. Retrieved September 2007, from <http://weather.uwaterloo.ca/data.html>.

- [60] Zondag, H.A., Vries, D.W., Van Hendel, W.G.J., Van Zolingen, R.J.C., & Van Steenhoven, A.A. (2003). The Yield of Different Combined PV-Thermal Collector Designs. *Solar Energy* 74(3), 253-269.